Risk stratification and targeted neuroprotection in Parkinson disease utilising the glucocerebrosidase pathway

Dr. Stephen Mullin

64,106 words

For my wife Tanya and my darling daughter Jessica. This thesis took too many evenings and weekends which should have been spent with you both. Without your love and support it would never have been completed.

Acknowledgements

Above all I must express my gratitude to all the participants who took part in the studies that make up this thesis. Their commitment to research is humbling and inspiring. Moreover, I must also thanks the support of the Gaucher association (in particular Tanya Histed Collins, Jeremy Manuel and Dan Brown) and Parkinson's UK. Their support was crucial to all of the work presented here.

This thesis is a grounded on foundations of the previous work, good will and patience of numerous people. My mother and father who took on the uneviable task of proof reading it. Prof. Sandip Patel, Dr. Bethan Kilpatrick and Dr. Lizzie Yates took a neophyte and taught him, in spite of his medic tendencies, to carry out single cell imaging. Dr. Joana Magalhaes and Dr. Ania Migdalska showed considerable restraint in showing me how breed and harvest mice primary cultures. Dr. Michelle Beavan and Dr. Alistair Mcneil passed on a cohort of patients which most PhD students would be the envy of most PhD students. The efforts of Dr. Marco Toffoli and Dr. Micol Avenali were vital to the cohort study. Jonathan Bestwick tolerated my very tentative and unprepared immersion into the world of repeated measures statistics. Prof. Henrik Zetterberg and Prof. Kevin Mills offered considerable time, capital and above all expertise in carrying out the various biomarkers studies, while Dr.Wendy Heywood and Jenny Hallqvist carried out many of these assays.

Dr. Morton Stokholm and Prof. David Brooks supported and funded the PET imaging studies and looked after me during my myriad expeditions to Denmark. Dr. Alistair Noyce, Prof. Anette Schrag, Helen Brooker, Prof Keith Wesnes, Any Cartwright enabled the hugely complicated rapsodi portal to become a reality. Dr. Steven Lubbe and Prof. Huw Morris were invaluable sources of advice and expertise for the meta analysis of genetic case control data. AiM PD would not have been possible without Laura Smith, Katherine Lee, Gayle De Souza, Prof. Tom Foltynie, Dr. Phil Woodgate, Dr. Vincenzo Libri, Laura Henelly, Mark Elliot, Kerry Guile, Bryony Barling, Rita Smith and Edwina Sanders.

Sarah Cable was the bedrock of most of the clinical work carried out in this thesis. Her energy and tireless commitment to subjects of tremendous sensitivity as well as her near infinite work ethics saved a number of projects on a number of occasions. Dr. Derralyn Hughes and Prof Atul Mehta have between them educated me about lysosomal storage diseases with patience and enthusiasm. Equally the staff of the lysosomal storge disease unit and most notably Patricia Pilgrim, June perry, Juniebel Cook and Linda Patridge must be thanked. Rob Baker, Dr. Matt Gegg, Dr. Christos Proukakis, Dr. Natalie Welsh, Dr. Christina Gewinner, Dr. Mark Cooper have provided help at advice throughout the thesis.

Finally, I must thank my supervisor and mentor Prof. Tony Schapira, who taught, guided and supported me through the myriad highs and lows. It is an opportunity I hope some day I may be able to repay.

Abstract:

Objectives:

Glucocerebrosidase mutations represent genetically the most significant risk factor for Parkinson disease, however their penetrance is incomplete and variable such that only a minority of glucocerebrosidase mutation carriers will develop Parkinson disease. In this thesis I aimed to investigate the basis for this incomplete penetrance, to identify indices which may be used to predict Parkinson disease conversion amongst glucocerebrosidse mutation carriers and to test a putative neuroprotective drug designed to modify the glucocerebrosidase pathway.

Methods:

In **chapter 2** we used meta and joint analyses to calculate the odds ratio of developing Parkinson disease with individual glucocerebrosidase mutations. In **chapter 3** we prospectively assessed a cohort of glucocerebrosidase mutation carriers without Parkinson disease for prodromal signs of Parkinsonism. In **chapter 4** we sought to extend the scope, scale and sustainability of this study by producing a prototype study to assess these patients remotely through the internet. In **chapter 5** we investigated whether novel imaging (PET using the PK-1195 and DAT ligands), serum (alpha synuclein, tau and inflammatory markers) and urine (hypothesis generating screen) could be used to predict PD conversion. In **chapter 6** we used single cell calcium imaging in a primary neuronal mouse model carrying the

N370S glucocerebrosidase mutation to investigate whether deranged calcium homeostasis might be the basis for the selective vulnerability of dopaminergic neurons in glucocerebrosidase mutation carrying cells. In **chapters 7 and 8** we present optimisation and preliminary data from AiM PD, a phase II, open label, non placebo controlled trial of ambroxol, a small molecular chaperone of the glucocerebrosidase enzyme.

Results:

Chapter 2: We derived quantifiable estimates of Parkinson disease risk for 84GG, E326K N370S, L444P, D409H, RecNcil as well as important data relating to the ethnic distribution of these mutations.

Chapter 3: The University of Pennslyvannia smell identification test and Montreal cognitive assessment scores of glucocerebrosidse mutation carriers were worse than those of controls. There is a clustering effect amongst glucocerebrosidse mutation carriers whereby poor scores in these assessments and the Beck's depression index seemed to be present together in a subset of participants.

Chapter 4: We show the rapsodi portal is able, using validated assessments, to detect Parkinson disease features. Preliminary data shows cognitive deficits amongst Glucocerebrosidase mutations carriers exist compared to controls.

Chapter 5: PK11195 signal is increased in the substantia nigra of glucocerebrosidase mutation carriers compared to controls and this signal increase correlates with olfactory loss. Serum alpha synuclein levels in glucocerebrosidase carriers correlate with the number of severe (neuronopathic) mutations and a risk score derived from prospective assessment of prodromal Parkinson disease features. The hypothesis generating urine proteomics

screen identified a number of potential markers of Parkinson disease conversion including elements of the IgG kappa light chain.

Chapter 6: We found no evidence of deranged calcium homeostasis

Chapter 7: The glucocerebrosidase enzyme activity assay has been optimised to be reproducibly used in cerebrospinal fluid samples in our hands. The optimal time to carry out the assay to prevent degradation of activity following freezing is within 2 weeks of collection. *In vitro* addition of ambroxol to control CSF at physiologically relevant concentrations caused a 50% reduction in activity levels, due presumably to anatagonistic binding to the active site of the enzyme.

Chapter 8: Preliminary results show that ambroxol delivers a statistically significant increase in leucocyte glucocerebrosidase activity amongst glucocerebrosidase mutation carriers with Parkinson disease. These patients seem to have worse features of non motor Parkinson disease symptoms than idiopathic Parkinson disease cases.

Conclusions:

Our results collectively suggest it may be feasible to stratify risk of Parkinson disease conversion amongst glucocerebrosidse mutation carriers on the basis of genetic, clinical, imaging and biochemical indices. Moeover they suggest that ambroxol has potential as a neuroprotective agent in Parkinson disease.

Publications

Publications from thesis

Arkadir, David, Tama Dinur, Stephen Mullin, Atul Mehta, Hagit N Baris, Roy N Alcalay, and Ari Zimran. 2016. “Trio Approach Reveals Higher Risk of PD in Carriers of Severe vs. Mild GBA Mutations..” *Blood Cells, Molecules & Diseases*, November. doi:10.1016/j.bcmd.2016.11.007.

Mullin, Stephen and Anthony H V Schapira. 2015. “Pathogenic Mechanisms of Neurodegeneration in Parkinson Disease.” *Neurologic Clinics of NA* 33 (1). Elsevier Inc: 1–17. doi:10.1016/j.ncl.2014.09.010.

Mullin, Stephen, and Anthony Schapira. 2015. “The Genetics of Parkinson's Disease..” *British Medical Bulletin* 114 (1): 39–52. doi:10.1093/bmb/ldv022.

Pakpoor, Julia, Alastair Noyce, Raph Goldacre, Marianna Selkihova, Stephen Mullin, Anette Schrag, Andrew Lees, and Michael Goldacre. 2017. “Viral Hepatitis and Parkinson Disease.” *Neurology*, March, 10.1212/WNL.0000000000003848. doi:10.1212/WNL.0000000000003848.

Porcari, Riccardo, Christos Proukakis, Christopher A Waudby, Benedetta Bolognesi, P Patrizia Mangione, Jack F S Paton, Stephen Mullin, et al. 2015. “The H50Q Mutation Induces a 10-Fold Decrease in the Solubility of A-Synuclein..” *Journal of Biological Chemistry* 290 (4): 2395–2404. doi:10.1074/jbc.M114.610527.

Manuscripts in preparation

Mullin, Stephen, Katherine Lee, Laura Smith, Gayle De Souza, Phil Woodgate Vincenzo Libri Sarah Cable, Tom Foltynie, Anthony Schapira 2017 “Rationale and protocol for ambroxol in modification of Parkinson’s disease (AiM PD) trial.” *Movement disorders*

Mullin, Stephen,, Laura Smith, Derralyn Hughes, Atul Mehta, Christos Proukakis, Huw R Morris, Vittorio Belloti, Steven Lubbe, Tony Schapira 2017 "Meta and pooled joint analyses of risk of Parkinson disease quantifies pathogenicity of individual *GBA* mutations." *Annals of Neurology*

Mullin, Stephen Michelle Beavan, Wendy E Heywood, Jonathan Bestwick, Alisdair McNeil, Christos Proukakis, Timothy M Cox, Derralyn Hughes, Atul Mehta, Kevin Mills, Henrik Zetterberg, Anthony HV Schapira 2017 “Evolution and clustering of prodromal Parkinsonian features in *GBA* carriers: a prospective cohort study” *Neurology*

Mullin, Stephen, Morten Stokholm, Derralyn Hughes, Atul Mehta, Nicola Pavese, David Brooks, Anthony Schapira 2017 “Increased microglial activation in asymptomatic glucocerebrosidase mutation carriers: A cross-sectional PET study” *Lancet Neurology*

Index

Index of appendices

Index of figures

Index of supplementary figures

Index of tables

Index of Supplementary tables

Chapter 1 - Introduction

1.0 The glycosphingolipid pathway

Glycosphingolipids are a class lipids found in eukaryotic organisms. They share a common two tailed lipid, ceramide, which anchors the molecule in the cell membrane. The addition in most cases of a lactosylceramide forms the basic disaccharide whilst a number of other carbohydates can be attached to the galactose group by glycosidic linkage. Their concentration on cell membranes varies dramatically on the basis of cellular function.[1]

Genetically derived enzyme deficiencies at different stages of the glycosphingolipid catabolic pathway give rise to highly stereotyped diseases with varying severity and clinical presentations, reflecting accumulation of the respective sphingolipid substrates in various visceral organs [2,3]. The GM1 and GM2 gangliosidoses for instance, caused respectively by deficiencies in the Beta hexaminidase and Beta galctosidase, are severe and progressive diseases of childhood onset neurodegeneration [4]. Fabry disease, a deficit of alpha galactosidase, leads to accumulation of globotriaosylceramide through an as yet unidentified mechanism, and a variety of clinical phenotypes including cornea verticillata, peripheral neuropathy, cardiomyopathy, stroke, chronic renal failure and cutaneous angiokeratoma formation [5].

1.1 Glucocerebrosidase and Gaucher disease

Glucocerebrosidase (also called glucosylceramidase) is a lysosomal hydrolase enzyme which catalyses the breakdown of the sphingolipid glucosylceramide (Gb1) into ceramide and water. It is a particularly important component of this pathway because it lies downstream of the glycosphingolipids GM1 and globoside, meaning that it is implicit in the breakdown of these molecules and their catabolites [3]. In Gaucher disease, homozygous carriers of mutations in the glucocerebrosidase gene (*GBA*) cause an accumulation of Glucosylceramide, which is deposited in the spleen, liver and bones. A number of more "severe" *GBA* mutations are variably associated with symptoms of central nervous system involvement. Characteristically these neuronopathic forms of Gaucher disease, which are subdivided in an acute onset (invariably fatal) presentation (type 2) and a more chronic progressive form (type 3), give rise to supranuclear gaze palsy accompanying other features such as cognitive impairment, epilepsy and tremor [6-9]. In practice the demarcation between types 2 and 3 is more fluid and the presence of neuronopathic features is highly variable, even amongst those with identical genetic mutations of the *GBA* gene [10].

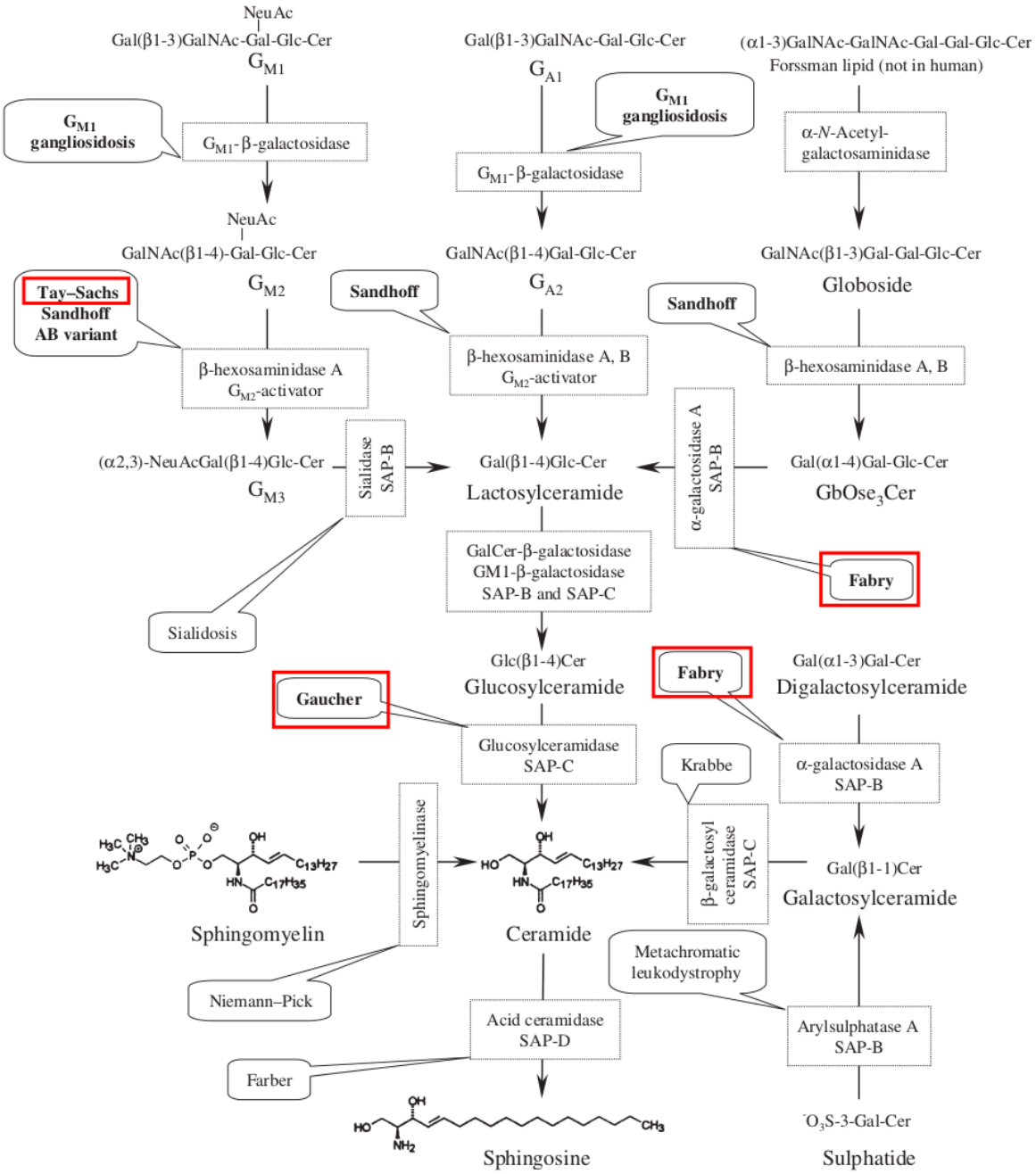

Fig 1. The sphingolipid pathway. Adapted from: Jeyakumar, M., Butters, T. D., Dwek, R. a, & Platt, F. M. (2002). Glycosphingolipid lysosomal storage diseases: therapy and pathogenesis. Neuropathology and applied neurobiology, 28(5), 343-57.

1.2 Glucocerebrosidase and Parkinson disease

In the 1990s it was noticed that there appeared to be a higher incidence of Parkinson disease amongst those with Gaucher disease and their kindred. Longitudinal studies amongst Gaucher disease cohorts suggest a conversion to Parkinson disease of approximately 10% by the age of 80 [11-13]. For heterozygous *GBA* carriers penetrance has been quoted as high as 30%, although this figure is controversial [14,15]. That said it is clear that the true penetrance is substantially lower than 50%, making *GBA* a genetic risk factor as opposed to an autosomal dominant allele in the traditional Mendelian sense. There are to date in excess of 300 known Gaucher causing *GBA* mutations and their prevalence (quantified using exon sequencing) has been demonstrated in the UK to be as high as 3% [16], although more usually this is reported around 1% [17-19]. Amongst Ashkenazi Jewish enriched population, where these mutations are more common, this can rise to around 6% [20,21].

There is substantial variation in the effect size (in terms of conversion to Parkinson disease and GD) of individual mutations. Strikingly those alleles which are associated with neuronopathic forms of Gaucher disease also appear to be those which carry a higher risk of Parkinson disease conversion [22]. Conversely there are a number of *GBA* gene variants which cause Gaucher disease only in combination with a 'severe' Gaucher disease allele. These variants have been suggested to be associated with Parkinson disease with marginal odd ratios [23,24]. Some of these individual alleles have been demonstrated with allele frequencies within the general population as high as 2% and up to 7% in idiopathic Parkinson disease

populations [16]. This makes *GBA* comfortably the most numerically significant genetic risk factor for Parkinson disease identified to date [25].

It appears that there are some clinical differences between the phenotype of GBA and idiopathic PD. Most prominently there is a striking cognitive phenotype which appears to be proportionate to the severity of the *GBA* mutation in question [26-30]. Interestingly *GBA* appears also to be a genetic risk factor for Lewy body dementia [31,32]. Some evidence suggests there is a more pronounced visuospatial deficit to this cognitive impairment [33]. Moreover age of onset of *GBA* Parkinson disease cases is approximately 4 years earlier and there appears to be a more symmetrical presentation with less evidence of unilateral tremor or rigidity [30]. Anecdotally there is evidence of more neuropsychiatric features and a faster disease progression, although there is a lack of high quality data to support these findings at present.

1.3 GBA and alpha synuclein

Alpha synuclein is a cystolic protein of unknown physiological function which is the substantive component of Lewy bodies, the pathological stigmata of Parkinson disease. There is compelling data to suggest a direct and reciprocal relationship between GCase activity and alpha synuclein. Biochemical inhibition of GCase activity with conduritol-B-epoxide (CBE) leads to an an increase in alpha synuclein levels [34]. In fibroblasts, mouse primary cultures, neural crest cells and induced pluripotent stem cells carrying *GBA* mutations, alpha synuclein is upregulated [35-37].

1.4 Putative pathogenic mechanisms of the contribution of GBA mutation's to Parkinson disease

The mechanism of the contribution of the mutant *GBA* gene to Parkinson disease is uncertain. A number of mechanisms have been proposed. Broadly these can be grouped into those which postulate that the loss on function of the catalytic activity of the GCase enzyme is the primary driver of disease and those which believe mutations lead to secondary biochemical consequences and Parkinson disease (gain of function).

1.5 Loss of function

There is evidence to suggest that dysfunction of GCase catalytic activity is associated with increased Parkinson's risk. Peripheral blood leucocyte GCase activity is reduced amongst idiopathic Parkinson disease patients and in the brains of idiopathic Parkinson disease subjects compared to controls [38,39]. Studies in cerebrospinal fluid of idiopathic Parkinson disease cases show lower GCase activity levels compared to controls [40].

That said there are major inconsistencies to this argument. In particular there is a relatively poor correlation between GCase activity levels and disease risk in Parkinson disease and indeed GD. For instance, one study showed that GCase activity from peripheral blood spots categorised by mutation did not correlate with the severity of those individual mutations in terms of Parkinson disease. *L444P* Parkinson disease cases for instance appear to have higher GCase activity than those with *N370S*, even though *L444P* mutations convey between 2-3 times the risk of Parkinson disease compared to *N370S* [30,38,41,42]. Equally heterozygous

carriers of the *84GG* mutation, which is a frameshift mutation and would be expected to be null in terms of GCase activity, had comparable enzyme activity with other missense *GBA* mutations [38].

It may be that this disparity is a reflection of the limitations of the GCase activity assay. Typically in leucocyte GCase is normalised to the protein concentration of the lysate produced and in cerebrospinal fluid there is no normalisation to protein concentration at all [43-45]. Differences in the expression levels of the mutant and wild type GCase protein (from the remaining non mutated allele) will substantially influence what is effectively an assay which measures the rate of substrate catalysis, yet to date there is no mechanism to normalise for GCase protein expression.

1.5a Substrate accumulation

Glycosylceramide accumulation has been demonstrated in both neuronopathic and non neuronopathic forms of Gaucher disease and has been shown to cause significant microglial activation in human brains and a number of mouse models in the former [46-48]. This mechanism (and central nervous system immune dysregulation more generally), has been postulated as a pathogenic mechanism is Parkinson disease [48-55], although of course it is highly non specific and could be caused by a wide variety of processes. Substrate accumulation has been suggested as a pathogenic mechanism of Parkinson disease in GCase mutation carriers [56]. To date substrate accumulation has not been demonstrated in Parkinson's brains, although one study did show a reduction in ceramide, the product of GCase catalysis [57,58].

1.5b Direct disposal of alpha synuclein by GCase

Nuclear magnetic resonance spectroscopy provides direct evidence of a pH dependent interaction between GCase and alpha synuclein [59-61]. Equally, as described previously, a reciprocal relationship has been reproducibly demonstrated between alpha synuclein levels and GCase activity [34,36]. Such a direct interaction implies a direct role of GCase in alpha synuclein breakdown.

Autophagic dysfunction is a well established paradigm within the field of neurodegeneration and in particular within Parkinson disease [62-65]. Chaperone mediated autophagy (CMA) dysfunction, by which transit of the substrate into the lysosome, aided by the a complex of the LAMP2A protein isoform and heat shock protein 70 (HSP 70), has been heavily implicated with Parkinson disease [66-68]. Interruption of this mechanism has been found in a variety of cell models as well as Parkinson disease brains. Alpha synuclein has been demonstrated to be degraded via CMA and some models additionally indicate direct inhibition of CMA by alpha synuclein [63,65,69,70]; in turn creating a vicious cycle of impaired CMA mediated disposal of the protein. It is tempting to speculate that a generalised interruption of physiological autophagic homeostasis - with GCase being a component of this pathway - may account for this association, however to date other lysosomal storage diseases have not been shown to be associated with Parkinson disease [71,72]. Further efforts to qualify the relationship between GCase and alpha synuclein are little more than speculative and have failed to reliably account for it.

1.6 Toxic gain of function

1.6a Endoplasmic reticulum GCase sequestration

Perhaps the most plausible hypothesis for mutant GCase mediated toxic gain of function comes from the lysosomal storage disease field. A series of elegant experiments has demonstrated that *GBA* mutations interrupt the physiological mechanism of post translational modification of the GCase protein [73,74]. This in turn results in a failure of trafficking of the protein from the endoplasmic reticulum. Consequently it not only may interrupt any putative interaction between alpha synuclein and GCase within the lysosome, but has been shown to result in an "unfolded protein response", whereby reactive oxygen species are produced in response to the sequestered protein, leading to cellular toxicity and ultimately death [75]. In terms of Gaucher disease, the degree of GCase sequestration has been shown to be a correlate of the clinical severity of the phenotype [76].

This hypothesis chimes with concurrent theories underlying the basis for the selective vulnerability of nigral neurons. Surmeier et al. have produced evidence to show that that the intracellular calcium homeostasis and specifically the rapid and characteristic oscillations of calcium which characterises "pacemaking" nigral neurons, is responsible for the overload of michondrial calcium buffering capacity [77]. Sequestration of protein within the ER has been shown to substantially upregulate calcium release [78] and hence provides a plausible explanation for the particular predilection of *GBA* mutations for the Parkinson disease phenotype.

1.6b Alpha synuclein aggregation dynamics and Impaired GCase

Alpha synuclein aggregation is thought to be pathogenic mechanism of neuronal death in Parkinson disease. In the native state alpha synuclein is monomeric. In the presence of a variety of factors such as oxidative stress, shaking, contact with lipid membranes and certain inorganic ions such as copper or iron, it defers to beta sheet rich fibrillar, oligomeric or aggregated forms [79-84]. It is these aggregated species that make up Lewy bodies. Monogenic forms of Parkinson disease caused by alpha synuclein mutations have been shown to have enhanced aggregation dynamics [85-88]. Morever increased cytosolic synuclein concentrations upregulate aggregation propensity [89,90]. Although the subject is controversial it is thought that oligomeric species are the predominant pathogenic form of the protein [91-96]. Moreover it appears that these aggregated species are able in the presence of monomeric synuclein, to cause it to defer to an aggregated form, as was shown initially in neuronal grafts transplanted into Parkinson disease cases which developed Lewy pathology [97]. These findings were subsequently replicated in a variety of models in which pre formed fibrils of alpha synuclein where injected into the brains of a variety of mammals [98-102].

To the knowledge of the author there has to date been little work looking at the direct effect of GCase or mutant GCase on alpha synuclein aggregation dynamics, short of the finding that alpha synuclein binds directly to the GCase active site [59]. It may be that an interruption of the GCase mediated physiological disposal of one or all of the synuclein species may increase aggregation propensity either by the failure to remove seeding fibrillary species or simply by increasing cystolic synuclein concentrations.

1.7 Toxic gain of function as a consequence of loss of function or loss of function as a consequence of toxic gain of function? chicken or egg?

There may of course be the potential for both loss of function and a toxic gain of function to be coexistent or perhaps more plausibly a product of one another. For instance any structural alteration to the GCase protein may give rise to gain in function but may incidentally reduce enzyme activity. Conversely a loss of enzyme activity may result downstream in an added gain of function as a result of disruption of the balance of substrate/product. As such the distinction between the two may well be no more than an exercise in semantics.

1.8 Understanding which GBA mutation carriers will convert to Parkinson disease

It is crucial that the distinction is made between *GBA* mutations, which (along with *LRRK2* mutations) are a genetic risk factor for Parkinson disease and other Mendelian forms of genetic Parkinson disease such as mutations in the alpha synuclein, *PINK* or *PARKIN* genes [25]. Crucially, on balance of probabilities, *GBA* mutations carriers are more likely **not** to develop Parkinson's [13,14,103]. The question of the variable penetrance of *GBA* Parkinson disease accordingly remains a major unanswered point in our understanding of Parkinson disease and is of particular interest because it mimics the inheritance of idiopathic Parkinson disease. More specifically, a family history of Parkinson disease is the single greatest risk factor for developing Parkinson disease, although only a small minority of cases develop Parkinson's in a Mendelian manner [25,104]. One can speculate that untangling the

factors which contribute to the conversion of *GBA* carriers to Parkinson's may also allow us to reveal those who will develop idiopathic Parkinson disease.

One aspect is of course the "potency" of the *GBA* mutations. There are to date over 300 Gaucher disease causing *GBA* mutations and many more polymorphisms, associated only with Gaucher disease in the conjunction only with a 'severe'/'neuronopathic' *GBA* allele [105,106]. It is now abundantly clear that so called severe Gaucher diseasecausing mutations are associated with a much greater risk of Parkinson disease than mild ones [22]. In the case of the most common mutations (*N370S* and *L444P*) it is even possible to quantify the risk individually, with each mutation respectively conveying an odds ratio of 3-4 of developing Parkinson disease [30,42] and 6-12 [30,41,42] respectively.

Even with this taken into account the cause of the variable penetrance of Parkinson's caused by *GBA* alleles remains unclear. The three most likely candidates would seem to be genetic, epigenetic and environmental cofactors [25], although to date a series of environmental exposures (such as smoking, NSAID exposure, coffee, outdoor lifestyle and head trauma [104]) have been implicated as protective or risk factors in Parkinson disease, none have been proven to be relevant in the context of *GBA* Parkinson disease, whilst evidence for specific genetic or epigenetic cofactors is scant.

1.9 Early detection of conversion in GBA Parkinson disease

It has been known for some years that a clinical prodrome which includes hyposmia, constipation, cognitive impairment and REM sleep disorder preceeds the onset of motor

Parkinson disease by up to 20 years [107-110]. Our own analyses of our longitudinal cohort has established some of these features are prominent amongst *GBA* carriers [111,112]. Equally genotyping of those with electrophysiologically proven REM sleep disorder dysfunction shows a higher prevalence of *GBA* mutation carriers compared to age matched controls [113]. It may be that by using a combination of genetic, clinical, biochemical and imaging biomarkers we are able to stratify the risk of developing Parkinson disease amongst *GBA* mutation carriers.

1.10 GCase targeted neuroprotection in Parkinson disease

Clearly the major draw of research looking at monogenetic risk factors for Parkinson's is that it offers the possibility of targeted neuroprotective interventions. It has been proposed that the GCase pathway is amenable to such modification through five predominant mechanisms.

1.10a Gene therapy

Gene therapy refers to the modification of specific genes within a subset of cells using a targeted vector such as a virus. Interest in gene therapy targeting the *GBA* gene has mostly been in the context of Gaucher disease and has been longstanding [114]. Of particular interest has been the realistic prospect of such therapy crossing the blood brain barrier and hence being a viable treatment for the neuronopathic form of the disease. Using invariant natural T killer cells it was shown in 2011 Gaucher fibroblasts could be transfected using a high-titer, amphotropic retroviral vector in which human *GBA*1 was driven by the mutant polyoma

virus enhancer/herpesvirus thymidine kinase gene promoter [115,116]. Unfortunately the clinical protocol that resulted achieved only a transfection efficiency of 1-10% which was insufficient to cause a clinically significant improvement in substrate levels [117]. Finding stable and safe means of efficient transfection remains the principle obstacle to the successful clinical application of this technology [118]. Using a murine *GBA* knockout model an intravenously injected lentiviral vector was shown to be able to deliver improved GCase activity, reduced substrate accumulation and improvements in a number of clinical outcomes [119], however, whether such outcomes can be replicated in human subjects is uncertain. In the context of Parkinson disease moreover it is unclear whether affected brain regions (e.g substantia nigra and striatum) could be reached by such vector technologies.

1.10b GCase replacement therapy

Direct supplementation of recombinant GCase enzyme has been a highly successful treatment in Gaucher disease and has extended the life expectancy of these patients by decades [120,121]. Systematically recombinant GCase has been shown to localise to the lysosome and upregulate enzyme activity. The limitation of this approach in the context of Parkinson disease is that GCase, as a 60 kd protein, is too large to cross the blood brain barrier in sufficient quantities to modify central nervous system GCase activity [122,123]: A variety approaches such as co therapy with pharmacological agents and inducing blood vessel inflammation have been suggested as mechanism to enhance central nervous system GCase uptake [124], although there is currently no evidence of their relevance to clinical practice. An alternative approach might be direct intrathecal administration of recombinant GCase [123,125]. A prototype for this approach exists in treatment of the lysosomal storage

disorders Hunter's and Hurler's diseases (Mucopolysaccharidosis type I and II) [126] although doubt remains about the ability of a intrathecally administered ERT to provide a sufficient concentration gradient to breach the parenchymal cells of the brain and hence penetrate neuronal tissues.

1.10c Substrate reduction

I have already discussed the paucity of evidence for the presence of substrate accumulation in Parkinson disease. None the less, there is significant interest in its use as a neuroprotective agent in Parkinson disease. This has primarily been driven by the finding that in synuclein overexpression cell lines GCase substrate inhibition appears to reduce alpha synuclein levels [56] Miglustat, a reversible inhibitor of glucosylceramide synthase has been used in the context of type 3 Gaucher disease, although concerns exist over the side effect profile and in particular the incidence of peripheral neuropathy [127-129]. A new agent (eliglustat) which also inhibits glucosylceramide synthase, is currently undergoing evaluation in clinical trials in Gaucher disease [130] and Parkinson disease [131].

1.10d Small molecular chaperones

Relying on the observation that mutant GCase is sequestered within the endoplasmic reticulum, small molecular chaperones act as molecular cofactors which aid physiological post translational folding and in turn, upregulate trafficking of mutant GCase to the lysosomal compartment of the cell [132-134]. Two types of chaperone exist, the prototype inhibitory chaperone (which binds to the active site of the GCase protein) and non inhibitory

chaperones, which bind to alternate parts of the structure yet are still able to modulate folding sufficiently to restore or partially restore post translational folding [135]. In both cases the change in the pH environment causes partial elution of the chaperone upon entry into the lysosomal compartment, although as we shall discuss later the degree of this elution is variable.

1.10e Inhibition of the proteosomal system

Misfolded GCase is removed from cytosol predominately by the proteosomal system. This mechanism is heavily reliant on heat shock protein 90, a chaperone which amongst a huge variety of other functions, removes misfolded GCase via the proteosomal system [136]. This occurs through the LAMP2A protein, which mediates recognition of defective proteins for translocation to the lysosome [137]. A mooted therapeutic strategy has been the interruption of the recognition of the GCase protein by the HSP 90 protein, in turn reducing the amount of GCase degraded via chaperone mediated autophagy (CMA) and increasing cytosolic concentrations of the protein [123]. Histone deacetylase inhibitors have been shown *in vitro* to reduce GCase degredation [136]. Given the wealth of evidence linking alpha synuclein to impaired degredation within the proteosomal system [137] it seems some what counterintuitive to impair this mechanism as a potential therapeutic strategy in Parkinson disease.

1.11 Outline of thesis

The focus of this thesis is to discern tools to construct and ascertain genetic, chemical, clinical and imaging biomarkers of conversion of Parkinson disease amongst *GBA* carriers. It will attempt to understand the basis for the variable phenotypic penetrance of *GBA* Parkinson disease and of the selective vulnerability of certain parts of the brain to *GBA*. Finally, I will detail the validation work and preliminary findings of clinical trial utilising a targeted neuroprotective strategy, namely small molecular chaperones of the GCase enzyme.

In **chapter 2** I will outline the basis of the genetic risk of Parkinson's caused by *GBA* alleles. There is already an established literature, based largely on genetic case control studies, which correlates the severity of the Gaucher phenotype of known *GBA* mutations and the risk of Parkinson disease. I develop this analysis further to attempt to quantify the disease risk of individual mutations, including the so called Parkinson disease associated Gaucher polymorphisms.

In **Chapter 3** I will present the prospective analysis of some 100 *GBA* mutations carriers without Parkinson disease for prodromal features of Parkinson disease. We will show globally that there is an increased prevalence of a number of these features and furthermore there is clustering of them amongst a 'high risk' group of patients who may be at increased risk of Parkinson disease.

In **Chapter 4** I will describe the development of rapsodi, an internet based platform for assessment of prodromal Parkinson disease features. The portal aims to increase the power of these analyses and, in turn, provide a means for the prediction of future Parkinson disease conversion. I will also outline preliminary validation data for the portal which will show its utility in terms of remotely assessing *GBA* carriers.

Chapter 5 will show work looking for prospective chemical biomarkers of Parkinson disease conversion amongst *GBA* carriers . It will also detail the results of PET imaging scans using the dopamine active transporter (DAT) and the PK11195 ligands, which provide preliminary evidence of nigral glial activation and inflammation amongst non Parkinson disease *GBA* carriers. Additionally I shall describe work carried out within the same cohort looking for urine and serum biomarkers, which implies a role for systemic inflammation in the pathogenesis of *GBA* Parkinson disease in addition to some more established neurodegenerative pathways.

Drawing heavily on the work of Mia Horowitz and James Surmeier, in **chapter 6** I will postulate a theoretical basis for both the incomplete penetrance of *GBA* Parkinson disease and the selective vulnerability of dopaminergic (and other) neuronal subtypes in chapter 3. I will suggest that the unfolded protein response brought about by mutant GCase sequestration gives rise to a chain of intracellular calcium evoked calcium release which overwhelms mitochondrial buffering capacity and ultimately leads to neuronal death. Unfortunately this work did not produce results which corroborate this hypothesis.

In **chapter 7** I shall outline the design and validation studies for the AiM PD trial, a phase II, open label, non placebo controlled clinical trial of the the inhibitory small molecular chaperone ambroxol amongst *GBA* and idiopathic Parkinson disease subjects. I shall detail work necessary to validate reproducibly the GCase activity assay in cerebrospinal fluid and blood leucocytes, assays to detect ambroxol in serum and cerebrospinal fluid and mass spectrometry assays to detect and quantify GCase and glucosylceramide in cerebrospinal fluid.

In **Chapter 8** I will describe the preliminary data from the Aim PD study. We will present blood GCase activity pre and post commencement of ambroxol and baseline cerebrospinal fluid GCase data. These data will show an upregulation of leucocyte GCase, supporting the putative action of ambroxol. The cerebrospinal fluid data will be discussed in terms of its relevance to prevailing debates and controversies within the field, with particular focus on the role of GCase activity in the pathogenesis of *GBA* Parkinson disease.

In **chapter 9** I shall conclude by suggesting that *GBA* Parkinson disease provides a prototype for the targeting of "bespoke" neuroprotection. I will suggest that using the presence of *GBA* mutation as a baseline screening assessment it may be possible to identify and treat high risk individuals with neuroprotective agents targeted at the GCase pathway. More broadly, given that an estimated 70% of the heritability of Parkinson disease remains unaccounted for, I shall suggest that such an approach may have wider applications to idiopathic Parkinson disease as a whole.

Chapter 2 - Characterising the mutation specific genetics of *GBA* Parkinson's

2.0 Introduction

The mutations spectrum within the *GBA* gene has been ably defined over the last two decades by research into the Gaucher disease. Over 300 Gaucher causing mutations have been defined and a crude measure of their potency has been produced on the basis of whether they have been described in subjects with neuronopathic forms of the disease [105,106]. The relevance of this classification has been highlighted by work which has revealed that 'severe' Gaucher causing mutations are collectively associated with an odds ratio of Parkinson's ≈ 16 as opposed to 'mild' mutations which are associated with an odds ratio ≈ 3 [22]. These data are based on genetic case control studies, in which an odds ratio and confidence intervals are constructed from the allele frequency of carriers of the mutation in question with and without Parkinson disease [138]. Moreover in a small cross sectional survey a significant majority of the Parkinson disease affected offspring of Gaucher patients carrying one severe and one mild mutations had a severe Gaucher disease causing mutation [139].

Conversely Gaucher associated polymorphisms, which cause Gaucher disease but only in conjunction with a severe disease causing allele, have been associated with Parkinson disease, although the subject is controversial. The two most prominent of these, *T369M* and *E326K* have been variously shown to be both pathogenic and non pathogenic in a number of studies [16,23,24]. These contradictory findings may be a reflection of the low odds

ratios of the effect size (which on the whole are within the range of 1-2) and which will accordingly require large sample sizes to reach the threshold for significance.

These rudimentary studies have established stark variability in the 'potency' of *GBA* mutations in terms of Parkinson disease. Such variation is of key importance as the penetrance of *GBA* Parkinson disease has collectively been estimated between 10-30% [13,14], but it becomes less perplexing if one infers that the type (and potency) of mutations that make up the cohorts upon which these estimates are based may vary substantially. Taking this line of argument to its logical end, it may be feasible to stratify the risk of development of Parkinson disease based on the specific individual mutations in question.

2.1 Methods

A full outline of the methods of this study is detailed in the appendices. (section 10.0).

In order to attempt to derive assessments of the risk of Parkinson disease associated with individual *GBA* mutations a comprehensive literature search was carried out using the following terms: "glucocerebrosidase" (or "*GBA*"), risk (or "odds ratio" or "OR" or "risk ratio" or "RR") and "Parkinson's" (or "Parkinson" or "Parkinson disease"). High quality case-control genetics studies were selected according to the following criteria:

- Estimated the odds ratio or risk ratio of developing Parkinson disease due to a *GBA* mutation
- Appropriately matched control groups

- *GBA* genotyping using a recognised and validated method that prevented amplification of the pseudogene *GBAP1* (either whole/partial gene Sanger sequencing or mutation/variant specific microarray screening)
- No duplication/sharing of datasets in studies included in the analysis

Articles were short listed in November 2016 on the basis of abstracts and rejected/selected following review of the full text. The selected articles were supplemented by articles identified by reviewing the references of established meta-analyses [22,30,42,140,141] or from the private databases of the authors (SM and AHVS). A flow diagram of the selection process is shown in Fig. 1 and a complete list of studies from which data was taken is available in the appendix (sup. table 1)

Each study was individually reviewed by a single reviewer (SM) and variant alleles detected amongst the case and control groups were recorded. Any variant detected in two or more separate studies was included in the final analysis. Where applicable, the microarray design was reviewed and if unable to differentiate between individual mutations which also appear as part of a haplotype (*e.g. L444P* and *L444P*;*A456P*;V460V), the study was excluded from relevant analyses. The total number of cases and controls from all studies in which genotyping covered the variant in question (*i.e.* full exon Sanger sequencing, partial exon Sanger sequencing covering region of variant, or variant specific microarray screening) was calculated as were the total number of case and control subjects who were mutation/variant carriers.

We initially carried out meta-analysis to determine the risk associated with developing

Parkinson disease for each mutation. A fixed effects model was employed in all cases to calculate an OR of the risk of developing Parkinson disease. A pooled OR was calculated using the Mantel-Haenszel test [142]. Homogeneity of the sample was assessed using Woolf's test for heterogeneity [143]. To assess for publication bias we carried out Begg's test [144].

We then carried out further joint analyses, one which used the pooled count data for that mutation and a second where this dataset was augmented with ethnically matched control count data derived from the The Exome Aggregation Consortium (ExAc) database (ExAc.broadinstitute.org) [145,146]. Where mutations/variants appeared to be specific to one ethnicity we excluded all studies not drawn from that ethnicity for the joint analysis (full details in individual mutations section within appendicies) . We then used Firth logistic regression (which has been shown to minimise type 1 errors in both balanced and unbalanced case-control datasets) to calculate the risk of Parkinson disease associated in these amalgamated datasets [147]. In all cases we applied a Holm-Bonferroni correction for multiple comparisons [148]. The details of the exact methods used for each mutation are shown in the supplementary materials (section 10.0).

Selection of articles, compilation of count data and primary data analysis was carried out by myself. Dr Steven Lubbe advised on aspects of data analysis.

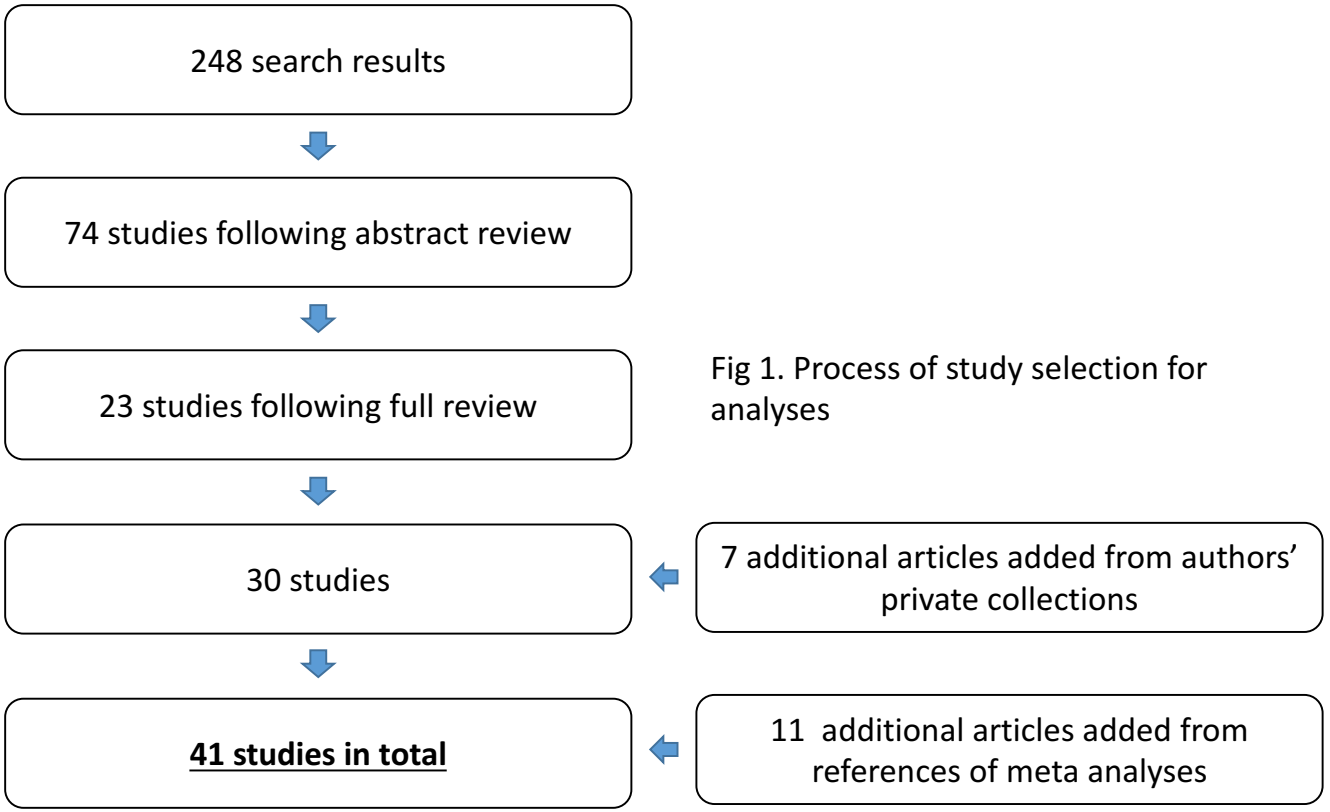

Fig 1. Process of study selection for analyses

2.2 Results

A more detailed summary of the findings for each individual mutations are detailed in the appendices together with forest plots and Begg plots (section 10.0). A breakdown allele frequency/counts by ethnicity is shown in Table 1. Summary effect sizes of significant mutations are shown in Fig 2.

2.2a Major variations in mutation composition with ethnicity

Its has been previously reported that *N370S* is almost exclusively found amongst Caucasian and Ashkenazi cohorts and this was indeed replicated in our study [41,42,149]. Disproportionally the severe Gaucher causing mutations *R120W*, *L444P* and *RecNcil* (a haplotype combining *L444P*, *A456P* and the silent mutant V460V) were found amongst East Asian populations. This may provide an explanation for the consistently high odds ratios encountered in meta analyses of the effect sizes of *GBA* mutations amongst these populations [41] *R463C*, *E326K* and *T369M* were almost exclusively found amongst Caucasian populations while *84GG* was disproportionately found amongst Ashkenazi (and to a lesser extent east Asian) populations.

We chose the ethnic classifications of the cohort on the basis of definitions used in the ExaC database, however, it was clear that within these regions (Caucasian, Hispanic, African, East Asian) substantial country by country variation also exists. One hundred percent of *H255Q* mutations were found amongst the two Greek cohorts whilst 24/28 *R120W* mutations were from the two Japanese cohorts included in the study.

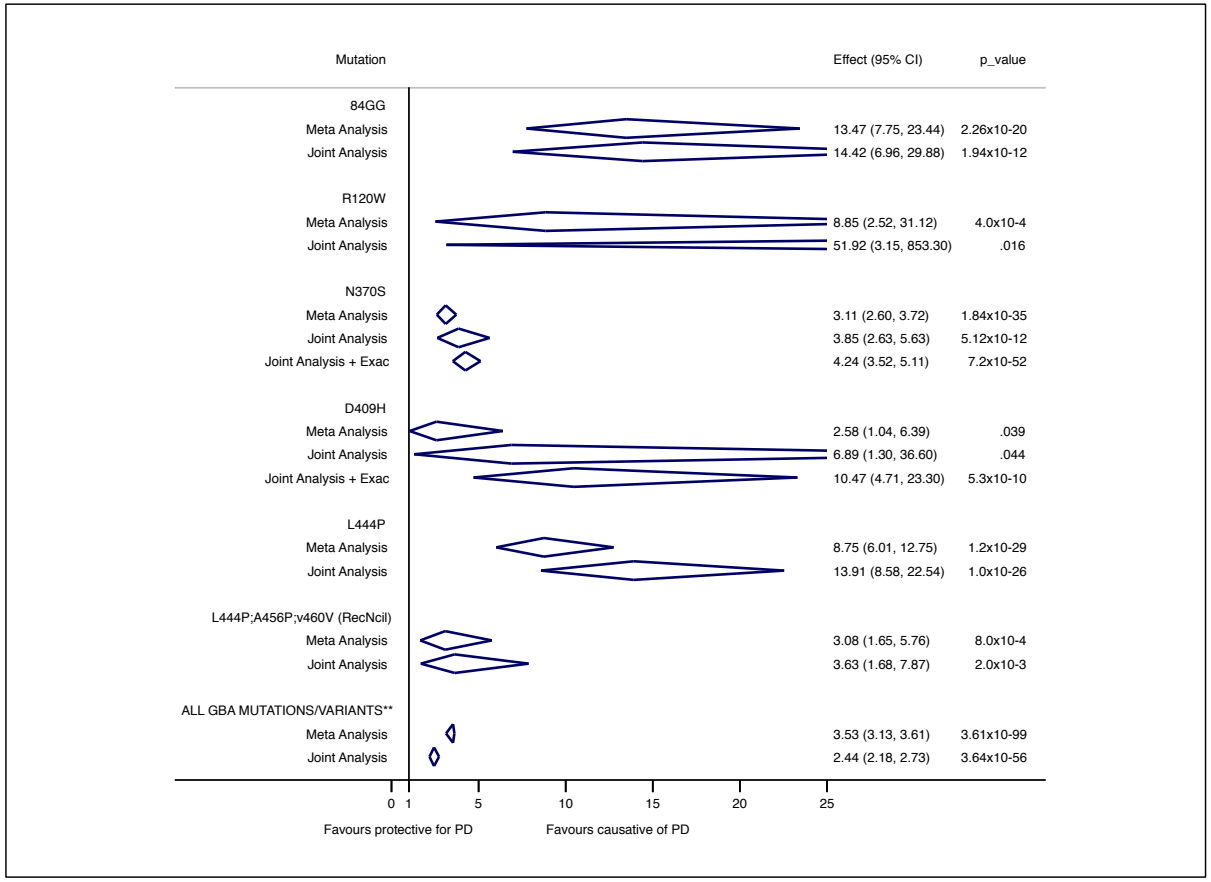

Fig 2. Effect size (OR) with 95% CI of PD risk associated with 84GG, R120W, N370S, D409H, L444P and L444P;A456P:V460V (RecNcil) and all GD causing mutations. ** all GBA mutations estimate is significantly heterogenous. It is displayed for illustrative comparative purposes and should not be considered a reliable risk estimate (see text for details)

Table 1. Distribution of Mutation/Variant count data by ethnicity

	Caucasian n Parkinson disease(%)/ n CTL (%)	**East Asian n Parkinson disease(%)/ n CTL (%)**	**Hispanic n Parkinson disease(%)/ n CTL (%)**	**North African n Parkinson disease(%)/ n CTL (%)**	**Ashkenazi n Parkinson disease (%)/ n CTL (%)**	**Total n Parkinson disease/n CTL**
84GG	0(0.0)/0(0.0)*	8(21.0)/1(10.0)	-	0(0.0)/0(0.0)	30(79.0)/9(90.0)*	38/10
R120W	3(10.7)/0(0.0)	25(89.3)/0(0.0)	-	0(0.0)/0(0.0)	0(0.0)/ 0(0.0)	28/0
H255Q	8 (100.0)/ 0(0.0)	0 (0.0)/ 0(0.0)	-	0(0.0)/0(0.0)	-	8/0
H255Q;D409H	12(100.0)/3(100.0)	0(0.0)/0(0.0)	-	0(0.0)/0(0.0)	-	12/3
E326K	165(98.8)/76(98.8)*	1(0.6)/0(0.0)	-	1(0.6)/1(1.2)	-	167/77
T369M	75(96.7)/23(95.8)*	1(0.0)/0(0.0)	-	2(3.3)/1(4.2)	-	78/24
N370S	179(48.8)/28(7.8)*	6(1.6)/2(0.6)	2(0.5)/1/(0.3)	2(0.5)/0(0)	178(48.5)/320(91.1)*	367/351
D409H	8 (57.1)/0(0.0)	6 (42.9)/0(0.0)	-	0(0.0)/0(0.0)	0 (0.0)/0(0.0)*	14/0
L444P	173()/12()*	104(34.3)/5(15.7)	21(4.1)/0(0.0)	2(0.9)/0(0.0)	5(1.8)/4(21.1)*	305/21
***L444P;A456P*; V460V(*RecNcil*)**	15(33.3)/1/(14.2)	27(60.0)/6(85.7)	1(2.2)/0(0.0)	2(4.4)/0(0.0)	-	45/7
R463C	11(100.0)/0(0.0)	0(0.0)/0(0.0)	0(0.0)/0(0.0)	0(0.0)/0(0.0)	-	11/0

CTL- control, n – number of samples, Parkinson disease – Parkinson disease *. Excludes Alcalay et al. As distribution of mutations within Ashekenazi/non Ashkenazi subjects unclear

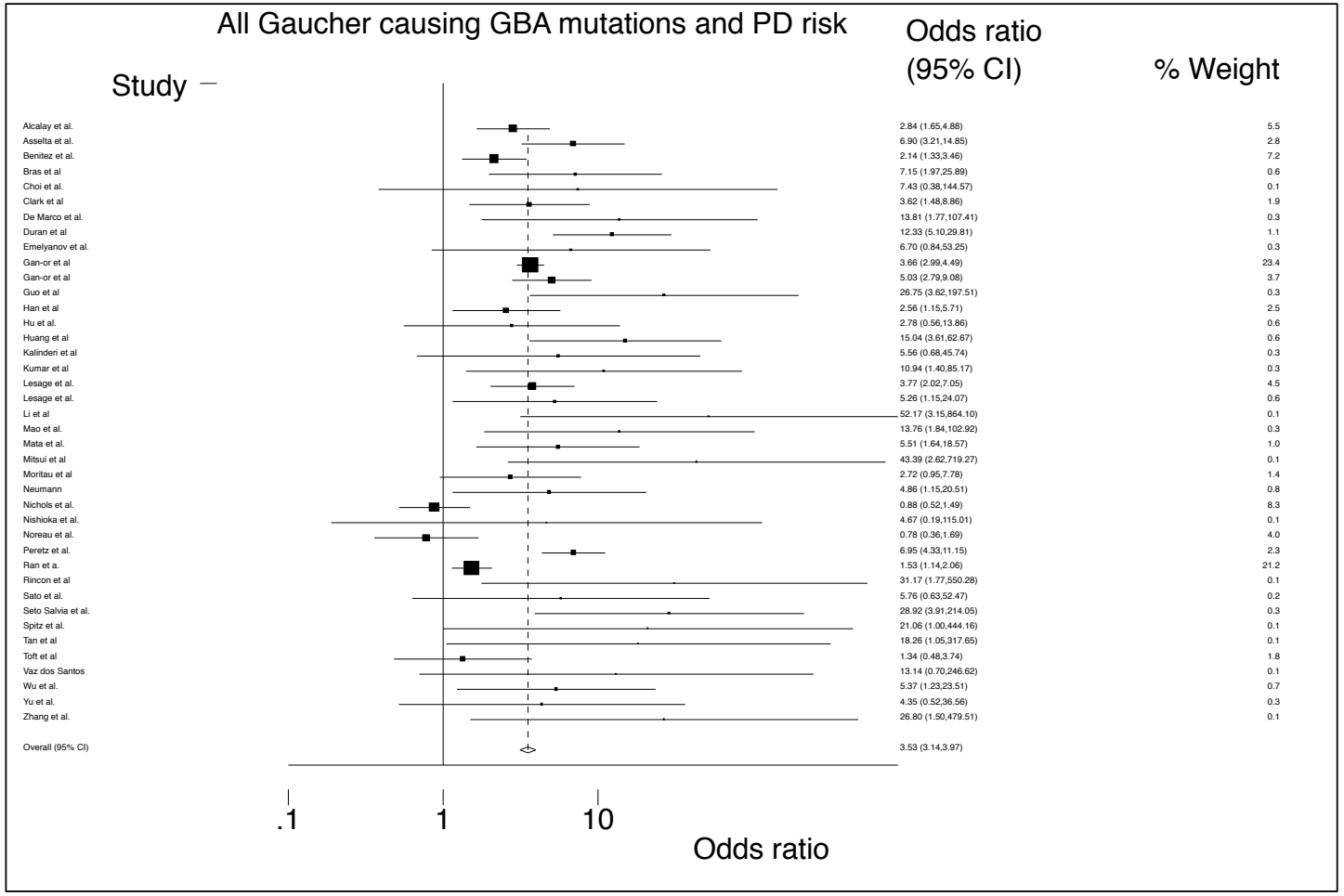

Fig. 3. Forest plot of risk of PD (with 95%CI) associated with all GD causing mutations. Please note sample significantly heterogenous and is displayed for illustrative comparative purposes and should not be considered a reliable risk estimate (see text for details)

2.2b Wide variations exist amongst the odds ratios of Parkinson disease risk amongst individual Gaucher causing mutations

Fig. 2 shows the odds ratios of all those Gaucher disease causing mutations found to be causative of Parkinson disease in all analyses undertaken. Reassuringly there is substantial concordance between the estimates obtained for *N370S*, *L444P* and all *GBA* variants in the analysis and those derived from established meta analyses [30,41,42]. Forest ands Begg plots of these two mutations and all Gaucher disease causing mutations are available in the appendices (Supplementary Fig 1,2 & 6, section 10.0). The latter is however of dubious significance because the heterogeneity test failed to confirm the sample was homogenous (I^2=71.1 p=1.6x10^{-12}), suggesting that the constituent studies that make up the estimate are not sufficiently similar in terms of their findings to be able to derive an accurate estimate of the cumulative effect size. The forest plot of the meta analysis is shown in Fig 3. This has been an issue which has been encountered previously in this context [30] (i.e meta analyses of *GBA* mutations) and highlights the difficulty of deriving risk estimates cumulatively from mutations with substantially different odds ratios associated with them.

Amongst the highest odds ratios derived are those derived from the *84GG* mutation (sup. Figures 3 & 7, section 10.0), a severe frameshift caused by a Guanine duplication at position 84 of the DNA sequence [150]. This gives rise to a null protein with an entirely distinct protein sequence compared to wild type. It is unclear whether this provides evidence that GCase activity is the presiding mechanism of pathogenicity or whether there is broader disruption of the GCase structure leading a secondary loss/gain of function.

RecNcil (supp. figures 3 & 6, section 10.0) is a complex haplotype comprising substitutions at *L444P*, *A456P* and the silent mutation V460V. In common with *L444P* it gives rise to a severe neuronopathic Gaucher disease phenotype, although in both the joint and meta analyses undertaken the odds ratio of the haplotype was significantly lower than the *L444P* mutation in isolation. This result is puzzling and implies that the additional structural modifications produced by these three mutations may lessen the pathogenicity of the *L444P* mutation. There are precedents for such a reduction in pathogenicity. The RecTL mutation, a haplotype of *L444P*, *A456P*, V460V and *D409H* has been described as having a significantly milder clinical Gaucher disease phenotype than either the *L444P* or *D409H* mutations in isolation, both of which are severe neuronopathic mutations [151].

The odds ratios and confidence intervals for all those mutations which failed consistently across all analyses undertaken to reach significance are shown in sup. Fig 1.

2.2c The E326K polymorphism is a genetic risk factor for Parkinson disease, however T369M is not.

In all three analyses we were able to demonstrate the *E326K* polymorphism (supp. figures 4 and 7, section 10.0) as a genetic risk factor for Parkinson disease. To our knowledge is the first time this has been shown. Conversely, in contrast to a recent meta-analysis [24], our analyses of *T369M* (sup. figures 4 and 7, section 10.0) did not (although trends were demonstrated across all analyses and the meta analysis narrowly

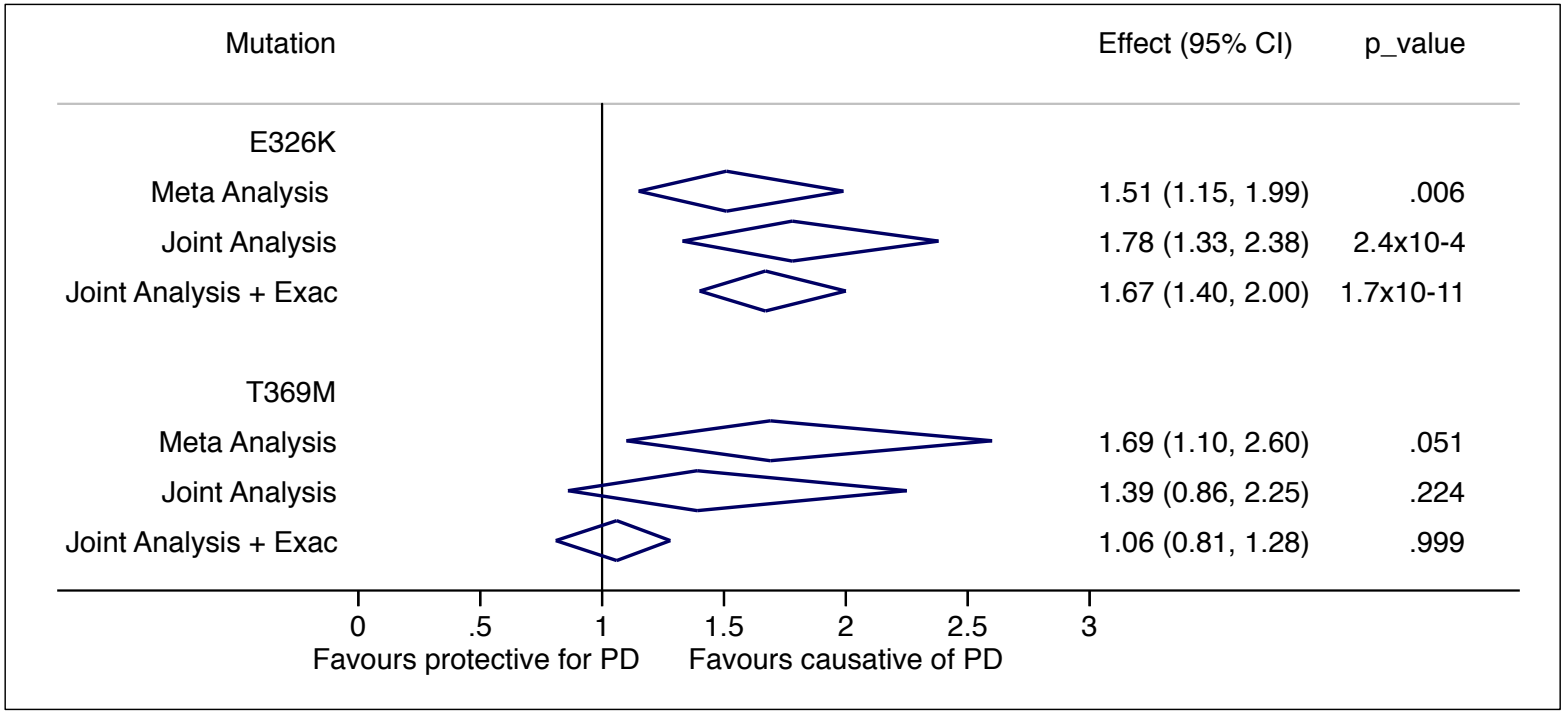

Fig 4. Effect size (OR) with 95% CI of PD risk associated with E326K and T369M variants

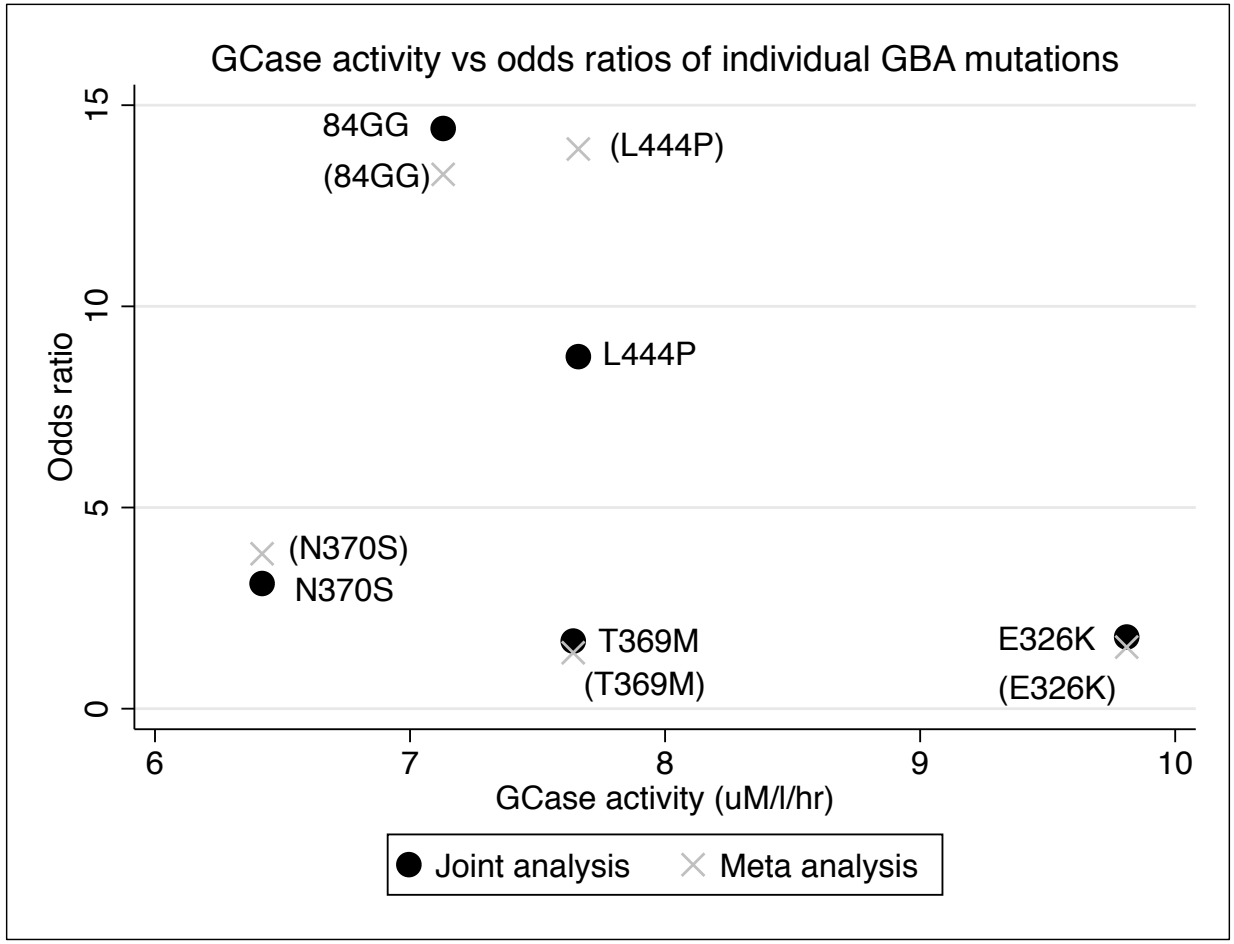

Fig. 5. Blood leucocyte GCase activity (Alcalay et al. 2016) plotted against the odds ratios of individual GBA mutations)

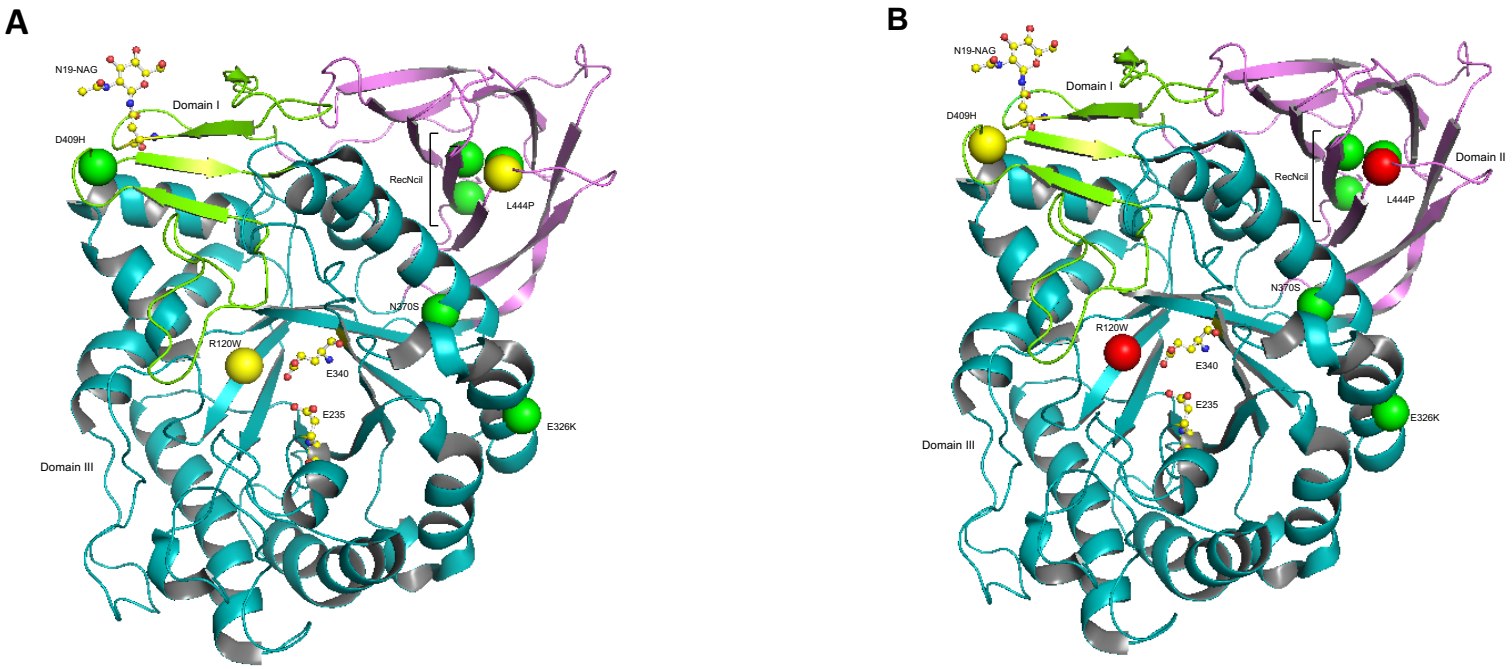

Fig 6. The X-ray structure of glucocerebrosidase (PDB code 3GXI). Domain I is shown in green. The glycosylation site at N19 is shown as a ball-and-stick model. Domain II is shown in pink. Domain III, the catalytic domain, is shown in blue and contains the active-site residues E253 and E340 which are shown as ball-and-stick models. The six significant glucocerebrosidase mutations (R120W, L444P, E326K, N370S, D409H and RecNcil) are shown with spheres. The colour of the spheres corresponds with the odds ratio associated with the mutation: green (<5); yellow (5-10) and red (10<) from the meta analyses **(A)** and joint analyses **(B)**.

missed significance (p=0.051) following correction for multiple comparisons. This may be because the aforementioned meta analysis contained unpublished data to which we did not have access. Effect sizes of these two mutations/variants are shown in Fig 4.

2.2d No clear structural correlations with the odds ratios of individual GBA mutations or with GCase activity in peripheral blood.

We explored whether our results could be used to provide insights into the mode of pathogenicity of the GCase protein by comparing these odds ratios with measured peripheral blood GCase activity in *GBA* Parkinson disease heterozygotes [38] (Fig 5). We also mapped the mutations on the crystal structure of the GCase protein [152,153] to crudely understand whether any commonalities exist between the structural locations/disruptions caused by individual mutations and their severity (Fig 6). In both cases were were unable show a clear pattern/correlation between the scale of the odds ratio and the parameter is question.

It may be that these approaches are too rudimentary to tackle adequately this question. As discussed previously there is enormous variation in peripheral blood GCase activity, even between subjects with the same mutation. It is also unclear whether peripheral blood GCase activity is an adequate reflection of central nervous system activity, (although experiments carried out in **chapter 5** on Parkinson disease leucocytes and cerebrospinal fluid do provide some clarity on this point). In heterozygotes the expression levels and relative activity of GCase derived from the remaining wildtype allele have a substantial impact. That said, it is revealing that in a relatively substantial sample of 40 *N370S* and 8 *L444P* carriers *N370S*

activity is lower than that of *L444P* even though the odds ratio is 3-4 times greater in the latter [38].

In terms of the structural characterisation of these mutations, this model is of course static and so gives only a broad indication of the modification produced . It may be that these mutations give rise to common or dynamic structural modifications which are beyond the scope of this approach. Of these mutations, only *N370S* has had it's crystal structure described [154]. The structure of wild-type and mutant GCase are virtually indistinguishable at both acidic and neutral pH, however *N370S* GCase was more stable at neutral pH in both analyses supporting the hypothesis that in *N370S* mutant protein the pH optima shifts from 4.5 to 6.4 [155]. Analysis of both the x-ray structure [154] and molecular dynamic simulations [156] suggest that the biggest change is the orientation of loop 3. At neutral pH loop 3 adopts an extended conformation which transitions to a helical conformation in acidic conditions for catalysis. However, just one conformation for loop 3 is observed in *N370S* GCase, presenting only in the extended conformation across the pH range [154,156] again providing evidence that the Asn 370 residue is important in stabilising the helical turn of loop 3. This, it is suggested, results in a rigid structure, potentially reducing substrate binding, access to the active site and catalytic dyad integrity.

In terms of the other mutations analysed, a number of mechanisms for structural dysfunction can and have been postulated, although it is hard to identify a common theme relating them to the pathogenicity identified. *R120W* for instance (which lies immediately adjacent to the active site – Fig 6) may directly reduce enzyme kinetics [157]. The Arg120 residue has a crucial role in the stability and polarity of the cavity of the active site of the

enzyme and through the guanidine center supports an array of hydrogen bonds with Asp 282, Asn 234, Ser 177 and a salt bridge with 340. This role is dramatically subverted by the replacement of the bulky hydrophobic structure of the tryptophan. Other mutations may more drastically interfere with the protein structure leading to sequestration. The replacement of L444 by a Pro, just at the edge of two beta strands is likely to likely perturb the kinetics of formation of the hydrogen bonds between the main chains of Asp 445 and Leu 461. It has been shown that this proline substitution causes rigidity in the protein backbone, disrupting the hydrophobicity of domain II and in turn improper domain folding and impaired enzyme function [158], Likewise, *D409H* causes a destabilised protein through prevention of proper hydrogen bond networks [158]. For *E326K* the kinetics of protein folding and stability of the tertiary structure should be expected to be disrupted by the replacement of Glu 326 by a Lys. The Glu 326, in fact, is engaged in the formation of highly stabilizing bonds with the guanidine group of Arg 329. A Lys in position 326 introduces a repulsive force toward Arg 329 thus generating a negative tension on the polypeptide which disfavors the helix formation.

2.3 The principle of quantifiable risk stratification of individual GBA mutation for Parkinson disease risk is feasible and realistic

The analyses carried out here show that is possible on the basis of existing case control data to quantify the risk of Parkinson's associated with individual *GBA* mutations. The stark variation in risk associated with each mutation is emphasised. Some are more useful than others. The broad confidence intervals of a number of the estimates are a reflection of the relatively small numbers of individuals with some of the less common mutations, however

the example of *E326K* shows, quantification is feasible even in the case of comparatively weak mutations when the mutation is sufficiently common.

This approach may be able to provide precise estimates (i.e odds ratios with narrow confidence intervals) for the more common mutations. For *RecNcil* for instance a power calculation (Firth logistic regression [147] and assuming equal Parkinson disease and control groups) shows that to produce an odds ratio with confidence intervals with a range of 3.0 would require a sample of ≈100,000 Parkinson disease cases which although ambitious is a plausible cohort size across a number of centres nationally or internationally. Conversely equivalent estimates are probably unrealistic in the case of less common mutations such as *D409H*, where the same calculation estimates a sample size of 30 million Parkinson disease cases. That said the scale of these estimates will still be useful in stratification of Parkinson disease risk even if they are crude and unsuitable for genetic counselling. For instance it is clear that *84GG* is associated with a very high Parkinson disease risk even if exact quantification is hindered by the scale of the confidence intervals. This information could be used as a flag for 'enhanced scrutiny and screening' for prodromal Parkinson disease signs in carriers. Finally, in the case of very rare variants in the *GBA* gene, larger cohort sizes would allow confirmation or refutation of pathogenicity and decision making as to whether screening for prodromal Parkinson disease signs is necessary.

2.4 Concluding remarks

These data provide considerable information as to the ethnic variability of *GBA* mutants, the widespread disparity of Parkinson disease risk associated with them and in some cases

precise quantification of these risks. They give an invaluable insight as to how a future screening strategy for *GBA* variants, in order to select subjects for early neuroprotection, might operate and are an indication of its potential utility.

Chapter 3 - Prodromal Parkinson disease features amongst *GBA* carriers as a tool for stratification of Parkinson disease conversion

3.0 Introduction

GBA is distinct from the Mendelian forms of genetic Parkinson's which preceeded it in that has an autosomal dominant inheritance. It has an incomplete penetrance of between 10-30% [11,13,14]. This figure is calculated on the basis of all *GBA* mutations with all the limitations discussed previously which accompany this approach. None the less, it is clear that *GBA* carriers are substantially more likely **not** to develop Parkinson's. The estimates quoted above refer only to Gaucher causing mutations and do not take into account polymorphisms such as *E326K* and *T369M*. On the basis of the approximate odds ratios calculated in the previous chapter and estimated Parkinson's prevalence at age 80 [159] (which produces the highest estimate of this figure) this would mean that between 1.9-3.9% of carriers of the *E326K* mutations will develop Parkinson disease assuming they lived to age 80. In this case, given an allele frequency of 0.02 (2%) in western European populations [159], blanket administration of a neuroprotective agent would be at best uneconomical and at worst potentially dangerous depending on the side effect profile of the compound in question.

The clinical prodrome of Parkinson disease includes constipation [104,107], hyposmia [160], anxiety , depression [160], rapid eye movement sleep disorder [161]). These features are postulated to correlate with the spread of alpha synuclein from the enteric nervous system (constipation) to various autonomic ganglions, the vagus nerve, midbrain (dysautonomia and other motor features), olfactory bulb (hyposmia) and eventually the cortex and

neocortex (cognitive impairment, anxiety and depression), mimicking the pattern of lewy pathology development postulated by Braak [162].The neuroanatomical correlates of REM sleep disorder are unclear although it seems likely to invlove a variety of brainstem (predominately pontine) structures [163].

The difficulty in terms of broader screening strategies for Parkinson disease is that these symptoms are common amongst the general population. All age self reported rates of constipation are estimated to be as high as ≈ 40% in some studies whilst those with clinically diagnostic features of constipation number some 15% [164]. From the age of 30 onwards 20-30% of subjects have been shown to have clinically defined hyposmia with a similar number being defined as anosmic from the age of 50 [165]. Mild cognitive impairment has been reported as high as 28% amongst over 60s and 39% in over 70s.[166] Up to 7% [167] and 17% of the population respectively have been reported to have anxiety disorder or a diagnosis of depression in western Europe and the United States. REM sleep disorder is an exception to this, because true electrophysiologically proven REM sleep disorder is present amongst ≈0.5% of the population (and these studies were carried out in elderly populations) [168], although all age prevalence of so called subclinical REM sleep disorder (i.e reported predominately on the basis of validated questionnaires without electrophysiological confirmation) may be as high as 5% [168].

The possibility of using a tandem population based screening for *GBA* mutation carriers (and then assessing for prodromal features of Parkinson disease) as a means to target neuroprotective therapies is attractive, as it can be presumed to substantially increase the specificity of the approach. This would in turn avoid unwarranted expense and side effects.

As such, we carried out a five year extended follow up of *GBA* mutation carriers, assessing them for prodromal Parkinson disease features and comparing them with a control group.

3.1 Methods

A more detailed summary of the assessment and analysis procedure is included in the appendices (section 10.2).

Briefly 117 (35 controls, 39 heterozygote *GBA* carrier and 43 biallelic *GBA* carriers) were assessed over a 5 year period at three timepoints for prodromal Parkinson disease features. Hyposmia, cognitive impairment, depression, REM sleep disorder, autonomic features, motor symptoms and signs of Parkinson disease were assessed respectively using the University of Pennsylvania smell identification test (UPSIT) [169], the Montreal cognitive assessment (MoCa) [170], the Beck depression inventory (BDI) [171], the Rapid eye movement sleep behaviour disorder questionnaire (RBDSQ) [172], a subscale of the unified multi system atrophy rating scale (UMSARS) [173] and the unified Parkinson disease rating scale parts II and III. For the latter we performed comparisons of assessments between assessors to minimise inter assessor variability and found minimal varance (range 0-4 points, section 1.2c Appendices). We compensated for the effect of missing data using multiple imputation [174] (details Appendices section 10.3b). The demographics of the study groups together with significance testing of differences in the three study groups (Mann-Whitney U test for het/bia/ctl or Fishers exact test for *GBA*/ctl) are shown in table 1. SM collected data for the 2014/15 (75%) in conjunction with Dr Michelle Beavan (25%). Analysis was carried out by SM.

Table 1. Demographic and significance testing amongst participants			
	baseline	**timepoint 1**	**timepoint 2**
control median age	61	59	59
bia median age	51	52	52.5
het median age	60	63	61.5
Significance level	**P=0.002**	**p=0.017**	**p=0.031**
***GBA* median age**	55	56	56
Significance level (vs ctl)	p=0.142	p=0.505	p=0.748
ctl % male (n)	47	57	56
bia % male (n)	58	61	55
het % male (n)	45	40	35
Significance level	p=0.537	p=0.282	p=0.221
***GBA* % male (n)**	51	50	49
Significance level (vs ctl)	p=0.396	p=0.404	p=0.350
ctl % Fhx Parkinson disease/dementia (n)	6	8	11
bia % Fhx Parkinson disease/dementia (n)	23	21	22
het % Fhx Parkinson disease/dementia (n)	10	15	19
Significance level	p=0.062	p=0.308	p=0.315
***GBA* % Fhx Parkinson disease/dementia (n)**	17	17	22
Significance level (vs ctl)	p=0.084	p=0.253	p=0.226
ctl % university educated (n)	68	63	74
bia % university educated (n)	48	49	43
het % university educated (n)	50	53	50
Significance level (vs ctl)	p=0.247	p=0.625	p=0.100

***GBA* % university educated (n)**	49	50	48
Significance level (vs ctl)	p=0.075	p=0.199	**p=0.030**
ctl % smoker (n)	31	33	42
bia % smoker (n)	30	29	29
het % smoker (n)	36	33	42
Significance level	p=0.851	0.904	p=0.459
***GBA* % smoker (n)**	27	31	34
Significance level (vs ctl)	p=0.527	p=0.510	p=0.361

Table 2. Summary table of results

Comparison of prevalence of Parkinson disease prodromal features all *GBA* carriers vs controls	
baseline (2010/11)	**p value, OR [95%CI]**
UPSIT	**p=0.003, 4.0 [1.6-10.4]**
MOCA	**p<0.001, 6.0 [2.3-15.2]**
timepoint 1 (2012/13)	**p value, OR [95%CI]**
UPSIT	**p<0.001, 7.6 [2.7-21.8]**
MOCA	**p=0.002, 7.3 [2.1-24.9]**
timepoint 2 (2014/15)	**p value, OR [95%CI]**
UPSIT	**p=0.002, 6.8 [2.0-23.1]**
MOCA	**p=0.024, 4.0 [1.2-13.6]**
BDI	**p=0.029, 10.6 [1.3-90.0]**
Repeated measures model for prodromal Parkinson disease features in *GBA* carriers vs controls	
	p value, OR [95%CI]
UPSIT	**p=0.006, 5.0 [1.6-16.1]**
MOCA	**p=0.007, 5.7 [1.5-20.0]**
BDI	p=0.158, 2.3 [0.7 - 7.4]
RBDSQ	p=0.120, 3.2 [0.7-13.4]
Correlation of prodromal feature risk scores with UPSIT risk score in all *GBA* carriers	
	p value, OR [95%CI]
MOCA	**p=0.033, 1.5 [1.03-2.3]**
BDI	**p=0.030, 1.3 [1.02-1.8]**

3.2 Results

A summary table of results are presented in Table 2. A more detailed presentation of descriptive statistics and analyses undertaken is presented in supplementary tables 3 and 4 (section 10.2),

3.2a Hyposmia and cognition are globally worse amongst heterozygous and bi-allelic GBA mutation carriers compared to controls.

At all three timepoints for *GBA* mutation carriers compared to controls, UPSIT and MOCA scores were worse (UPSIT baseline OR 4.0 p=0.003, timepoint 1 OR 7.6 p<0.001, timepoint 2 OR 6.8 p=0.002, MOCA baseline OR 6.0 p<0.001, timepoint 1 OR 7.3 p=0.002, timepoint 2 OR 4.0 p=0.024). Subset analyses showed that for the UPSIT both bi-allelic (baseline OR 4.2 p=0.006, timepoint 1 OR 6.3 p=0.002 and timepoint 2 OR 6.8 p=0.005) and heterozygous groups (baseline OR 4.3 p=0.011, timepoint 1 OR 9.0 p<0.001, timepoint 2 OR 7.2 p=0.004) also had worse scores at all timepoints. MOCA scores were worse amongst bi allelic and heterozygous groups at baseline (bia OR 5.0 p=0.003, het OR 6.8 p<0.001) and at timepoint 3 for the bi-allelic group (OR 5.9 p=0.011). Strong trends were exhibited at timepoint 2 for both bi-allelic (p=0.069) and heterozygous groups (p=0.072). BDI scores were significantly worse at timepoint 2 only (OR 10.6 p=0.029) which was mirrored in subset analysis in the biallelic group (OR 6.3 p<0.001) but not the heterozygous groups (p=0.069). There were no significant differences cross sectionally for RBDSQ scores.

Although there were clear trends showing worse autonomic dysfunction, REM sleep disorder, and UPDRS II and III scores in *GBA* mutation carriers compared to controls (see Figures 1 and 2), these only reached statistical significance in the case of UPDRS III at timepoint 2 (p=0.020), UPDRS II at timepoint 3 (p=0.022) and UMSARS at baseline (p=0.040) with some subset analyses in bi allelic and heterozygous groups mirroring these finding. (see supplementary Table 4 for further details).

Deterioration of UPSIT and MOCA was worse amongst the combined group of *GBA* carriers compared to controls with the steepest deterioration seen for UPSIT (OR 21.3 p<0.001) then MOCA (OR 5.7 p=0.007). This was replicated amongst both bi-allelic and heterozygous carriers compared to controls (supplementry Table 2). Although trends were exhibited there was no significant difference in the rate of decline of RBDSQ (p= 0.120) or BDI scores (p=0.158) compared to controls (supp. Table 4).

3.2b 'High risk' GBA mutation carriers develop a combination of impaired cognition, hyposmia and depression

We hypothesized the existence of a high-risk group with accelerated progression of multiple premotor features. To do so we produced a novel system of risk scoring which attached equivalent weight to both the extent of the deficit and its rate of decline. Briefly over the three assessment timepoints participants were scored 1 point for each half standard deviation the average score was below the trimmed mean of the combined *GBA* carrier group (max. 4 points) and 1 point for every half standard deviation reduction in scores from

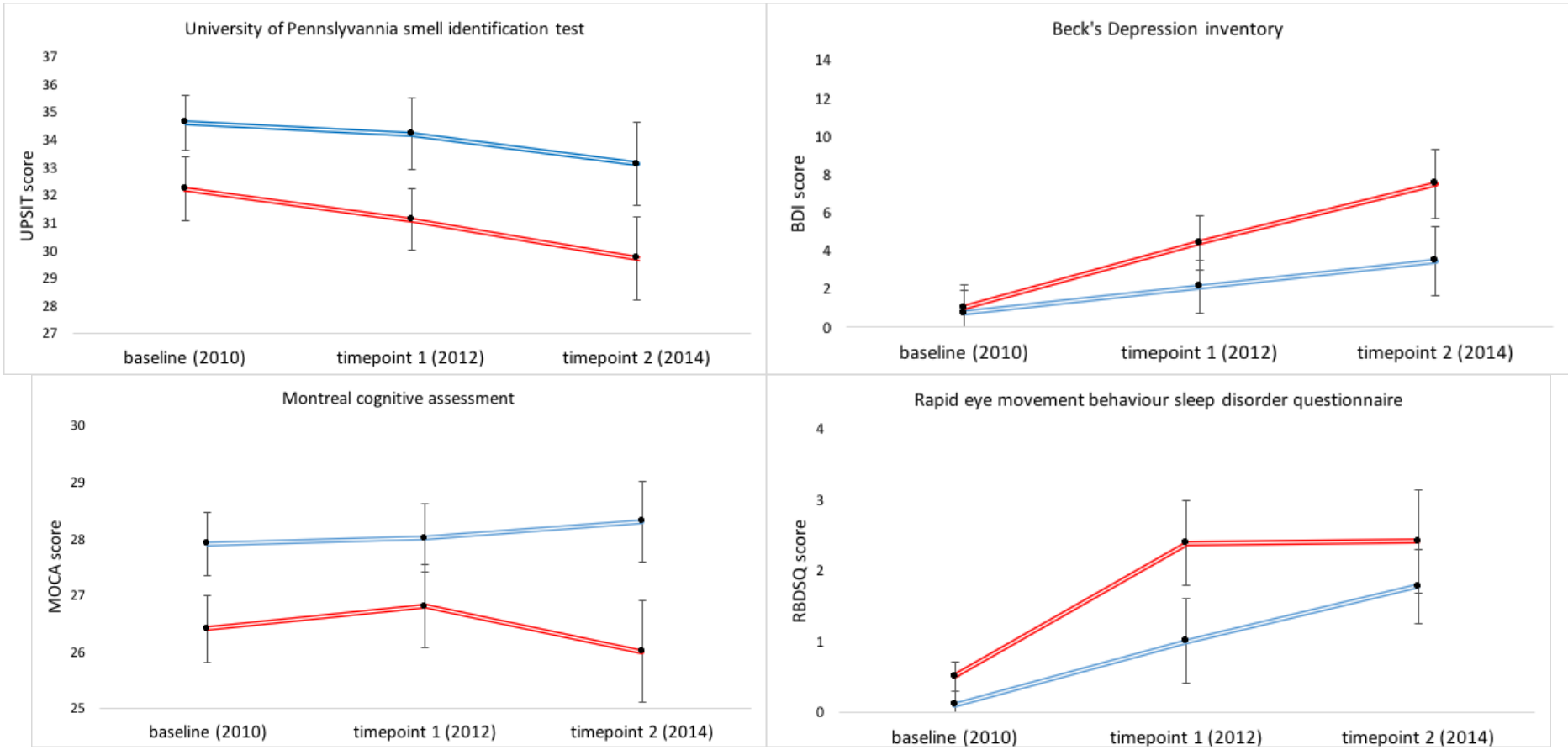

Fig 1. Trimmed means of UPSIT, MOCA, BDI scores and RBDSQ of combined cohort of GBA carriers (red) and controls (blue) with exact confidence intervals

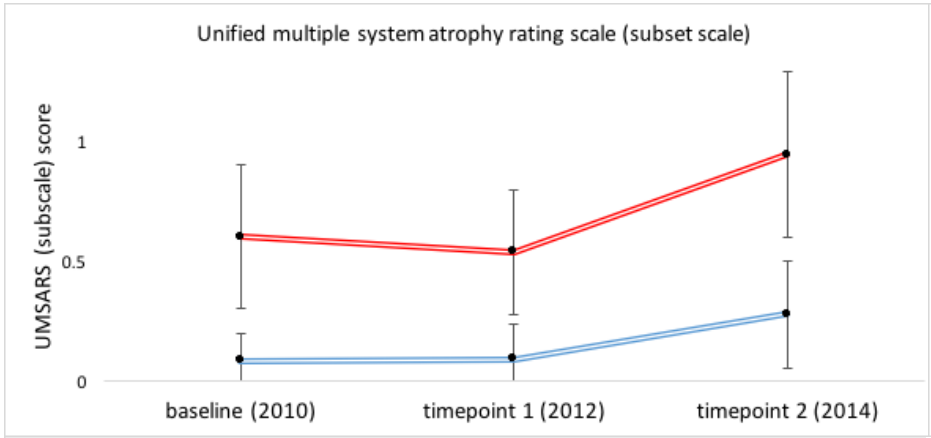

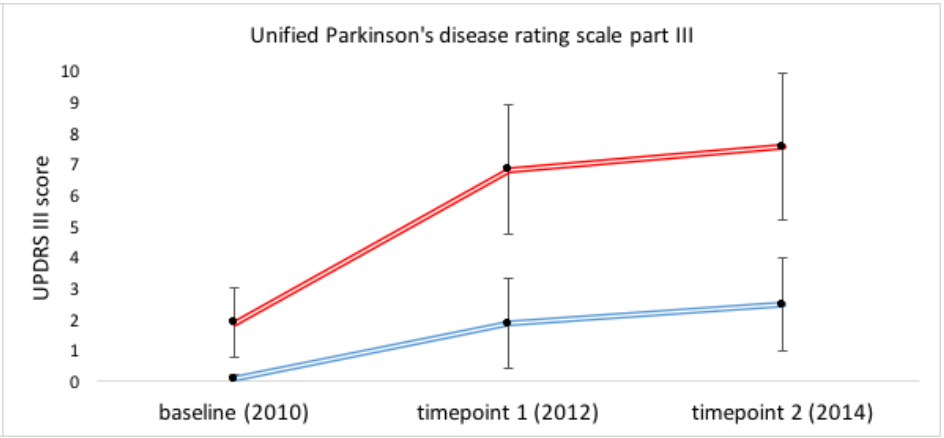

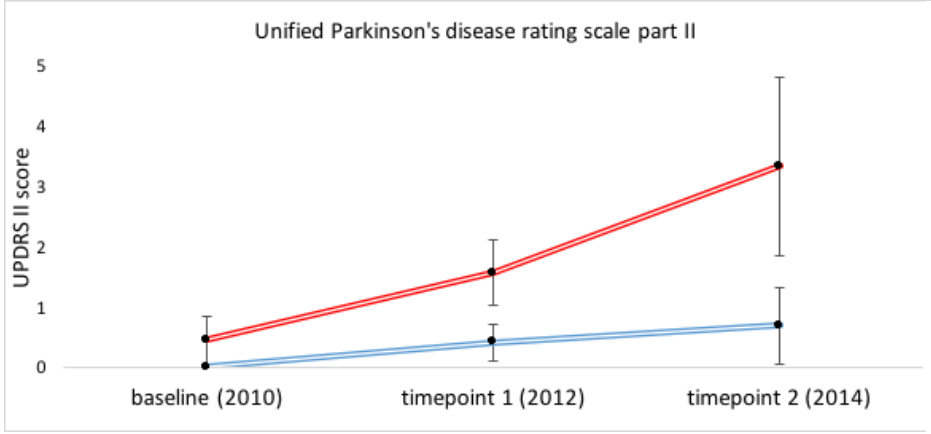

Fig 2. Trimmed means of UPDRS II, UPDRS III, RBDSQ and UMSARS (subscale) scores of combined cohort of GBA carriers (red) and controls (blue) with exact confidence intervals

the beginning to end (max 4 points), (Fig 3 and Appendices section 10.2d). Using this system, and compatible with recent data suggesting that patients at risk of Parkinson disease share a common risk profile [104,109], we discovered that those with olfactory deficits were also more likely to have deficits of cognition (MOCA OR 1.5 p=0.033) and depression (BDI OR 1.3 p=0.030). Figure 4 shows that overlap of those with these prodromal features of the approximately 10% of participants with the worst/fastest deteriorating prodromal features based on our risk stratification system. (UPSIT = 3/8 86th centile and above, MOCA = 3/8 91th centile and above, BDI = 4/8 86th centile and above) compared to the control group (UPSIT 2/8 89th centile, MOCA 3/8 89th centile, BDI 2/8 87th centile). Subset analysis showed that this was also true amongst bi-allelic *GBA* carriers alone, in terms of cognition (MOCA, OR 2.95 p=0.006) but not depression. There were no correlations between these risk scores amongst the control group (Figure 4 and supplementary Table 4). Figure 5 shows the prospective trimmed mean scores of these 3 prodromal features in those with the worst UPSIT scores, compared to the rest of the cohort and emphasise this clustering effect,

3.2c Illustrative case GBA bi-allelic participant who developed Parkinson disease

In March 2013 one 53 year-old male with established Gaucher disease developed bradykinesia, rigidity and a unilateral resting tremor. At this time he developed a marked cognitive deficit which fulfilled diagnostic criteria for dementia with Lewy bodies (DLB). He was homozygous for *R463C*, a severe Gaucher diseasecausing mutation [105] which has been

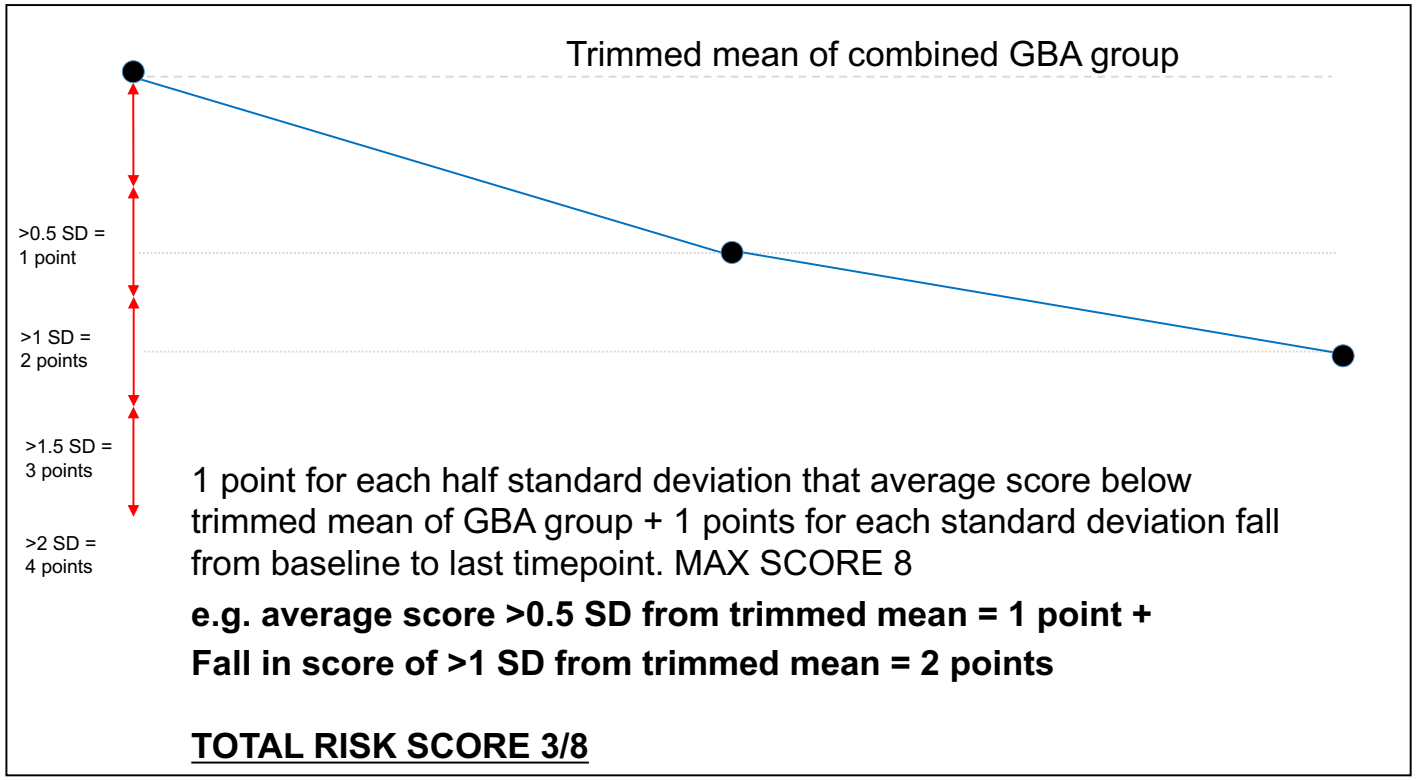

Fig 3. Explanation of risk stratification system of prodromal PD features

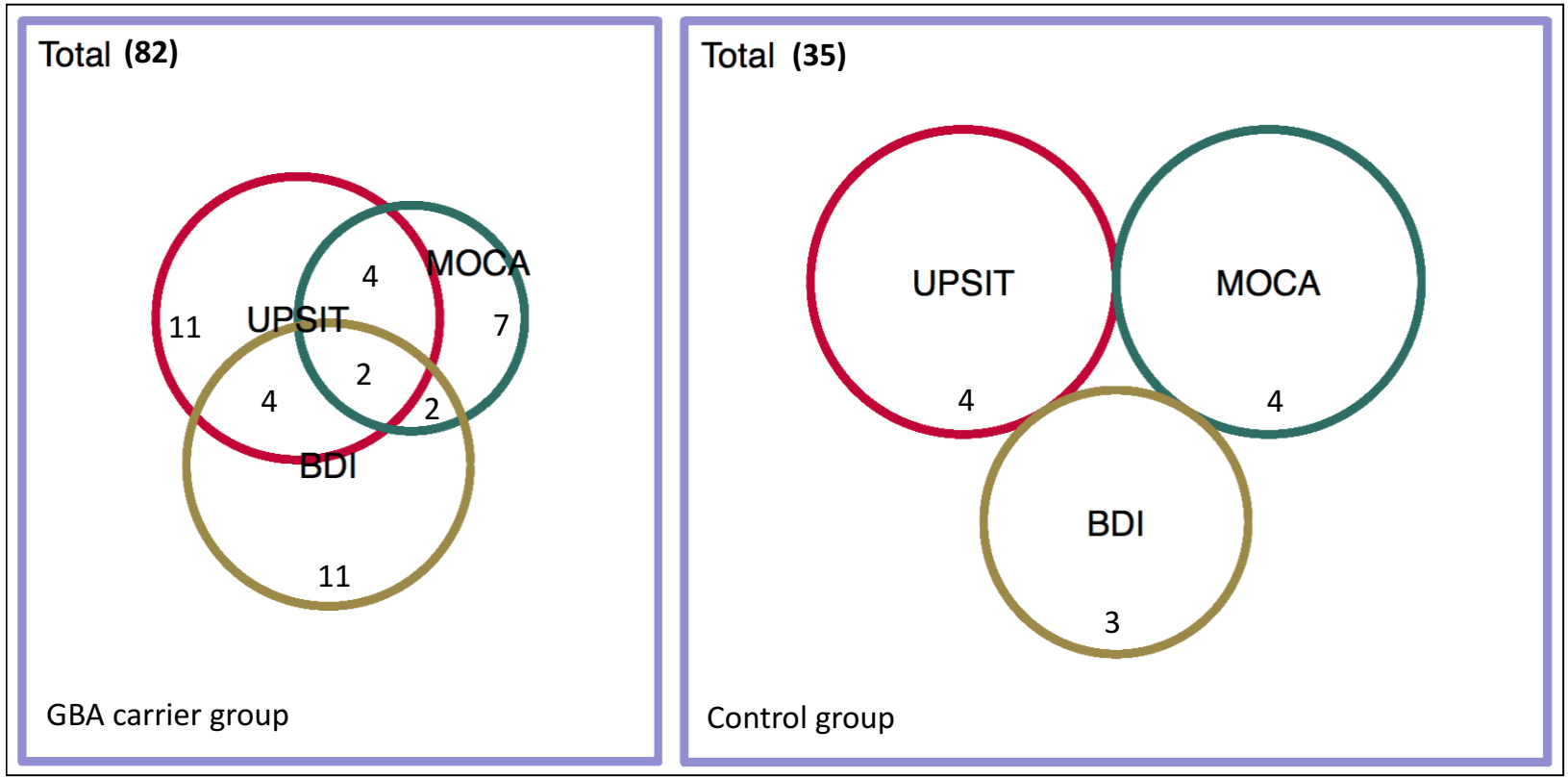

Fig 4. Venn diagrams of overlap between *GBA* mutations carriers (left) and controls (right) with the worst UPSIT (red GBA/ctl 86th/89th centile and above), MOCA (green GBA/ctl 91st/89th centile and above) and BDI scores (brown GBA/ctl 86th / 87th centile and above)

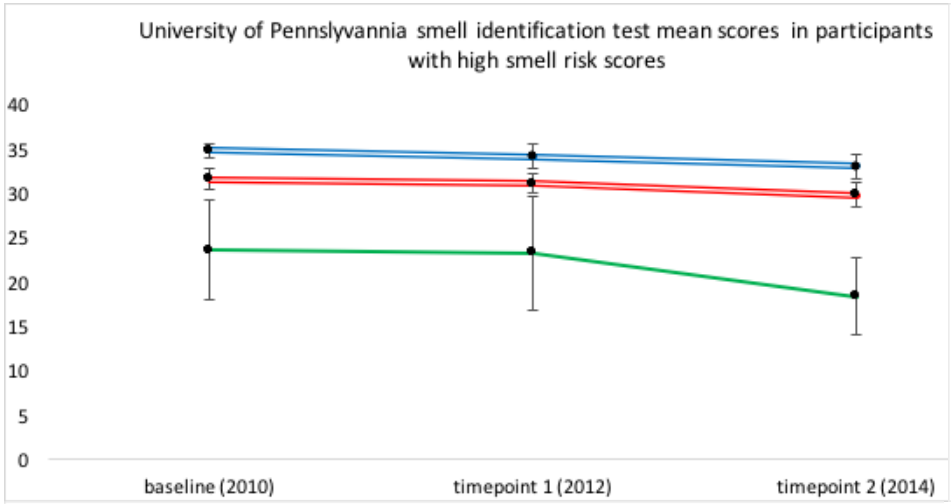

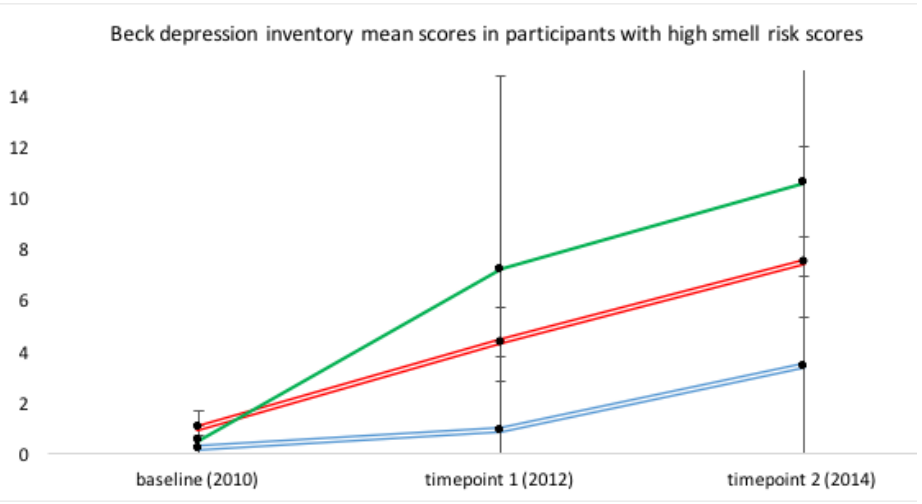

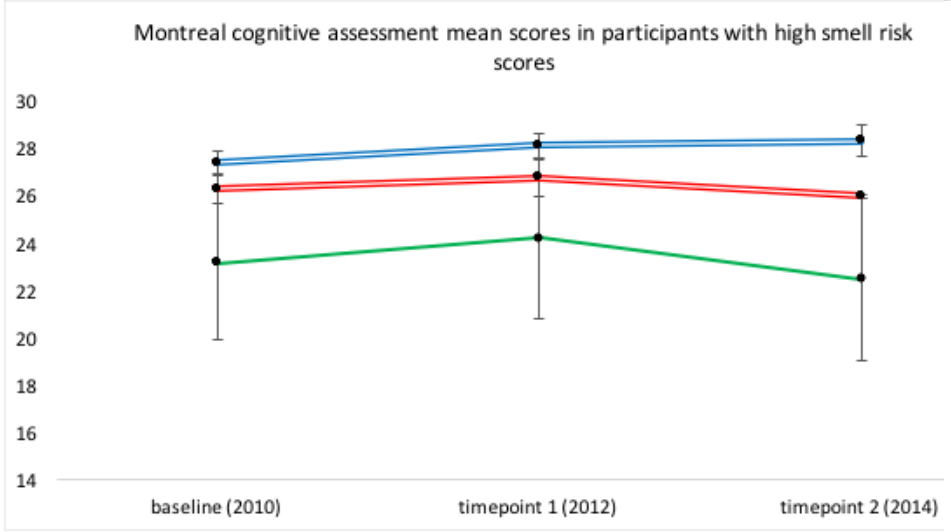

Fig 5. Trimmed means of UPSIT, MOCA and BDI scores of those with highest smell risk score (green) compared to scores of combined cohort of GBA carriers (red) and controls (blue) with exact confidence intervals

described in several patients with Parkinson disease and DLB [26,30,175]. A breakdown of his prodromal feature scores are presented in table 3 and (in the case of cognition, depression and hyposmia) are plotted graphically in figure 6.

Table 3. prodromal Parkinson disease risk scores of participant who developed Parkinsonism			
	Baseline (2010) Score [centile]	**timepoint 1 (2012) Score [centile]**	**timepoint 1 (2014) Score [centile] *Parkinsonism DIAGNOSIS**
UPSIT	20 [93]	14 [96]	17 [95]
MOCA	27 [54]	27 [57]	21 [87]
BDI	4 [82]	4 [50]	25 [95]
UMSARS	0	3 [95]	5 [97]
RBDSQ	0	2 [52]	5 [85]
UPDRS II	0	3 [85]	29 [99]
UPDRS III	0	3 [50]	45 [99]

3.2d Clinical course of those with Parkinsonian features

A number of participants presented with clinical features of Parkinsonism. A summary of these characteristics is listed below in table 4. The trimmed mean of their UPSIT, MOCA and BDI scores is plotted for illustrative purposes against those of the rest of the cohort and the participant who developed Parkinsonism in Fig 6.

Table 4 Clinical characteristics of participants with parkinsonian features

age	sex	genotype	Clinical features
80	m	*N370S*/*N370S*	Parkinson disease: Bilateral rigidity with activation, asymmetrical bradykinesia, gait impairment, bilateral postural tremor GD: ERT 4 weekly. Thrombocytopenia
85	m	*N370S*/*L444P*	**Parkinson disease: More prominent** right pill rolling tremor with **postural component.** No bradykinesia or rigidity GD: ERT 4 weekly. splenomegaly. Bone pain (teeth)
75	m	*N370S*/*N370S*	Flexed posture, bilateral rigidity, kinetic and postural tremor GD: ERT 4 weekly
63	m	*N370S*/*L444P*	Parkinson disease: Flexed posture, resting head tremor, **bilateral kinetic hand tremor GD: ERT 2 weekly.**
53	m	*R463C*/*R463C*	**Parkinson disease: Asymmetrical rigidity and bradykinesia, resting head and leg tremor** **Parkinson disease DIAGNOSIS 2014 GD: ERT. Avascular necrosis.** **Hypergammaglobulinaemia.**
80	F	wt/G250V	bradykinesia, **asymmetrical resting tremor**
80	m	wt/*N370S*	left-arm kinetic tremor, and flexed posture

New features since timepoint 2 marked in **bold**

ERT: Enzyme replacement therapy GD: Gaucher disease Parkinson disease: Parkinson disease wt: wild type

3.2e What is the significance of global deficits of hyposmia, cognition and depression amongst GBA carriers?

Our results show that *GBA* carriers have deficits in a number of criteria which sweepingly are labelled prodromal Parkinson disease features. But what are these deficits actually indicative of pathologically? It has been shown previously that type 1 Gaucher disease patients do exhibit cognitive deficits [176] in spite of the received wisdom that their central

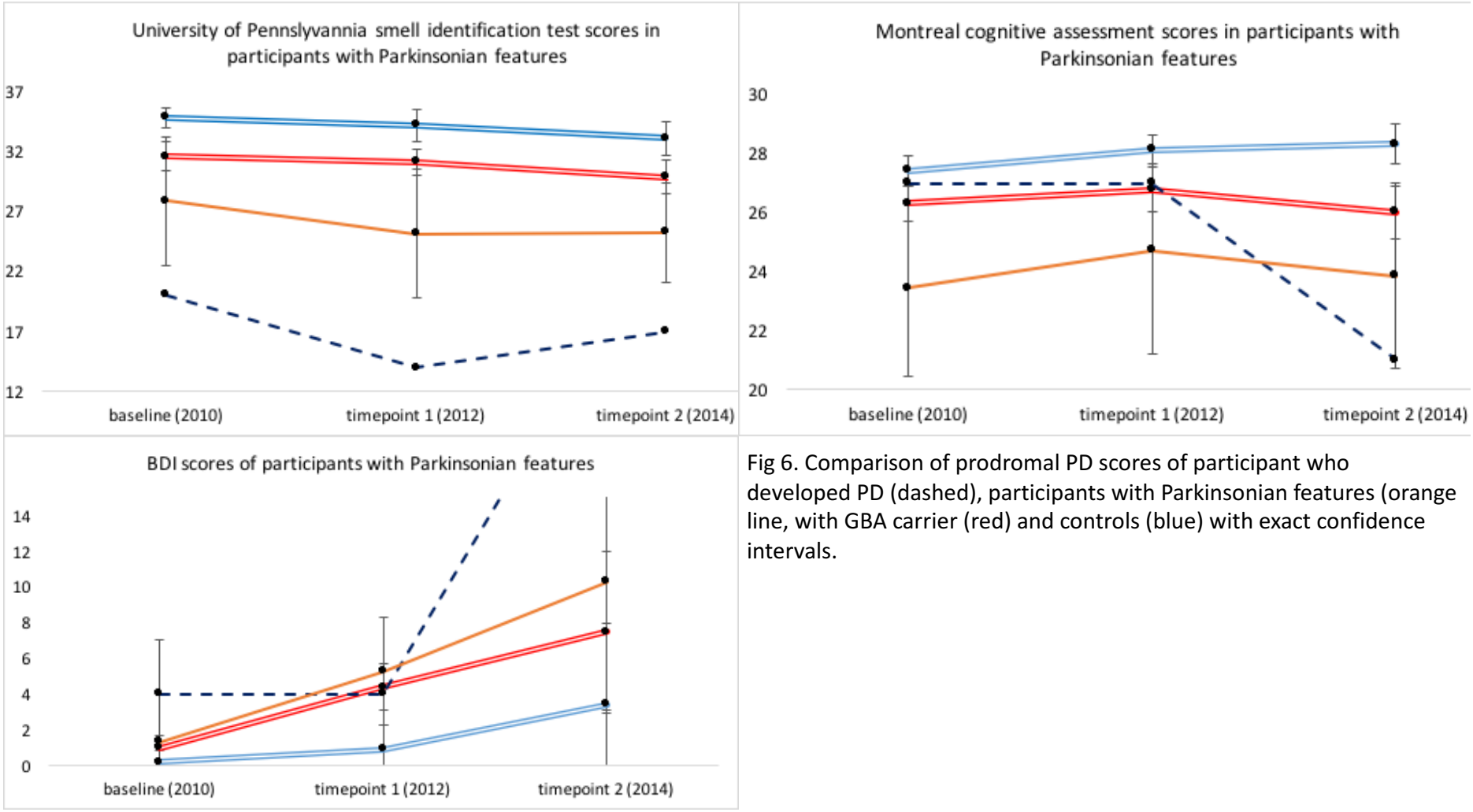

Fig 6. Comparison of prodromal PD scores of participant who developed PD (dashed), participants with Parkinsonian features (orange line, with GBA carrier (red) and controls (blue) with exact confidence intervals.

nervous system is spared. It is useful at this point to consider the substantial body of literature which shows that *GBA* Parkinson disease has a more pronounced cognitive phenotype and that equally *GBA* is a genetic risk factor for dementia with Lewy bodies [31]. Does development of Lewy pathology (or indeed some other pathological process implicated in Parkinson disease) occur to a variable degree in all *GBA* carriers?.

The clinical phenotype of neuronopathic Gaucher disease includes supernuclear gaze palsy, cognitive impairment, epilepsy, ataxia, bulbar dysfunction, myoclonus and hydrocephalus, a broad range of neurological features which is suggestive of generalized rather than focal neurodegeneration [6,7,10]. That said the former is almost universally present, although this may be a reflection of physicians' reluctance to make the diagnosis in its absence. None the less it is interesting that the apparent primary presentation of neuronopathic Gaucher disease is one which affects midbrain structures, albeit with input from the thalamus and cerebellum [177]. Parkinson disease similarly has a has a predilection for brain stem structures, causing as it does hyposmia (olfactory nucleus and bulb), REM sleep dysfunction disorder (predominately pontine structures) [163] and indeed sometimes supranuclear gaze palsies themselves (although these are more commonly a feature of the taupathy progressive supranuclear palsy) [178]. It is appealing to hypothesise that *GBA* mutations give rise to variable brainstem neurodegeneration with some unknown factor determining whether sufficient nigral damage occurs to cause the conversion to motor Parkinson disease and this is a theme we shall develop further in **chapter 4**.

3.2f Clustering of prodromal Parkinson disease features

The use of our novel risk score system allows us to quantify the extent of MoCa, BDI and UPSIT the deficit across all timepoints and the rate of decline of these scores. Clearly the hope is that detection of deficits in a number of prodromal Parkinson disease features may increase the sensitivity of detection of Parkinson disease conversion as a prelude to targeting neuroprotective compounds. Whether amongst *GBA* carriers clustering of depression, cognitive impairment and hyposmia actually occurs in advance of Parkinson disease conversion remains to be seen and can only be answered by further prospective assessment. Considering the clinical course of our Parkinson disease convertor the most striking point is the extent of his hyposmia, which was by some way the most profound across the entire cohort. There was evidence of mild features of depression, however his cognitive impairment was in fact slightly better than the average scores of *GBA* carriers. It may be, of course, that not all Parkinson disease convertors develop the 'full house' of prodromal symptoms, but rather only a subset of those which are indicative of neuroanatomical location of the pathology. Conversely, of those other participants with Parkinsonian features MoCA, UPSIT and BDI scores were consistently below the average of the *GBA* affected participants (Fig 6).

3.3 Concluding remarks

In this chapter we have presented a five year follow up of 'asymptomatic' *GBA* carriers and demonstrated convincing deficits of cognition and olfaction. As we have stated there is no guarantee that these features are indicative of Parkinson disease conversion. However, the

specificity of olfaction in particular to neurodegenerative disease does lead to a reasonable postulation that common histological processes are underway. Furthermore, the clustering of prodromal Parkinson disease symptoms in a subset of individuals further emphasises our hypothesis. Whilst synuclein pathology has yet to be noted in Gaucher cases without clinical signs of Parkinsonism, only a handful of post mortems have been carried out to date on these patients [46,179,180] and in many cases it is not clear whether synuclein immunofluorescence was convincingly assessed. It would be interesting at post mortem to assess the prevalence of lewy bodies amongst the brains of aged *GBA* carriers without Parkinson disease compared to controls, although logistically this is of course highly problematic. The existing cohort study is underpowered to answer the range of questions which arise from these findings (e.g are there differential prodromal Parkinson disease features in different *GBA* mutations, can these be correlated with biomarkers and can higher risk individuals be selected for neuroprotective therapies). In the next chapter we shall propose a mechanism to address this issue and hence to expand the size and increase the sustainability of prospective follow up of these participants.

Chapter 4 - Internet based Parkinson disease prodromal assessment shows feasibility of remote assessment for prodromal Parkinson disease signs amongst *GBA* carriers

4.0 Introduction

The inherent difficulties associated with prospective assessment of disease cohorts are well known, namely that ageing, disease burden or simply study fatigue lead cumulatively to a very high attrition rate amongst participants. Moreover, conventional assessment of cohorts (especially one as in this case that is geographically disparate) is time consuming and expensive, primarily on account of the travel and time costs associated with participants travelling to assessors (or vice versa). Finally the necessity for different assessors to carry out assessments at different timepoints introduces a degree of inter assessor variability which is particularly pertinent for clinical assessments associated with a degree of subjectivity, such as the UPDRS. In all cases these limitations are compounded with increasing years of assessment.

In the above analyses we have shown trends towards a difference in the motor symptoms and signs (UPDRS II and III respectively), REM sleep behaviour disorder (RBDSQ), BDI (BDI), autonomic symptoms (UMSARS subscale) as well as the significant differences in hyposmia (UPSIT) and cognition (MoCa) already exhibited. Speculatively we can suggest that with a larger cohort size these trends would be likely to translate into significant differences. Moreover the requirement for larger cohorts is not only academic. A recurrent theme of this thesis is the potential be able to risk stratify *GBA* mutation carriers in terms of their Parkinson disease risk, with an eye to effective targeting of future neuroprotective drugs. If

this is to be realised then a reliable, convenient, reproducible and above all cost effective method must be found to clinically assess *GBA* carriers for signs of prodromal Parkinson disease.

4.1 An internet based platform for clinical assessment of prodromal Parkinson disease amongst GBA carriers

The obvious solution to this problem is an internet based platform. At first glance the concept is entirely feasible. Of the assessments carried out in the study described in chapter 2, only the UPDRS III and MoCa must be carried out in person, the rest being either questionnaires or smell tests that have been used and validated as postal assessments. Moreover, in terms of both motor dysfunction and cognition, online assessments exist which have been validated in Parkinson disease patients. A prototype for this approach exists in the PREDICT PD study [181,182]. PREDICT PD is an online assessment portal which aims to identify prodromal signs of Parkinson disease amongst members of the general population. The model involves subjects signing up by logging on to the website. On a yearly basis participants undertake a series of online questionnaires (hospital anxiety and depression scale, REM sleep behaviour disorder questionnaire and a number of validated questions related to other prodromal Parkinson disease features and risk factors such as constipation, head trauma and outdoor living). Participants also undertake the BRAIN test, a validated assessment of bradykinesia in which participants tap sequentially the ";" and "s" keys as fast and accurately as possible [183]. Stratification of the cohort using an algorithm based on established odds ratios of Parkinson disease risk associated with the various

features found that higher risk participants had worse features of hyposmia (UPSIT), REM sleep behaviour disorder (RBDSQ) and bradykinesia (BRAIN test).

Using this prototype we sought to develop a platform for longitudinal assessment of this cohort. Whilst we were able to directly mimic many aspects of the PREDICT PD portal, there were a number of areas in which it was necessary to develop or enhance it for our own purposes. These were namely; the addition of more comprehensive questionnaire of non-motor Parkinson disease symptoms which prompted the addition of the UPDRS part II questionnaire to the portal and more significantly the incorporation of facility to allow cognitive testing of participants within the portal. This is of particular importance in this group because the cognitive phenotype phenotype appears to be more pronounced and *GBA* is an established genetic risk factor for dementia with Lewy bodies [26,28,31]. The latter was a significant challenge. Neuropsychometric testing entails considerable complexity and traditionally has required a facilitator to instruct and direct participants. Because of this we opted to acquire an 'off the shelf' solution in order to minimise the amount of development, testing and validation work required. After considering the products currently available we settled on the Cogtrack package. Based on the clinical dementia research assessment (CDR), a computerised package has been used for over 30 years. It is a multi domain cognitive assessment panel validated in both Parkinson disease and Alzheimers type dementia. Its principle advantage is its simplicity. The components of the package require input of either one or two keyboard based commands only (Fig 1-8). Moreover, they have been used prospectively in a number of clinical trials [184], a major consideration given the stated aim of

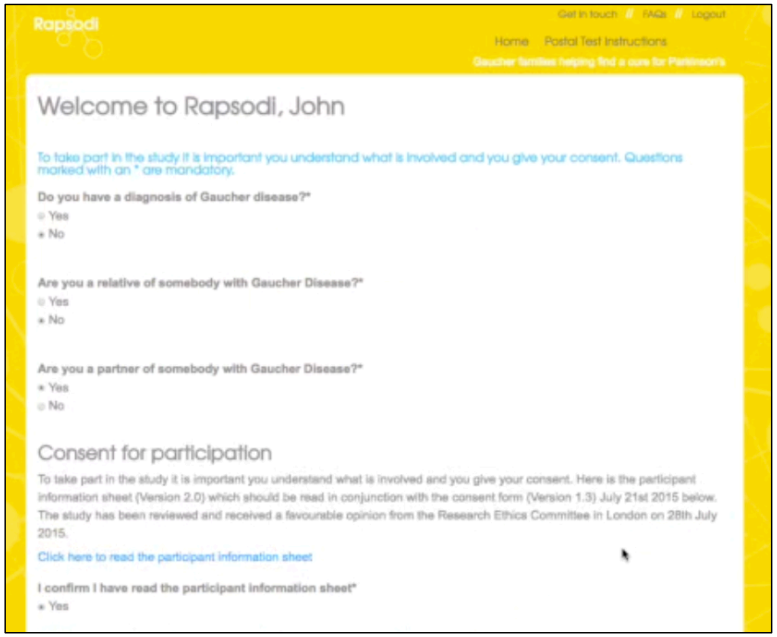

Fig 1. Screenshot of rapsodi consent screen

Fig 2. Screenshot of rapsodi BRAIN tap test

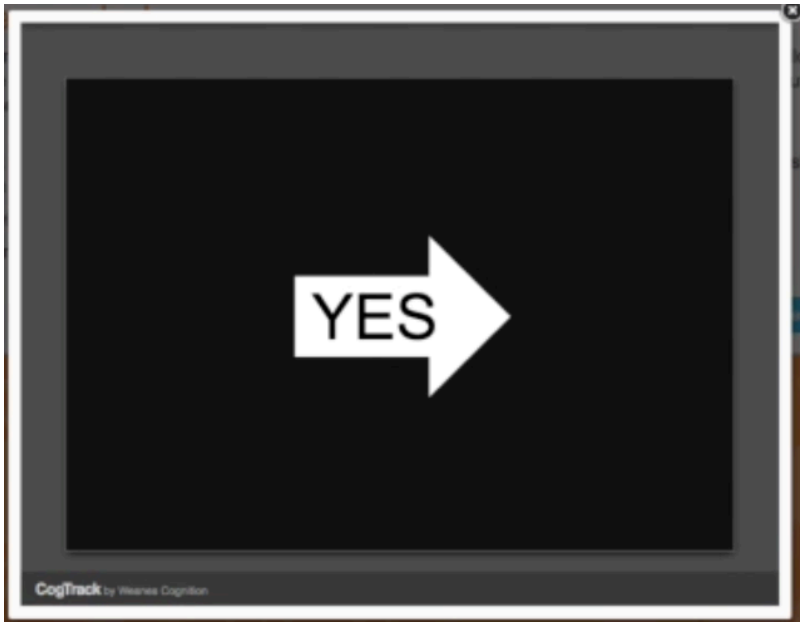

Fig 3 screenshot of simple reaction time task. The subject is asked to repeatedly press on the right key button when a "→ yes" cue appears on the screen.

Fig 4 screenshot of digital vigilance task. The subject is asked to press the right key button when a number cue matching a number permanently placed next to it on the screen appears.

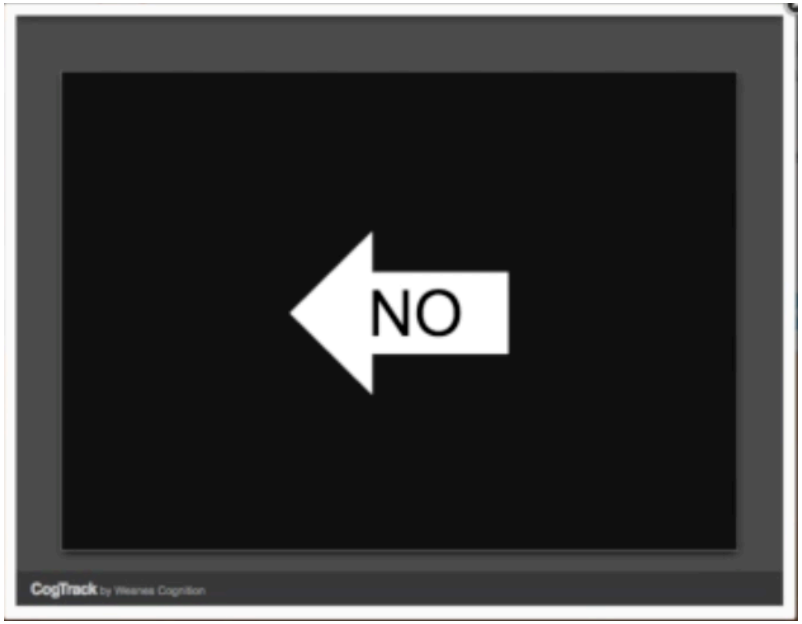

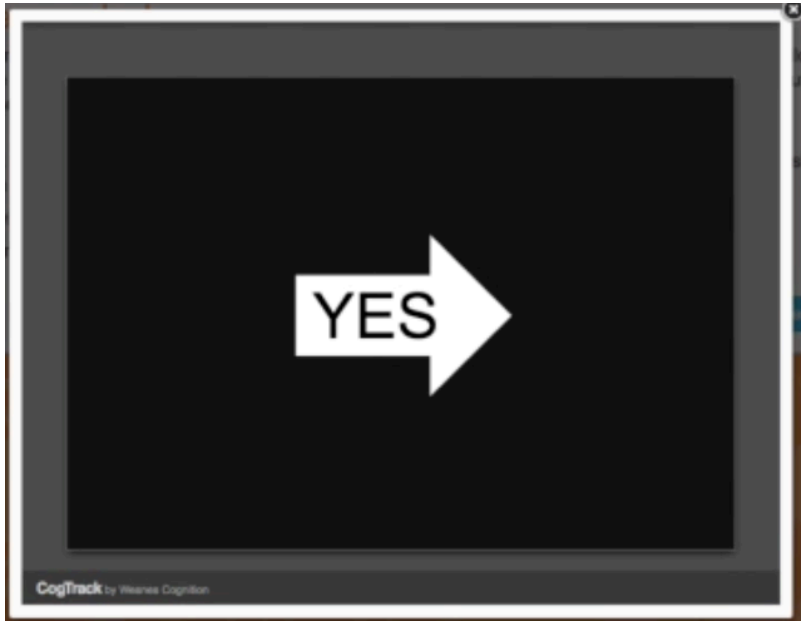

Fig 5. Choice reaction time The subject is asked to press the left and right buttons in response to cues indicating "yes →" and "no←".

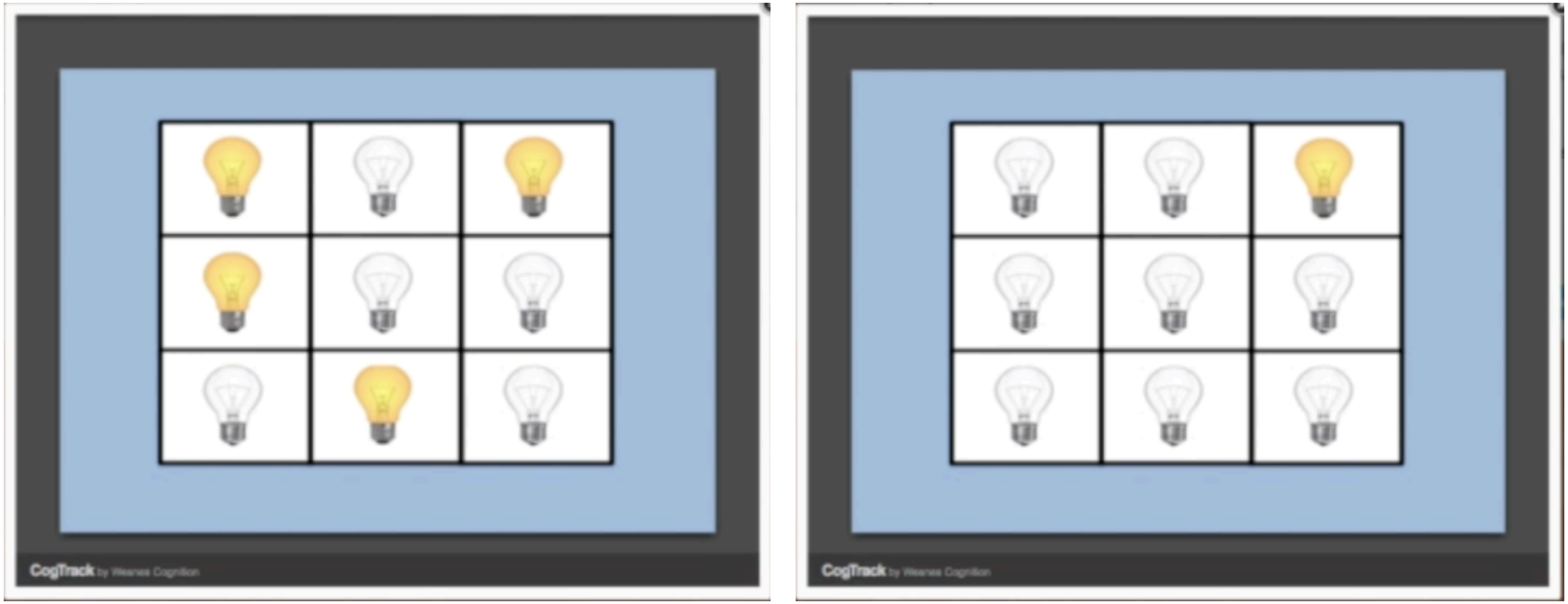

Fig. 6 Spatial working memory. A 3x3 grid with lightbulbs in four of the boxes in shown. In a new screen successively lightbulbs appear in one of the boxes and subjects indicate whether the light bulb was previously present in the box by pressing left (no) or right (yes).

Fi.g 7. numeric working memory. A series numbers are shown. The subject is then asked to assess whether sequential of numbers that flashes on the screen are part of that original sequence by pressing left (no) or right (yes).

Fig 8. A series of images are shown to participants at the beginning of the battery, the images interspersed with distractor images which are similar to the original stimulus (e.g a red car and a blue car, a flag blowing to the right and a flag blowing to the left). For each image the subject selects whether it is an original image (right) or a new image (left).

in the future utilising the rapsodi portal as a tool for the targeting of neuroprotective therapies.

4.2 Validation of Cogtrack cognitive tests

The most striking challenge was the lack of validation data for the unassisted use of the software. A panel of the software has been available for some years on the internet which has allowed the collection of data from some 93,334 participants who undertook assessment using the portal unassisted. This was compared with 5,989 age matched controls who undertook the portal in clinic. Therefore the utility of using the panel in such a manner is established. That said, no data exists on the applicability of unassisted use of the cogtrack panel in the Parkinson disease population. To test this we carried out some validation studies. Five Parkinson disease and three control subjects were asked to complete the cogtrack panel on two occasions (one assisted, one unassisted) 2-4 weeks apart. Participants were randomised as to whether they carried out the assisted or unassisted task first. Five control and five Parkinson disease participants were enrolled, however only 3 participants from each group completed both tasks. Although the cogtrack panel generates a number of outcomes which combine the measurements taken for each task, we chose to analyse a range of individual outputs. These outputs are displayed in figures 9-12. A full output of the medians and interquartile ranges of the outputs is listed in the supplementary table 5 (Appendices 10.3b). In all cases differences between assisted and unassisted outputs were not statistically significant amongst the unassisted and assisted groups. Data was collected by SM and Ana Sanz Perez. Analysis was carried out by SM.

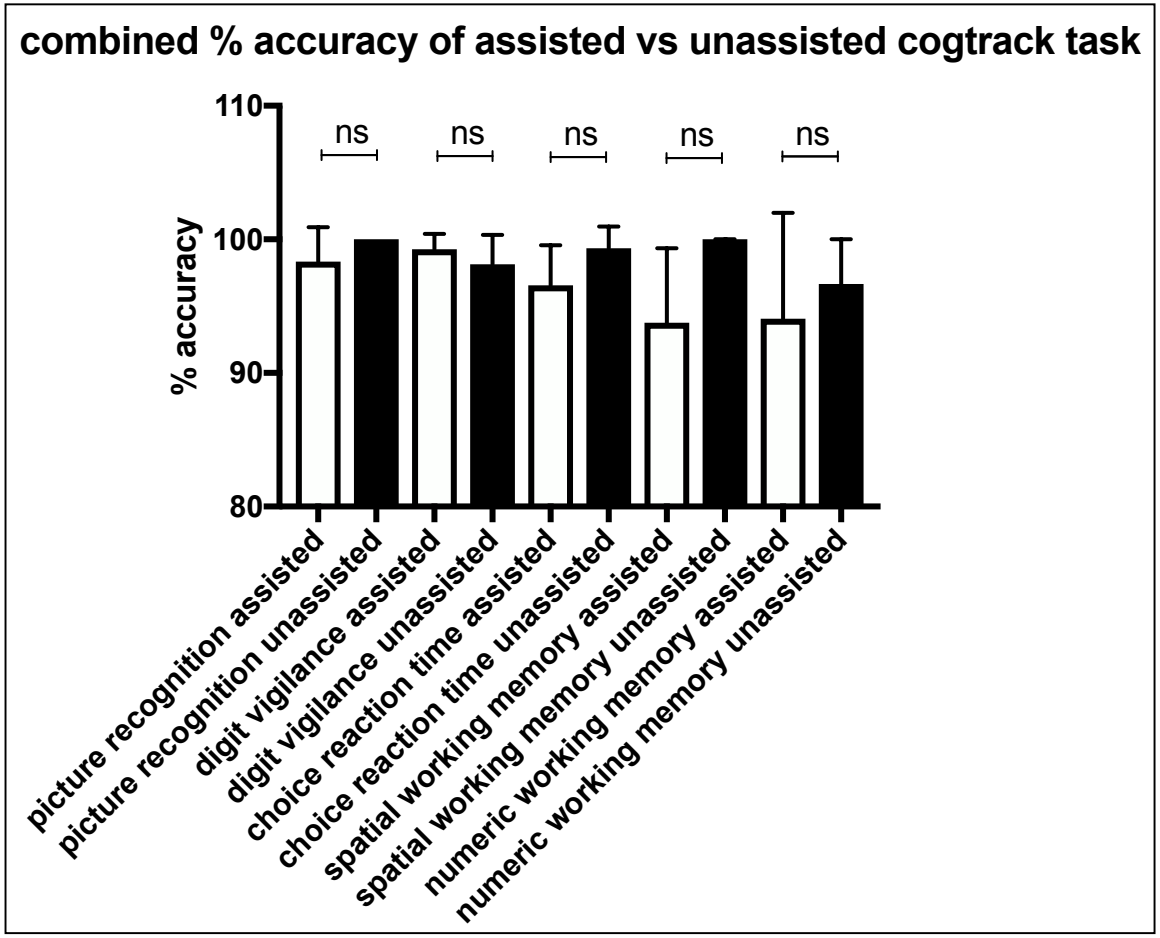

Fig 9. Comparison of median % accuracy of all participants (error bars IQR) with Wilcoxon rank sum significance testing between assisted and unassisted administration of tests

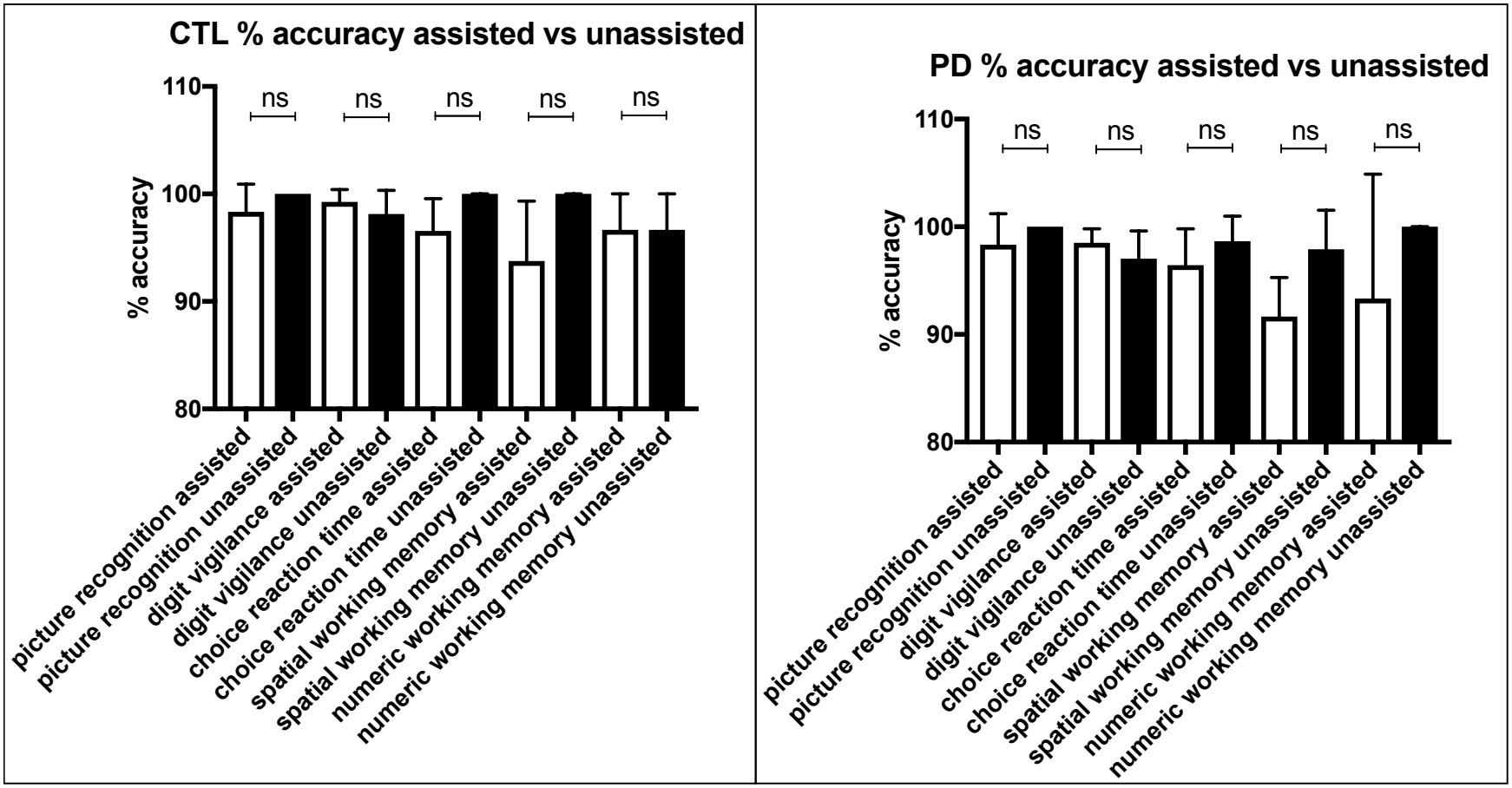

Fig 10. Comparison of median % accuracy (error bars IQR) with Wilcoxon rank sum significance testing between assisted and unassisted administration of tests in control and PD groups

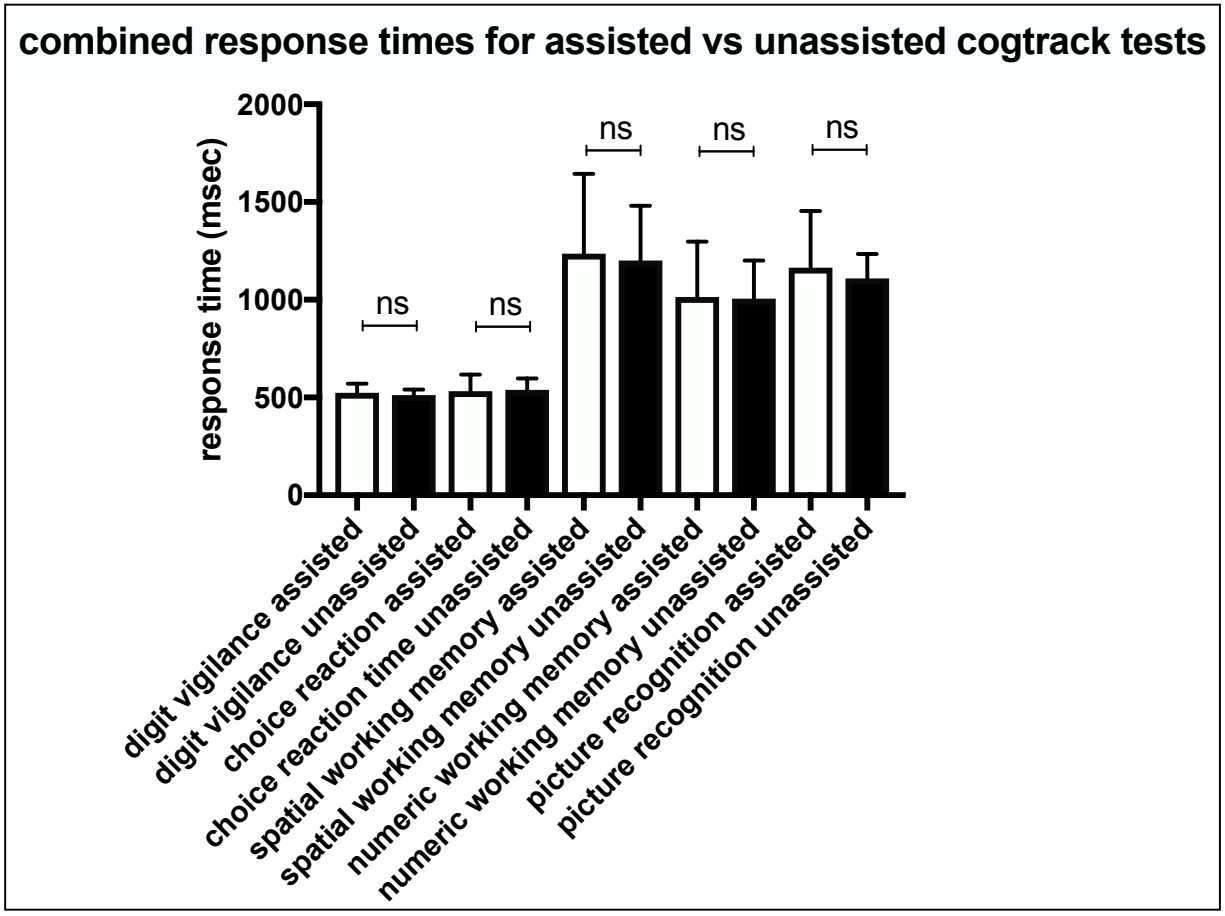

Fig 11. Comparison of median response time of all participants (error bars IQR) with Wilcoxon rank sum significance testing between assisted and unassisted administration of tests

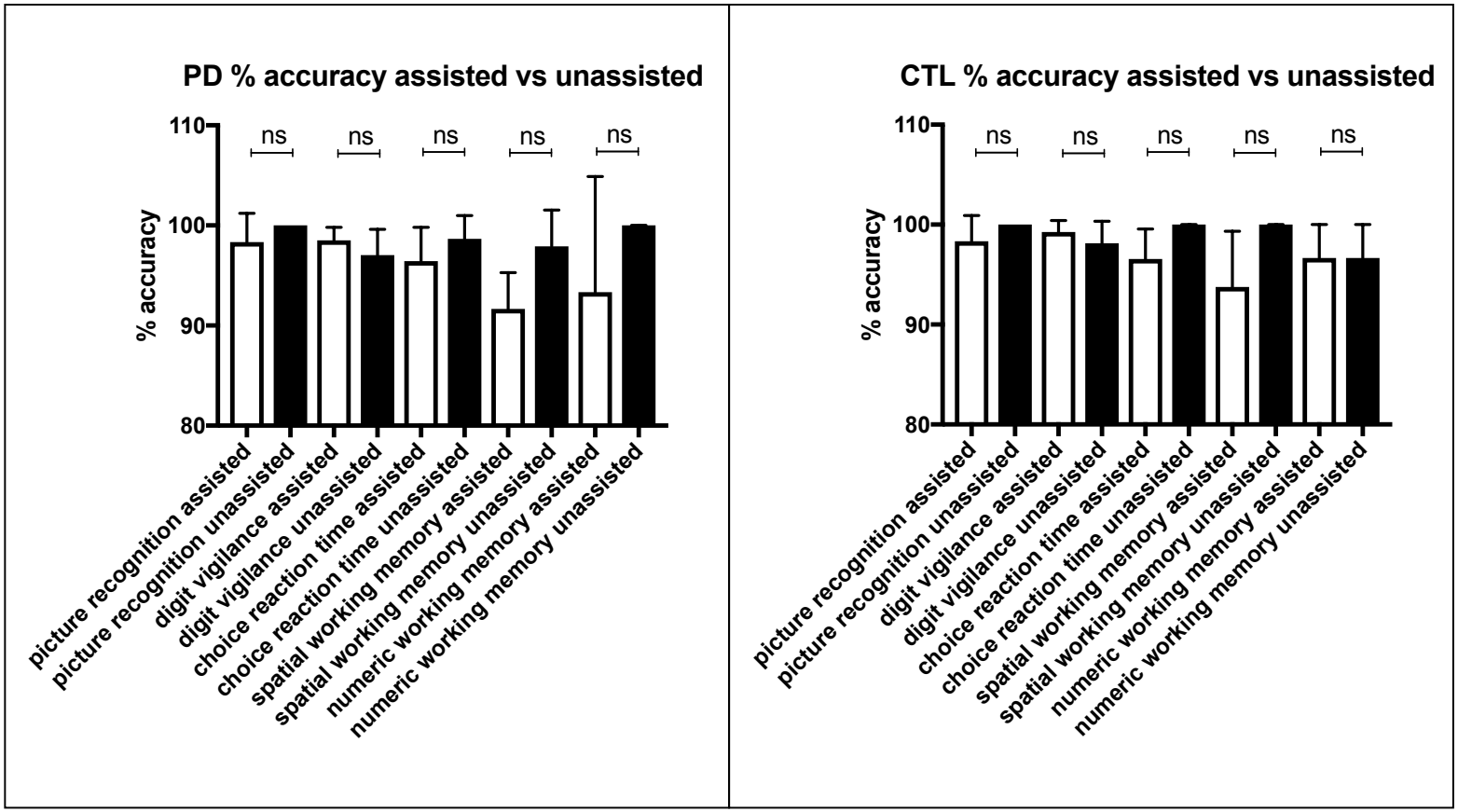

Fig 12. Comparison of median response times of all participants (error bars IQR) with Wilcoxon rank sum significance testing between assisted and unassisted administration of tests

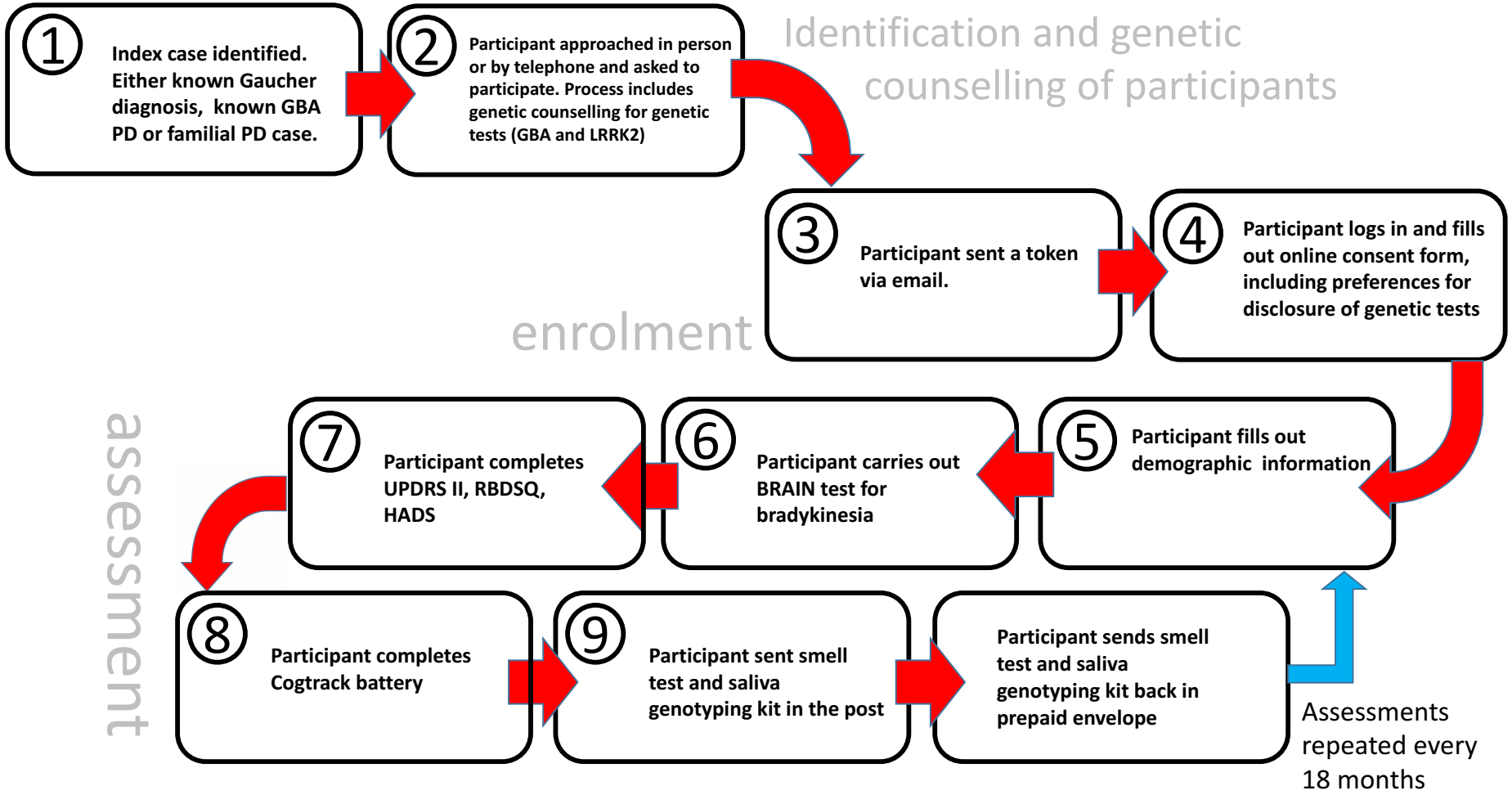

Fig 13. Flow diagram of the process of assessment in the rapsodi study

4.3 Logistical aspects of the rapsodi study.

The rapsodi study is designed ultimately to serve a cohort of a 1000+ subjects over a 25 year period. As such, it was vital to implement sustainable and scalable systems to allow the study to be conducted and data to be collected in a manageable and secure manner. Some of the particular challenges (and solutions) are described below. An overview of the study 'journey' is provided in Fig 13.

4.4 Online consent.

A major challenge was the necessity for the consent process to be online, as otherwise subjects would have to be visited in person, defeating the entire purpose of the study. This was also the case in the PREDICT PD study, but an added complication for rapsodi was that the process must also allow participants to make decisions regarding whether they wish to have the results of genetic testing for *LRRK2* and *GBA* revealed. We concluded in light of this that unlike PREDICT PD, a conversation, in person or by telephone prior to undertaking the consent process would be necessary. During this conversation genetic counselling for *GBA* and *LRRK2* mutations is offered in addition to more generalised overview of the study. Furthermore, the participant information sheet differed depending on the type of participant in question. A scheme was devised which utilised branching logic (i.e a series of questions directed participants to the correct PIS) in order to simplify the consent process. The design of this process was key in order to ensure subjects received adequate information prior to taking part in the study but in a manner which was not confusing or contradictory. A schematic of this consent process is included in Fig 14. We trialled the

procedure amongst a panel of Parkinson disease, Gaucher and *GBA* carriers and adjusted the process on the basis of the feedback obtained.

4.5 Processing of postal saliva samples

There were substantial complexities associated with DNA processing. We required a dynamic system that allowed DNA to be purified, analysed and the results available for discussion with participants as required. This process involved a number of operators at different sites. Briefly samples were received at the department of clinical neuroscience (DCN), UCL IoN, Royal Free Campus. DNA samples are purified in house, and delivered to health service laboratories (Health service laboratories (HSL) - Euston road) for genotyping and are then retrieved and databased at the DCN. We therefore chose to set up a cloud based database for the logging the receipt and transfer of DNA samples as well as recording the results of their analysis. This was achieved using the REDCAP platform. Date of receipt of initial sample (DCN), date of purification (DCN), date of receipt of purified DNA (HSL), genotyping date (HSL), genotyping result (HSL), date of databasing of purified DNA (DCN) are recorded in a pseudo anonymised manner (i.e study numbers only). A screenshot of the database is shown in Fig 15

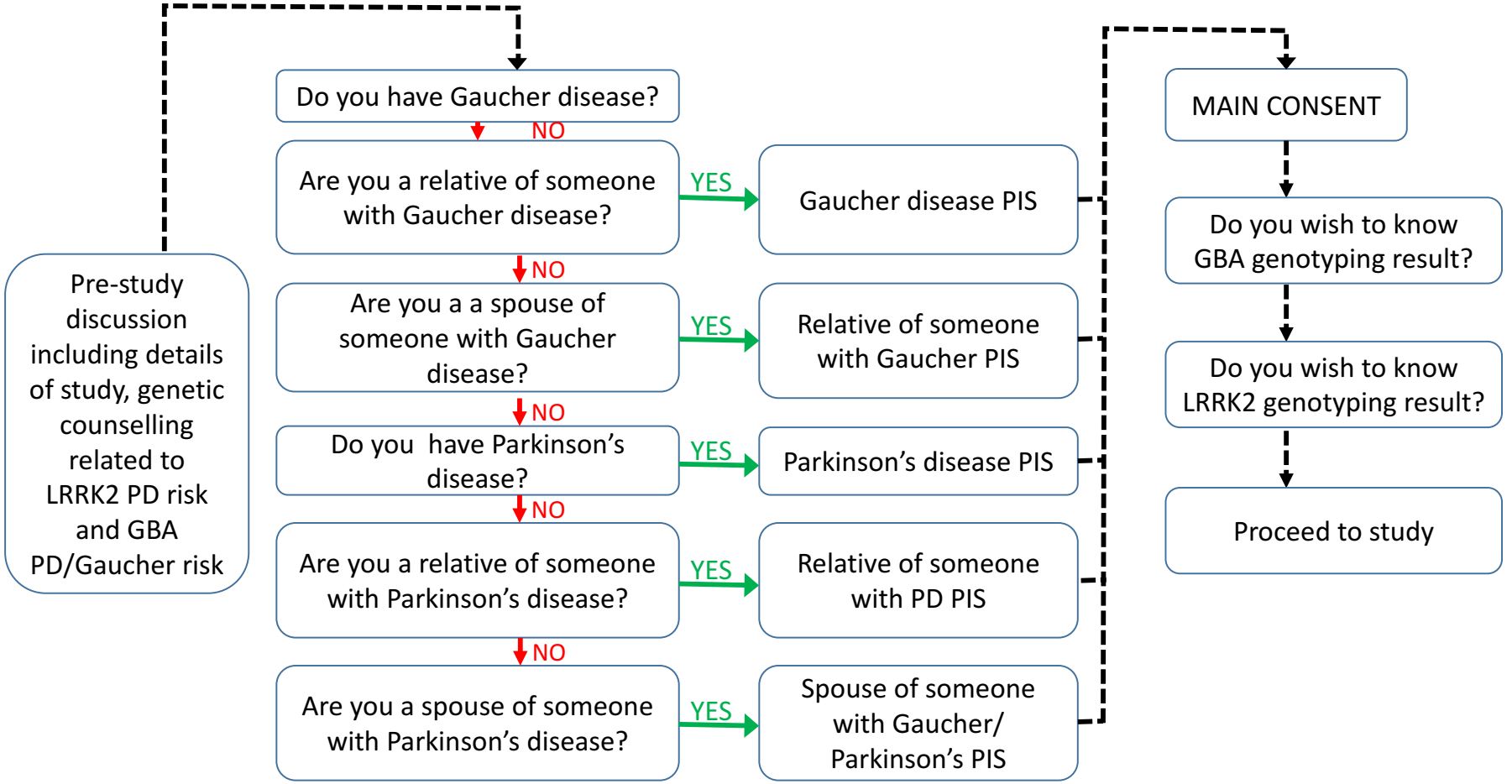

Fig 14. Flow diagram of the process of consent in the rapsodi study

4.6 Family tree mapping

A key component of the future analyses envisaged will be the impact of a family history of Gaucher disease, Parkinson's or (presumed lewy body) dementia in terms of the potential for Parkinson disease conversion. The rationale is of course that these factors are highly likely to be surrogate markers of genetic cofactors that may be implicated in the variable penetrance of these *GBA* mutation associated conditions. In a large cohort such as this, where many of the participants are likely to be related, the process of recording and using this information quickly becomes problematic. To resolve these issues we developed a specialist pedigree recording software programme. Screenshots of the programme are shown in Figure 16.

4.7 Data protection and security

Of paramount concern was ensuring the security of the data captured. To ensure this was the case we mimicked the approach adopted by PREDICT PD, namely that personal identifiers and assessments were stored on separate servers. We also specified that data should be stored on servers stamped with the ISO27001 accreditation. This is the highest level of security and is the same as used by the online banking industry. We also employed 24bit encryption to the site. Moreover the administrator logins for the site are protected with two factor user authentication, whereby in order to login, a user must enter a code sent to their email or mobile phone. A schematic of the layered security design in included in Fig 14

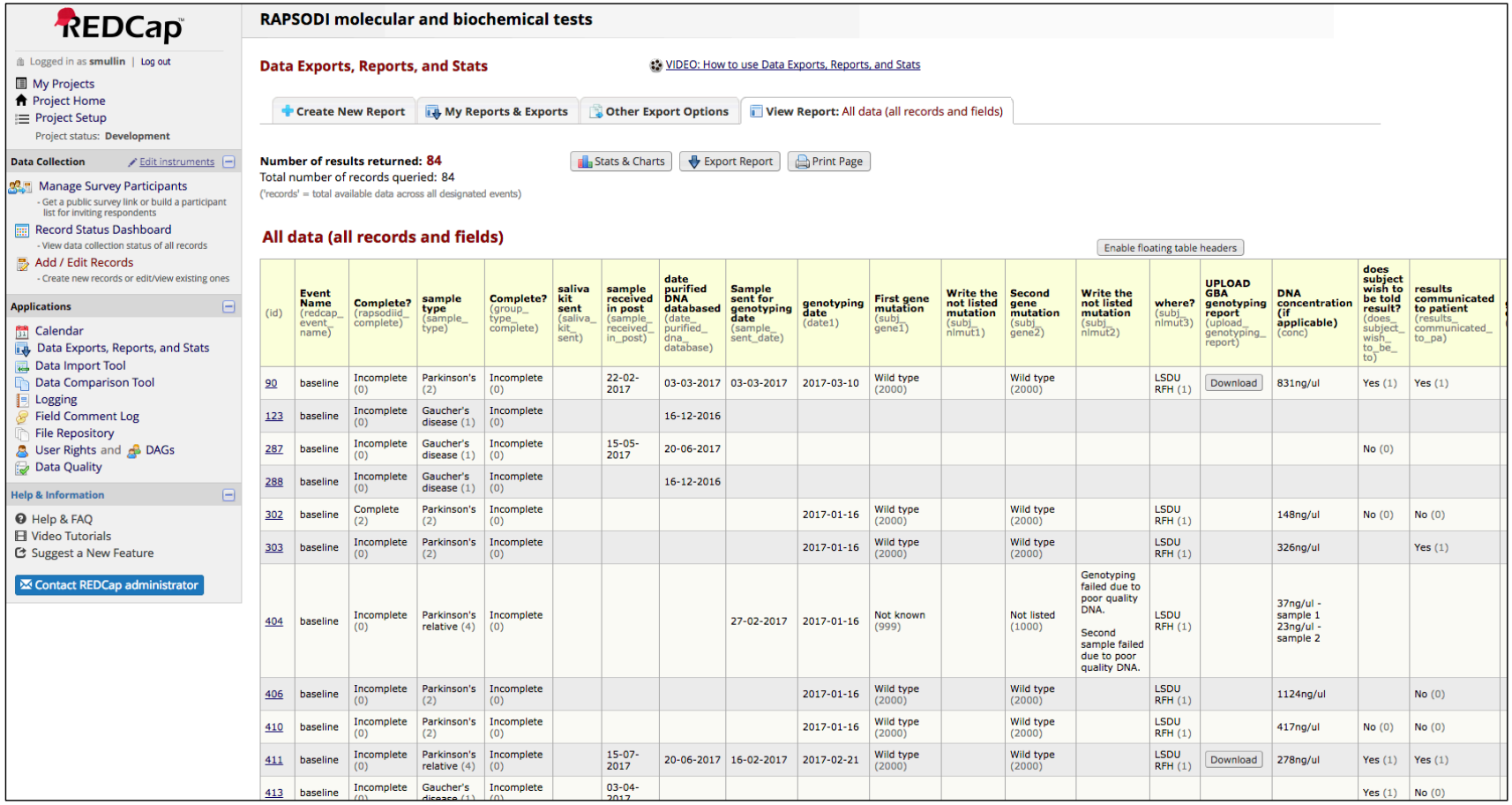

(id)	Event Name (redcap_event_name)	Complete? (rapsodiid_complete)	sample type (sample_type)	Complete? (group_type_complete)	saliva kit sent (saliva_kit_sent)	sample received in post (sample_received_in_post)	date purified DNA databased (date_purified_dna_database)	Sample sent for genotyping date (sample_sent_date)	genotyping date (date1)	First gene mutation (subj_gene1)	Write the not listed mutation (subj_nlmut1)	Second gene mutation (subj_gene2)	Write the not listed mutation (subj_nlmut2)	where? (subj_nlmut3)	UPLOAD GBA genotyping report (upload_genotyping_report)	DNA concentration (if applicable) (conc)	does subject wish to be told result? (does_subject_wish_to_be_to)	results communicated to patient (results_communicated_to_pa)
90	baseline	Incomplete (0)	Parkinson's (2)	Incomplete (0)		22-02-2017	03-03-2017	03-03-2017	2017-03-10	Wild type (2000)		Wild type (2000)		LSDU RFH (1)	Download	831ng/ul	Yes (1)	Yes (1)
123	baseline	Incomplete (0)	Gaucher's disease (1)	Incomplete (0)			16-12-2016											
287	baseline	Incomplete (0)	Gaucher's disease (1)	Incomplete (0)		15-05-2017	20-06-2017										No (0)	
288	baseline	Incomplete (0)	Gaucher's disease (1)	Incomplete (0)			16-12-2016											
302	baseline	Complete (2)	Parkinson's (2)	Incomplete (0)					2017-01-16	Wild type (2000)		Wild type (2000)		LSDU RFH (1)		148ng/ul	No (0)	No (0)
303	baseline	Incomplete (0)	Parkinson's (2)	Incomplete (0)					2017-01-16	Wild type (2000)		Wild type (2000)		LSDU RFH (1)		326ng/ul		Yes (1)
404	baseline	Incomplete (0)	Parkinson's relative (4)	Incomplete (0)				27-02-2017	2017-01-16	Not known (999)		Not listed (1000)	Genotyping failed due to poor quality DNA. Second sample failed due to poor quality DNA.	LSDU RFH (1)		37ng/ul - sample 1 23ng/ul - sample 2		
406	baseline	Incomplete (0)	Parkinson's (2)	Incomplete (0)					2017-01-16	Wild type (2000)		Wild type (2000)		LSDU RFH (1)		1124ng/ul		No (0)
410	baseline	Incomplete (0)	Parkinson's (2)	Incomplete (0)					2017-01-16	Wild type (2000)		Wild type (2000)		LSDU RFH (1)		417ng/ul	No (0)	No (0)
411	baseline	Incomplete (0)	Parkinson's relative (4)	Incomplete (0)		15-07-2017	20-06-2017	16-02-2017	2017-02-21	Wild type (2000)		Wild type (2000)		LSDU RFH (1)	Download	278ng/ul	Yes (1)	Yes (1)
413	baseline	Incomplete (0)	Gaucher's disease (1)	Incomplete (0)		03-04-2017											Yes (1)	No (0)

Fig 15. Screenshot of REDCap database for genotyping sample processing and results

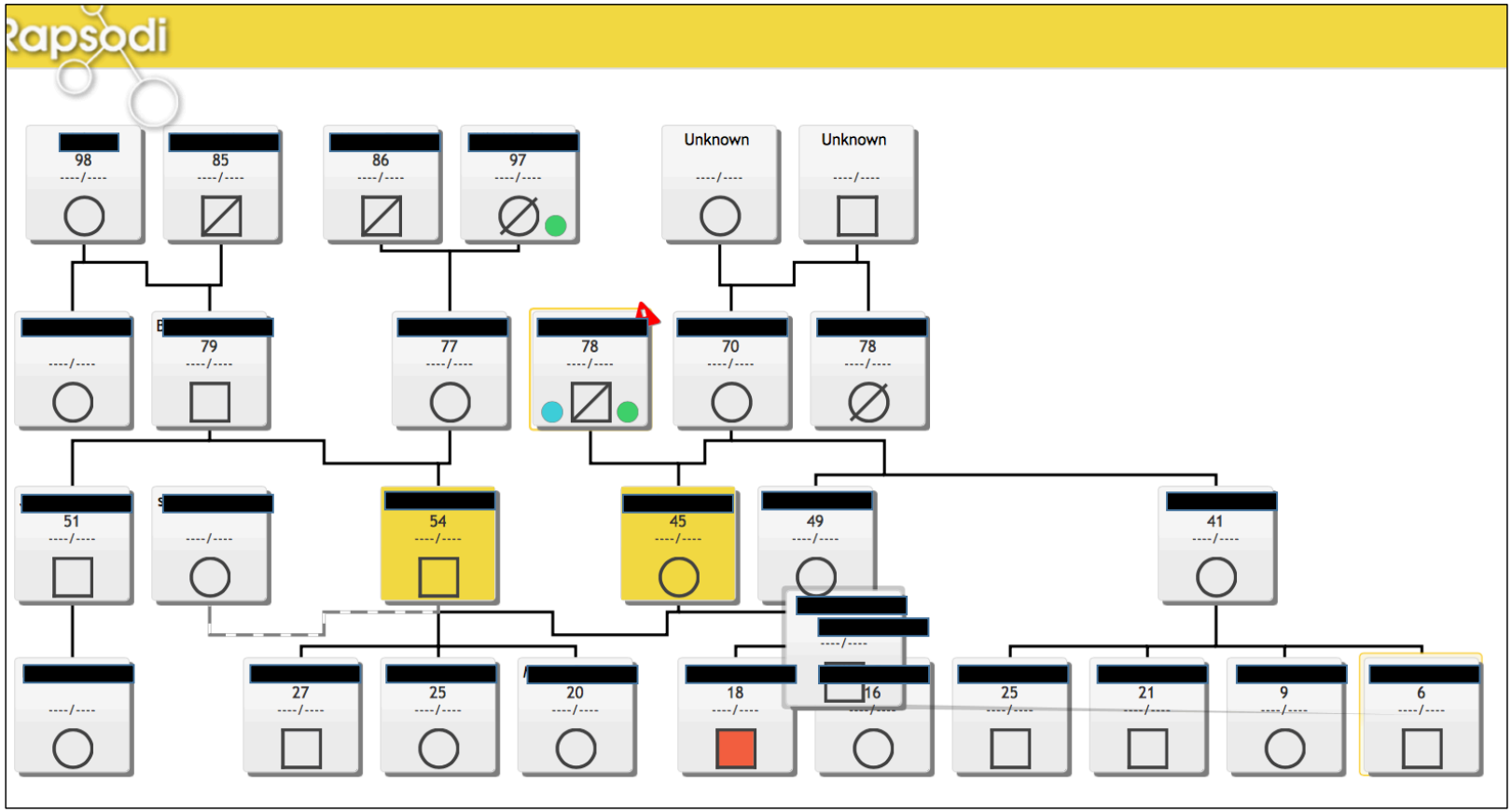

Fig 16. Screenshot of bespoke family tree mapping software developed for the rapsodi portal; the programme can be used to quickly and efficiently recorded detailed and complex family histories as part of the initial telephone consulantion with the patient.

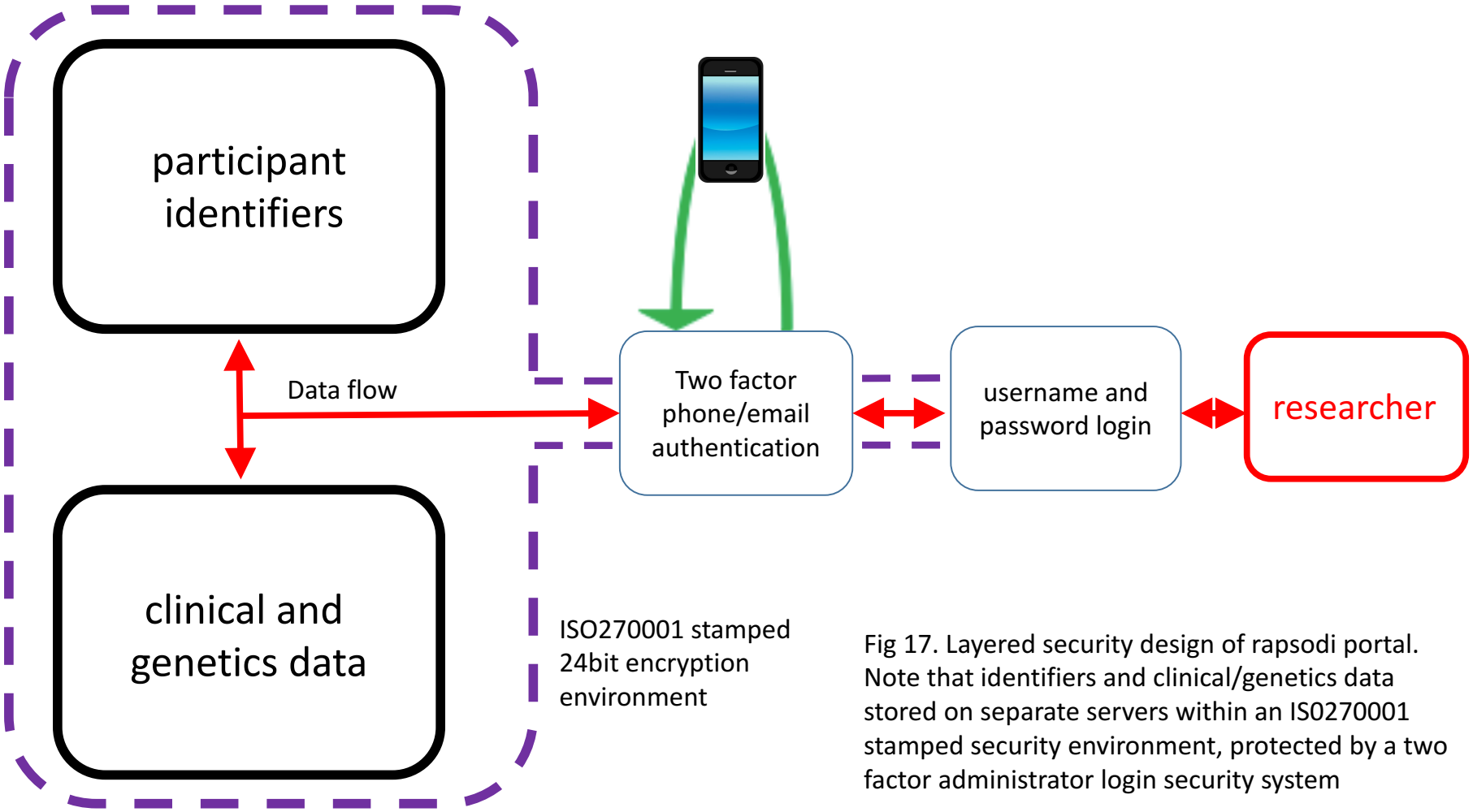

Fig 17. Layered security design of rapsodi portal. Note that identifiers and clinical/genetics data stored on separate servers within an IS0270001 stamped security environment, protected by a two factor administrator login security system

4.8 Cohort Characteristics

Table 1 - Characteristics of rapsodi cohort from September 2016 – May 2017						
		age (yr)	**male (%)**	**fhx Parkinson disease (%)**	**years of full time education (yr)**	**ever smoked (%)**
control N=38	**mean**	51.4	63.2%	34.2%	15.6	28.9%
	median	51.0			16.0	
carrier n=57	**mean**	60.7	49.1%	24.6%	13.1	33.3%
	median	63.0			13.0	
bilalleic N=59	**mean**	49.4	52.5%	28.8%	14.9	30.5%
	median	51.0			15.0	
Parkinson disease N=40	**mean**	64.8	57.5%	30.0%	15.1	20.0%
	median	63.0			16.0	
Significant difference?		**p<0.05**	ns	ns	**p<0.05**	ns

4.9 Analysis plan

Please note at the time of analysis data from the UPSIT assessments was not available

4.10a Questionnaires

Broadly speaking we have adhered to the analysis plan stipulated in **chapter 3**. Examination of data by visual inspection showed that none of the questionnaire assessments was normally distributed. This was mostly due to the ceiling and floor effects of the various assessment. Where recognised clinical thresholds exist we have used these to convert the assessments into an ordinal dataset. These are namely:

- RBDSQ: >5 REM sleep disorder [172]
- HADS: >11 Depression [185]

In these cases we then entered the variables into an ordinal logistic regression model which included the following coovariates; age, sex, FHx Parkinson disease, years of education, smoking status. The primary analysis compared all *GBA* participants with the control group and all Parkinson disease participants with the control group. Subset analysis comparing carrier and biallelic participants individually with controls was then undertaken in the event of a significant correlation of the former.

Where transformation of the dataset into ordinal categories was not possible (UPDRS II) we undertook a Mann U Whitney test once again comparing controls with a) the combined group of *GBA* carriers and b) the Parkinson disease group. Subset analyses then compared individual carrier and bi-allelic groups to controls in the event of associations.

4.10b Bradykinesia akinesia assessment (BRAIN)

The BRAIN test asks the subject to sequentially tap on the "s" and ";" keys as quickly, regularly and accurately as possible. It has three major outputs. The Kinesis score (KS30 - how many tap in 30 seconds), the akinesis time (AT30 - dwell time over keys), the dysmetria score, a weighted index which defines the number of incorrectly hit keys activated (DS30 - 1 point for correct key, 2 points for adjacent key, 3 for other keys) and the variance of the time interval between each keystroke (IS30). Validation studies show it is able to identify Parkinson disease subjects with sensitivity and specificity [183]. A screenshot of the BRAIN test is shown in figure 2.

We began by assessing outcomes for normality. Of the four outcomes outcomes only the KS30 score was parametrically distributed (visual inspection and Schapiro wilks test). For this outcome we elected to use a linear regression model which included age as a covariate to test for significant differences. For the other analyses the distribution was not parametric and so a Kruskal Wallis test was performed and pairwise analyses (comparing control with *GBA*, Parkinson disease, het and biallelic populations) was made using a Wilcoxon rank sum test.

4.10c Cogtrack

Overview of the Cogtrack battery and outputs.

The Cogtrack battery used consisted of the following components:

Simple reaction time (Fig 3).

The subject is asked to repeatedly press on the right key button when a "→ yes" cue appears on the screen. Mean (SRT) and median reaction time (SRT), standard deviation of reaction time (SRTSD) and coefficient of variance are recorded (SRTCV).

Digital vigilance (Fig 4).

The subject is asked to press the right key button when a number cue matching a number permanently placed next to it on the screen appears. Reaction time (VIGRT), Percentage of targets detected (VIGACC), Number of false alarms (VIGFA), Standard deviation of reaction time (VIGSD) and Coefficient of variance of reaction time (VIGCV) are recorded.

Choice reaction time (Fig 5).

The subject is asked to press the left and right buttons in response to cues indicating "press →/← now". Mean (CRT) and median (CRTM) reaction time, reaction time standard deviation (CRTSD) and coefficient of variance (CV%) were all recorded.

Spatial working memory (Fig 6).

A 3x3 grid with lightbulbs in 4 of the boxes in shown. Successively lightbulbs appear in the boxes and subjects indicate whether the light bulb was previously present in the box by pressing left (no) or right (yes). Mean and median reaction time to the original stimuli (i.e

bulbs which were present in the presented image – SPMORT, SPMORTM) and new stimuli (those that weren't – SPMNRT, SPMNRTM), accuracy of response to presented stimuli to original (SPMOACC1) and new stimuli (SPMNACC1), the standard deviation of the reaction time (SPMSD) and the coefficient of variance of the reaction time (SPMCV) are recorded.

Numeric working memory (Fig 7).

A series of numbers are shown. The subject is then asked to assess whether a series of numbers that flash on the screen are part of that original sequence. Mean and median reaction time to the original stimulus (NWMORT and NWMORTM), new stimulus (NWMNRT and NWMNRTM), a combined reaction time to both stimuli (NWMRT and NWMRTM), the standard deviation (NWMSD) and coefficient of variance (NWMCV) are recorded.

Picture recognition task (Fig 8).

A series of images are shown to participants at the beginning of the battery, the images interspersed with distractor images which are similar to the original stimulus (e.g a red car and a blue car, a flag blowing to the right and a flag blowing to the left). For each image the subject selects whether it is an original image (right) or a new image (left). Accuracy of responses to original (DPICOA) and new stimulus (DPICNA), mean and median reaction time to the original (DPICORT, DPICORTM), new stimulus (DPICNRT, DPICNRTM), combined reaction time (DPICRT, DPICRTM), standard deviation of the reaction time (DPICSD), and coefficient of variance of the reaction time (DPICCV) are recorded.

Approach to analysis of dataset.

Validation data (from Wesnes cognition previous research portfolio) exists based on 484 Parkinson disease and 1896 age matched controls exists. These data revealed deficits in a number of domains (Fig 18). Most prominently this was evident in the power of attention. This score is the sum of SRTM, CRTM, VIGRT outputs. Moreover, differences were also noted across the following outcomes SPMORTM, SPMNACC, DPICNACC, DPICNACC, DPICNRTM. Previous data based on assessments of Gaucher patients found deficits in power of attention and speed of memory composite scores [186]. Unfortunately this latter score includes outcomes drawn from the word recognition task that we chose to omit from the battery because our testing showed a disproportionate number of dropouts from this task.

Although guided by these data, given that this is the first time these tools have been used on heterozygote *GBA* carriers, we chose to analyse each output individually and then where possible (power and continuity of attention), to also compare these composite scores.

For each outcome variable normaility was assessed using the Schapiro Wilks test. The overwhelming majority of outcomes failed to meet the criteria for disproval of the null hypothesis that results distribution were non Gaussian (sup. table 7, section 10.4). This left us with a problem. Because formal thresholds were not available for the cogtrack tests we were unable to construct an ordinal regression model and hence were unable to include co-ovariates in the analysis. Although in most respects the populations were broadly balanced, there were discrepancies in the age and years of education which were inherent

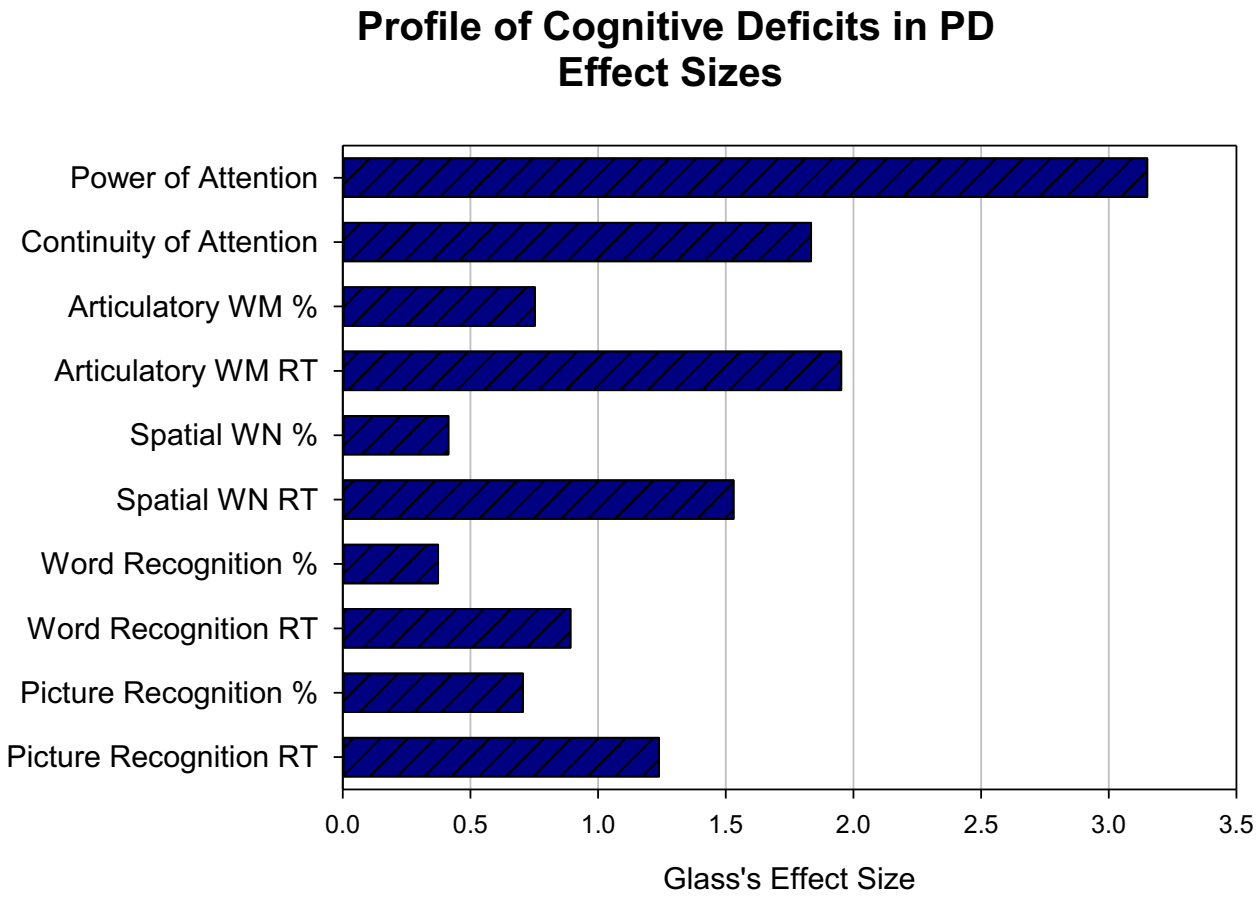

Fig 18. Summary Glass effect size of cogtrack battery comparing 484 PD patients (mean age 66.7 yrs, SD 10.4) and 1896 age-matched controls (courtesy of Prof. Keith Wesnes)

to the study design as described previously. Although sub optimal we chose to analyse the data without taking into account coovariates. We were conscious of the risk of type 1 error due to multiple comparisons, so in the first case a kruschal Wallis test looking for differences between the four study groups. In the event of significant associations we carried out further pairwise analyses comparing 1) *GBA* vs control 2) Parkinson disease vs control 3) carrier vs control 4) biallelic vs control 5) carrier vs biallelic

4.11 Results

Data was collected by SM and Sarah Cable.

4.11a Questionnaires

Descriptive statistics together with statistical test results are shown below in Tables 2 and 3.

Table 2 – Questionnaire scores from, rapsodi portal					
	CTL	**Parkinson disease**	**HET**	**BIA**	***GBA***
RBDSQ , median (mean)	3 (4.0)	5 (5.4)	2 (3.0)	3 (3.2)	2 (3.1)
HADS, median (mean)	5 (8.3)	10 (10.6)	5 (7.2)	8 (8.8)	7 (8.0)
UPDRS II, median (mean)	0 (1.5)	8 (8.9)	0 (2.8)	0 (1.5)	0 (2.1)

Table 3 – significance testing of questionnaires vs controls			
	RBDSQ* OR [95%CI], p value	**UPDRS II** Z score, p value**	**HADS* OR [95%CI], p value**
GBA	0.69 [-0.26-1.81] p=0.453	-0.499 p=0.62	0.57 (0.08-4.10) p=0.581
Parkinson disease	**1.18 [1.14-9.35] p=0.027**	**-5.688 p<0.0001**	1.02 (0.12-8.17) p=0.980

*Ordinal logistic regression **Wilcoxon rank sum

These findings are interesting in that for both RBDSQ and UPDRS II the assessments were able to show definable deficits amongst Parkinson disease subjects. This is not suprising in

itself, however does show that within this population these symptoms can be detected by remote online assessment. The HADS score shows no difference between the Parkinson disease and control group. Exploration of the dataset shows that the median values are distinct. The thresholding value 5/6 may not adequately differentiate the differences in depression scores between the two groups. Indeed a Wilcoxon rank sum pairwise analysis using the continuous data does show a significant difference (z=-2.129 p=0.033) between the two, which perhaps implies the thresholding value is too low. Altogether, using a positive control population of those with established Parkinson disease, these data suggests this approach is able to detect these prodromal Parkinson disease features.

It is unsurprising that the assessments were not able to discern any differences in UPDRS II, HADS or RBDSQ scores. Associations using only marginally smaller group sizes were not seen in **chapter 3.**

4.11b Bradykinesia akinesia assessment (BRAIN)

group	KS30	AT30 (msec)	DS30	IS30
control mean	57.82	83.54	1.04	74549.77
control median	60.00	77.50	1.00	13514.33
heterozygote mean	54.74	101.69	1.04	68335.57
heterozygote median	53.00	88.00	1.00	17588.59
biallelic mean	60.50	84.50	1.09	31627.65
biallelic median	60.00	80.00	1.00	6402.78
***GBA* mean**	58.32	93.07	1.06	51063.86
***GBA* median**	58.00	82.00	1.00	9768.34
Parkinson disease mean	48.40	102.05	1.04	96806.40
Parkinson disease median.	46.50	94.50	1.00	36413.95

Table 4. Summary outputs of BRAIN test

These analysis is shown below and box plots are displayed in figures 19-21.

group	Coef.	t	p value	95% CI
heterozygote	-.5558149	-0.18	p=0.859	[-6.73-5.62]
biallelic	0.4292081	0.15	p=0.883	[-5.36- 6.22]
Parkinson disease	-7.352564	-2.06	**p=0.042**	[-14.42-0.28]

Table 5. Linear regression results of KS30 model including age and study group

	multivariate	Parkinson disease	*GBA*	het	bia
AT30	p=0.1915				
IS30	**p=0.0151**	**p=0.0248**	p=0.9605	p=0.3805	P=0.3496
DS30	p=0.8246				

Table 6. Kruskal Wallis (+/- spearman's rank) testing for differences between study groups.

For the KS30 and AT30 significant differences were shown between the Parkinson disease and control groups. These results are unsurprising, although do prove the utility of the tool in these studies. Otherwise there are no significant differences between *GBA* carriers and controls, although there are hints of a trend toward this result in terms of the KS30, AT30 and IS30 scores in the heterozygote group. This trend is, however, not replicated amongst the biallelic group. One explanation might be that these participants are younger. Our regression model clearly showed that age was a highly significant determinant of the KS30 score ($p<0.0001$), and accordingly the fact that this group is some 10 years younger may provide an explanation for the difference. To date we have found no convincing evidence of motor deficits aside (amongst these patients) from trends amongst the UPDRS II and III scores (chapter 2) and quite simply it may be that such deficits do not exist. Alternatively it may be that a more stratified approach is required which we shall discuss more in depth at the conclusion of the chapter.

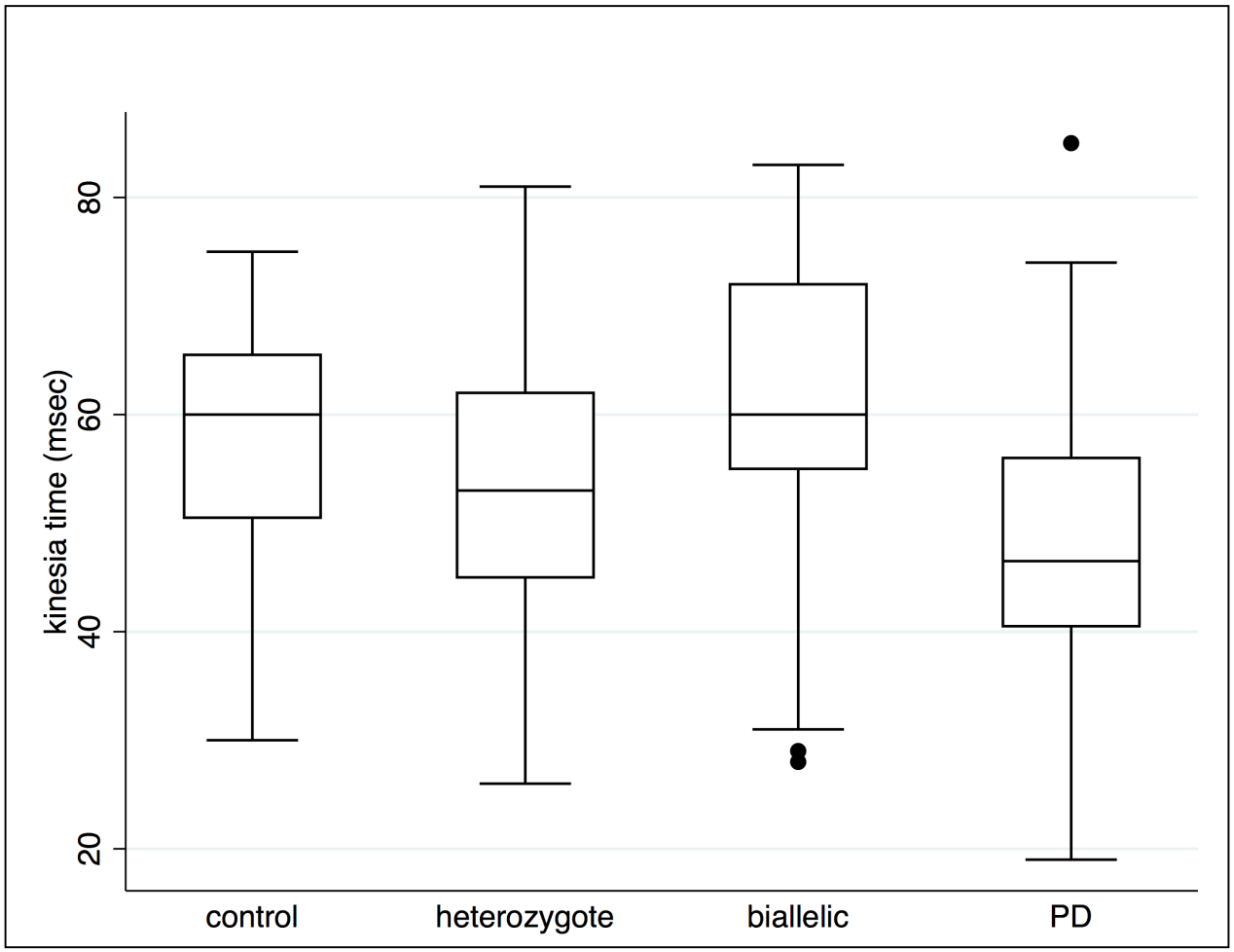

Fig.19 Box plots of kinesia times (KS30) of control, hetrozygote, biallelic and PD individuals. NB no significance bar as regression model used.

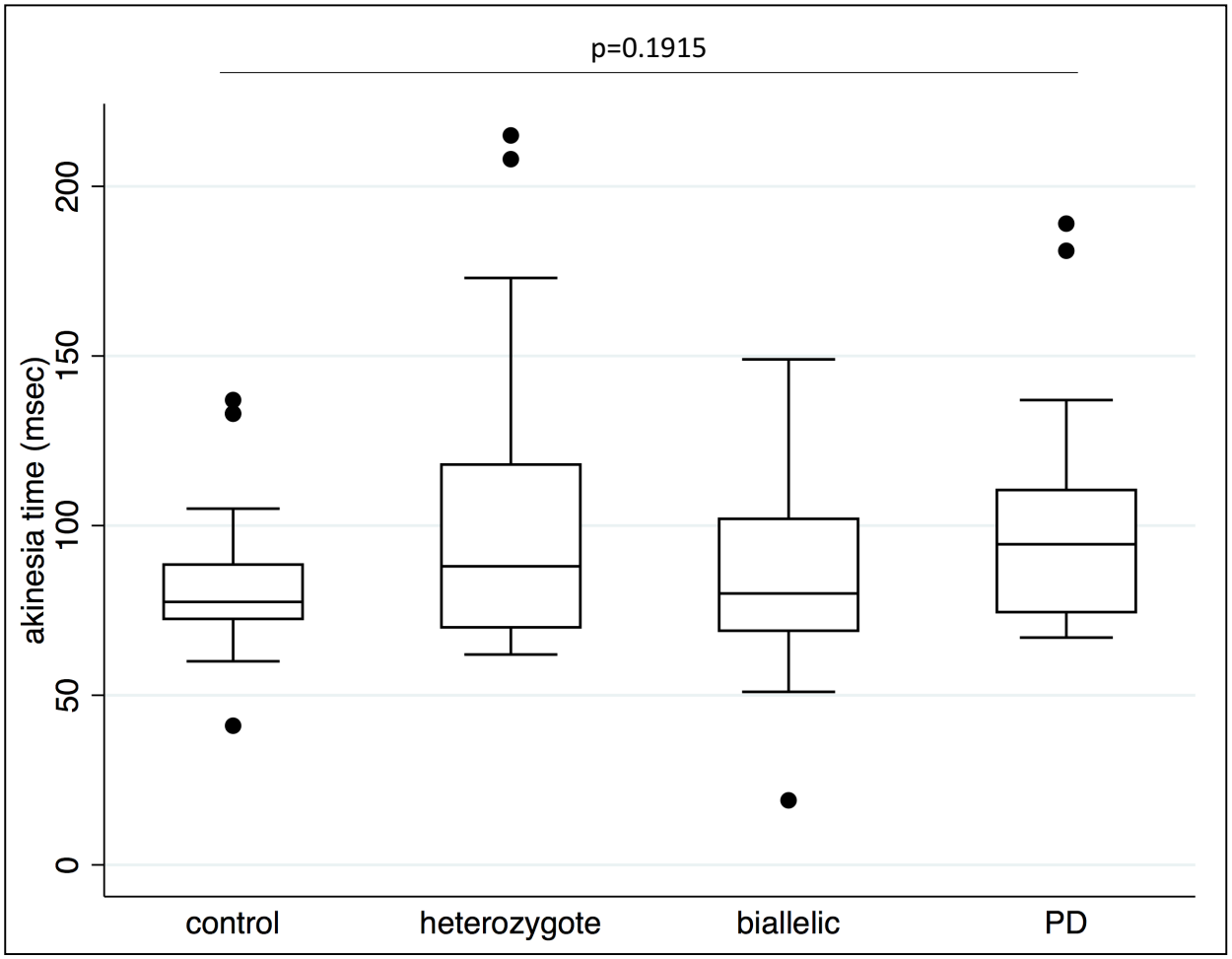

Fig.20 Box plots of akinesia times (AT30) of control, hetrozygote, biallelic and PD individuals

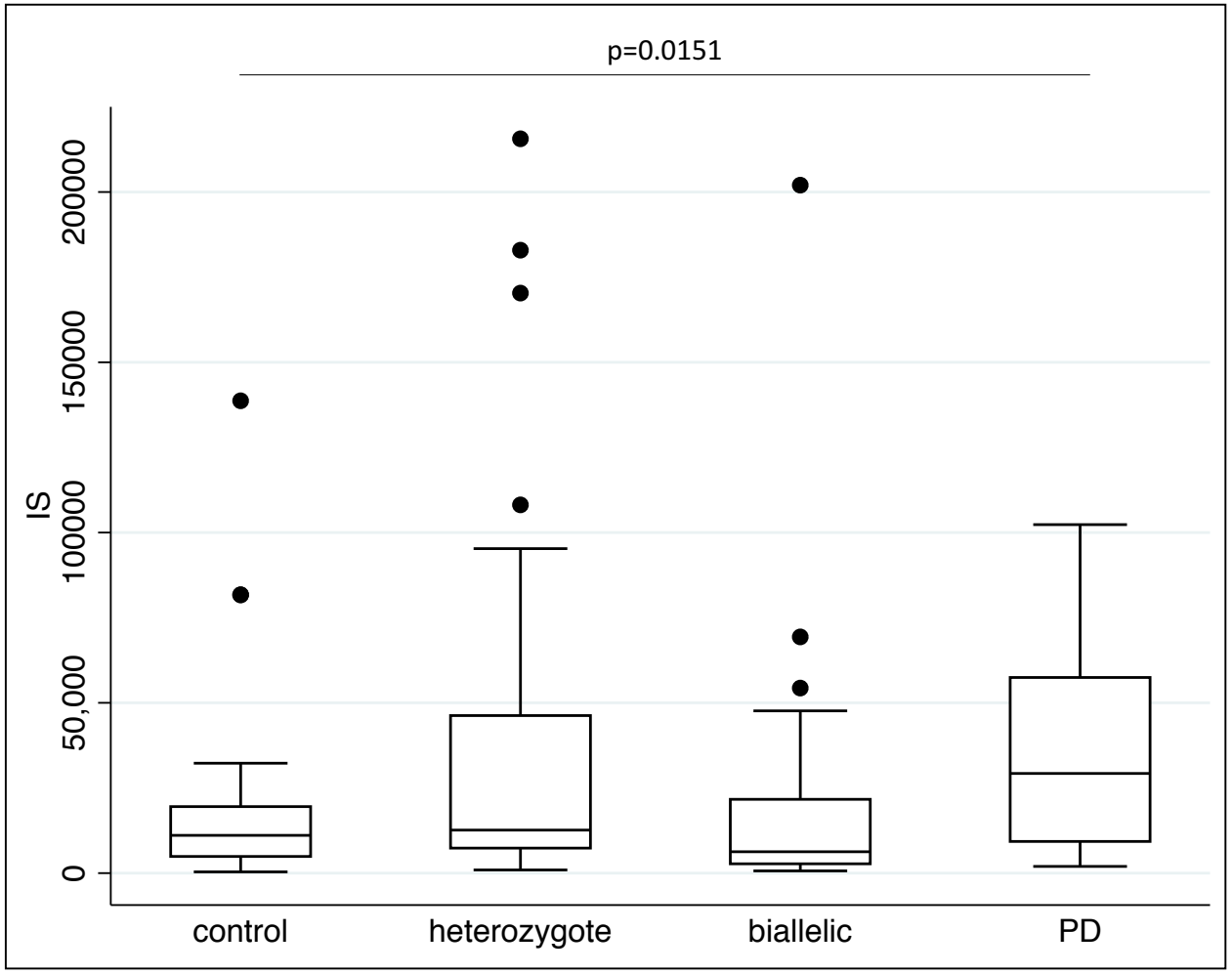

Fig.21 Box plots of IS30 score of control, hetrozygote, biallelic and PD individuals

4.11c Cogtrack

A total of 171 (25 controls, 55 carriers, 52 biallelic, 38 Parkinson's) undertook the cogtrack battery. A summary table of statistics (median and mean) for the outputs are displayed in the appendices (supp. table 6, section 10.4). Analyses based on the plan described above are shown in table 7.

Visual memory is impaired in all groups compared to controls.

GBA carriers appear to display deficits in reaction time across a range of tasks. The most interesting finding is the very consistent differences in reaction times compared to controls amongst all groups in the spatial working memory task. Moreover in *GBA* and biallelic vs control subjects significance differences exist in terms of the accuracy of response to the original stimulus (and this is mimicked in terms of strong trends in the other two pairwise analyses (carrier z=1.876 p=0.0607, Parkinson disease z=1.954 p=0.0507). Box plots of these outputs are displayed in Figures 22-23.

Visual deficits are an established field of enquiry in the context of Parkinson's[187] and there is evidence this is a disproportionate feature amongst *GBA* Parkinson's cases. [33] It is therefore striking that amongst this task the differences in reaction times are so prominent. The task combines tests of both visual memory and visual perception, therefore it would be interesting if future assessments could further dissect the relative contributions of the two processes.

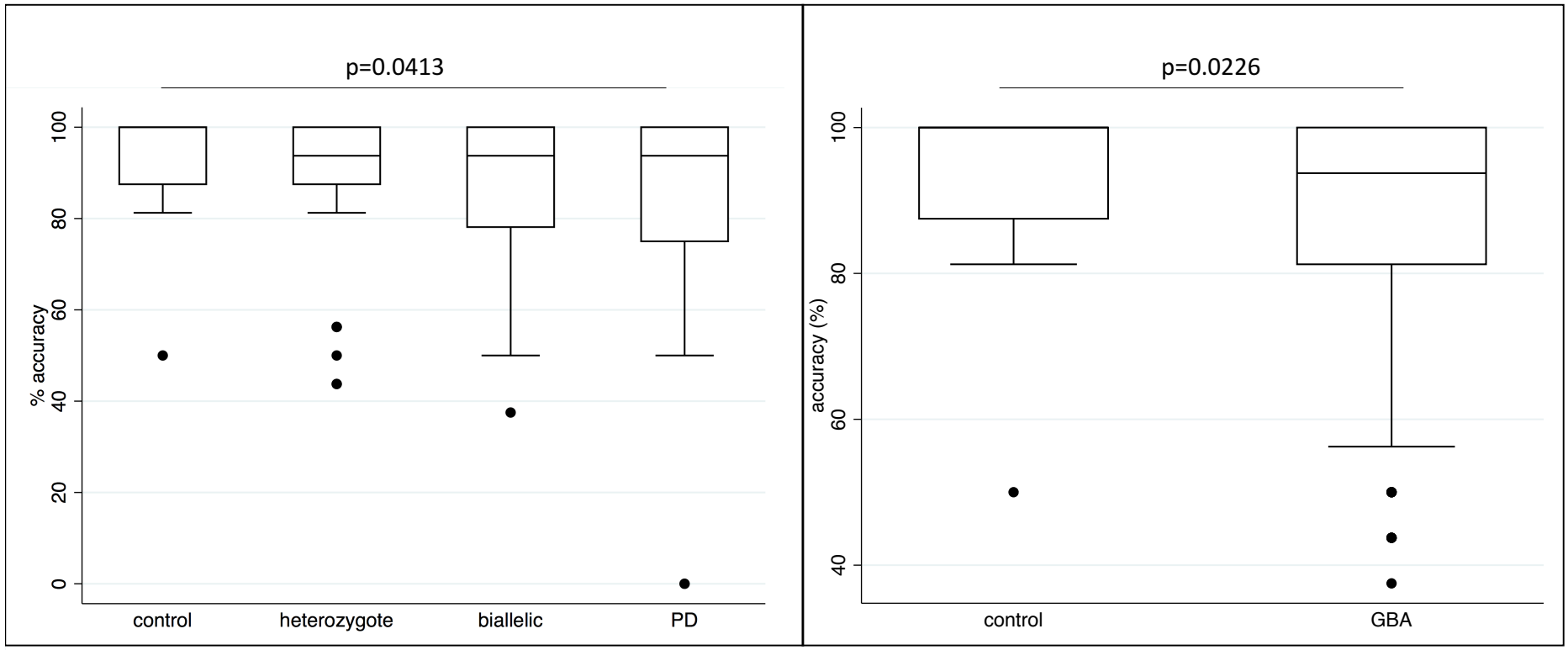

Fig.22 Box plots of % accuracy of response in spatial working memory task (SPMACC) of control, hetrozygote, biallelic and PD individuals

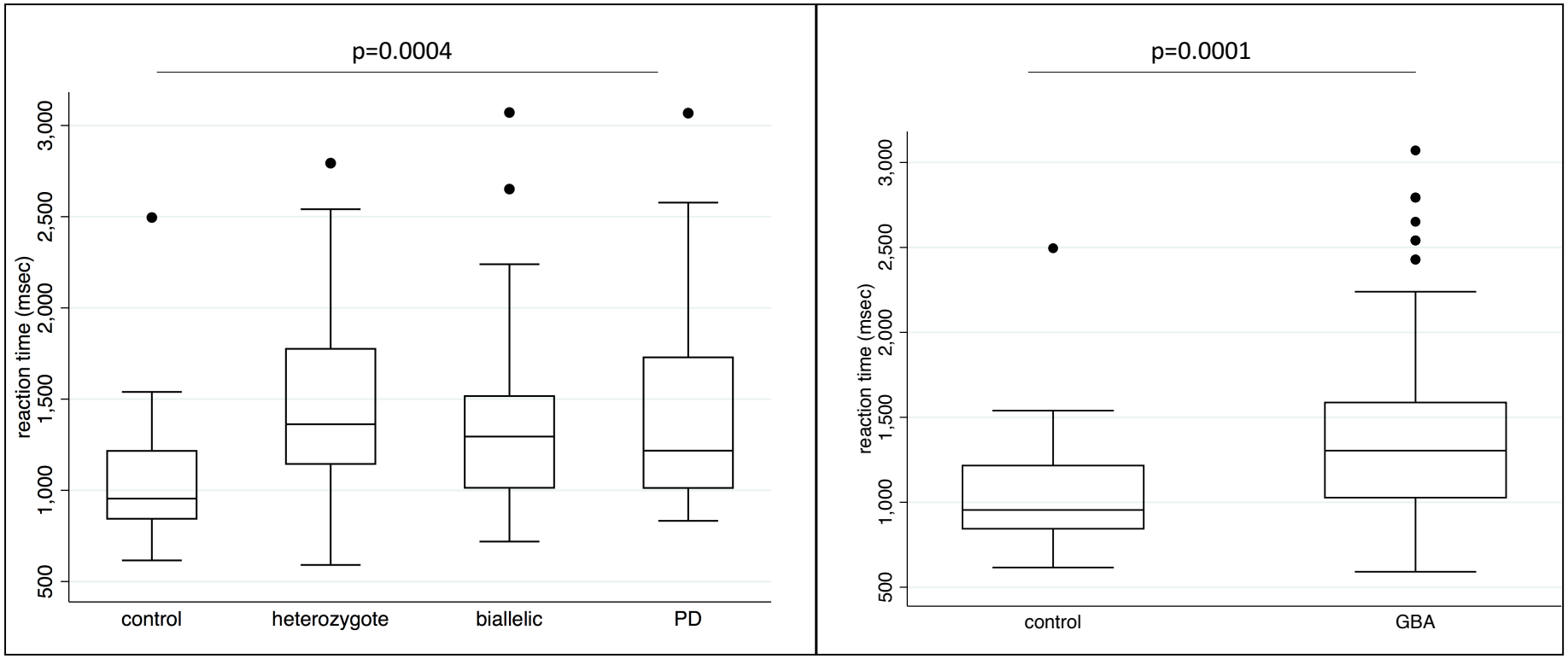

Fig.23 Box plots of reaction time in spatial working memory task (SPMRT) of control, heterozygote, biallelic and PD individuals

More generally its seems that there are deficits in the reaction times of all groups compared to controls. This is consistent with previous validation data which found that the power of attentions composite score is reduced in Parkinson disease subjects (Fig 18). The continuity of attention composite is comprised of the reaction time elements of the simple reaction time, choice reaction time and digital vigilance tasks and was reduced in *GBA* vs CTL and HET vs CTL in these data. Trends (biallelic z=-1.414 p=0.1572 and Parkinson disease z=-1.546 p=0.1221) were present amongst the other two groups. It is likely therefore that given sufficient power all study groups would show a significant result.

These results are primarily informative because they will allow rationalisation of the portal in order to minimise the number of tests undertaken. The intent of the rapsodi project is, rather than to phenotype the cognitive impairment present in these participants, to provide a screening assessment which will enable stratification of the cohort. The current battery takes on average 20min. Retention within the study is aided by making the patient experience as quick as possible, hence we hope the basis of these results, to rationalise the battery based on the most sensitive assessments.

4.12 Concluding remarks

In this chapter we have demonstrated the utility of an internet based assessment for prodromal Parkinson disease features amongst *GBA* carriers. It will hopefully assure the sustainability of the assessment of cohorts of *GBA* carriers for these signs and the drastic enlargement of this cohort. Significant differences were recorded for aspects of the

cognitive assessment; in particular reaction times across the board (and in particular for spatial working memory tasks) showed consistent and definable deficits. In terms of the other assessments it may be that increased study numbers may bring these deficits out, or on the other hand that by identifying outliers within the groups we may be able to define higher risk individuals.

The process of optimisation of rapsodi is still underway and is unremitting, as the key will be making the process of prospective assessment as simple and engaging as possible and refining and scaling the processes. New challenges lie ahead such as incorporating and validating the use of touch screen devices. That said, the promise of such an approach is nearly limitless. For instance there is the very real prospect of incorporating biomarkers such as GCase activity (which can be collected on peripheral blood spots) into the assessment process. Stratification of the cohort into high and low risk participants could

Table 7. Significance testing for outputs for cogtrack battery											
x	**multivariate**	***GBA* vs CTL**	**Parkinson disease vs CTL**	**HET vs CTL**	**BIA vs CTL**	**test**	**multivariate**	***GBA* vs CTL**	**Parkinson disease vs CTL**	**HET vs CTL**	**BIA vs CTL**
SRT	**p=0.0092**	**p=0.001**	ns	**p=0.0015**	**p=0.049**	**SPMSD**	**p=0.0054**	**p=0.0012**	**p=0.0011**	**p=0.0041**	**p=0.0021**
SRTM	**p=0.0351**	**p=0.014**	ns	ns	**p=0.007**	**SPMCV**	**p=0.0040**	**p=0.0035**	**p=0.0009**	**p=0.0066**	**p=0.0085**
SRTSD	ns	-	-	-	-	**NWMOACC**	ns	-	-	-	-
SRTCV	ns	-	-	-	-	**NWMNACC**	ns	-	-	-	-
VIGACC	ns	-	-	-	-	**NWMORT**	**p=0.0117**	**p=0.0174**	**p=0.0097**	**p=0.0048**	ns
VIGRT	**p=0.0001**	**p=0.0024**	**p=0.0003**	**p=0.0003**	ns	**NWMNRT**	ns	-	-	-	-
VIGFA	**p=0.0065**	ns	ns	ns	**p=0.0282**	**NWMRT**	ns	-	-	-	-
VIGSD	**p=0.0062**	**p=0.0161**	**p=0.0004**	**p=0.0058**	ns	**NWMORTM**	**p=0.0235**	ns	ns	**p=0.0115**	ns
VIGCV	ns	-	-	-	-	**NWMNRTM**	ns	-	-	-	-
CRTACC	ns	-	-	-	-	**NWMRTM**	**p=0.0400**	ns	**p=0.0204**	ns	ns
CRT	**p=0.0179**	ns	ns	**p=0.0403**	ns	**NWMSD**	**p=0.0495**	**p=0.0100**	**p=0.0076**	**p=0.0137**	**p=0.0250**
CRTCV	-	-	-	-	-	**DPICNA**	ns	-	-	-	-
SPMOACC	**P=0.0413**	**p=0.0226**	ns	ns	**p=0.0197**	**DPICORT**	ns	-	-	-	-
SPMNACC	ns	-	-	-	-	**DPICNRT**	ns	-	-	-	-
SPMORT	**p=0.0026**	**p=0.001**	**p=0.0094**	**p=0.0003**	**p=0.0182**	**DPICRT**	ns	-	-	-	-
SPMNRT	**p=0.0010**	**p=0.0001**	**p=0.0025**	**p=0.0002**	**p=0.0008**	**DPICORTM**	ns	-	-	-	-
SPMRT	**p=0.0004**	**p=0.0001**	**p=0.0007**	**p=0.0001**	**p=0.0021**	**DPICNRTM**	ns	-	-	-	-
SPMNRTM	**p=0.0024**	**p=0.0021**	ns	**p=0.0015**	**p=0.0139**	**DPICSD**	ns	-	-	-	-
SPMRTM	**p=0.0002**	**p=0.0001**	**p=0.0134**	**p<0.0001**	**p=0.0047**	**DPICCV**	ns	-	-	-	-
Composite scores											
POA	**p=0.0097**	**p=0.0151**	ns	**p=0.0027**	ns						

allow development of new biomarkers of Parkinson disease conversion. There is a realistic prospect of extending the study of a multinational basis to other Parkinson disease and Gaucher cohorts. Such big data allows us to tackle questions touched on already in this thesis, such as the risk associated with the 300 individual Gaucher associated *GBA* mutations in terms of Parkinson disease or the role of other genetic and epigenetic modifiers in this conversion.

Chapter 5 - Novel biomarkers implicating neuroinflammation in the aetiology of *GBA* Parkinson disease

5.0 Introduction

Biomarkers which correlate with the conversion to Parkinson disease amongst *GBA* carriers are of interest for two reasons. In the first case they may help to identify those who are at high risk of conversion to allow targeting of novel neuroprotective therapeutics. More broadly they may have relevance as screening tools to identify those in the prodromal phase of idiopathic Parkinson disease. We have discussed the use in **chapter 4** of clinical assessments to identify features of the so called prodromal phase of Parkinson disease. These assessments are cheap, non invasive and as we have shown have utility in the context of an internet based assessment portal, making their use in population based screening plausible. That said the features they define are on the whole common and although we have presented evidence of clustering in certain subjects, in isolation they may be insufficient to adequately define who is at risk of Parkinson disease conversion. In this case a second line of screening and assessment may increase their specificity. As such there is a requirement for robust markers of Parkinson disease conversion amongst *GBA* carriers. In this chapter I shall describe various experiments which have attempted to validate and reveal novel biomarkers of Parkinson disease conversion amongst *GBA* carriers, namely PET imaging assessing for dopaminergic loss and glial inflammation, serum ELISA antibody screening for a number of known neurodegenerative and inflammatory markers and a hypothesis generating screen in the urine of *GBA* carriers with evidence of prodromal Parkinson disease signs. Our findings directly implicate the established alpha synuclein

pathway is the pathogenesis of Parkinson disease conversion amongst *GBA* carriers as well more broadly highlighting the role of central nervous system inflammation (and to an extent peripheral inflammation) in this process.

5.1 PET imaging of dopaminergic loss and glial activation

5.2 PET imaging

PET imaging is an established diagnostic tool in Parkinson's and other neurodegenerative conditions. Ligands designed to mimic molecules (such as glucose) or to bind to epitopes on other proteins (such as beta amyloid) accumulate in the brain. Gamma rays emitted indirectly by the positron emitting radionucleotide attached to the biologically active molecule are detected and form the basis of images produced. PET's use in Parkinson's is established. SPECT Dopamine active transporter (DAT) has been shown to be able to detect dopaminergic loss within the brain of Parkinson's patients with sensitivity and specificity [188]. SPECT imaging measuring cerebral perfusion has been shown to increase the specificity of the diagnosis of Alzheimer's disease and ligands which bind to the beta amyloid appear to be able to detect the accumulation of plaques in the brain [189]. It would therefore seem the obvious tool to investigate *in vivo* processes ongoing in those at higher risk of developing Parkinson disease.

5.3 PET imaging of GBA mutation carriers

Only a few molecular imaging studies have investigated the integrity of the dopaminergic nigrostriatal system in Parkinson disease patients positive for *GBA* mutations and the

number of patients included is limited. Reduced striatal ^{18}F-DOPA uptake has been observed [190,191] as has reduced striatal dopamine transporter (DaT) binding [192,193] and altered striatal asymmetry [194]. There have to date been no PET imaging studies in *GBA* carriers who do not Parkinson disease.

5.4 Neuroinflammation in Parkinson disease

Since the discovery of increased numbers of MHC class II activated glial cells in the substantia nigra of Parkinson's patients [195,196] neuroinflammation and specifically the role of glial activation in the aetiology of Parkinson disease has been closely scrutinised [197] Under normal physiological conditions, microglia are quiescent and distributed across the central nervous system. However, microglia become activated in response to a pathologic insult, primarily at the site of injury, causing a prolonged release of pathological cytokines [198] Epidemiological evidence suggests a protective effect associated with various non steroidal anti inflammatory drugs.[199-201] Genetic studies have shown that a number of polymorphisms in the TNF alpha and other immunomodulatory genes have protective or causative effects in terms Parkinson disease development [202,203]. A number of studies have found upregulated levels of various peripheral cytokines in Parkinson disease patients implying that peripheral immune upregulation may be a surrogate of these central inflammatory processes [204-206]. Thus there is significant evidence from a number of sources of a role for immune dysregulation in the aetiology of Parkinson disease, it however remains to be seen whether central immune modulation is a pathogenic or protective mechanism.

5.5 Immune dysregulation in Gaucher disease

Immune dysregulation is a profound feature of Gaucher disease and has been linked to a variety of clinical phenotypes. [207-210] Although limited post mortem data exists from neuronopathic Gaucher diseasepatients, glial activation does appear to be an established feature [48,211], and these findings are replicated in mouse models of the disease [212]. Peripherally, Gaucher disease patients have been shown to have upregulation of IL-6 and 10 [213]. Given the correlation of those neuronopathic Gaucher diseasemutations with increased Parkinson disease pathogenicity [22], it would seem plausible that neuroinflammation forms a significant aspect of *GBA* Parkinson disease.

5.6 PK11195 – a ligand for the detection of glial activation

The isoquinolone PK11195 is an experimental ligand which is thought to bind to regions of microglial activation. It is a partial antagonist of central benzodiazepine receptors associated the GABA related channels, however what the exact source of the upregulation of PK11195 binding is in the presence of microglial activation is not clear. Variously PK1195 has been described to bind to astrocytes, various haematogenous infiltrates and microglial cells themselves.[198] None the less it appears to be a robust *in vivo* measure of glial upregulation as shown by a number of *in vivo* studies [51,214,215]. Two studies using the ligand have shown upregulation of PK11195 binding in the midbrain and brainsterm respectively [49,216] and additionally in the former within the frontal and temporal cortex [216]. On the basis of these findings we selected the PK11195 ligand as suitable investigative paradigm for qualification

of the role of central nervous system glial activation and neuroinflammation in non Parkinson disease *GBA* carriers.

5.7 Aims

1) To investigate whether dopaminergic loss and glial activation are present in pre specified regions of interest in the brains of *GBA* carriers.
2) To see whether these changes correlate with the presence of features of prodromal Parkinson disease, mutations severity, GCase activity and various serum biomarkers of neurodegeneration/inflammation.

5.8 Methods

The current study was conducted between the 16th of November 2015 and 17th of November 2016. Nine subjects who were either bilallelic (homozygous or compound heterozygous) or heterozygous carriers of a Gaucher disease associated *GBA* mutation (Table 1) were recruited from an established cohort at the Department of Clinical Neuroscience, University College London, United Kingdom to participate in the current PET study. All subjects were genotyped at the lysosomal storage disease unit (LSDU), Royal Free hospital London, UK, using a two stage process of high resolution melting of exons 1-11 of the *GBA* gene with subsequent sanger sequencing of any exons which deviated from the reference curve. Biallelic carriers were all type 1 (non neuronopathic) Gaucher disease subjects whilst heterozygous carriers were drawn from kindred of Gaucher diseasepatients.

No subjects in this study were genetically related. GBA subjects were recruited by SM, controls were recruited by Dr Morten Stokholm.

Carriers were each examined with two PET scans using ^{11}C-PK11195 and ^{18}F-DOPA, one MRI scan, and a clinical neurological examination. Prodromal Parkinson disease features were further characterised with the following assessment scales: University of Pennslyvannia smell identification test (UPSIT – hyposmia) [169], Montreal cognitive assessment (MoCA - cognition) [170], Rapid eye movement sleep behaviour disorder questionnaire (RBDSQ - REM sleep behavious disorder) [172], Non motor symptoms scale (NMSS – non motor Parkinson disease features) [217,218], Unified Parkinson disease rating scale parts II and III (UPDRS II & III – motor symptoms and signs of Parkinson disease) and Beck's depression inventory (BDI) [171].

All scans and examinations were performed at the Department of Nuclear medicine & PET centre, Aarhus University Hospital, Denmark. For comparison of PET studies, in-house PET data from 29 healthy controls subjects were included, 20 healthy controls with ^{11}C-PK11195 PET and 9 with ^{18}F-DOPA PET. These control subjects have been previously recruited recruited [219].

5.8a PET and MRI

In brief, PET scans were performed on an ECAT HRRT CTI/Siemens system with an intravenously injection of tracer and dynamic PET images were obtained for 60.5 and 94.5 minutes and subsequently rebinned into 24 and 26 frames, for ^{11}C-PK11195 and ^{18}F-DOPA respectively. One hour prior to ^{18}F-DOPA PET an oral 150 mg dose of carbidopa was

administered to the participants. Both image series were reconstructed using 3D OSEM (ordered subsets expectation maximization) and resolution recovery modelling (PSF) with 10 iterations and 16 subsets. Reconstructed images consisted of 207 axial image slices with a 1.22 mm voxel size. Each study participant had a structural MRI 3D sequence performed for co-registration of PET images (3 T MAGNETOM Skyra or Trio, Siemens Healthcare).

5.8b Image analysis

PET images were examined with a region of interest (ROi) approach using the PNEURO module in PMOD software v 3.6 (PMOD technologies Ltd. Switzerland) and at a voxel level using Statistical Parametric Mapping (SPM12, Wellcome Trust Centre for Neuroimaging, UCL). Image analysis was performed as previously described [219]. In brief, parametric maps with regional binding potentials (BP_{ND}) and influx constants (Ki) were generated for the ^{11}C-PK11195 and ^{18}F-DOPA PET images, respectively. It is reasonable to expect that microglial activation may be present throughout the brain in a population at-risk of developing neurodegenerative disorders. In view of this, one cannot depend on an anatomic brain region devoid of specific ligand binding to be used as reference region. Therefore, we used the supervised cluster analysis to extract an individual reference tissue non-specific input function and the simplified reference tissue model [219] to generate parametric BP_{ND} maps with ^{11}C-PK11195. The ^{18}F-DOPA parametric maps with influx constants (Ki) were generated using the Patlak graphical approach with occipital lobe grey matter as a non-specific reference tissue input function. The equilibration time was set to 25 minutes. Image analysis was carried out by Dr Morten Stokholm.

5.8c Selection of regions of interest

The caudate and putamen have been established to be the most sensitive areas of the brain for detecting dopaminergic loss using the ^{18}F-DOPA ligand and hence were selected as sole regions of interest for the ^{18}F-DOPA analysis. ^{11}C-PK11195 is an experimental ligand which binds in the presence of migroglial activation. Previously signal was increased amongst early Parkinson disease cases across the basal ganglia, therefore the pallidum, caudate and substantia nigra were selected as regions which were representative of this region.

5.8d Statistical analysis

Statistical analyses and graphs were performed on Stata v14.2 (StataCorp 4905 Lakeway Dr., College Station, TX 77845). Distributions of DOPA and ^{11}C-PK11195 signal intensity and Parkinson disease prodromal assessments were assessed by visual inspection. Because all distributions could not consistently be confirmed to be parametric DOPA and PK signal for specified regions of interest were compared in carrier and control groups using the Wilcoxon Rank sum test ($p<0.05$). Secondary analyses were undertaken correlating ^{18}F-DOPA /^{11}C-PK11195 signal intensity with prodromal risk scores, GCase activity, number of severe mutatations possessed and serum ELISA quantification of levels of alpha synuclein, IL6, IL8, TNF alpha (Spearman's rank test, $p<0.05$). Statistical analysis was carried out by SM.

5.9 Results (PET imaging)

Nine *GBA* positive carriers (5 biallelic and 4 heterozygote) and 29 age and sex matched controls were included in the final analysis. Demographics and clinical characteristics of the *GBA* positive and control participants are listed in table 1. Genotypes of the *GBA* carriers are listed in table 2.

Table 1. Characteristics of control and *GBA* carrier groups					
	Bi-allelic *GBA*	**Heterozygous *GBA***	**Combined *GBA***	**Control (PK11195)**	**Control (F-DOPA)**
N	**5**	**4**	**9**	**20**	**9**
mean age [median] (yr)	64.5	62	63.5	66.5	64.7
male (%)	50.0	40.0	44.4	55	56
% with a severe mutation	60.0	50.0	55.5	-	
mean UPSIT [median]	33.5 [33.5]	32.0 [31]	32.7 [33]	-	
mean MoCa [median]	27.0 [26]	28.0 [29]	27.6 [27]	-	
mean MMSE [median]	29.8 [30]	27.6 [28]	28.6 [29]	-	
mean UPDRS II [median]	1.8 [1]	3.0 [3]	2.4 [2]	-	
mean UPDRS III [median]	13.3 [10]	5.8 [6]	9.1 [6]	-	
mean BDI [median]	2.5 [3]	3.4 [4]	3.0 [3.2]	-	
mean NMSS [median]	10.5 [13.25]	16.8 [16]	15.2 [15]	-	
mean GCase activity [median]	1.34 [1.34]	8.53 [7.52]	4.77 [1.98]		

Table 2. Mutations of *GBA* carrier group; *denotes severe mutation, **denotes null mutation	
Biallelic	**Heterozygous**
N370S/*L444P**	*N370S*/wt
N370S/IVS 2+1*	*N370S*/wt
N370S/F216Y	V394L*/wt
N370S/R359X**	*RecNcil* (*L444P*/*A456P*/V460V)*/wt
N370S/V447E	

5.9a GBA carriers exhibit microglial activation restricted to substantia nigra but without evidence of dopaminergic loss

Of the regions of interest surveyed (full breakdown in table 3) only the substantia nigra showed a significant increase in ^{11}C-PK11195 uptake (Wilcoxon rank sum, left p=0.0008, right p=0.0016) amongst *GBA* carriers compared to controls (Figure 1). Increased nigral uptake was relatively consistent across the *GBA* group compared to controls (Figure 1). The specificity of the increase in glial activation is intriguing. One might expect a more generalised increase in PK11195 uptake in these patients, but the very defined increase in inflammation in the region most prominently affected neuropathologically in Parkinson disease implies that some as yet unknown factor makes the region especially prone to glial activation of this type. There is already a substantial literature on the selective vulnerability of this and other regions preferentially affected in Parkinson disease [77,220,221]. Whatever its underlying basis, the implication of these findings is that to some extent, the biochemical process that lead to Parkinson disease conversion is ongoing to a variable extent in the vast majority of *GBA* Parkinson disease carriers with the caveat that in only a proportion will it be sufficient to cause the development of motor Parkinson disease features [14]. There was no

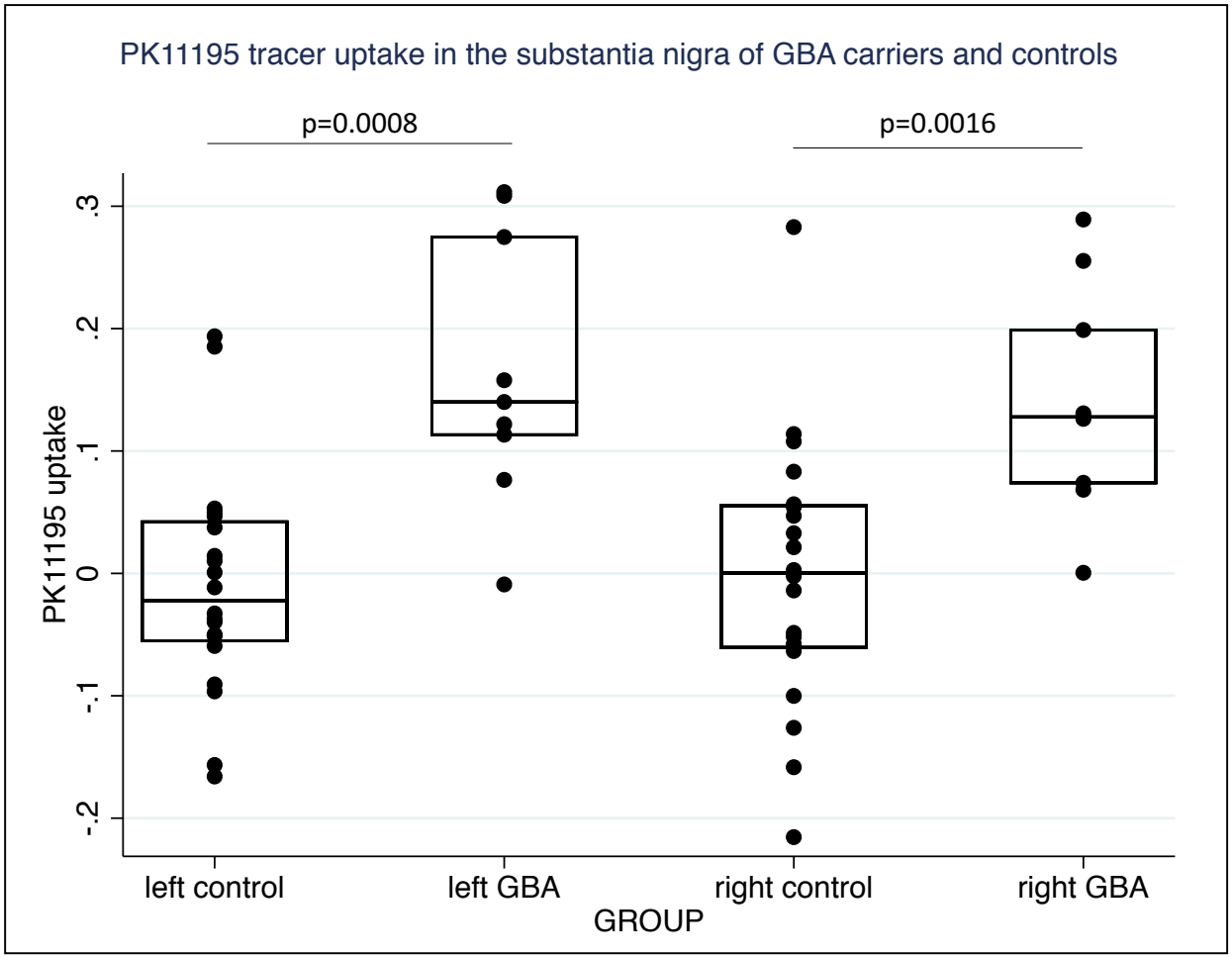

Fig 1. Box plots of PK11195 uptake in the left and right substantia of control and GBA carrier participants

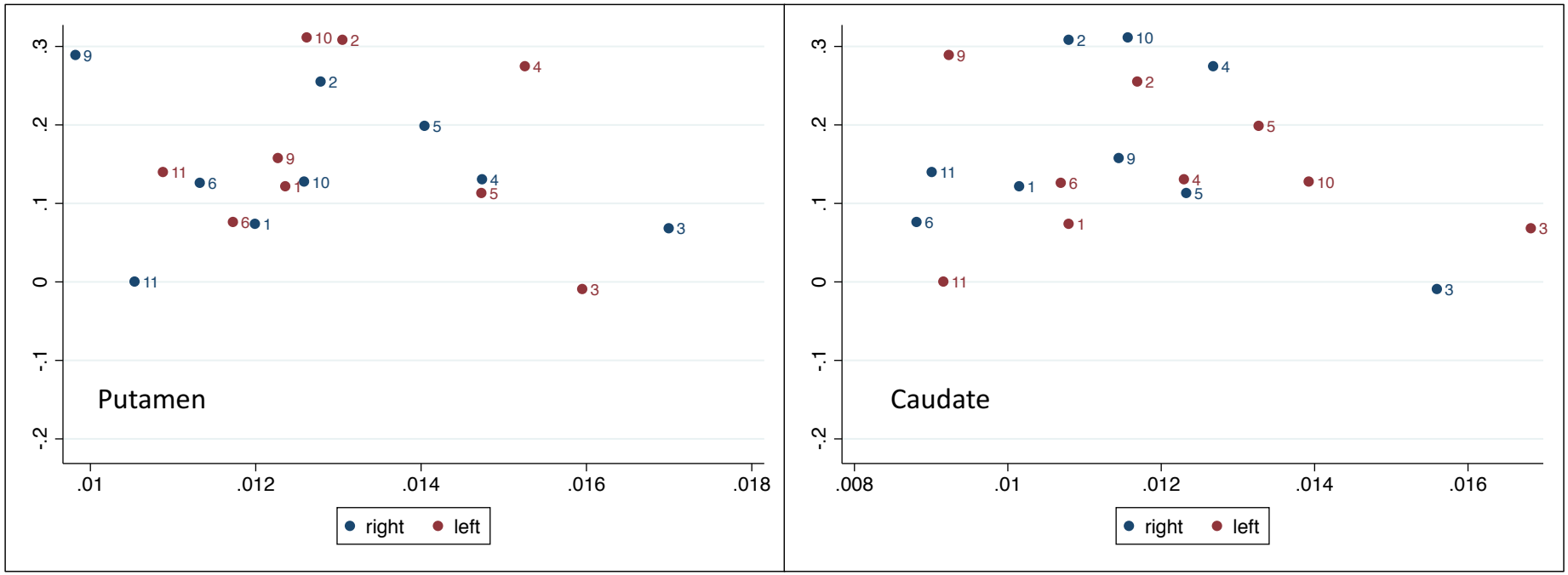

Fig 2. scatter plot showing DOPA uptake (x) PK11195 uptake (y) in left (red) and right (blue) Putamen (left) and Caudate (right) of GBA carriers

correlation between nigral PK11195 with Putamen (left p=0.8984, right=0.9322) or Caudate (left p=0.9661, right 0.9661) L-DOPA signal (scatter graph Fig. 2), implying that the inflammation is independent (or possibly in advance) of dopaminergic loss.

Table 3. p values for comparison (Spearman's rank) of DOPA and PK11195 signal in *GBA* carrier and control group (p<0.05)				
	DOPA (left)	**DOPA (right)**	**PK11195 (left)**	**PK11195 (right)**
Substantia nigra	-	-	**p=0.0008**	**p=0.0016**
Putamen	p=0.681	p=0.509	p=0.220	p=0.220
Caudate	p=0.719	p=0.627	p=0.300	p=0.509

5.9b Increase in nigral ^{11}C-PK11195 uptake correlates with deficits in olfaction amongst GBA carriers

There was a negative correlation between nigral ^{11}C-PK11195 uptake and UPSIT score (left p=0.0058, right=0.0317 Figure 3). There were no other significant correlation for the other prodromal Parkinson disease features assessed (full details in table 4). It is certainly noteworthy that the only correlation obtained in these analyses was with the degree of olfactory loss. Hyposmia has been shown to be increased in established Parkinson disease subjects compared to controls [222,223] and as we saw in the previous chapter is consistently worse and deteriorates at a faster rate amongst *GBA* carriers. Anatomically the olfactory nucleus and substantia nigra are spatially close within the upper mesencephalon and direct projection are present from the olfactory nucleus to the striatal system.[224]. It therefore seems plausible that nigral glial activation projects to the olfactory nucleus and bulb and is either causative of or a result of underlying neurodegeneration in both regions.

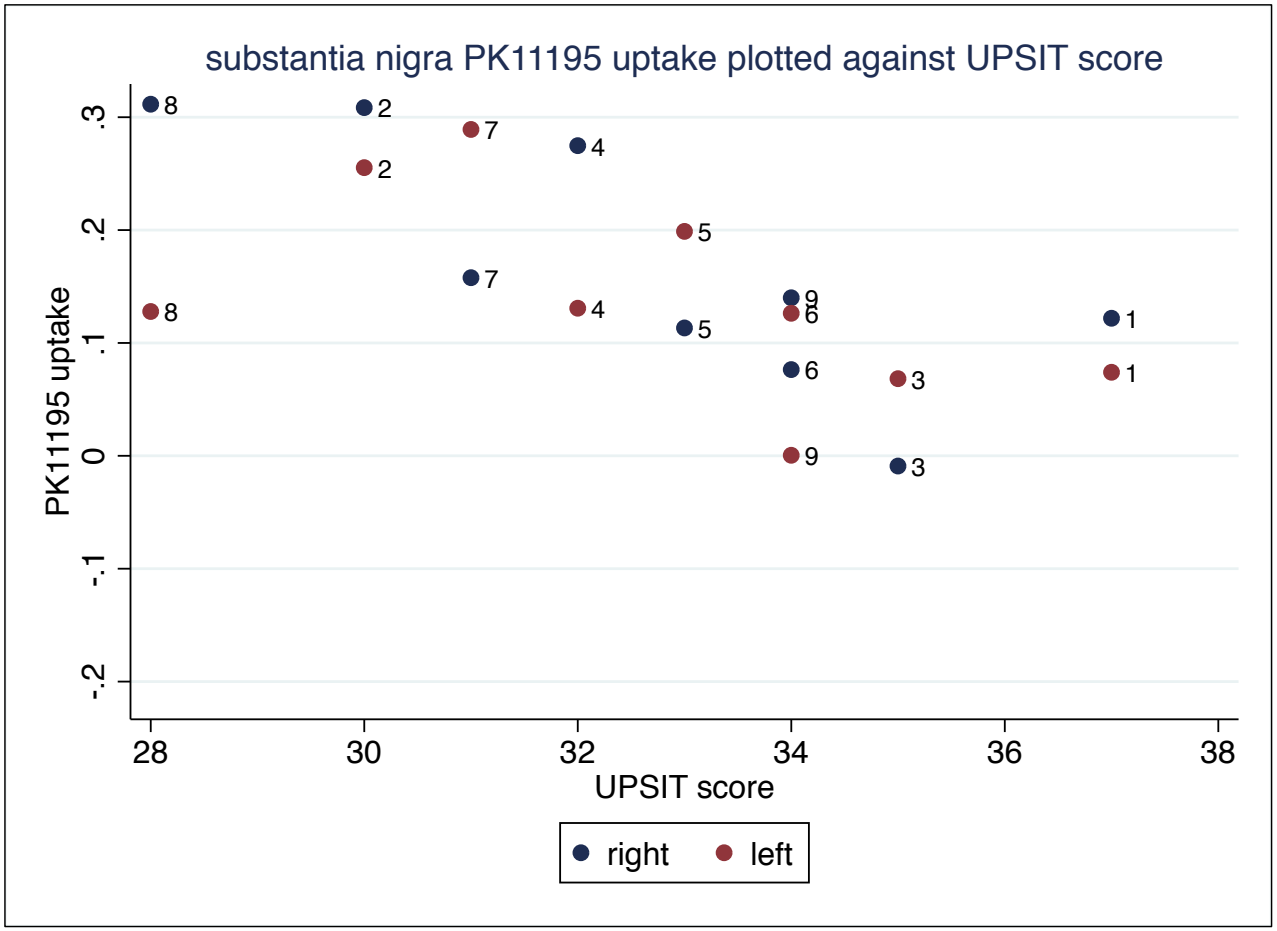

Fig 3. scatter plot of correlation of UPSIT score (x) PK11195 uptake (y) in left (red) and right (blue) substantia nigra amongst GBA carriers

Table 4. p values for correlation (Wilcoxon rank sum) of nigral PK11195 signal and prodromal Parkinson disease feature assessment scores/ putative Parkinson disease biomarkers (p<0.05)		
	left	**right**
UPSIT	**p=0.006**	**p=0.031**
Blood leucocyte GCase activity	p=0.076	**p=0.016**
MoCa	p=0.192	p=0.174
RBDSQ	p=0.379	p=0.328
BDI	p=0.542	p=0.095
MMSE	p=0.423	p=0.110
UPDRS II	p=0.343	p=0.525
UPDRS III	P=0.764	p=0.813
NMSS	p=0.949	p=0.177
severe/null mutation	p=0.379	p=1.000

5.9c GCase activity is positively correlated with nigral ^{11}C-PK11195 uptake

There was a positive correlation between GCase activity and nigral ^{11}C-PK11195 uptake on the right (p=0.0159) and strong trend on the left (p=0.0769). This is a puzzling finding given the established literature. Reduced GCase activity as has been discussed previously is thought to be implicated in the pathological mechanism under Parkinson disease conversion in both idiopathic Parkinson disease and in terms of Parkinson disease risk amongst *GBA* carriers. This correlation must be treated with caution. Biallelic *GBA* carriers have extremely low GCase activity whilst heterozygotes have much higher levels on account of the remaining wild type allele. In this population, this has resulted in a binomial distribution (Figure 4) which may have given rise to a false correlation (Fig 5). Alternatively this may provide evidence of a potential neuroprotective effect associated with the glial activation at the substantia nigra.

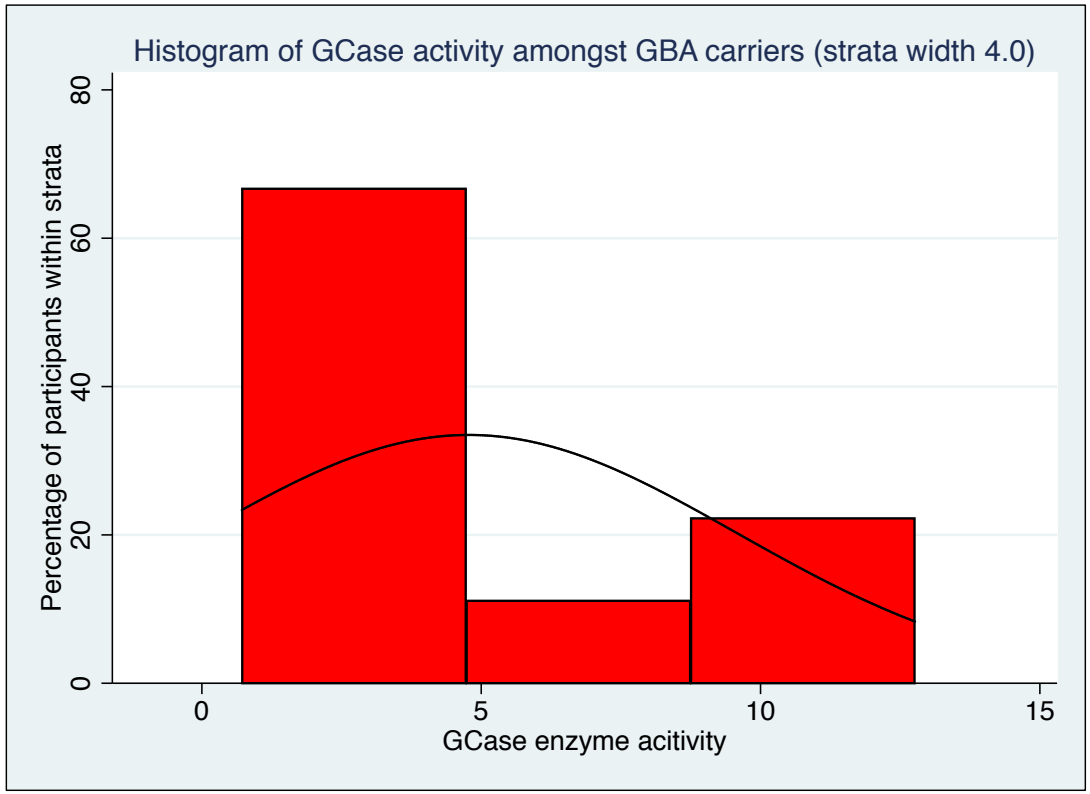

Fig 4. Histogram (red) showing binomial distribution of GCase enzyme activity amongst mixed population of heterozygote and biallelic carriers with normality curve plotted in black

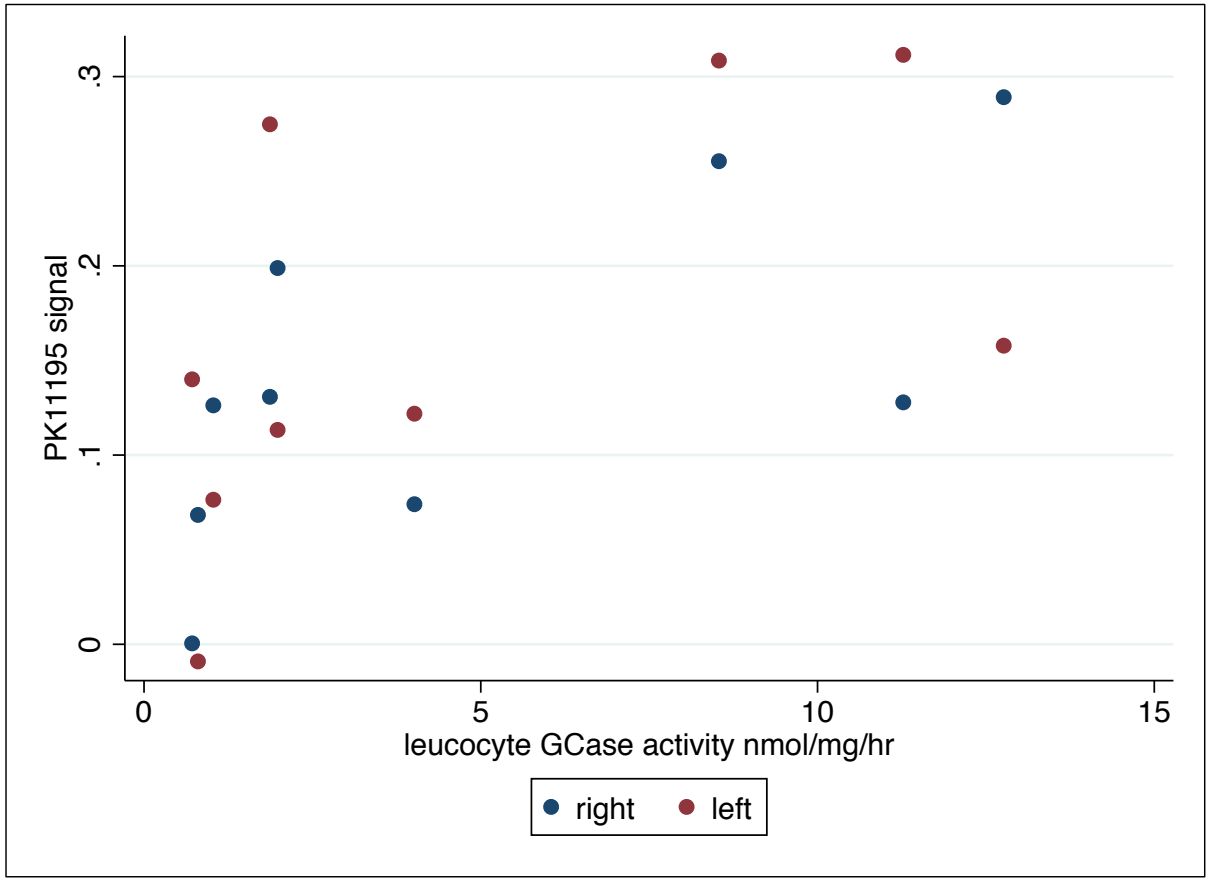

Fig 5. Scatter graph of leucocyte Gcase activity (x) against left (red) and right (blue) PK11195 uptake (y)

5.9d No deficits in ^{18}F-DOPA signal amongst GBA carriers

There were no significant decrements in ^{18}F-DOPA uptake amongst *GBA* carriers compared to controls. There did not appear to be a correlation between the increase nigral ^{11}C-PK11195 and putamen (left p=0.898, right=0.932) or caudate ^{18}F-DOPA reduction in the *GBA* group (left p=0.9661, right p=0.9661). Interestingly there was substantial variability of DOPA signal in both the putamen and caudate compared to the control group with highest and lowest DOPA signals within the study recorded amongst a portion of the *GBA* carrier participants (Figure 6). Upregulation of DOPA signal has been recorded in other 'at risk' Parkinson disease groups other studies [225]. Speculatively this might represent a positive feedback mechanism in the context of ongoing (but not complete) dopaminergic neuronal damage, although I must stress we have no evidence to support this hypothesis. Normal DOPA scans are common in the context of established idiopathic Parkinson disease [226-228], therefore it is not surprising that in the these patients, who are largely free of motor features of Parkinson disease, these scans are otherwise broadly unremarkable. In terms of potential neuroprotective interventions these findings are encouraging, as they show that in those with possible prodromal signs of Parkinson disease the dopaminergic system is still broadly intact and, plausibly, could be saved if some mechanism to halt the underlying pathological process were found.

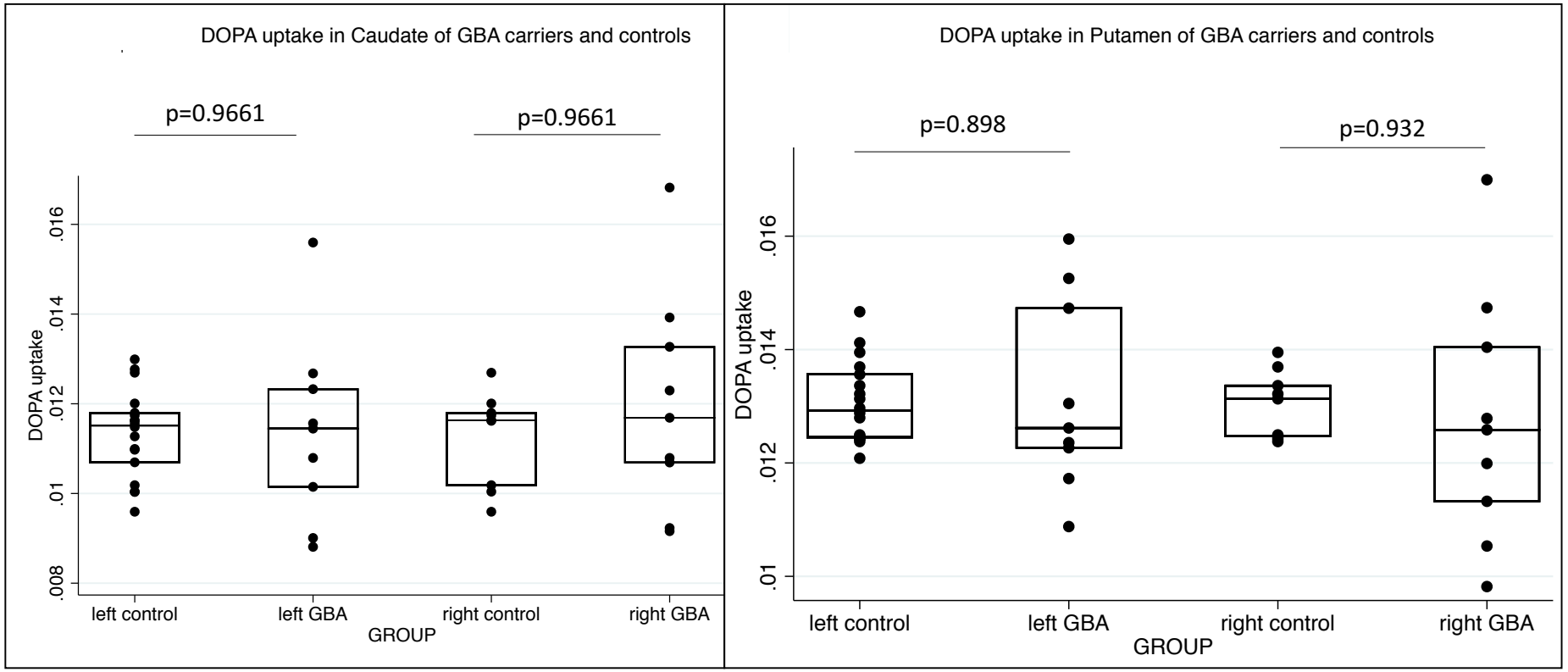

Fig 6. Box plots of DOP uptake in the left and right Caudate (left) and Putamen (right) of control and GBA carrier participants

5.10 Peripheral markers of neurodegeneration and inflammation as putative biomarkers of Parkinson disease conversion amongst GBA carriers

Given the literature described in the introduction to this chapter and the focal glial activation found using the PK11195 ligand, we endeavoured to find out whether there was evidence of peripheral immune dysregulation and or other markers of neurodegeneration in *GBA* carriers compared to controls and whether these increases correlated with Parkinson disease prodromal features amongst *GBA* carriers.

5.11 Aims (ELISA biomarkers)

1) To understand whether IL6, IL8, TNF alpha, alpha synuclein and tau were upregulated amongst *GBA* carriers compared to controls in blood serum.
2) To ascertain whether the above biomarkers correlated with the presence of prodromal Parkinson disease features, number of severe mutations or GCase activity.

5.12 Methods (ELISA biomarkers)

We collected serum (11 heterozygotes, 28 biallelic) of 39 members of the existing cohort supplemented by 27 controls, 17 heterozygous, 39 homozygous, 19 idiopathic Parkinson disease and 7 *GBA* Parkinson disease subjects. We measured concentrations of three cytokines (Interleukin 6, interleukin 8 and TNF alpha) which have been previously been

suggested to be upregulated in Parkinson disease along with the established neurodegenerative markers alpha synuclein and tau.

Separately we collected blood leucocyte pellets and carried out a GCase activity assays on 59 samples (12 controls, 21 heterozygotes, 26 biallelic- charactersitics table 5). Of these there were ELISA and GCase data available for 14 biallelic and 5 hetrozygote carriers only for whom qualification of ELISA biomarkers had been carried out. Samples were collected by SM and Dr Michelle Beavan, analysis was carried out on our behalf in the laboratories of Henrik Zetterberg. GCase assays were carried out by Dr Marco Toffoli and Dr Micol Avenali.

Median values of the levels of these cytokines in each respective group are shown below together with the demographics of each group (table 5). Because of the relatively small study numbers and the large number of study groups, we kept comparisons to a minimum, opting to carry out one primary analysis, namely a comparison of control participants with a combined group of *GBA* carriers. In the event of significant correlations we carried out a further subset analysis comparing biallelic and heterozygous groups individually with controls. For each cytokine we also attempted to correlate levels with the combined risk score derived from UPSIT, MOCA and BDI scores (see chapter 3, section 3.2b). We carried out further subset analyses correlating biomarkers levels with GCase activity and with the number of severe mutations.

Because there was substantial variation in the age and sex of participants we opted to use an ordinal regression model (see **chapter 2**) taking into account age and sex for all analyses. This was also necessary as the for ELISA/GCase/number of severe mutations the data was

not consistently parametric. In the case of the ELISA samples upper and lower limits of sensitivity of the assay also precluded the use of parametric statistical tests. To do this we divided the continuous outputs into 10 equal strata scores, low to high: 0-10) In the analysis looking at cytokine levels and risk score we also included family history of Parkinson disease/dementia and smoking status as coovariates.

Table 5. Demographics and median levels of serum ELISA assays measured.					
	control	**heterozygous *GBA***	**biallelic *GBA***	**Idiopathic Parkinson disease**	***GBA* Parkinson disease**
n	27	17	39	19	7
age median	64	60	5 2	75	69
% male	65	55	53	57	79
IL6 median	0.542	0.690	0.685	0.716	1.045
IL8 median	11.70	11.58	13.42	10.67	10.28
TNFa median	1.74	1.88	1.87	1.60	2.35
alpha synuclein	17599	17077	26188	18167	13969
tau	0.417	0.631	0.448	0.985	0.360

Table 6. Statistical comparisons using biomarkers			
	Comparison of *GBA* group with controls		**Correlation with combined risk score of participants**
IL6	OR 1.82 [95%CI 0.76-4.35] p=0.173		OR 1.04 [0.865-1.27] p=0.628
IL8	**OR 3.51 [1.18-10.37] p=0.023**		OR 0.90 [0.674-1.20] p=0.488
IL8 (subset)	**bialleic OR 5.45 [1.85-16.0] p=0.002**	**heterozygous OR 4.13 [1.21-14.05] p=0.023**	
TNF alpha	0.68 [0.14-3.34] p=0.653		OR 0.93 [0.479-1.81] p=0.838
alpha synuclein	1.78 [95%CI 0.59-2.94] p=0.109		**OR 1.4 [1.04-4.95] p=0.025.**
tau	OR 2.2 [1.41-3.92] p=0.055		OR 1.6 {0.84-2.74] p=0.111

Table 7. Correlations of biomarkers with number of severe mutations	
	OR [95% CI] p value (<0.05)
alpha synuclein	**OR 5.33 [1.68 -16.85] p=0.004**
tau	OR 1.88 [0.79-4.5] p=0.153
IL6	OR 1.29 [0.54 – 3.05] p=0.567
IL8	OR 1.94 [0.775-4.85] p=0.157
TNF alpha	OR 1.87 [0.752-4.68] p=0.177

5.13 Results (ELISA biomarkers)

Summary statistics for all analyses undertaken are shown in tables 6 and 7. The ELISA assays were carried out on our behalf by the laboratories of Prof. Henrik Zetterberg.

5.13a Interleukin 8 is upregulated in GBA subjects compared to controls

The only significant increase found in the *GBA* versus control group was interleukin 8. Subset analysis showed this was increased amongst both heterozygous and bi allelic participants compared to controls. This finding is interesting although what relevance it has to the course of Parkinson's is debatable. The primary driver of this trend are Gaucher patients and immune dysregulation has previously been documented amongst them. None the less the fact it was present also amongst carriers is revealing although the lack of relationship to the risk score of prodromal features implies it may not correlate with central immune dysregulation. Such evidence of immune upregulation in asymptomatic *GBA* carriers does imply that that these processes are ongoing within these patients.

5.13b Serum alpha synuclein levels correlate with severity of prodromal Parkinson disease features and number of severe mutations present

There was a trend towards an increase in alpha synuclein amongst the *GBA* group (OR 1.78 [95%CI 0.59-2.94] p=0.109) and a correlation with the combined risk score OR 1.4 [1.68-16.85] p=0.025). Moreover, alpha synuclein levels correlated strongly with the number of severe Gaucher causing mutations possessed by a participant (OR 5.33 [1.68 -16.85] p=0.004, Fig 7). These correlations are interesting and add further weight to the hypothesized link between alpha synuclein upregulation amongst *GBA* mutation carriers. The significance of alterations in blood synuclein levels is unclear. Variously serum synuclein levels have been shown to upregulated and downregulated is idiopathic Parkinson disease populations [229-232]. Given the increased risk of Parkinson disease that severe *GBA* mutations convey, they imply a direct role for synuclein in the pathogenesis of *GBA* Parkinson disease.

There is no clear evidence as to what the relationship between serum synuclein and Parkinson's is or indeed whether peripheral upregulation correlates with central upregulation. Plausibly increases in serum synuclein may be representative of removal of the protein from the intracellular compartment, which may be a direct result of the failure of the autophagic pathway to process the protein adequately [62,65]. There are precedents for such findings. Amongst heterozygous carriers of the complete penetrance autosomal dominant SNCA triplication gene, SNCA was found to be upregulated in both serum and brain lysates, albeit the brain and blood samples were from different subjects and study numbers were low.[229] In recent years evidence has accumulated that alpha synuclein and oligomeric alpha synuclein in particular transfer directly between cells, contributing to the observed prion like propagation of the protein.[233] Alpha synuclein has been shown to be

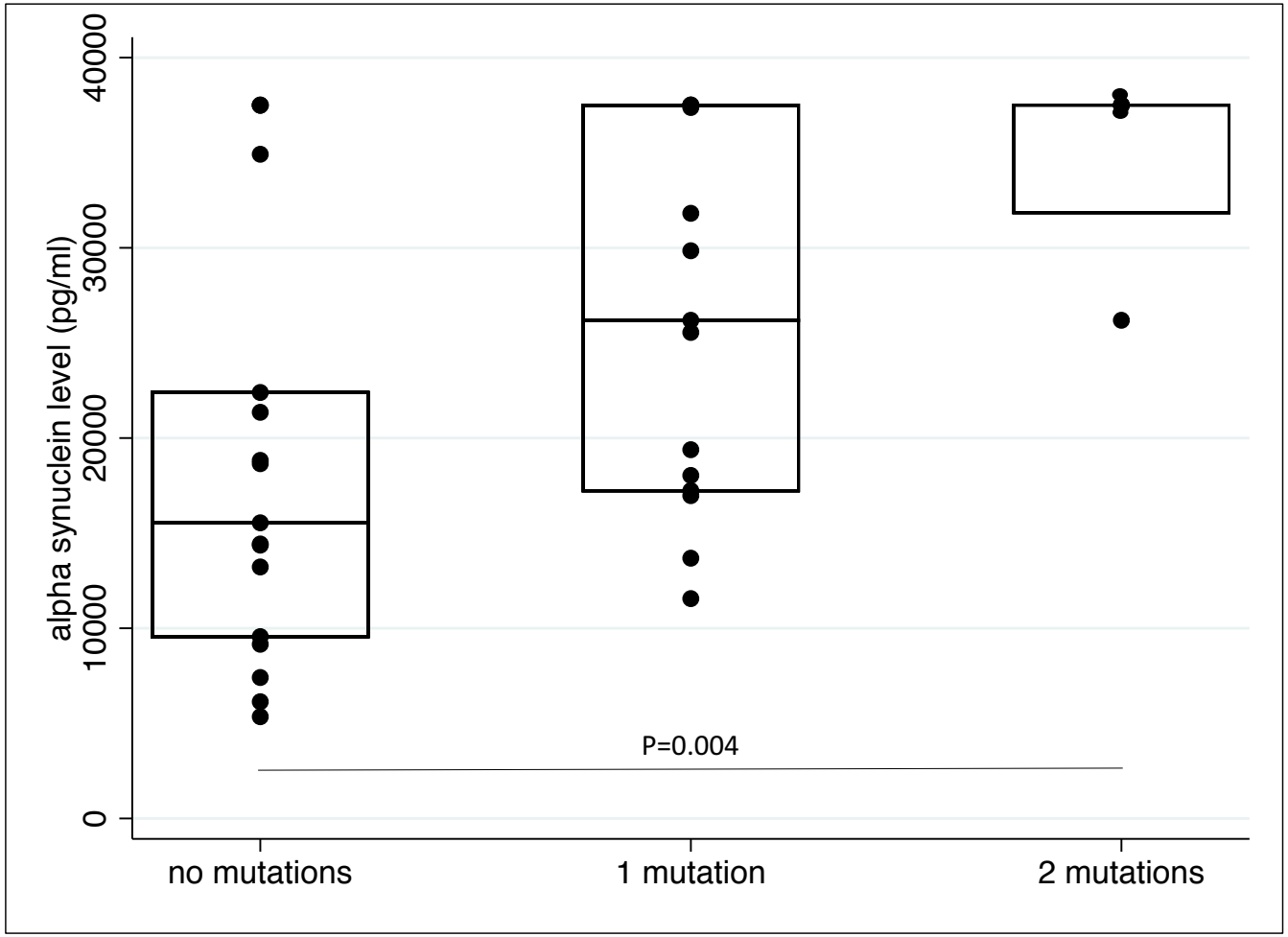

Fig 7. Box plot of alpha synuclein ELISA concentration in those with no 'severe" GBA mutations, one severe mutation and two severe mutations

exported in exosomes and increases intracellularly upon blockage of lysosomal pathway [234]. From. Exosomal independent pathways have also been implicated in this process.. [235,236]. There is the suggestion that the aggregated and fibrillar forms are preferentially exocytosed from the cell, implying this is a mechanism to remove toxic forms of the protein.[236] Significantly exocytosed alpha synuclein levels are increased amongst *GBA* knockout cell lines [237].

5.13c GCase activity correlations with ELISA biomarkers

We were able to carry out GCase activity assays in a subset of the patients who were part of the biomarkers experiment. Demographics and summary statistics of GCase activity are shown in table 8 below.

	CTL	**HET**	**BIA**
N	5	6	6
Median age	59	62	54
% male	60	50	50

Table 8. Characteristics of participants where GCase activity was measured

A summary of the analyses undertaken is presented in Table 9. As would be expected, GCase activity was significantly different across the three groups (Kruskal Wallis p=0.0012, Fig 8) and followed an expected pattern in proportion to the number GBA mutations carried. We attempted to correlate GCase activity with levels of the following ELISA biomarkers amongst *GBA* positive participants (Table 10). The only significant correlation seen was with IL6 (p=0.026, Fig. 9). The result is interesting as it implies reduced GCase activity may contribute to an upregulation of peripheral immune response, although the result must be treated with significant caution as there are no consistent increases across

the analyses undertaken with IL6, nor across the full range of cytokines tested. It is interesting that no correlation is present between leucocyte GCase activity and alpha synuclein. *In vitro* inverse correlations have been observed in a number of model systems. It may be this discrepancy is a result of variation between GCase activity levels in the central nervous system and peripheral leucocytes (see **chapter 8**), or that this this correlation is in fact not causal.

Table 9. Correlations of biomarkers and GCase activity	
	OR [95% CI] p value (<0.05)
IL6	**0.76 [0.60-0.96] p=0.026**
alpha synuclein	1.07 [0.85-1.36] p=0.546
tau	0.99 [0.81-1.21] p=0.956
IL8	0.92 [0.742 - 1.16] p=0.516
TNF alpha	0.95 [0.79-1.16] p=0.642

5.14 A hypothesis generating screen of urine for novel biomarkers of GBA Parkinson disease conversion

In contrast to the hypothesis based approaches described above we used a hypothesis generating proteomics screen in order to identify novel biomarkers of Parkinson disease conversion. Urine was chosen as the platform for this screen because lipid rich components of glycosphingolipid pathway are particularly abundantly excreted in acidic conditions of urine [238-240].

We compared control samples (n=5 median age 58, 3 Males, 2 Females), *GBA* bi-allelic (n= 17, median age 52, 10 Males, 7 Females), *GBA* heterozygotes (n=8 median age 58.5 , 1 Males, 7 Females) and a combined cohort of *GBA* samples dichotomised into a high risk (risk score >/= 1.5, n= 7 median age 52, 4 Males, 3 Females) or a low risk (risk score <1.5, n=21, median age 55.5, 7 Males, 11 Females). Mutations carried in these groups are shown

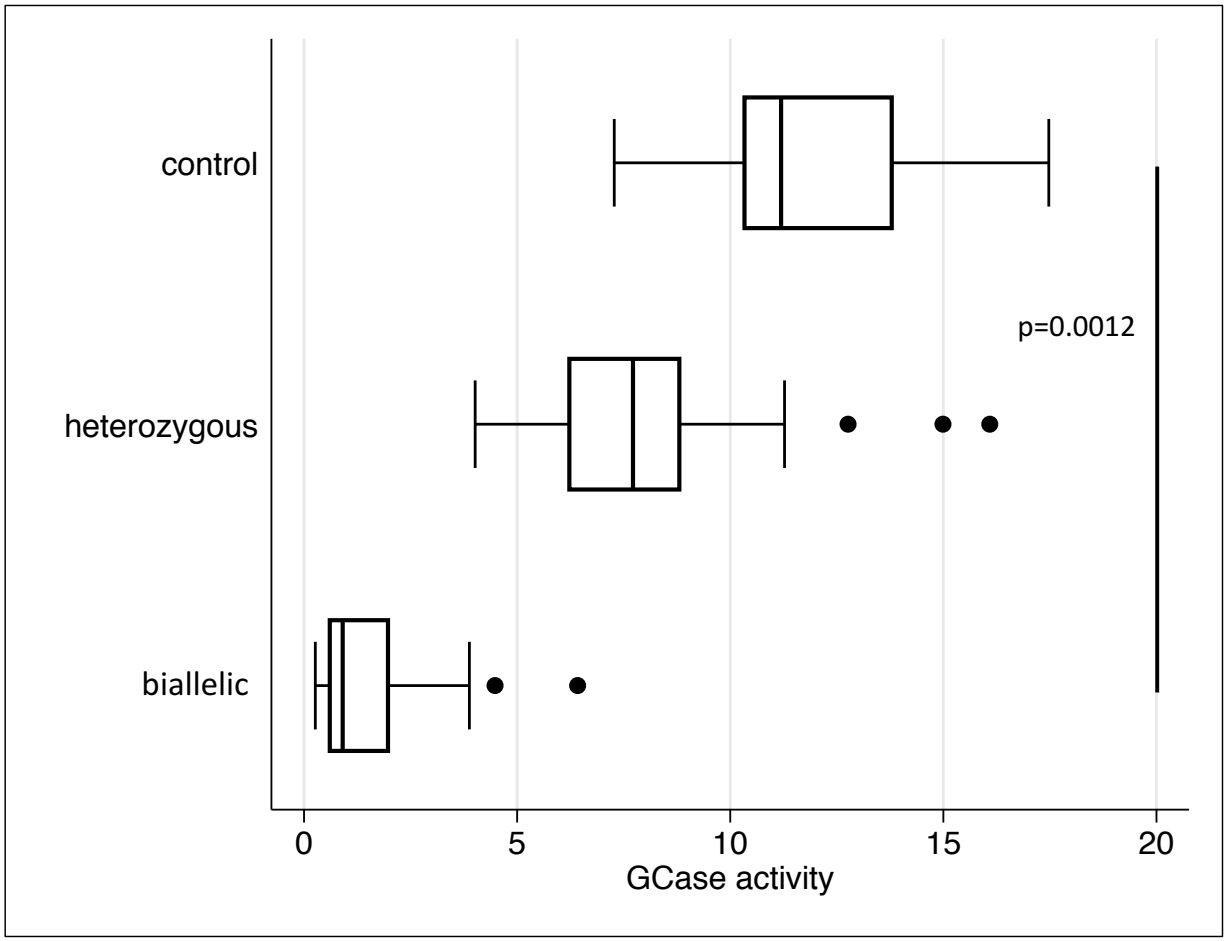

Fig 8. Box plot of Gcase enzyme activity amongst control, heterozygous and biallelic participants.

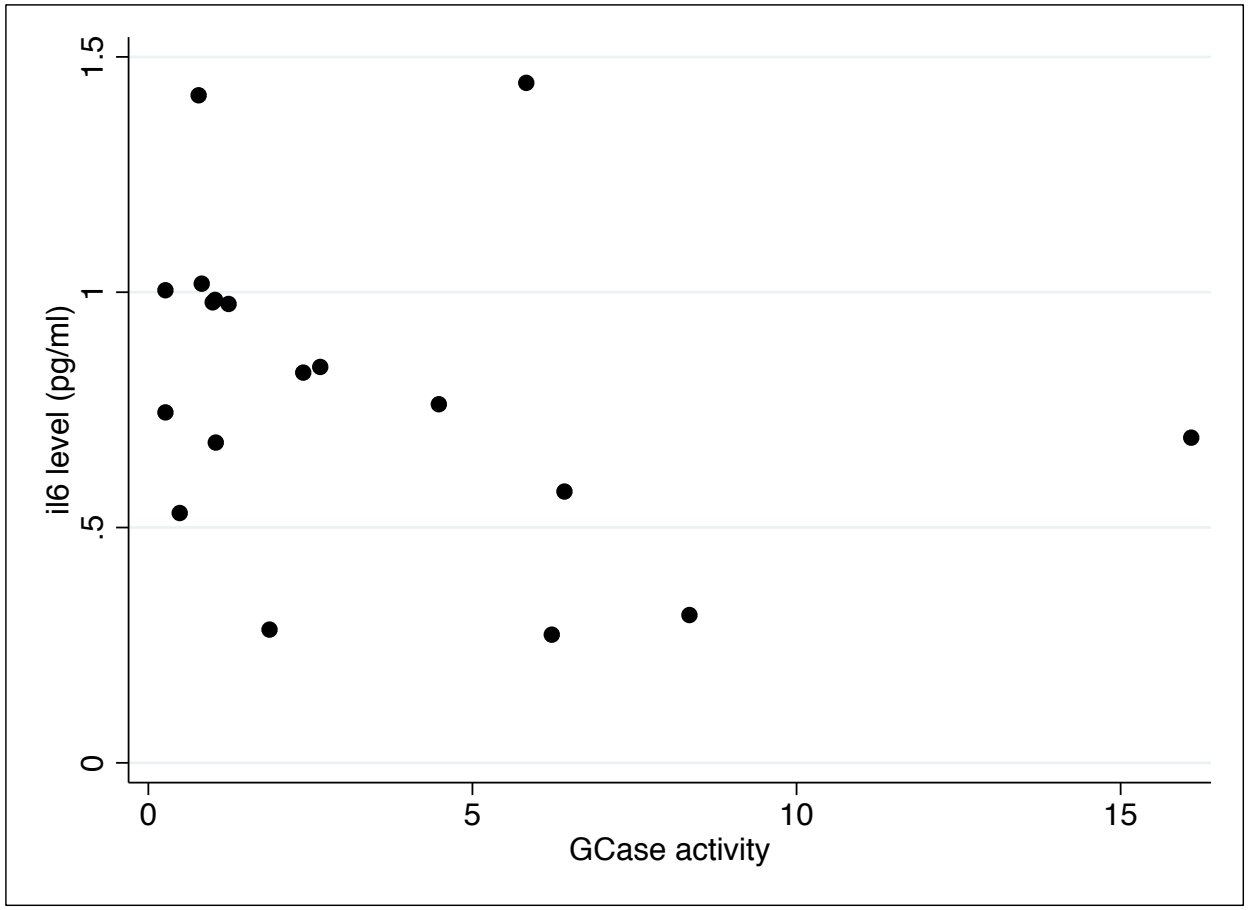

Fig 9. Scatter plot inverse correlation of GCase enzyme activity (x) and interleukin 6 (y, IL6)

in table 11 and their prodromal risk scores are shown in table 12. These analyses were carried out on our behalf by Dr. Wendy Heywood. Sample preparation was performed as described previously [241]. Urine was thawed, centrifuged and filtered using a 3 kDa filter (Millipore, UK). Desalted urine was protein assayed by BCA (Sigma UK). 25 mg of protein was freeze dried, trypsin digested. Yeast enolase peptide internal standard (Waters Corp. Milford, MA) was added to digests to a final concentration of 50 fmol/µl and the digests desalted prior to analysis using C18 solid phase extraction (Agilent, UK). Digested peptides were re-suspended in 3% ACN, 0.1% TFA and analysed on a Waters Synapt G2 Si HD mass spectrometer coupled to a 2D NanoAquity UPLC. Online high pH-low pH fractionation was performed over 2 fractions (19 and 50% ACN) on a 85 min LC-MSe analyses as described previously in our laboratory.[242] Proteins were identified and analysed for differential expression using Non-linear dynamics Progensis QI with a downloaded UniProt human reference proteome database to which the sequence of P00924 yeast enolase and P00761 porcine trypsin were added manually. Fixed modifications of carboamidomethylation of cysteines, dynamic modifications of deamidation of asparagine/glutamine and oxidation of methionine, up to 2 missed cleavage sites and false discovery rate set at 4% mass tolerance for ion and fragments were set to auto. Only protein identifications with >95% confidence and more than 1 peptide were included in the differential expression analysis. A two way analysis of covariance test with a false discovery rate correction for multiple comparisons [243] was used to determine differences in protein expression between controls vs bi- allelic carriers/heterozygous carriers, bi-allelic vs heterozygous carriers and high vs low risk *GBA* carriers. Samples were obtained by SM and Dr Michelle Beavan. Samples were analysed on out behalf by Jenny Hallqvist.

5.15 Results (hypothesis generating screen)

Five proteins were upregulated in the high risk versus low risk groups. These results are shown in table 10. Each of these candidate proteins is considered separately below.

Protein name	Gaucher disease vs control	het vs control	Gaucher disease vs het	High vs low
Ig kappa V-I region AU	**OR 3.51 p=0.005**	**OR 3.16 p=0.002**	ns	**OR 3.35 p=0.003**
Isoform of Tyrosin protein phosphate non receptor 6	ns	ns	ns	**OR 0.62 P=0.004**
Neutrophil defensin 1	ns	ns	ns	**OR 0.03 P=0.005**
Guanlylin	**OR 4.41 p=0.003**	ns	ns	**OR 2.05 p=0.031**
Ig kappa V-I region Ni	**OR 2.79 p=0.025**	ns	ns	**OR 3.52 p=0.023**

Table 10. Summary of proteomics analyses undertaken

5.15a Ig kappa V-L region AU and Ni

Both proteins are constituent parts of the variable region Ig kappa light chain produced by B cells as part of the humoral immune response. This region determines the antigenic characteristic of the resulting immunoglobulin. Increases in both proteins imply the presence of these patients of a monoclonal or polyclonal gammopathy. In Gaucher disease this has been described as has the increase in frequency of malignancies associated with it, in particular multiple myeloma but also chronic lymphocytic leukemia and b cell lymphoma [210,244].

Table 11. Mutations present amongst the high and low risk *GBA* groups	
low risk	**high risk**
L444P/F216Y	*R463C*/*R463C*
N370S/*R120W*	*N370S*/R359X
N370S/*N370S*	*L444P*/*R463C*
N370S/L105R	*N370S*/*N370S*
N370S/*L444P*	N370S/D409H
R469H/R359X	595-596delCT c.595_596delCT p.Leu199AspfsX62
RecNcil/R262G + S271G	*N370S*/wt
N370/*L444P*	
N370S/*L444P*	
D409H/*D409H*	
595-596delCT c.595_596delCT p.Leu199AspfsX62	
N370S/wt	
G250V/wt	
D409H/*D409H*	
N370S/wt	
c.1388+1 G>A	
N370S/wt	
L444P/wt	
L444P/wt	

Table 12. Prodromal risk scores of high and low risk groups at last assessment.		
	Low risk	**High risk**
UPSIT median	30	26
MoCa median	27	23.5
UPDRS II median	1	4
UPDRS III median	5	9
BDI median	3.5	6

Typically around only 0.001% of plasma immunoglobulins cross the blood brain barrier, hence it is unlikely that the increase in these light chain is derived from the central nervous system [245]. Nonetheless, data derived from fragments of monoclonal antibodies targeted at

the A beta 42 protein showed that even at these microscopic concentrations, fragments of intravenously administered immunoglobulin were able to activate glial to produce a highly specific central nervous system immune response against the protein [246]. In the case of one of the monoclonal antibodies (AN1792), 6% of those administered the antibody developed a meningoencephalitis, which is indicative of the magnitude of the immune can produce [247].

The correlation therefore increases in Ig kappa with those with the worst prodromal features of Parkinson disease is interesting although its significance remains to be seen. Plausibly, the gammopathy peripherally may be indicative of a concurrent central nervous system immune activation. If this is the case IgG Kappa light chain components may have utility as potential biomarkers of early Parkinson disease and potentially disease progression.

5.15b Neurophil Defensin 1

Neurophil defensin 1 is a cytotoxic peptide which is abundant in granules of neutrophils and is widely expressed in intestinal, respiratory and urinary tract epithelia. It is an effective cytotoxin against a variety of prokaryotic and eukaryotic cell types[248]. In recent years the role of the microsomal pathogens in Parkinson disease has been in the news. The work of Braak and other suggests a progression of synuclein pathology from the gut to the midbrain via the vagus nerve and various other autonomic and non autonomic nerve ganglions [162,249]. Synuclein pathology has been identified decades in advance of the development of motor Parkinson disease in a number of studies [250,251]. Gut inflammation has been described in Parkinson disease patients and expression of various cytokines has been shown to be

upregulated amongst these patients [252]. It has been suggested that this is a reflection of aberrant gut flora and faecal transplant has even been suggested as a viable neuroprotective strategy [253]. Colonic biopsy has been suggested to be a potential mechanism for diagnosis of the prodromal phase of Parkinson disease. Should urinary neutrophil defensin in fact turn out to be a correlate of gut inflammation this could serve as a cheap and non invasive biomarker of Parkinson disease development.

5.15c Guanylin

Guanylin is an endogenous protein hormone which activates the guanylate cyclase enzyme. Its predominant function is thought to be regulation of intestinal natriuretic peptides and in turn regulation of natriusis, kaliuresis and diuresis in the kidneys. It is expressed within the central nervous system but, to date, has not been associated with any neurological disease. It is known to be implicated in a number of diseases including cystic fibrosis, asthma, intestinal cancer, kidney failure, heart failure and the metabolic syndrome [254]. It is unclear what relevance the pathway has to our existing understanding of Parkinson disease pathogenesis.

5.16 Concluding remarks

This chapter has described a variety of studies aimed at developing novel biomarkers of Parkinson disease conversion. Perhaps the most striking finding is that PET imaging studies reveal focal inflammation of the substantia nigra of *GBA* carriers in the absence of any definable dopaminergic loss. The correlation of this glial activation with the olfactory deficits

of the participants implies that it is indicative of glial activation across a variety of midbrain structures. The sample size here is small and so validation in larger cohorts is clearly required; however this limitation accepted, our results provide exciting evidence which suggest it is feasible to detect the pathological processes underlying Parkinson disease development prior to dopaminergic loss occurring.

Additionally we attempted to understand whether a number of cytokines and proteins associated with peripheral inflammation were upregulated in *GBA* carriers and whether they correlated with the presence of prodromal Parkinson disease features, number of severe *GBA* mutations and GCase activity. In truth the significance of these findings is unclear. There are a large number of variables and assumptions which must be made in the interpretation of the data. Moreover, the results are some what inconsistent. Interleukin 8 was upregulated amongst *GBA* carriers compared to controls and in both biallelic and heterozygous carriers, however, the correlation did not extend to prodromal Parkinson disease features. Conversely IL6 seemed to inversely correlate with GCase activity whilst TNF-alpha levels seemed consistently flat across our analyses. That said, our hypothesis generating proteomics screen picked up two components of the Ig kappa light chain raised across *GBA* carriers compared to controls and in 'high' vs 'low' risk groups. There does therefore appear to be a common theme across these analyses implicating immune dysregulation peripherally and centrally in the process of Parkinson disease conversion. However, there is no evidence of generalised immune upregulation or of any individual cytokine; therefore whilst interesting, it is difficult to draw any firm conclusions on the basis of these data, although they do provide interesting leads which may be pursued in larger cohorts.

Our hypothesis generating screen of urinary proteins has revealed a number exciting targets as putative urinary biomarkers of Parkinson disease conversion. It also highlights the utility of using prodromal Parkinson disease features as a potential surrogate of Parkinson disease conversion. The next step will be validation of these biomarkers amongst idiopathic and *GBA* Parkinson disease subjects and this work is already ongoing.

Chapter 6 – No evidence of disturbance of calcium homeostasis in *N370S* embryonic mouse primary neurons

The question of why neuronal toxicity in Parkinson disease is predominately confined to dopaminergic cells of the substantia nigra pars compacta has attracted much interest in recent years. Initial attention was focused on whether this selective toxicity was a property of dopamine itself, however evidence for this is contradictory [87,228,255]. More pertinently, this model fails to explain why Parkinson disease involves a minority of non dopaminergic neurons [256] and equally why many dopaminergic neurons outside the SNc are spared in Parkinson disease [257,258].

More recently, attention has focused on the intrinsic physiological pacemaking properties of neurons within the substantia nigra pars compacta and other parts of the mesencephalon and brain- stem. This activity, essential in the case of the dopaminergic cells of the substantia nigra pars compacta for maintenance of basal dopamine levels (and hence movement), requires rapid spontaneous firing of neurons, which are highly dependent on transmembrane calcium currents [259,260].

6.0a Calcium flux as physiological messenging pathway

Calcium signaling is a vital cytosolic function. In addition to nigral pacemaking neurons, it is intrinsic to a vast array of cellular activities in a variety of cell types. For instance dendritic growth (neurons) [261], insulin synthesis and release (islet cells)[262], vesicular trafficking

(variety of cells) [263] and oocyte fertilization [264] are mediated by cytosolic calcium flux. It primary advantage is the versatility of the signaling it allows. This can either be ultra rapid (mediated through fast amplification and then dissipation of intracellular calcium currents) or slow cell signaling (mediated through gene transcription) [265,266].

With reference to neurons it is thought that the mechanism for this process is as follows. Neuronal depolarization stimulates the opening of voltage gated calcium channels allowing intracellular entry of calcium into the cytosolic compartment. As the cell repolarizes closure of these channels is gradual, causing an influx of calcium ions, with the duration of closure correlated to the magnitude of calcium influx. Local calcium current then are propogated across the cytosol causing stimulation of IP3, NAADP and other receptors within intracellular organelles such as the endoplasmic reticulum and lysosome. This causes rapid amplification and propagation of these calcium currents. This intracellular calcium is then rapidly removed from the cytosolic compartment back into the endoplasmic reticulum, lysosome and pertinently the mitochondria and also through active efflux via plasma membrane pumps [77]. Mitochondria are particularly suited to such buffering activities as they have negatively polarized matrix which allows rapid uptake of positively charged calcium ions. The mitochondrial membrane potential can then be repolarised by a rapid upregulation of oxidative phosphorylation [267].

6.0b Calcium current within cells affected by Parkinson disease

Cells of the substantia nigra display intrinsic pacemaking action potentials which maintain

basal neurotransmitter tone. This entails a near constant broad spiking (slow closing voltage gates calcium channels) depolarization with reduced buffering capacity [77] It is hypothesized that because of the heightened calcium influx and reduced intrinsic buffering capacity, over the course of a lifetime, mitochondria become overloaded by the perpetual effect of this continuous higher level of calcium buffering. Ultimately it is suggested, this results in the mitochondrial incompetence which has been recognized for some years as a major component of the pathogenesis of Parkinson disease [268]. An interesting caveat to this is the epidemiologic finding that dihydropyridines, commonly used antihypertensives that antagonize L-type calcium channels, seem to exhibit a protective effect against Parkinson disease [269,270]. It may be that blocking of these channels limits pathologic calcium flux, reducing neuronal toxicity during periods of enhanced energy demand, slowing the progression of Parkinson disease.

6.1 GBA mutations and calcium flux

It has been suggested that certain genetic forms of Parkinson disease may lead to disturbances of calcium homeostasis which accelerate the process of mitochondrial overload. In a fibroblast model of G2019S *LRRK2*, it was shown that compared to controls, NAADP induced global cytosolic calcium signal was increased and this was reversible through inhibition of the lysosomal two-pore channel [271]. In *GBA*-positive fibroblasts carrying the *N370S* mutation cytosolic calcium there was an increased cyclic ADP ribose induced cytosolic evoked calcium reponse. Dissection of the contributions of individual

organelles showed an increase in endoplasmic reticulum and a decrease in lysosomal calcium stores [272]. Moreover, amongst homozygous and some heterozygous *GBA* carrier derived induced pluripotent stem cells, basal calcium levels and calcium flux upon stimulation of ryanodine receptors with caffeine were increased compared to controls. Both were reversible by Zinc finger nuclease (ZFN) genetic modification of mutant alleles to the wild-type [273]. Mutations of the *GBA* gene induce aberrant folding which compromises the post translational modification and transport of the of enzyme from the endoplasmic reticulum to to lysosome [74]. Mutant *GBA* becomes sequestered in the endoplasmic reticulum, resulting in an unfolded protein response and in turn upregulation of calcium release into the cytoplasm [75,76,274]. We hypothesize that this additional calcium release from the endoplasmic reticulum results in an increase of calcium flux, in turn overloading the mitochondria and leading to the Parkinson disease phenotype.

Using a mouse primary neuronal model carrying the *N370S* mutation, we shall investigate whether deranged calcium homeostasis is present and dissect the underlying organellar contributions to any derangement. We believe that this is a more physiological model in which to test this hypothesis than the primarily fibroblast based work that has preceeded it. All experiments in this chapter were carried out by SM.

6.2 Characterisation of a mouse primary neuronal model

Prior to commencing experiments, we elected to test a number of the primary neuronal models in terms of their suitability for these experiments. Two preparations using wild type mice were compared, an embryonic preparation harvested between day 14-18 pre partum and a post partum preparation at between 2-5 days gestation. Both preps were cultured for 5-7 days prior to experiments. We carried out immunohistochemistry to establish the

neuronal purity of the preparations (full protocol, appendices section 10.6). Beta three tubulin (abcam ab18207) was used as neuronal marker and glial fibrillary acidic protein (GFAP - abcam ab4674) as a marker of glia microscopy showed that the embryonic prep was made up entirely of neurons, whilst the post partum prep was substantively glial (Fig 1), with sporadic neurons found within.

We further assessed the neuronal character of the two preparations by measuring cytosolic Ca^{2+} flux upon depolarization, by incubating them with Fura-2AM (2.5 uM) and 0.005% v/v pluronic acid (Invitrogen) for 1 h and stimulating with 52mM KCl. Fura-2 is a ratiometric dye which upon binding with Ca^{2+} ions changes its excitation spectra from 360nm to 340 nm (full protocol, appendices 10.7). By dividing the intensity of the emission at 340 and 380nm, a ratio is obtained which is comparable from sample to sample and will compensate for any change in focus which occurs during signal recording. The neurons in the embryonic preparation (Fig 2) consistently underwent a characteristic neuronal depolarization whilst the evoked calcium signal trace in the post partum prep neurons was heterogeneous and morphologically inconsistent (Fig 3). Equally there was a more sparse distribution of neurons amongst the post partum prep (Fig 1), indicative of a worse state of baseline cellular health. We concluded from these studies that the embryonic prep had a higher neuronal purity and represented a healthier and more physiological platform upon which to base further functional imaging.

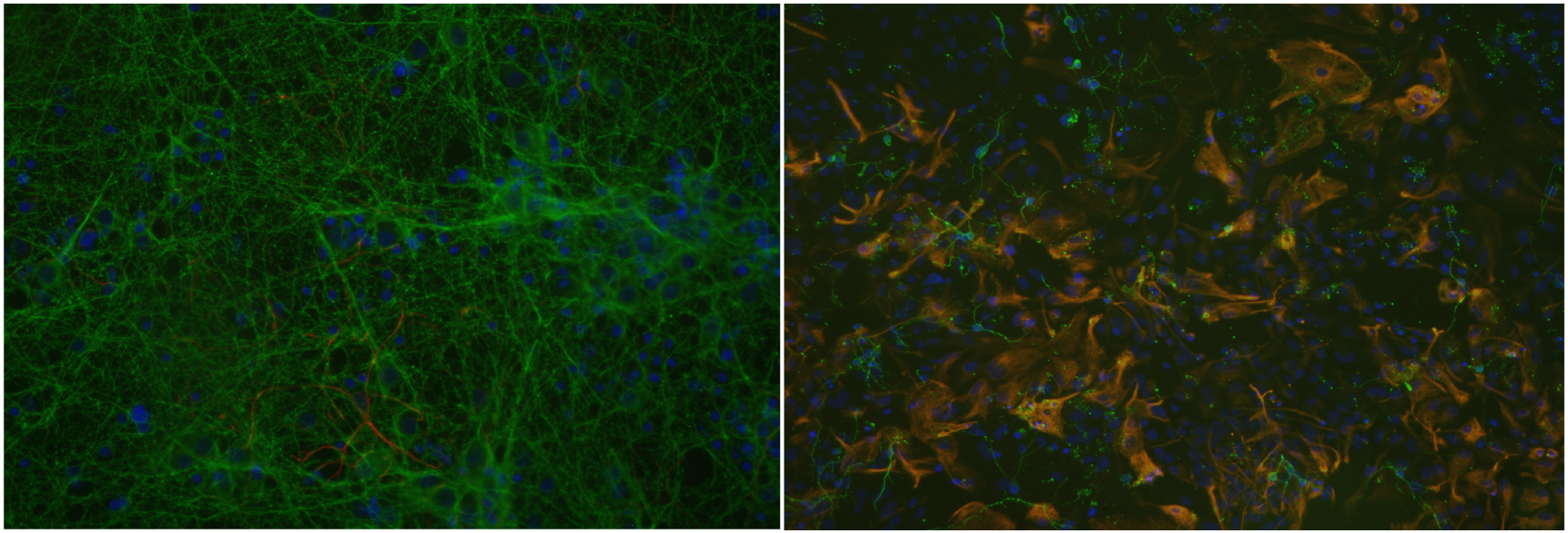

Fig 1. Immunohistochemistry of 5 day old embryonic neuronal prep (left) and 5 day post partum mixed glial and neuronal prep (right). Beta 3 tubulin (green), GFAP (red), DAPI (blue). X20 objective.

6.3 Optimisation of assessment of evoked calcium signal through stimulation of SERCA ATPase inhibitor thapsigargin in embryonic primary neuronal prep

To quantify endoplasmic reticulum Ca2+ stores, we carried out preliminary studies to assess the response in wild type embryonic primary neurons to the SERCA ATPase inhibitor thapsigargin (for full protocol see appendices). Thapsigargin blocks the active transport of Ca2+ ions from the cytosol to the lumen of the endoplasmic reticulum, thus allowing (through leakage of calcium ions across the polarized ER membrane) estimation of ER calcium stores by quantification of the evoked change in calcium signal in the cytosol. In order to prevent extracellular influx of calcium ions the experiment must be carried out in calcium-free HBS which must be added (in replacement of normal HBS) just prior thapsigargin in order to ensure neurons were fully equilibrated in terms of cytosolic and extracellular calcium concentration.

The discernable change in evoked calcium signal following administration of 1uM thapsigargin was extremely small but quantifiable (Fig 4). An additional complicating factor was the tendency of the basal calcium signal to fall after the addition of calcium free HBS, a well known phenomenon which tended to negate the smallest thapsigargin-evoked increases of calcium signal (Fig 4).

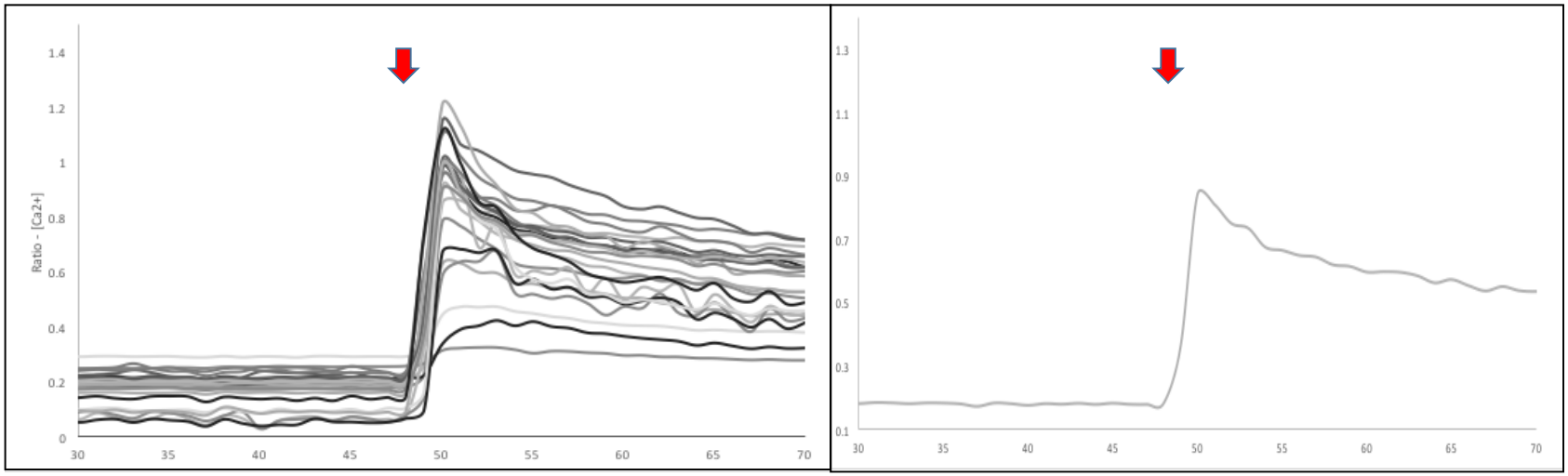

Fig 2. Indicative trace of Ca2+ signals evoked by 52mM KCL (red arrow) in embryonic preparation of mouse primary neurons. All cell traces left, average trace right.

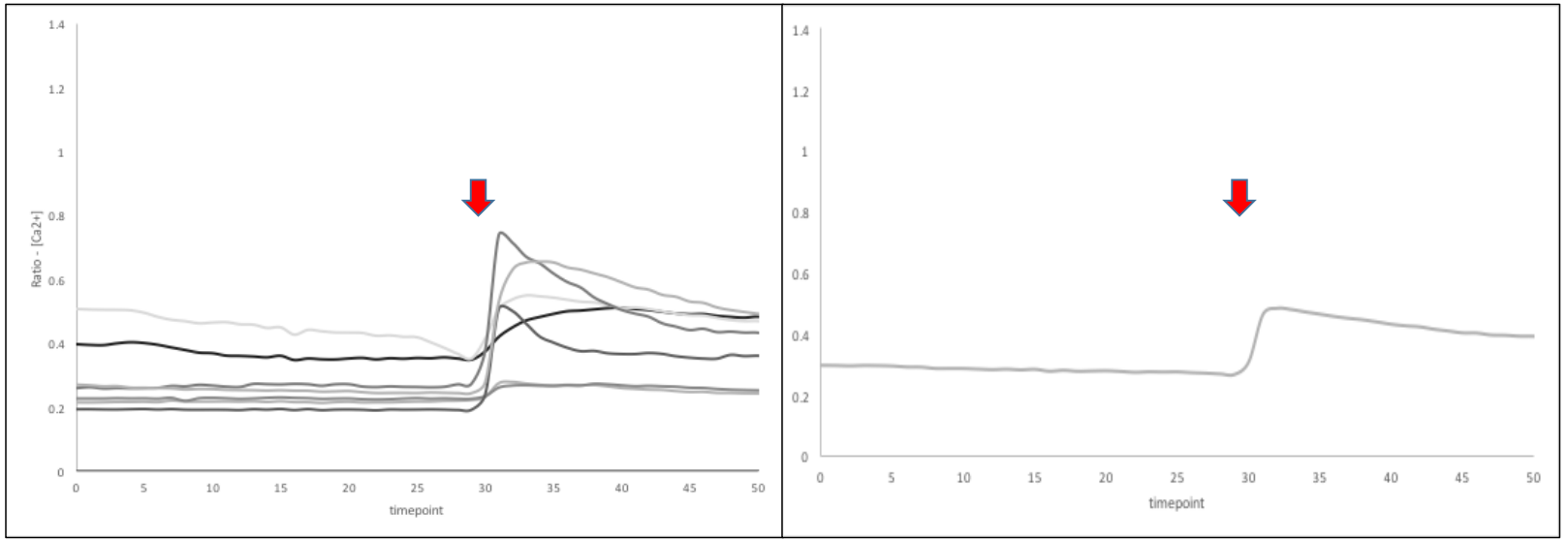

Fig 3. Indicative trace of Ca2+ signals evoked by KCL (52mM) in post partum preparation of mouse primary neurons. All cell traces left, average trace right

6.4 Inconsistent caffeine evoked calcium signal in mouse embryonic primary neurons

We attempted to obtain a more robust measure of ER calcium: by stimulation with caffeine, a ryanodine receptor agonist which has been shown to stimulate cytosolic ER calcium store mobilisation (for full protocol see appendices 10.7) [275]. We found that responses to caffeine were inconsistent. For the most part there was little if any response, however in a few cases there was a more robust response across all neurons (Fig 5). Unfortunately because of this inconsistency, we felt we were unable to utilize this paradigm in further experiments.

6.5 Primary neurons appear to have minimal lysosomal calcium stores

We wished to assess lysosomal stores of calcium. To do this we elected to use Gly–Phe–β-naphtylamide (GPN), a lysosomal permeabiliser which causes release of calcium into the cytosolic compartment (for full protocol see appendices 10.7). Responses of these neurons to GPN were poor, with vast majority of neurons not giving rise to any evoked calcium response (Fig 6). We used lysotracker red (a flourofore dye that stains acidic compartments and hence localizes to the lysosome) to confirm that GPN was permeabilising the lysosome (for full protocol see appendices). We found that the lysotracker signal dissipated in a manner consistent with lysosomal permeabilisation as described previously (Fig 7). As such we concluded that the basis for this was must be an innate lack of lysosomal calcium stores.

6.5 GCase activity reduced in N370S heterozygote and homozygote primary neurons

Details of the GCase activity assay are provided in the appendices (10.9). We found statistically significant in GCase activity in wildtype, heterozygous and homozygous mouse brain (Kruschal Wallis, p0.0001, hom 12, het 23, wt 13). Results are presented graphically in Fig. 8.

6.6 No difference in basal calcium signal in N370S compared to control primary neurons

Basal cytosolic calcium levels can be a surrogate measure of cellular health (Fig. 9). In an induced neuronal pluripotent stem cell model carrying *GBA* mutations, it has been reported basal calcium levels are raised which may be indicative of increased levels basal of cytosolic calcium flux [273], however we were unable show any difference in basal calcium levels upon assessment in heterozygous, homozygous and control primary neurons (Fig 8, 15 cover slips total 4 homozygous, 8 heterozygous, 3 wild type). Analysis using Kruskal-Wallis equality-of-populations rank test showed no evidence of significant differences across the groups (p=0.6648).

6.7 No difference in KCl-evoked calcium signal following stimulation in N370S primary neurons compared to controls

Next we attempted to quantify the KCL evoked calcium signal by subtracting the peak ratio from the basal ratio (Fig 11. 15 cover slips total 4 homozygous, 8 heterozygous, 3 wild type).

Kruskal-Wallis equality-of-populations rank test showed no evidence of significant differences across the groups (p=0.5037)

6.8 No difference in thapsigargin-evoked calcium signal in N370S primary neurons compared to controls

We then attempted to quantify the thapsigargin evoked calcium signal. As previously discussed in our optimization experiments, there was a great deal of heterogeneity in thapsigargin-evoked calcium responses. Kruskal-Wallis equality-of-populations rank test showed no evidence of significant differences across the groups (p=0.8151) (Fig. 12)

We speculated that there might be a differences in the character of thapsigargin-evoked calcium signal in *N370S* neurons compared to controls. We did so qualitatively by superimposing and comparing averaged (by genotype) traces of each genotype. Comparison of the morphology of traces showed no discernable qualitative difference (Fig 11). We also attempted to quantify any different by calculating the total change in calcium concentration by calculating the total area under curve, but were unable to show any difference between genotypes (Fig 14, Kruskal-Wallis equality-of-populations rank test p=0.2954).

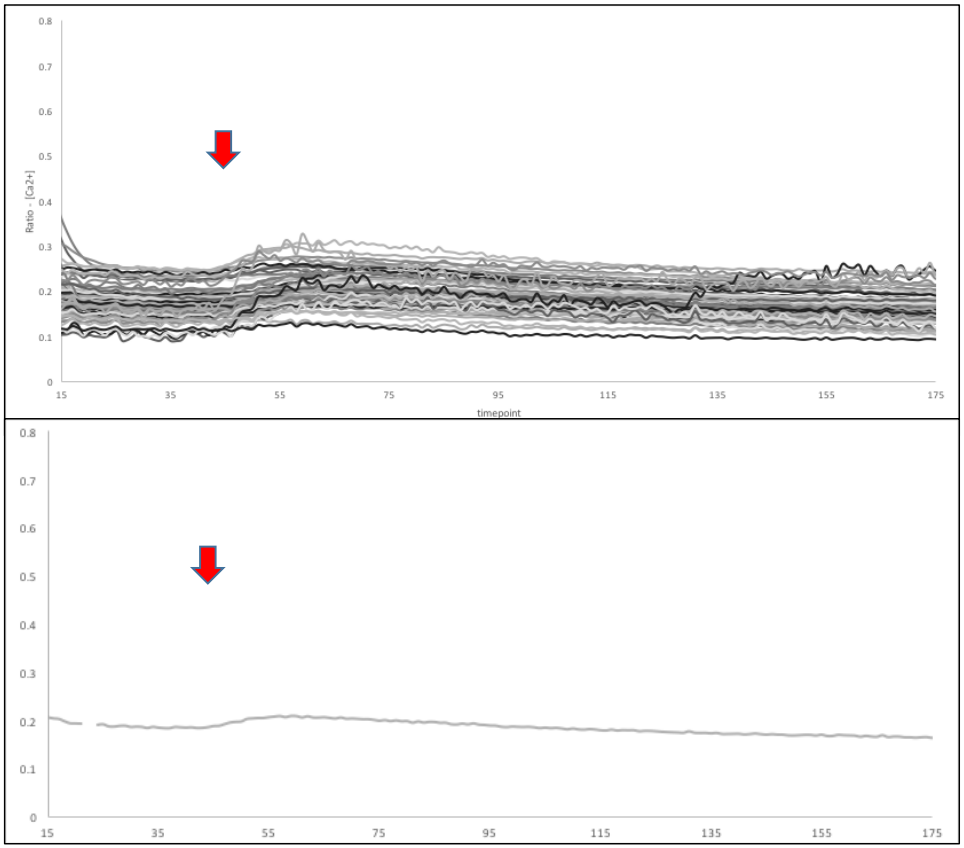

Fig 4. Indicative trace of Ca2+ signals following stimulation by thapsigargin 1uM (red arrow). Note fall in baseline during trace. All cell traces top, average trace bottom

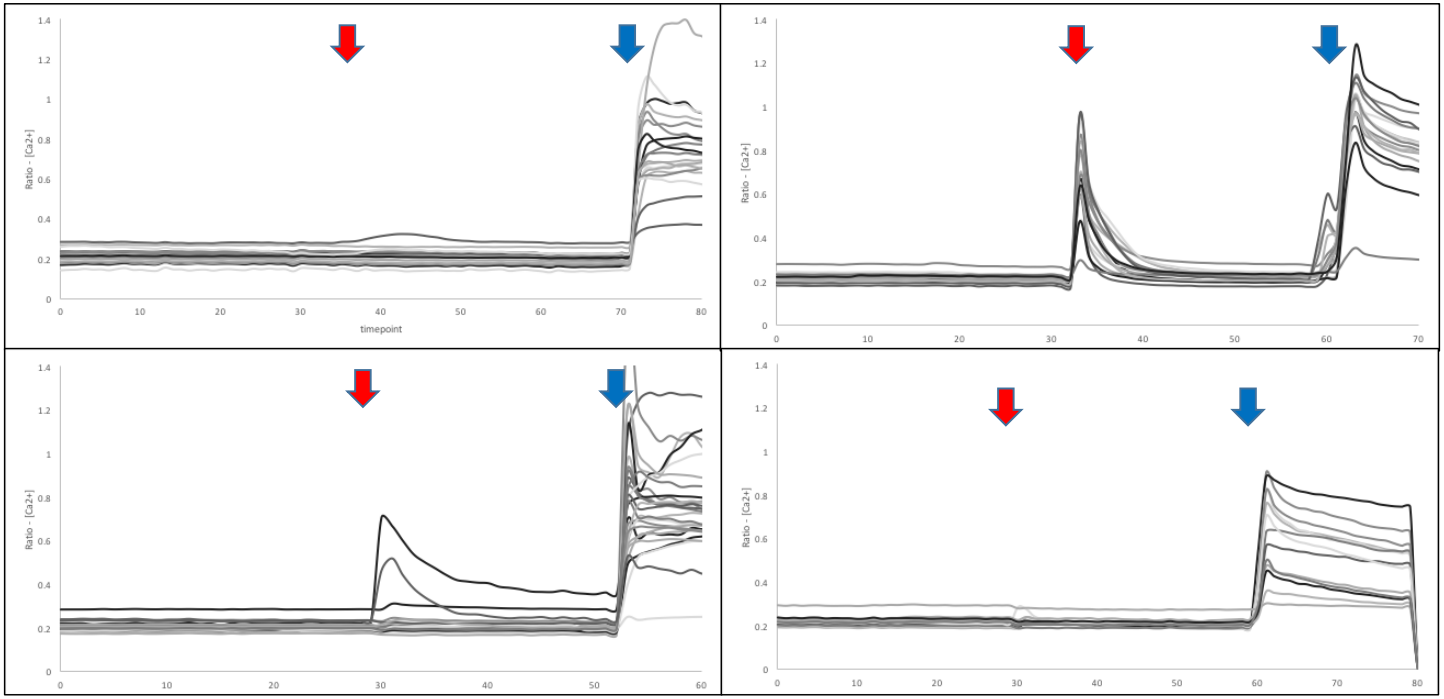

Fig 5. Inconsistent responses to stimulation with 2mM caffeine (red arrow) followed by 52mM KCL (blue arrow). All cell traces left, average trace right

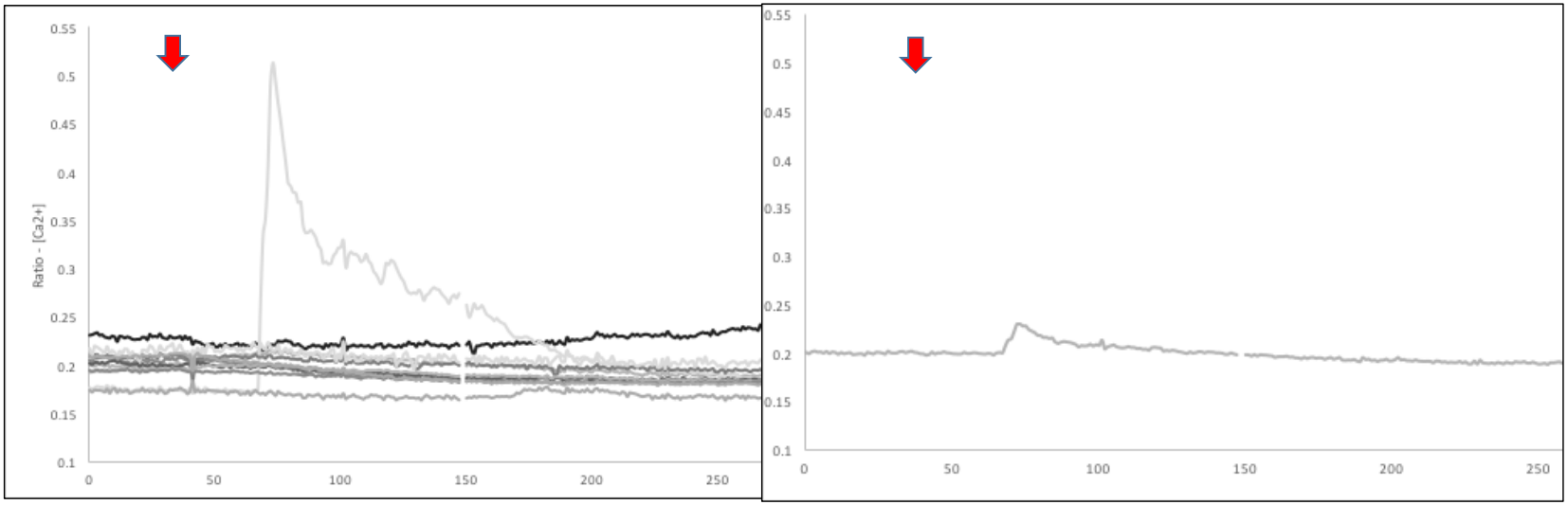

Fig 6. Representative trace of calcium evoked potential following stimulation with GPN 200uM (red arrow). All cell traces left, average trace right

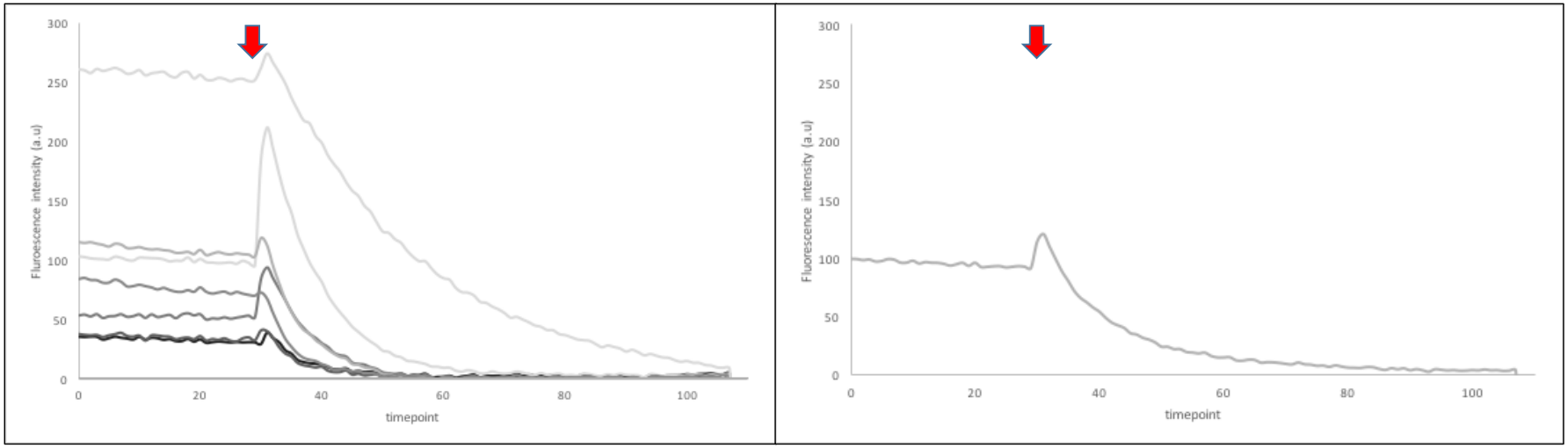

Fig 7. Fluorescence intensity of lysotracker red (25nM) after addition of 200uM GPN (red arrow) in wild type primary neurons. All cell traces left, average trace right

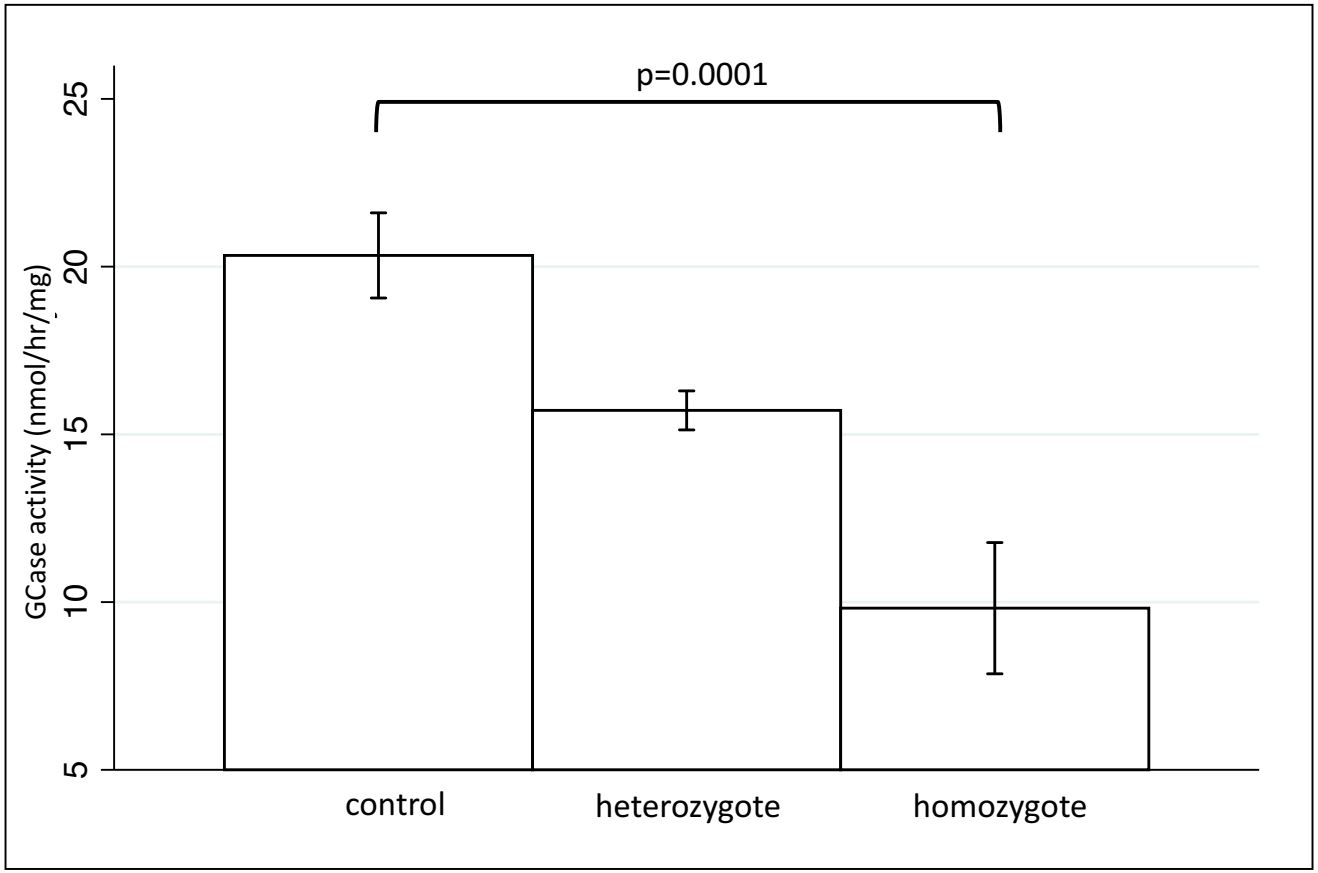

Fig. 8. GCase activity measure in brain lysate of control, heterozygote and homozygote N370S mice

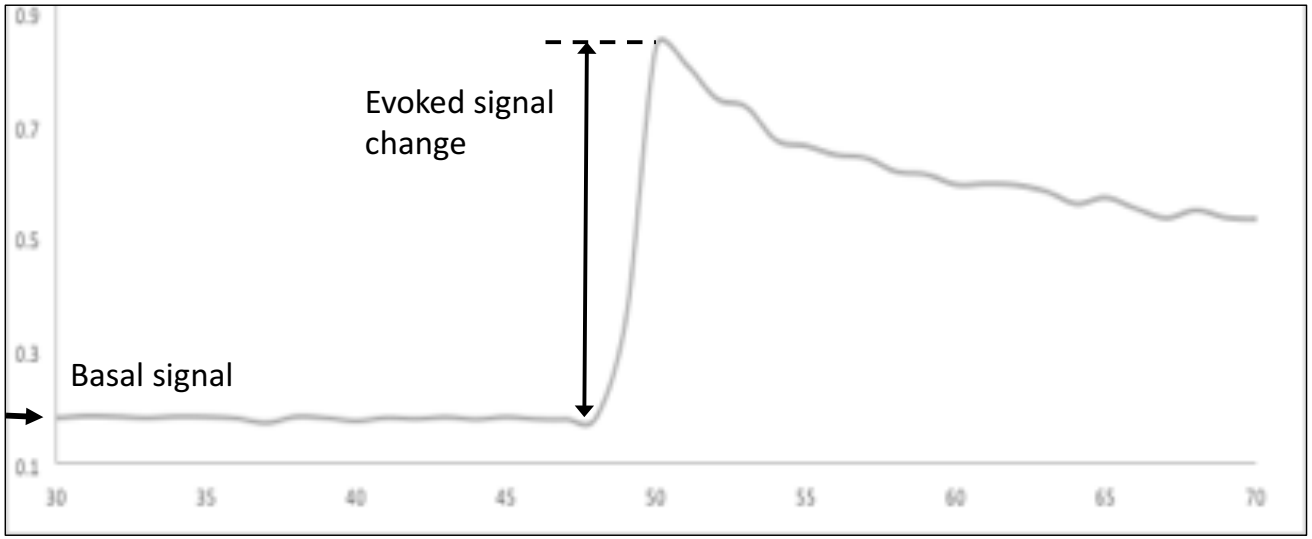

Fig 9. Explanation of basal and evoked calcium signal using illustrative KCL evoked signal

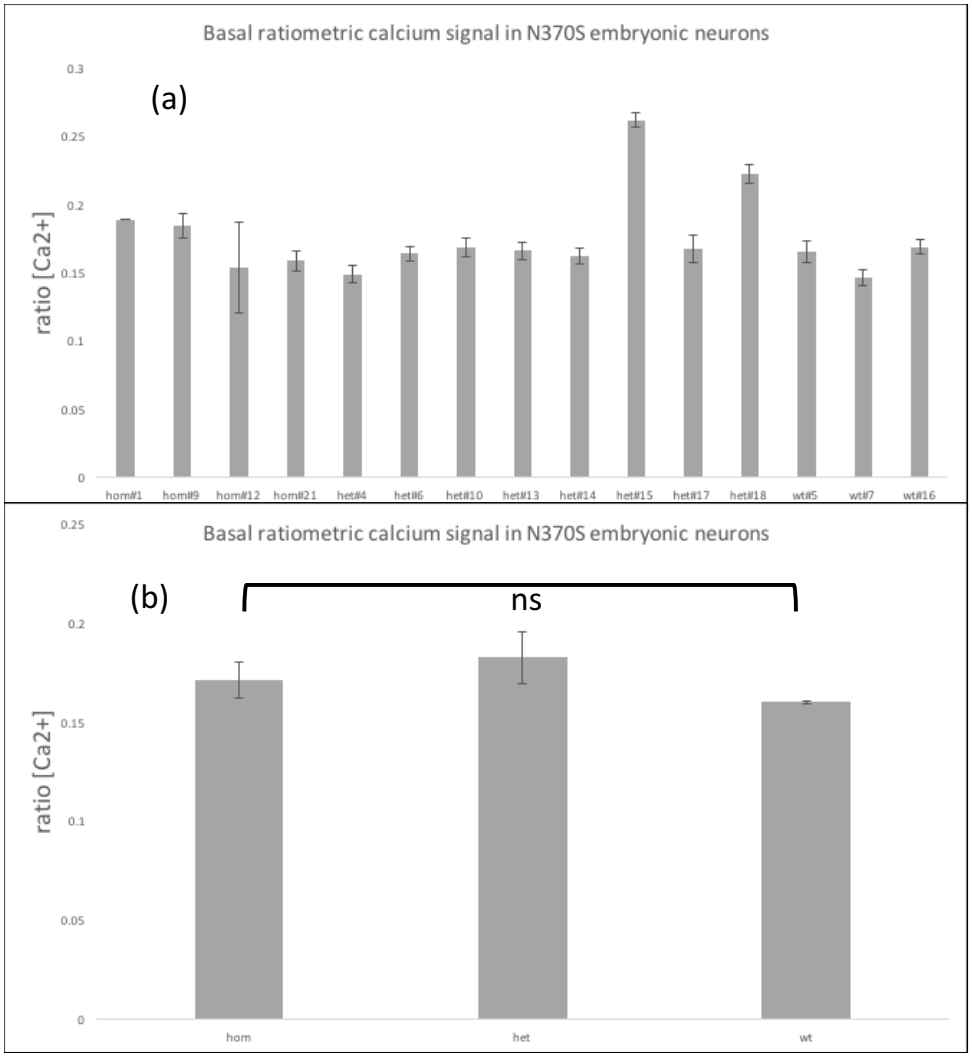

Fig. 10 Basal calcium signal in N370S homozygous, heterozygous and wildtype embryonic primary neurons (a) individual cover slips with confidence intervals (S.E.M) (b) averages with confidence intervals (S.E.M)

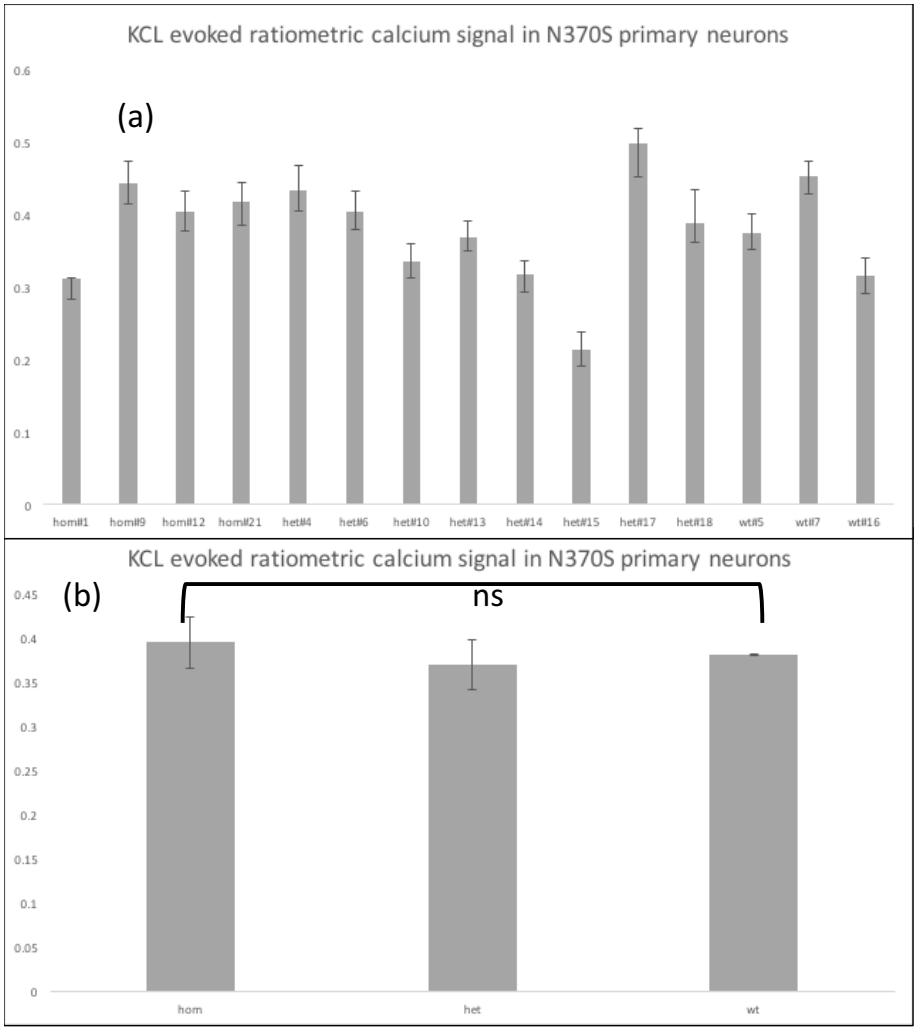

Fig. 11 52mM KCL evoked calcium signal signal in N370S homozygous, heterozygous and wildtype embryonic primary neurons (a) individual cover slips with confidence intervals (S.E.M) (b) averages with confidence intervals (S.E.M)

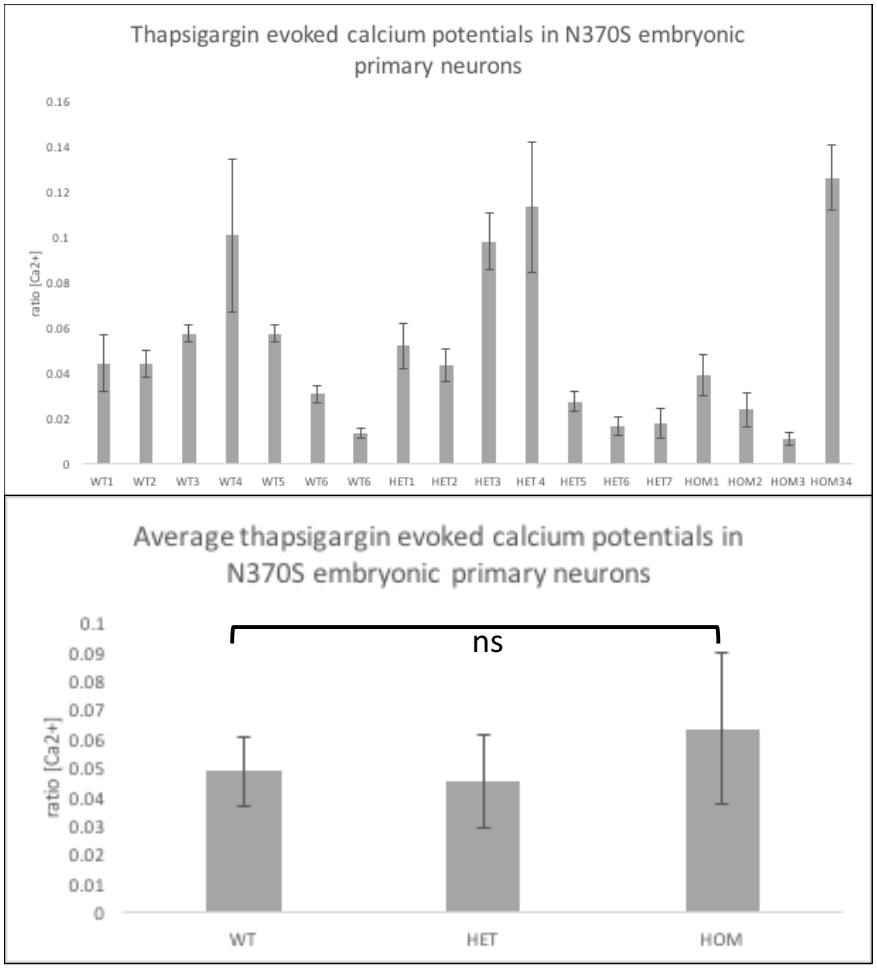

Fig. 12 Thapsigargin evoked calcium signal signal in N370S homozygous, heterozygous and wildtype embryonic primary neurons (a) individual cover slips with confidence intervals (S.E.M) (b) averages with confidence intervals (S.E.M)

6.9 No deficit in mitochondrial membrane signal of GBA mutation carrying fibroblasts compared to controls

Our hypothesis speculated that aberrant cytosolic calcium homeostasis lead to mitochondrial overload and eventually Parkinson disease in *GBA* mutations carrying cells. Previous live cell imaging of *GBA* knock out primary neuronal cultures revealed reduced basal mitochondrial membrane signal which a fragmented histological appearance with evidence to suggest this was due to complex V (ATP synthase) reversal [276]. In order to establish preliminarily whether mitochondrial impairment was present in cell lines carrying the *GBA* mutation we carried out an experiment to measure mitochondrial membrane by loading with Tetramethylrhodamine, methyl ester (TMRM), a cell-permeant, cationic, orange fluorescent dye that is readily sequestered by active mitochondria [277]. TMRM localizes to the mitochondrial intermembrane space in a membrane signal-dependent manner. It thus provides a surrogate marker of mitochondrial membrane signal and in turn, mitochondrial health. Using the ImageXpress, a high throughput microscopy platform which assesses individual cells in a 96 well plate format, we were able to quantify the intensity of the TMRM signal,

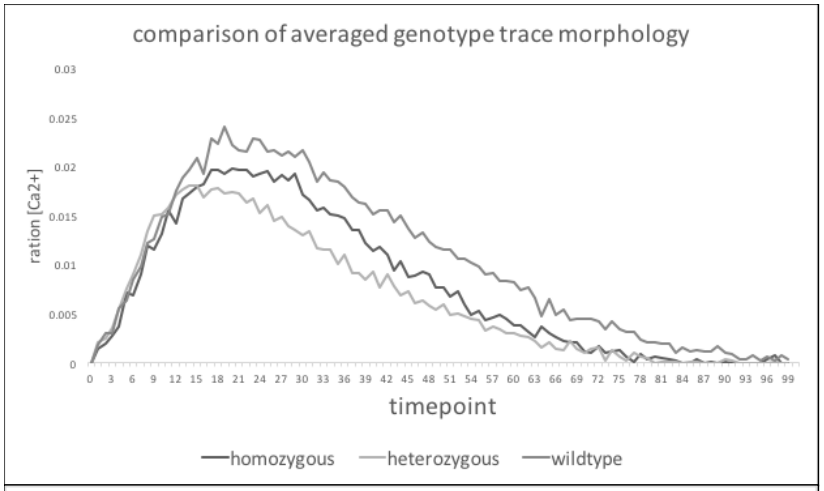

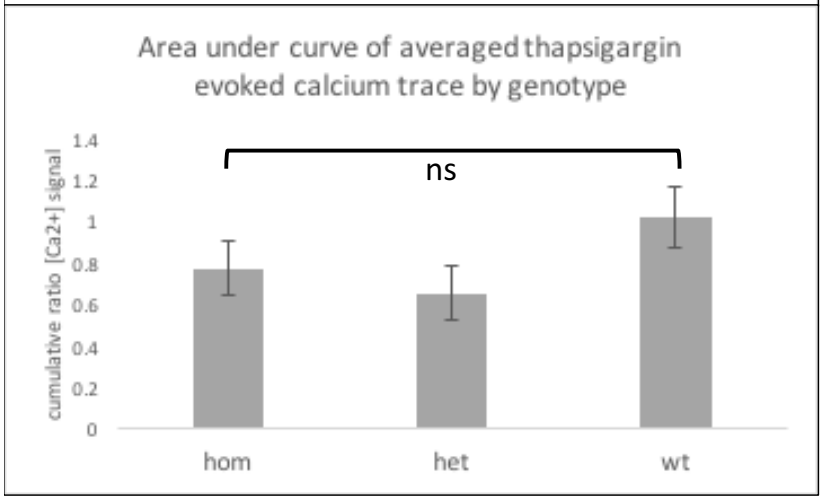

Fig. 13 AOC analysis of 1uM thapsigargin evoked calcium signal signal in N370S homozygous, heterozygous and wildtype embryonic primary neurons (a) individual cover slips with confidence intervals (S.E.M) (b) averages with confidence intervals (S.E.M)

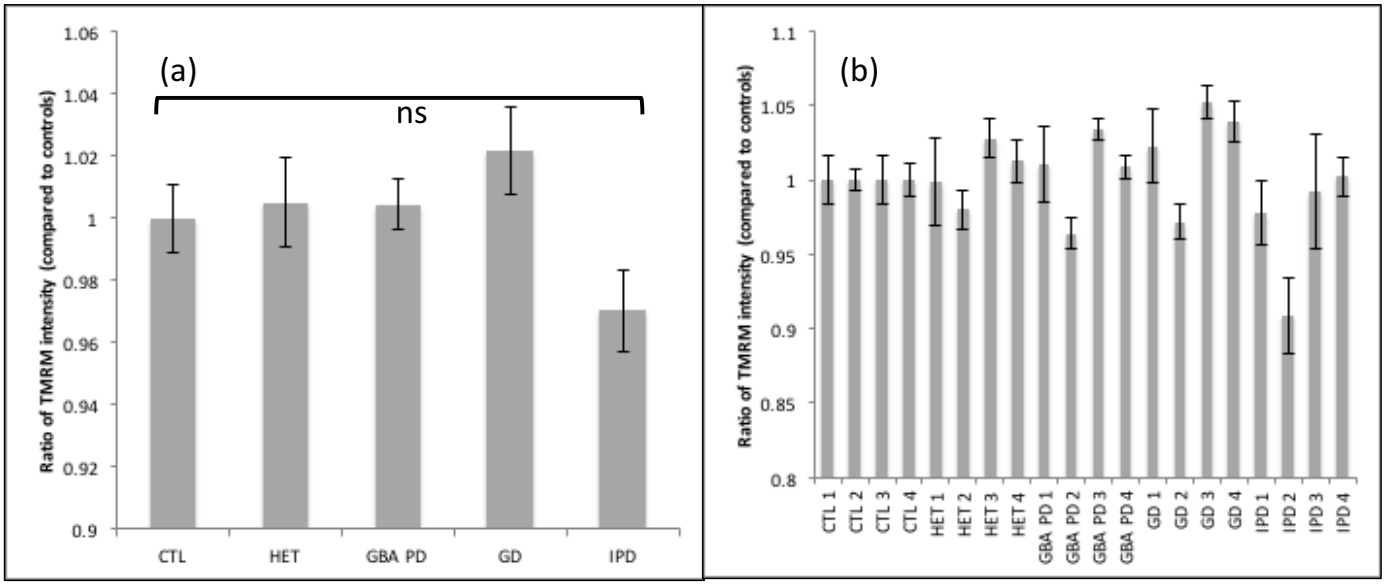

Fig 14. (a) Average ratio of TMRM intensity compared to controls of control, heterozygote, homozygote, Gaucher disease and idiopathic PD fibroblasts (b) Individual ratios of TMRM intensity from each cell line

thus producing a surrogate marker of mitochondrial membrane signal across thousands of fibroblasts.

Our results showed no significant difference between TMRM intensity across *GBA* carrying cell lines compared to one another or controls (Fig 12a, Kruschal Wallis p=0.3324) . There was a trend towards TMRM intensity being reduced amongst idiopathic Parkinson disease cases (Fig 12a), implying a reduced mitochondrial membrane signal. Reference to the individual measurement shows that this differences in predominately driven by subject IPD2, who had a TMRM signal some 10% lower than the other idiopathic Parkinson disease cases (Fig. 12b). Subset pairwise statistical analysis using the Mann u Whitney (idiopathic PD Parkinson disease vs control) test confirmed that this result was not significant (p=0.288).

6.10 Concluding remarks

The data collected reveals no evidence of either aberrant calcium homeostasis or impaired mitochondrial function within *N370S* carrying primary neurons and fibroblasts respectively. This is in contrast to the established literature. There are a number of possible explanations for this. The first is discrepancies in the disease models selected. The most relevant data collected was based on a neuronal induced pluripotent stem cell model carrying a combination of two mutations, *L444P* and *RecNcil*. The paper showed an increase in basal cytosolic calcium and of KCl-evoked calcium flux [273]. Both mutations give rise to a severe form of Gaucher disease[105], whilst *L444P* has been shown to cause a more penetrant Parkinson's phenotype [42]. *N370S* on the other hand is associated with a milder form of Gaucher disease, with incomplete penetrance in the homozygous state and concurrently a

less penetrant Parkinson disease phenotype.[105] As such, it may be that the severity of the *N370S* mutation is not sufficient to cause detectable impairment of calcium homeostasis.

With reference to existing data quantifying mitochondrial membrane potential, the most pertinent study used a *GBA* knockout model [276], once again it is likely that this gives rise to a more severe phenotype than our *N370S* model. Moreover our mitochondrial studies were carried out in a fibroblast model. Fibroblasts to do not experience voltage-gated calcium channel mediated influx of calcium. Without this influx and without a cellular phenotype which gives rise heightened calcium flux (such as in dopaminergic nigral neurons), it would seem unlikely that such mitochondrial overload would occur.

Perhaps the most comparable disease model tested to date is that of fibroblasts carrying the *N370S* mutation. In this paper, an increase was seen in thapsigargin (ER)derived evoked signal and a concurrent decrease in lysosomally derived calcium [278]. The most notable difference between this model and the primary neuronal mouse model we used was the scale of the evoked signals. Responses to thapsigargin recorded in the fibroblast model, were in the order of a ratio value 0.2 → 0.5 compared to an average change of 0.2→0.22 in our primary neuronal model. This discrepancy was exacerbated by the declining baseline calcium signal caused by the need to use calcium free HBS which caused gradual leakage calcium ions extracellularly. In terms of lysosomal calcium stores, with the exception of a few individual neurons, responses to GPN were not detectable, even though we were able to demonstrate successful permeabilisation of the lysosome. The implication of these findings is that the lysosomal and endoplasmic reticulum calcium stores are substantially

reduced in neurons compared to fibroblasts. This is in keeping with previous work which was unable to produce a significant thapsigargin evoked calcium signal.

Two contrasting conclusions may be drawn. The first is that because of the small scale of the calcium stores released, our experiments lacked the sensitivity to detect the discrepancies in evoked calcium signals, and as such that upregulation of ER derived calcium and subsequent cytosolic calcium 'overload' may still play a role in the predilection for Parkinson disease to develop in the brains of *GBA* carriers. Although possible this conclusion seems unlikely. The reason for this is the scale of calcium flux brought about by depolarization. Although it should be noted that 52mM KCL is a concentration does not represent a physiological stimulus, it gives rises to a change in calcium ratio of approximately 0.2 →1.2, which would render the effects of any additional ER derived calcium release at best marginal and at worst insignificant. It would seem unlikely that the tiny contribution of these additional stores would be the tipping point which would overload the cytosolic calcium buffering capacity of mitochondria.

It is interesting therefore that an increased basal calcium load and KCl-evoked action signal have been demonstrated in an induced pluripotent stem cell neuronal model. This data is compelling, especially the recapitulation of increased basal and calcium-evoked calcium signal with zinc finger transgenic modification of the cell lines [273]. If as suggested previously the reason this is not replicated in our results is more potent phenotype of the mutations in question, it may suggest that the increased calcium load results from upregulation of calcium entry through voltage gated calcium channels. One possible mechanism for this might be through alpha synuclein, the cytosolic protein of unknown aetiology which is the

principle component of Lewy bodies. It has been shown in a number of studies that alpha synuclein directly upregulates calcium influx by exerting a direct effect on voltage gated calcium channels. [279,280]. As mentioned previously there appears to be a bidirectional relationship between *GBA* activity levels and alpha synuclein, in which a reduction in *GBA* activity causes an increase in alpha synuclein levels and vica versa [36,281]. In this case it may be that the upregulation of alpha synuclein causes a direct increase in voltage gated calcium mediated calcium influx. This is an interesting hypothesis and would warrant further exploration in a more potent mutation carrying cell line such as *L444P*. This of course does not explain the reported rise in basal calcium signal, although this may be purely representative of poor cellular health rather than any innate dysregulation of calcium homeostasis. Such speculation aside we are unable to find any evidence of deranged calcium homeostasis in *N370S* mouse primary neuronal model.

Chapter 7 – Design and optimisation of AiM PD, a phase II open label, non-placebo controlled trial of ambroxol, a small molecular chaperone of the GCase protein.

7.0 Introduction

As described in the introduction, there is substantial interest in the GCase pathway as a potential target for neurointervention in Parkinson's. Small molecular chaperones offer perhaps the most plausible prospect of short term success in this field, primarily because of the volume of research which has been undertaken to date [135]. Chaperones alter chemical folding of a protein, in the case of enzymes stabilizing the catalysis of substrate. Under normal conditions the GCase protein is bound to the saposin C, a physiological chaperone molecule which is an intrinsic part of the ceramide synthesis pathway and is likely to aid interactions between the glucosylceramide substrate and the lipid membrane [282]. Nuclear magnetic resonance spectroscopy studies show that it binds to the GCase protein [61] and initiate the catalysis of glucosylceramide within the lysosome [283]. Its importance is emphasised by the finding that mutations in saposin C cause a clinical presentation of Gaucher disease but with a normal GCase enzyme activity [284].

Use of an external molecule to change the conformational properties of GCase is the principle underlying the use of small molecular chaperones. The GCase protein upon translation within the nucleus is transported within vesicles to endoplamic reticulum. Here it is post translationally modified in a number of steps in order to enable transport to the lysosome. Missense mutations in the GCase protein appear to disrupt this folding mechanism causing the protein to become sequestered within the endoplasmic reticulum[73].

The consequences of this are two fold. Firstly, whilst the active site of the mutant GCase protein is still suitable for catalysis, it does not reach the lysosome and hence is unable to catalyse the pH dependent breakdown of glucosylceramide. Secondly the sequestered protein causes an unfolded protein response. This physiological reaction to such protein sequestration includes halting of normal cellular translation, upregulation of molecular chaperones to aid folding and upregulated degradation of misfolded porteins, predominately by the proteasome system [78]. Until removed the sequestered protein gives rise cellular toxicity mediated predominately by reactive oxygen species production. If the unfolded protein response is able to overcome protein sequestration sufficiently quickly then the cell is restored otherwise the cell is marked for apoptosis and disposed of.

In the case of small molecular chaperones of the GCase enzyme, the conformational change resulting from its interaction with GCase (rather than directly assisting substrate catalysis) aids the physiological folding mechanisms and this allows transport of the enzyme away from the lysosome, and for at least a substantial portion of the protein, into the lysosome. An interesting observed finding is that the administration of small molecular chaperones causes an uplift in GCase activity in wildtype cell lines [37,285,286]. This presumably is a reflection of refolding of sequestered wildtype GCase in the ER to the cytosol. The desirability of this is debatable. If this GCase in question is functionally competent then additional protein reaching the lysosome is undoubtedly a positive. If on the other hand this sequestration serves as an intrinsic quality control mechanism for GCase, it could be argued that sending large amounts of compromised GCase protein to the lysosome may be potentially harmful.

As discussed in the introduction, it is unclear what the pathogenic mechanism of *GBA* Parkinson disease is. That said, whatever this mechanism is, it seems logical that mobilisation of mutant GCase from the endoplasmic reticulum can only be beneficial. If GCase were to have a direct role in in the disposal of alpha synuclein via autophagic pathways, as has been suggested by a body of evidence implying a direct interaction between the two [62,65,66,287-289], then clearly additional functionally active GCase reaching the lysosome would remove alpha synuclein and be protective in terms of Parkinson disease. Similarly, additional lysosomal GCase would aid removal of cellular glucosylceramide If substrate accumulation is the cause. If sequestration of the enzyme within the ER is the critical step [75,76], then removal of this protein by chaperones would dampen the unfolded protein response and reduce cellular toxicity. The only forseeable negative effect could be if the release of the sequestered GCase were to somehow overload the proteosomal system, mediated by the chaperone protein LAMP2A [68], which is responsible for the removal of compromised cellular GCase [136]. Such a mechanism would be dependent of overload of the Lysosomal Integral Membrane Protein-2 (LIMP2) protein. LIMP2 is the mediator of GCase transport to the *cis* and then *trans* golgi apparatus [290]. It binds to GCase to form a complex which is supplemented by AP-1 protein, allowing uptake of GCase into the late endosome.[290]. This could in turn potentially disrupt the removal of other proteins which may be contributory to Parkinson disease, including alpha synuclein, which there is some evidence to suggest is at least partially removed by the protesomal system [65,66].

7.1 Inhibitory and non-inhibitory chaperones

Small molecular chaperones can be subdivided into inhibitory and non-inhibitory subtypes [135].The inhibitory tag refers to the fact that these chaperones bind directly to the active site of the protein in order to induce conformational change, in turn antagonising the binding of enzyme substrate(s) and hence reducing enzyme activity. Upon reaching the acidic conditions of the lysosome, elution of the chaperone may occur leaving the active site available to allow enzyme catalysis. The degree of elution is dependent on the affinity of the chaperone for the substrate; if the affinity is too great or too high a dose is used then the active site will remain bound to the chaperone and no catalysis will occur. The concern here is clearly that far from aiding enzyme catalysis, prolonged binding at low pH to the active site of the protein will in fact inhibit its action. This was the case with isophagamine, which maintains a high binding affinity to the active site up to pH 4. Clinical trials of the compound in the context of Gaucher disease were unsuccessful and it may be this enhanced inhibition was the culprit [133,291,292]. The majority of chaperones discovered to date are inhibitory, hence careful consideration must be made of the choice of chaperone and the dose selected. The latter consideration is in two parts, namely whether peripherally chaperone concentration is sufficient to cause an inhibitory effect but high enough to reach the central nervous system and act as an effective small molecular chaperone once it gets there. The first was *N*-(*n*-nonyl)deoxynojirimycin

Physiological post translational handling of GCase protein

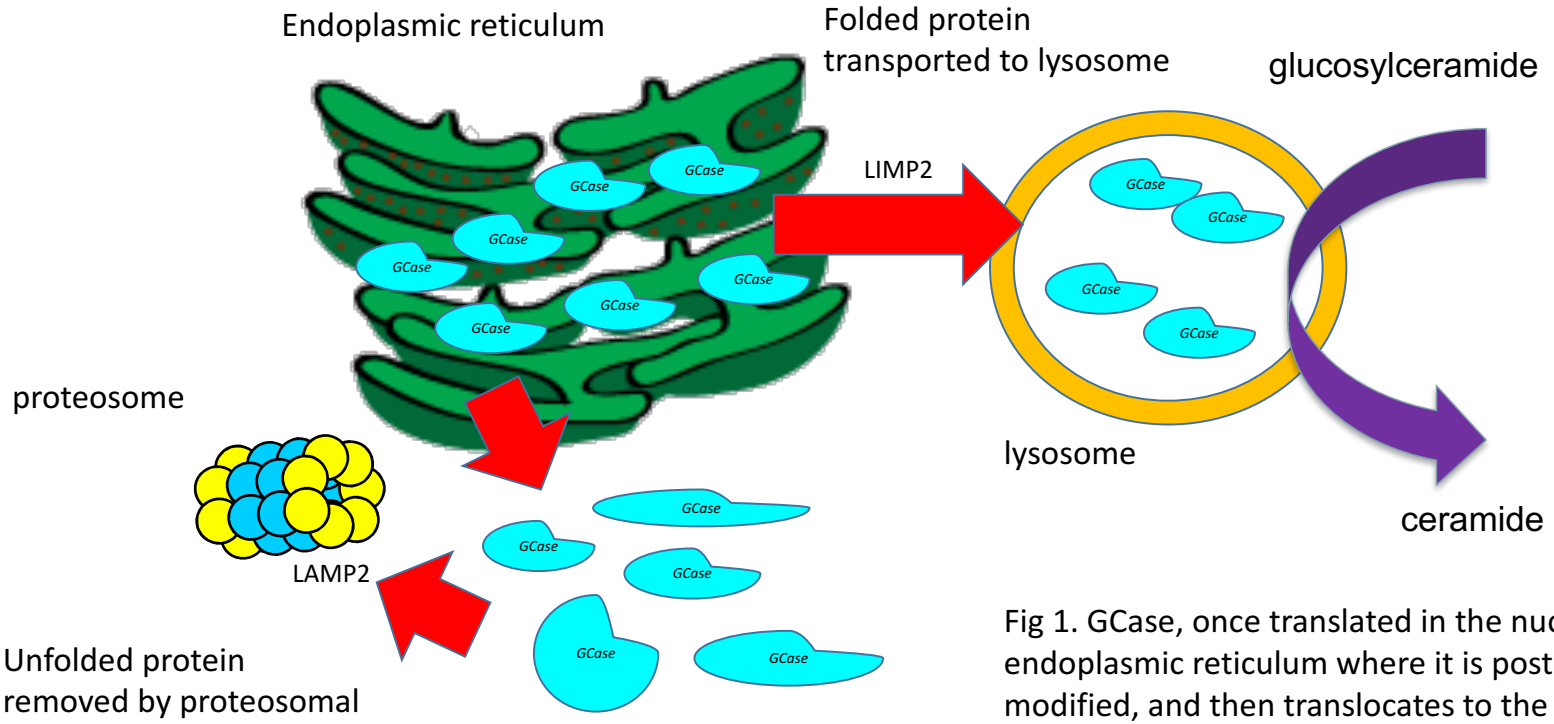

Fig 1. GCase, once translated in the nucleus moves endoplasmic reticulum where it is post translationally modified, and then translocates to the lysosomal mediated by LIMP2. Small quantities of aberrant or misfolded GCase is recognised by the LAMP2A protein and disposed of by the proteosome

Handling of GCase protein in the presence of GBA mutations

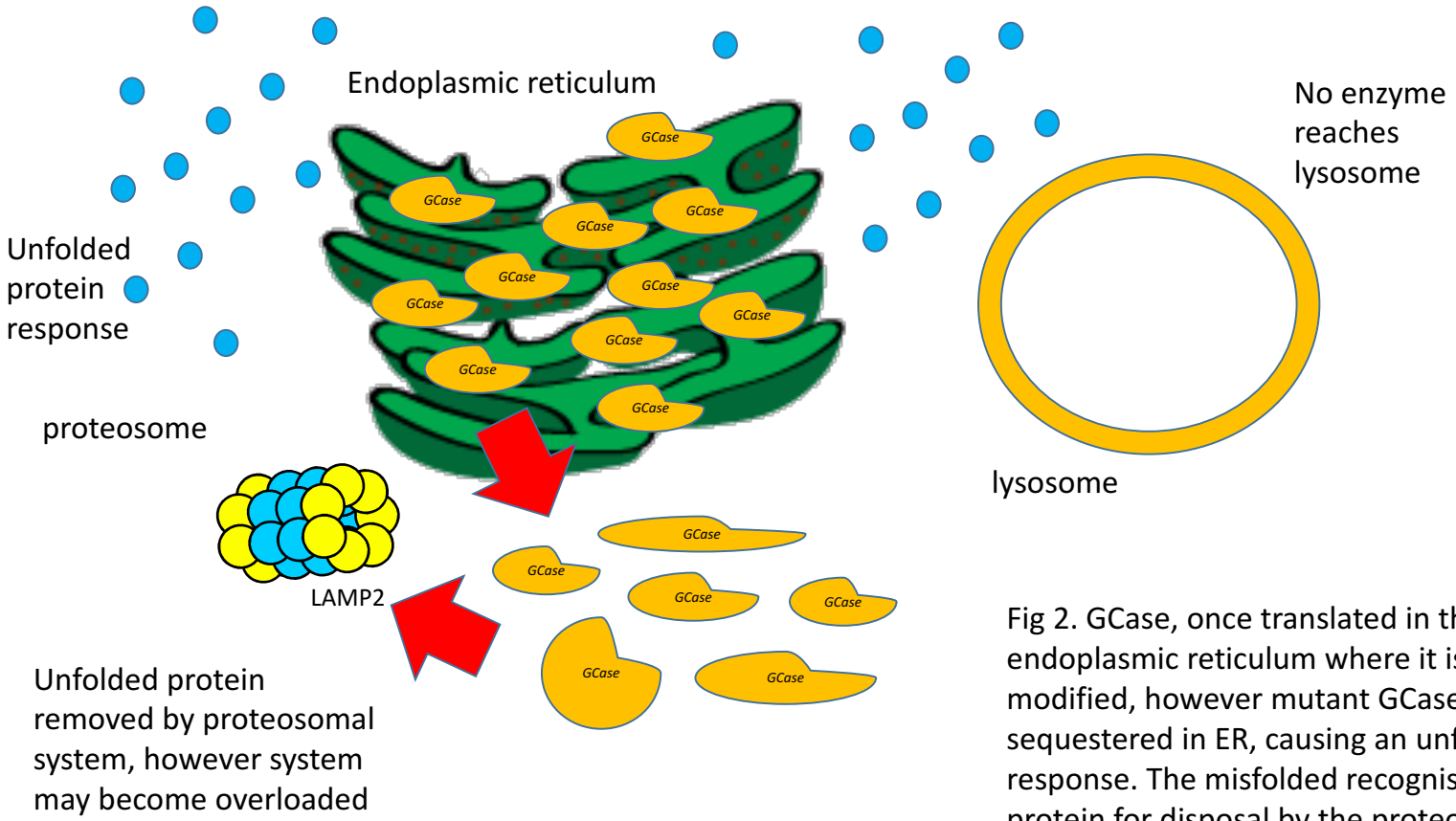

Fig 2. GCase, once translated in the nucleus moves endoplasmic reticulum where it is post translationally modified, however mutant GCase is misfolded and is sequestered in ER, causing an unfolded portein response. The misfolded recognised by the LAMP2A protein for disposal by the proteosome, however the system is unable to handle the volume protein.

(NN-DNJ), an iminosugar which at 10uM concentrations was found to cause a x2 increase in GCase activity. There have been subsequently a number of largely iminosugar based chaperones, however to date non have been found to be viable interventional medicinal products. That said, a recent study using an unnamed small molecular chaperone of GCase in induced pluripotent stem cells carrying a number of *GBA* mutations showed an upregulation of GCase within the lysosomal compartment, increased clearance of all synuclein species and a beneficial effect in terms of downstream neurotoxicity [293].

7.2 Ambroxol

Ambroxol is a metabolite of bromhexine. It has been used for over 30 years as a mucolytic and in the treatment of hyaline membrane disease [294]. In recent years it has also been suggested to be a novel treatment in acute respiratory distress syndrome [295]. Interestingly it has anaesthetic properties which may be mediated by blockage of voltage gated sodium channels and has been used as cough medicine [296]. It has also been suggested to be an inducer of exocytosis of calcium stores from the lysosome [297]. It has an excellent safety profile. The summary of product characteristics list only nausea as a common ((≥1/100 to <1/10); dyspepsia, vomiting, diarrhoea and abdominal pain as uncommon (≥1/1,000 to <1/100) and urticarial rash as a rare (≥1/10,000 to <1/1,000) side effect [298].

A screen of some 10,000 FDA approved compounds found that in fibroblast and lymphoblast cell lines of a number of Gaucher disease patients, showed that ambroxol was able to stabliise GCase during thermal denaturation, preventing any reduction in GCase

activity. Furthermore, it was reported that ambroxol was a mixed type inhibitor of GCase, with high binding at neutral pH but almost no inhibitory effect below pH 4.6. This was in stark contrast to isophagamine, which maintained a high binding affinity to pH 4.1 [133]. Their data indicated that a concentration of 60uM was the threshold at which concentration related inhibition occurred. Subsequently ambroxol was confirmed to increase GCase activity in fibroblasts and mouse models of Gaucher disease [35,134] and was shown to reduce levels of alpha synuclein in wildtype and mutant fibroblasts, work which was later confirmed in a neural crest stem cell model [37]. The latter study also showed upregulation of a number of autophagic pathways in response to the ambroxol [37].

7.3 Ambroxol and the blood brain barrier

In structural terms small molecular chaperones such as ambroxol are likely to cross the blood brain barrier. This principle was first confirmed in murine model of GM1 gangliosidosis where a small molecular chaperone molecule of β-galactosidase was able to successfully reduce GM1 substrate levels. [299,300] A number of studies have confirmed the brain penetrance of ambroxol. In *L444P* wildtype and synuclein overexpression mice respectively activity increased and in the latter alpha synuclein levels reduced [286]. The increase in GCase activity was mimicked in a wildtype human primate where GCase activity was increased following oral administration of ambroxol 100mg (≈ 40mg/kg) but not 22.5mg (≈ 10mg/kg) [301]. Moreover a phase II trial of ambroxol in 5 neuronopathic Gaucher patients at a dose of approximately 1.2g/day achieved 10-20% of the serum ambroxol concentration within the cerebrospinal fluid [302].

7.4 Safety and tolerability of ambroxol

Ambroxol has a long history of use in humans, which documents its very low level of toxicity. For several decades ambroxol has held market authorisation by the European Medicines Agency (EMEA) and in several countries across Europe for over-the-counter indications at doses up to 120 mg/day. There have been a number of clinical trials of ambroxol at a variety of doses. In one small study 12 participants with type I Gaucher disease took 150 mg daily in two divided doses for 6 months with minimal side effects [303]. A recent study in Japan treated 5 neuronopathic Gaucher disease patients with ambroxol at an escalating dose of 3mg/kg/day to 5mg/kg/dose for 12-31 months [302,304]. The only adverse event reported was mild hypouricaemia (Narita et al., 2016). Another study treated 12 healthy volunteers with 500 mg or 1g twice a day for 5 days and revealed no adverse effects [305]. A number of studies have demonstrated use of a 1g daily dose on (Intensive Therapy Unit) ITU in participants with acute respiratory distress syndrome (ARDS) for short periods. In one study 32 participants with Acute Respiratory Distress Syndrome (ARDS) were administered 40 mg/kg ambroxol in 4 daily divided doses for up to 10 days with no adverse effects [306] whilst a recent meta-analysis of 508 participants enrolled in studies using high dose ambroxol (15-20mg/kg/day) for short periods (3-7 days) to treat acute respiratory distress syndrome and acute lung injury did not reveal any significant adverse effects [295]. A further trial assesses the efficacy of ambroxol (1g dose administered every 12 hours for a maximum of 48 hours) prophylactically in pregnant women to prevent infantile acute respiratory distresss syndrome. The study demonstrated its safety to pregnant woman and the unborn child [307].

7.5 Ambroxol as a neuroprotective agent in Parkinson disease

The combination of its excellent safety profile, promising *in vitro* studies and rationale for use along with its robust brain penetrance at appropriate doses make ambroxol a highly promising neuroprotective target in both idiopathic and *GBA* Parkinson disease. We therefore decided to clarify its potential application in a phase II trial.

7.6 Objectives

Primary objective

- To confirm ambroxol central nervous system penetrance and GCase target acquisition in a population of Parkinson disease patients with and without *GBA* mutations

Secondary objectives

- To assess the safety and tolerability of the Glucocerebrosidase (GCase) enhancing chaperone ambroxol in Parkinson disease participants
- To quantify the effect of ambroxol on known neurodegenerative biomarkers
- To quantify the effect of ambroxol on glucosylceramide levels and GCase expression levels in cerebrospinal fluid

Exploratory objectives

- To explore whether ambroxol leads to improvement in cognitive performance, Montreal Cognitive Assessment (MoCA)

- To explore whether ambroxol leads to improvement in Parkinson Disease non-motor symptom assessment scale (NMSS) and non-motor symptom questionnaire

7.7 Design

Open label proof of principle non-placebo controlled interventional study.

Briefly participants undergo clinical and biochemical assessments and have cerebrospinal fluid, serum and urine samples taken at baseline prior to 5 weekly dose escalations to a target dose of 1.24g daily in three divided doses which is administered for a further 6 months. Following this there is 3 month washout period with subsequent reassessment at the end of this period. A summary of the assessment and assays used in the study is shown below (table 1). Study design was carried out by SM, Prof. Anthony Schapira, Prof. Tom Foltyniea and Dr Vincenzo Libri.

biochemical	**bl**	**10d**	**3m**	**6m**	**9m**
Leucocyte GCase	X	X	X	X	X
Serum ambroxol	x			x	x
Serum ELISAs	x		x	x	x
cerebrospinal fluid ambroxol	x			x	x
cerebrospinal fluid Glucocerebrosidase and Glucosylceramide estimation	x			x	
cerebrospinal fluid ELISAs	x			x	x
Proteomics, lipidomics, metabolimics (cerebrospinal fluid, serum, urine)	x			x	x
clinical	**bl**	**10d**	**3m**	**6m**	**9m**
UPDRS	(x2)		x	x	x
MoCa	x			x	x
NMS	x			x	x
NMSQuest	x			x	x

Table 1. Summary of clinical and biochemical assessments undertaken at each visit.

7.8 Optimisation and validation of exploratory assays

GCase assays were carried out by SM, Laura Smith or Katherine Lee. Analysis was carried out by SM.

7.9 GCase activity

The key assay in this study is the measurement of GCase activity. GCase activity is measured using a fluorogenic assay. Briefly, a known concentration of a synthetic substrate (4-methylumbelliferyl-D-glucopyranoside 4.8mM) is added to a known volume of leucocyte pellet lysate/ cerebrospinal fluid and incubated at 38 degrees celcius for a defined period. At this point, a known volume of an alkali glycine solution is added. The GCase will catalyse the substrate into 4-methylumbelliferone. In the presence of the alkali pH, the solution will fluoresce at 450nm following excitation at 365nm. By quantifying the intensity of the emitted light and comparing it to a standard containing a known concentration of 4-methylumbelliferone one can calculate the activity of the enzyme, normalized in the case of the leucocyte pellet to the protein concentration of the pellet and in the case of cerebrospinal fluid to the volume of cerebrospinal fluid used.

There are a number of limitations of the GCase assay. Most prominently it gives only a partial estimation of the catalytic capacity of the GCase protein because it takes no account of expression levels of the GCase protein itself. Moreover, the assay is extremely sensitive to a number of methodological factors which can substantially affect the inter and intra assay variability. This is especially pertinent for cerebrospinal fluid GCase because the

recorded activity levels are so low. In the preparatory work for this study it was vital to minimize the variability as much as feasible in order to minimize the possibility of type 2 error.

7.9a Previous reports of GCase activity in cerebrospinal fluid

In our hands cerebrospinal fluid activity were measured from 0.154-0.407 nmol/hr/ml cerebrospinal fluid whilst "normal" leucocyte GCase is considered to be 5-15nmol/hr/mg protein. Assuming cerebrospinal fluid protein concentration to be around 0.45g/l, we approximate our measured cerebrospinal fluid activity to 0.342- 0.904 nmol/hr/mg protein, an approximately 15 fold reduced level of activity.

In comparison Balducci et al [308] found mean activity in healthy controls to be 0.0312±0.0066 nmol/hr/ml. Parnetti et al [40,45] reported 0.0204-0.0966 nmol/hr/ml in cerebrospinal fluid of patients undergoing lumbar punctures for other neurological disorders, similar to our cerebrospinal fluid donors. Persichetti et al [44] however, reported activities between 0.0876-0.912 nmol/hr/ml, a similar range to those found in our results which probably reflects the similarity between the protocols used. A summary of the respective protocols used is shown below (Table 2).

Table 2. Summary notes comparing differences in protocols between recent papers			
Authors	**cerebrospinal fluid:substrate**	**Incubation**	**notes**
Balducci wt al. [308]	100µl:100µl	24hrs	3mM substrate, pH 4.5
Parnetti et al. [40,45]	50µl:100µl	24hrs	3mM substrate, pH 4.5
Perschetti et al. [44]	20µl:40µl	3hrs	10mM substrate, 0.2% sodium deoxytaurochol ate, pH 5.0

7.9b Degradation of cerebrospinal fluid and leucotye GCase activity with storage

A key issue during our design of the study was the observation that cerebrospinal fluid GCase activity appears to be affected by freeze thaw cycles and the length of storage at -80 degrees. Persichetti et al. noted serial reduction of GCase activity with freeze thaw cycles, with around a 5-10% loss activity noted at each cycle [44]. They also note an almost complete loss of GCase activity after only 7 days of storage at -20°C, whilst at -80°C they noted an approximately 20% loss of activity at 4 weeks and an almost immediate dip around 10% after thawing compared to fresh sample [44].

We wished to see what the GCase activity degradation rate was “in our hands” and so carried out an experiment to assess the serial loss of activity after long term storage. Fresh cerebrospinal fluid from control subjects being investigated for suspected normal pressure or idiopathic intracranial hypertension hydrocephalus were collected from the Royal Free

Hospital between January 2016 and November 2016. A cerebrospinal fluid GCase assay was performed within an hour of collection. Samples were aliquoted then frozen at -80 and thawed respectively at 3, 7, 10, 14, 21 and 28 days and GCase assays were repeated. At each time point 10 repeats were performed on 5 different cerebrospinal fluid samples.

Our results showed that there was an immediate drop in cerebrospinal fluid GCase activity of around 20% which then remained constant until 24 days, at which point activity fell to 30% and then to 40% at 28 days (Fig 3). In terms of leucocyte pellet GCase the immediate 20% drop was replicated, although over the four week course of the experiment this fall remained relatively consistent (Fig. 4) . On the basis of these findings we made the decision to process all samples within a 2 week window, to avoid variation inactivity measurements following prolonged storage.

7.9c Variation in substrate concentration

To date when carrying out GCase activity measures we had made up a fresh substrate solution. We realised that this was a substantial source of potential variability for two reasons. These were 1) that the volume of substrate added to the solution was extremely small, meaning that margins of error for weighing the samples could cause a substantial impact on the GCase activity. Assuming that at the stated concentration the active site of the GCase was not saturated, an increase in substrate concentration would equate to an increase in concurrent catalytic reactions and in turn and increase in GCase activity (and vica versa). We also noted 2) the solubility of the substrate powder was not complete even with prolonged vortexing. Once again any variation in concentration of soluble substrate could

effect the GCase activity. The latter problem was easily overcome by heating at 25 degrees for 20 minutes. We initially assessed whether any difference in GCase activity after a freeze thaw cycle and found there was no statistically significant differences between the two (n=5, 10 wells per sample, Wilcoxon rank sum p=1.00). We then compared the activity calculated with frozen aliquots of substrate solution which had been frozen at the beginning of the experiment, with GCase activity calculated using a fresh substrate solution (Fig 5) and found there was no significant difference between the two (n=5, 10 well per sample, week 1 Wilcoxon rank sum, p=0.386, week 2 p=0.772, week 3 p=1.00, week 4 p=0.563). On this basis we elected to use a frozen dissolved substrate solution from the same batch for all assays.

7.9d Variation in standard utilised

In order to prevent variation caused by disprecancies in the concentration of the standard caused by weighing discrepancies, we elected to use frozen and aliquoted standard from one batch for the duration of the study. To test whether freezing had any effect on the standard we carried out a test assay using frozen and fresh standard from the same batch. We found no significant difference between the two batches (n=4, 10 wells per sample p=0.848).

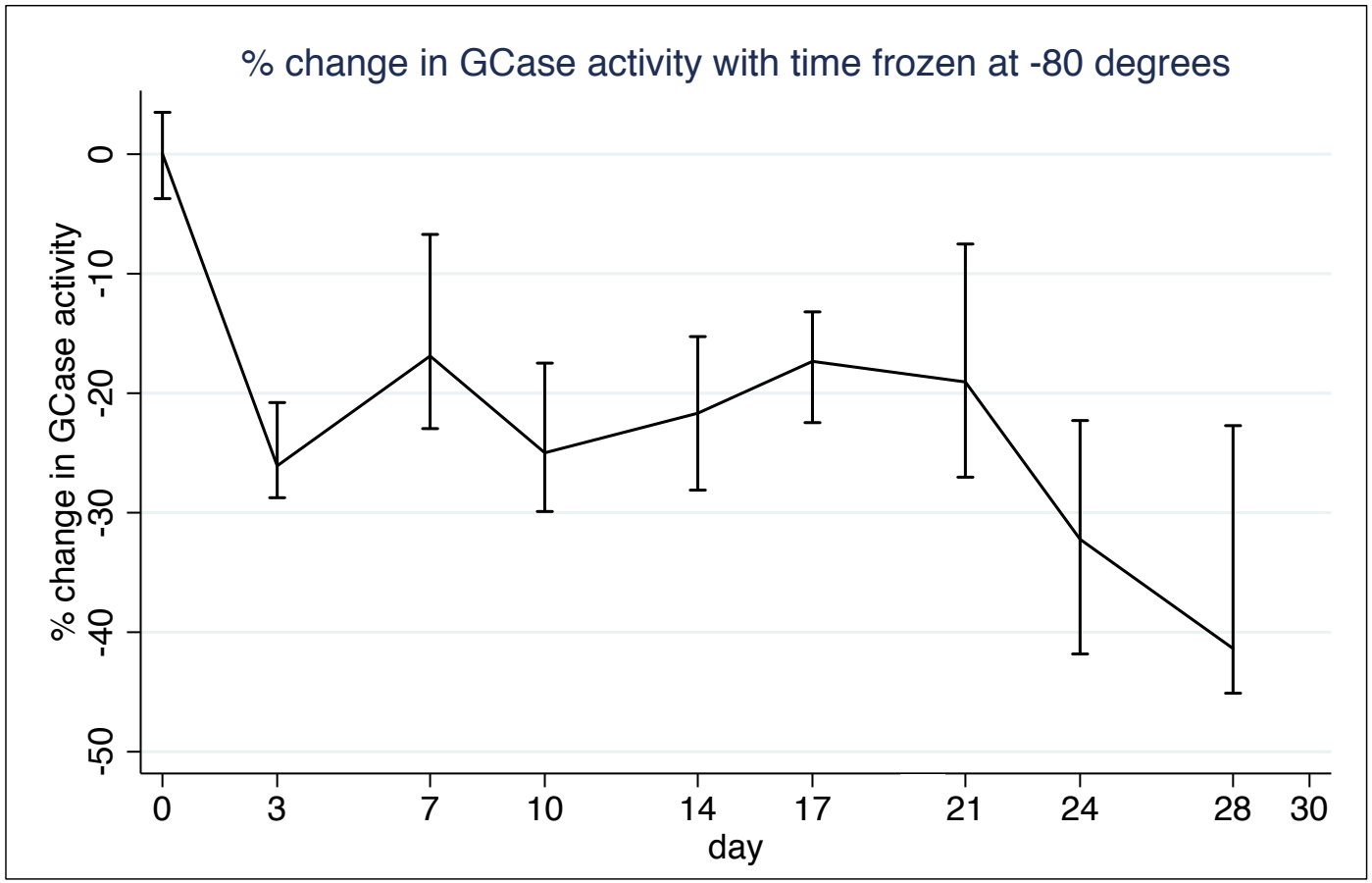

Fig 3. Percentage change of median CSF GCase activity following freezing at -80 degrees. Confidence intervals IQR

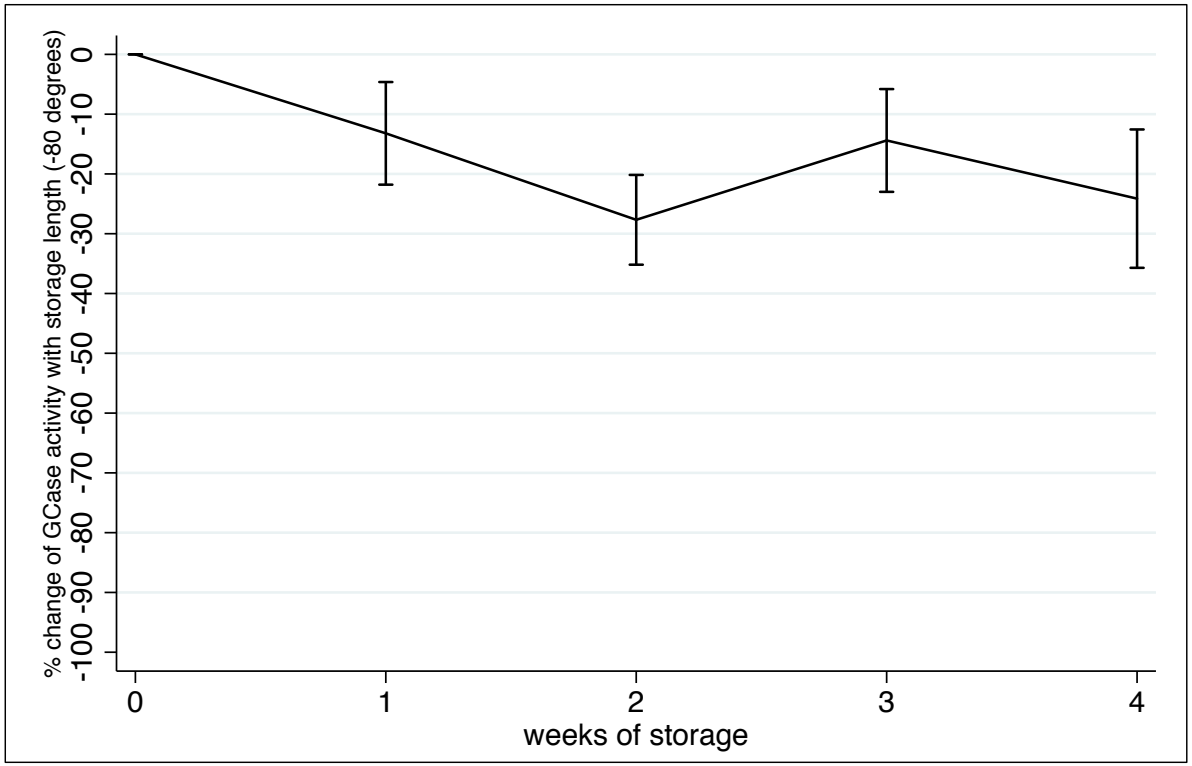

Fig 4. Percentage change of median CSF leucocyte GCase activity following freezing at -80 degrees. Confidence intervals IQR

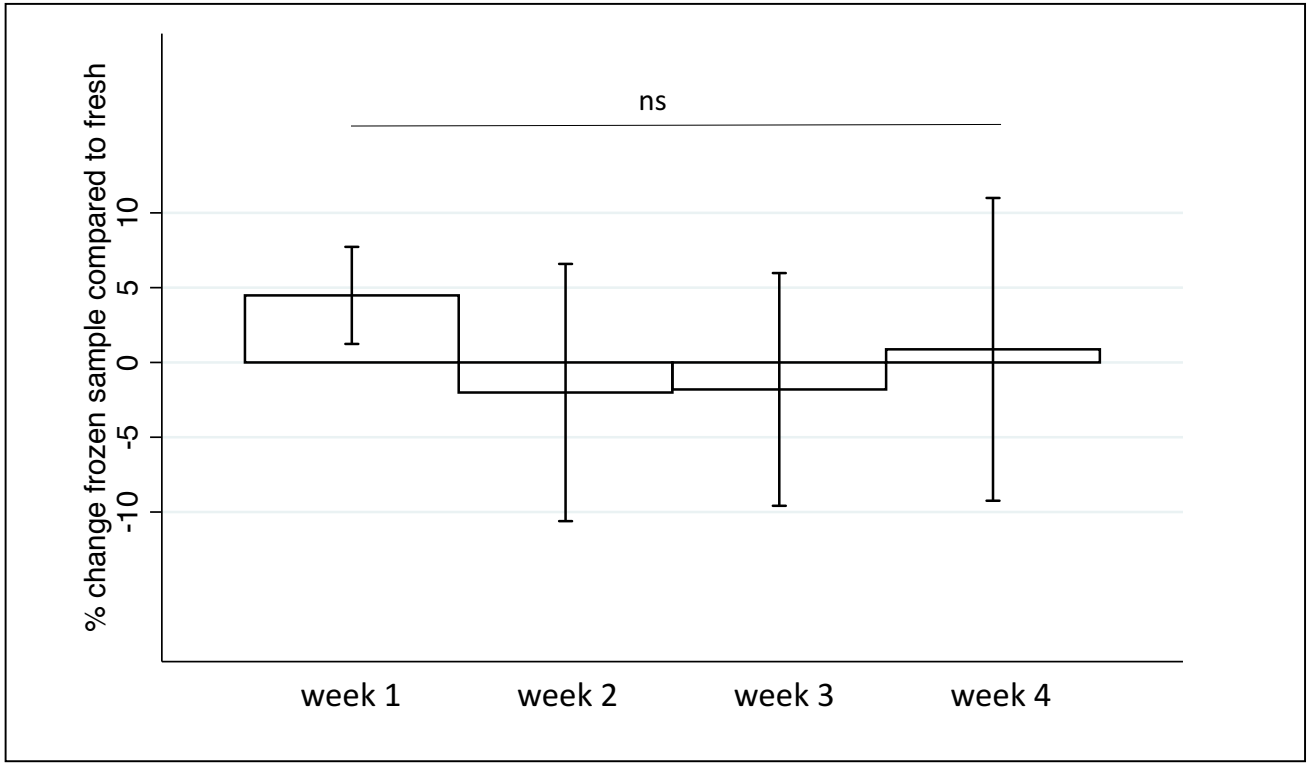

Fig 5. Percentage change of median CSF leucocyte GCase activity with freshly made up or frozen substrate solutionweeks denote number of weeks since freezing of substrate mix

7.9e Intra- and inter-assay variabilities

The cumulative % coefficient of variance (CV) for all the experiments (excluding storage assays) was 3.08% ($n_{samples}$=5) and 1.72% (n_{plates}=17) for the intra- and inter-assay CVs respectively. Although overall %CVs were low, there was a considerable range for the intra-assay CV, with 0.34% being the lowest and 13.33% the highest %CV found across all the experiments. In fact it is likely the CV is in real terms some what lower than this, as we saw an improvement in CV during the course of our optimisation. The highest %CV was from the first trial and 0.34% from one of the later experiments.

7.9f Expected effect on cerebrospinal fluid GCase of ambroxol

Ambroxol has been shown consistently to increase GCase activity in fibroblasts, neural crest stem cells, mouse brain lysates and non human primates [35,37,286,301]. That said, the effect of ambroxol binding to GCase in cerebrospinal fluid is unclear. The rationale for the observed increase in GCase activity in these various models is that chaperoning of GCase to the lysosomal portion of the cell allows pH dependent catalysis to occur. Cell lysis typically keeps lysosomes intact, hence GCase activity in these cell lines is increased in response to cellular incubation of ambroxol because the lysosomes are enriched for GCase protein. Conversely cerebrospinal fluid is broadly acellular (and samples are spun acellular prior to the assay), hence the detection of GCase activity in it means that free GCase protein must be present in the cerebrospinal fluid (albeit it at very low concentrations). In order to best

intepret the findings of the AiM PD trial we carried out a series of experiments to understand the relationship between cerebrospinal fluid GCase activity and the presence of ambroxol.

7.9g Incubation of cerebrospinal fluid with ambroxol causes a reduction of GCase activity

In order to understand the effect of central nervous system ambroxol penetration we added ambroxol to control cerebrospinal fluid derived from patients from the Royal Free hospital undergoing routine LP to rule out normal pressure hydrocephalus or idiopathic intracranial hypertension. Ambroxol was added at a concentration of 500nM, a figure based on measured concentrations in the cerebrospinal fluid in a recent clinical trial using a similar dose [302]. In addition we added isophagamine, another small molecular chaperone of GCase, again at a dose of 500nM [292]. We also carried out a number of positive controls of GCase inhibition, namely conduritol B epoxide (CBE), an inhibitor of GCase activity [309] and denatured cerebrospinal fluid (by heating cerebrospinal fluid for 30min at 80°C).

Ambroxol appeared to inhibit GCase activity by approximately 50% (rank sum, 95%CI 40.40-52.11%, $p<0.0001$) compared to control cerebrospinal fluid. Interestingly isophagamine, which has been previously shown to be a more inhibitory chaperone, reduced activity by a further 30% (80% reduction compared to controls) compared to ambroxol (rank sum, $p<0.0001$) producing about 20% of the GCase activity of control cerebrospinal fluid (95%CI 18.36-20.99%]. GCase activity was undetectable in both CBE treated and denatured cerebrospinal fluid. These results are displayed graphically in Fig. 6.

7.9h Speculating on the expected effect of cerebrospinal fluid GCase following ambroxol administration.

These findings are interesting as they confirm that ambroxol binds to the active site of the free GCase protein and causes direct inhibition of catalysis. As such any change other than inhibition of GCase activity implies an upregulation of GCase expression into the cerebrospinal fluid in response to ambroxol. This would not be a completely unexpected finding, for instance the newly unsequestered GCase protein might be available in sufficient quantities as to be surplus to the requirements of the lysosome, meaning it may be exocytosed from central nervous system cells and eventually into the cerebrospinal fluid. A sufficient increase in GCase concentration would be likely to outweight the inhibitory effect of the ambroxol. This emphasises the key importance of assessment of GCase and glucosylceramide levels within the cerebrospinal fluid as these will allow further interpretation of the basis of ambroxol's mode of action. For instance a static or increased GCase activity, with an increase in cerebrospinal fluid GCase levels and a decrease in glucosylceramide substrate levels would be consistent with this finding. A decrease in GCase activity with a static GCase concentration and a decrease in glucosylceramide levels would reveal ambroxol binding to the substrate and increased substrate catalysis. Even the combination of a reduced GCase concentration, reduced GCase activity and reduced glucosylceramide levels would imply increased GCase reaching the lysosome and a corresponding reduction of exported GCase into the cerebrospinal fluid.

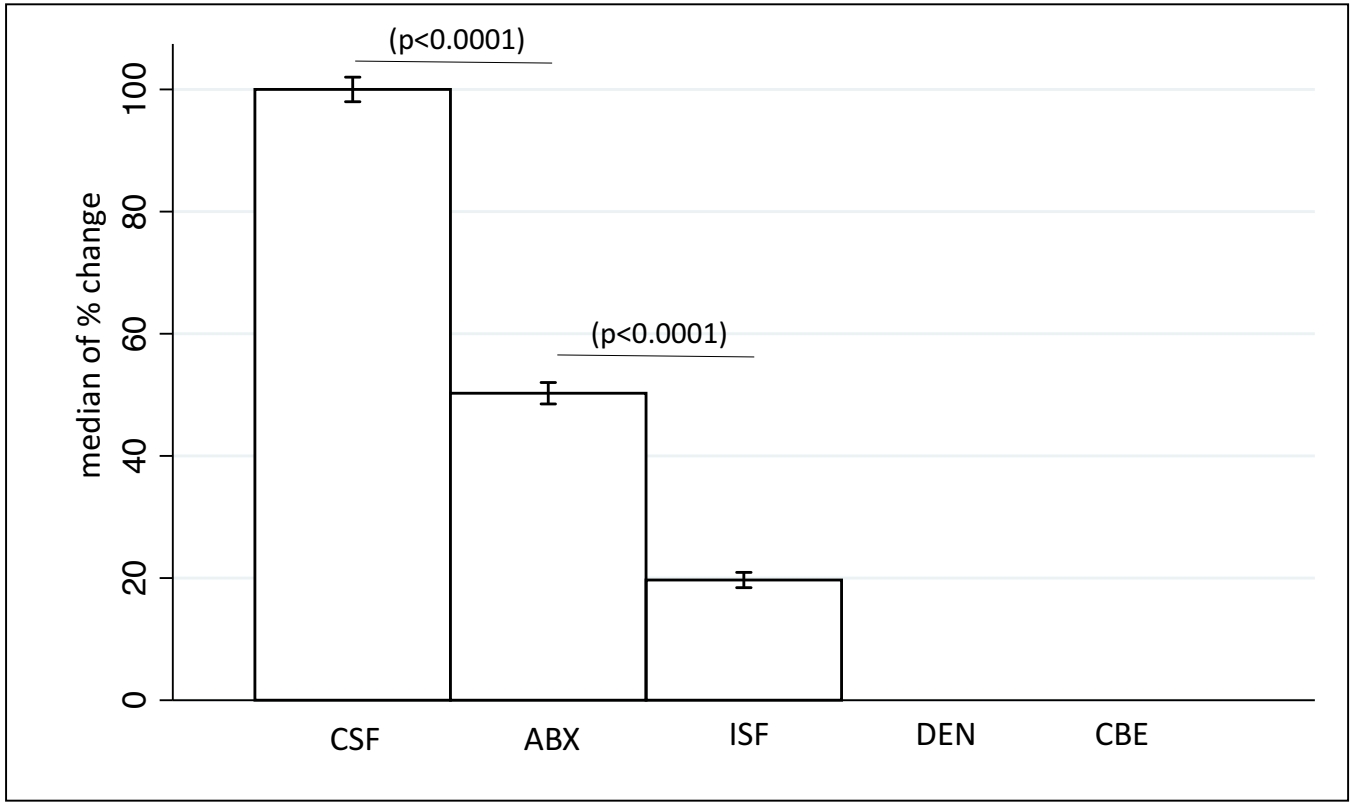

Fig 6. median of % change of CSF GCase activity in control CSF (CSF) and following incubation with ambroxol (ABX), isophagamine (ISF), denaturation at 80 degrees (DEN) and CBE (CBE).

7.9i Power calculations based on observed GCase activity reduction

Change of cerebrospinal fluid GCase activity is the primary outcome of the AiM PD study. Based on the dataset above (mean change activity 50.47%, SD 3.96%) we estimated the number of participants required to produce a statistically significant fall in GCase activity (baseline vs 6 month ambroxol treatment) assuming a power of 80% and confidence intervals of 95% (paired student T test) is 2 per study group, meaning that to detect changes within each study group a total cohort of 4 is required. Furthermore, I calculated a power curve to understand the limits of power of the study (Fig 7). Using this curve I calculated that given the proposed number of participants (N=20, 10 Parkinson disease, 10 *GBA* Parkinson disease), assuming a 50% fall in activity post ambroxol, a standard deviation of 50% in *GBA* and iParkinson disease groups and of 75% across all participants would be detectable. Based on these calculations we felt the study was amply powered to detect changes in the primary outcome.

7.9j Optimisation dilution of leucocyte pellet sample from CPT blood collection tubes

In order to standardise the collection procedure for leucocytes derived from human blood we purchased BD Vacutainer® CPT™ Mononuclear Cell Preparation Tube - Sodium Heparin (catalogue number 362753). Briefly the vacutainer tubes collect a set volume (8ml) of blood above an intermediate density material which allows blood cells to pass to the bottom of the tube upon centrifugation. Leucocytes, being too dense to pass through the material are collected underneath the serum and can be removed and pelleted with a

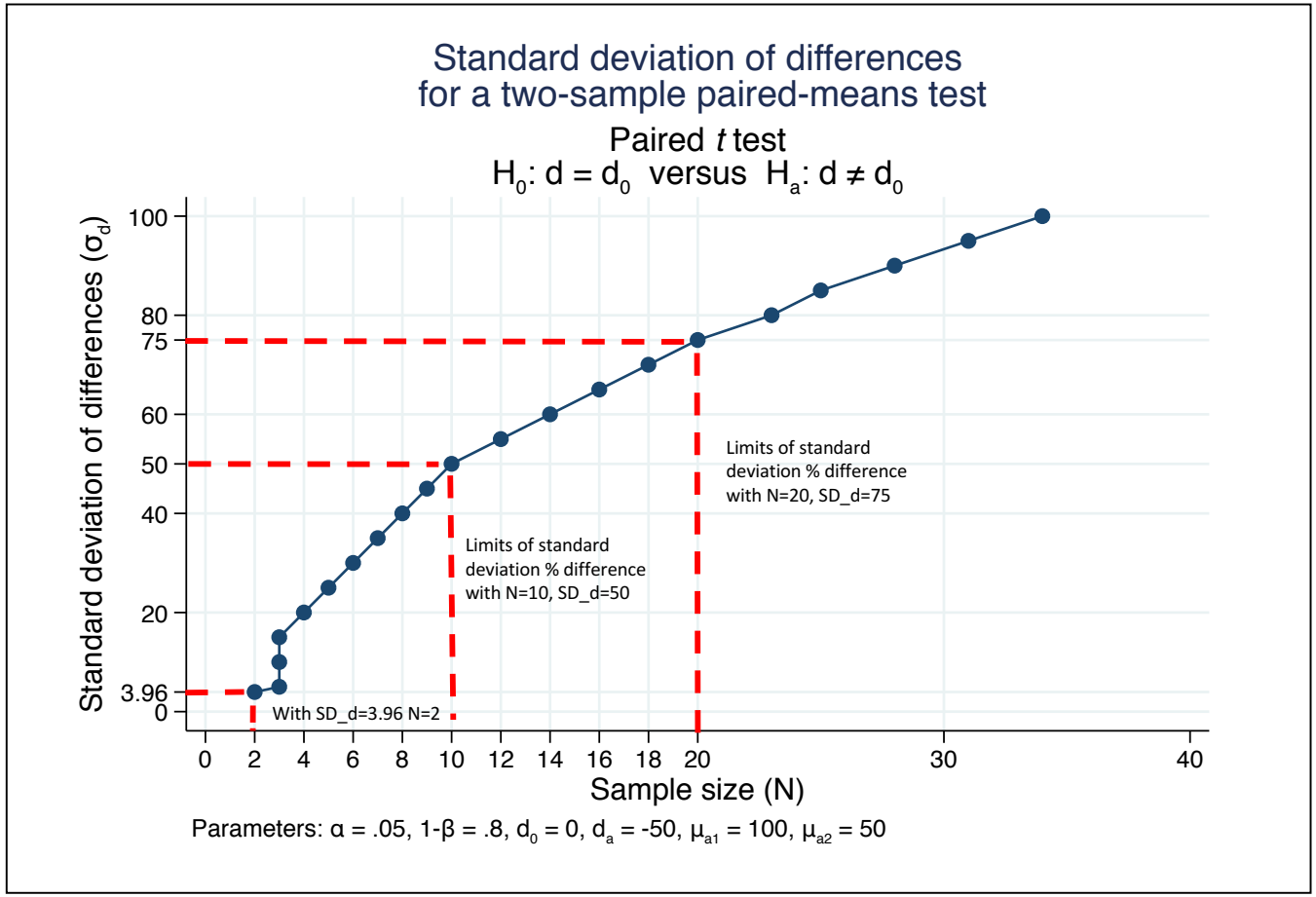

Fig 7. Power curve. Sample size (N) plotted against standard deviation of difference (y). Dotted red lines indicate standard deviation of preparatory assay (3.96), projected limits of significance testing with sample of 10 (number in each group) and 20 (total number in study)

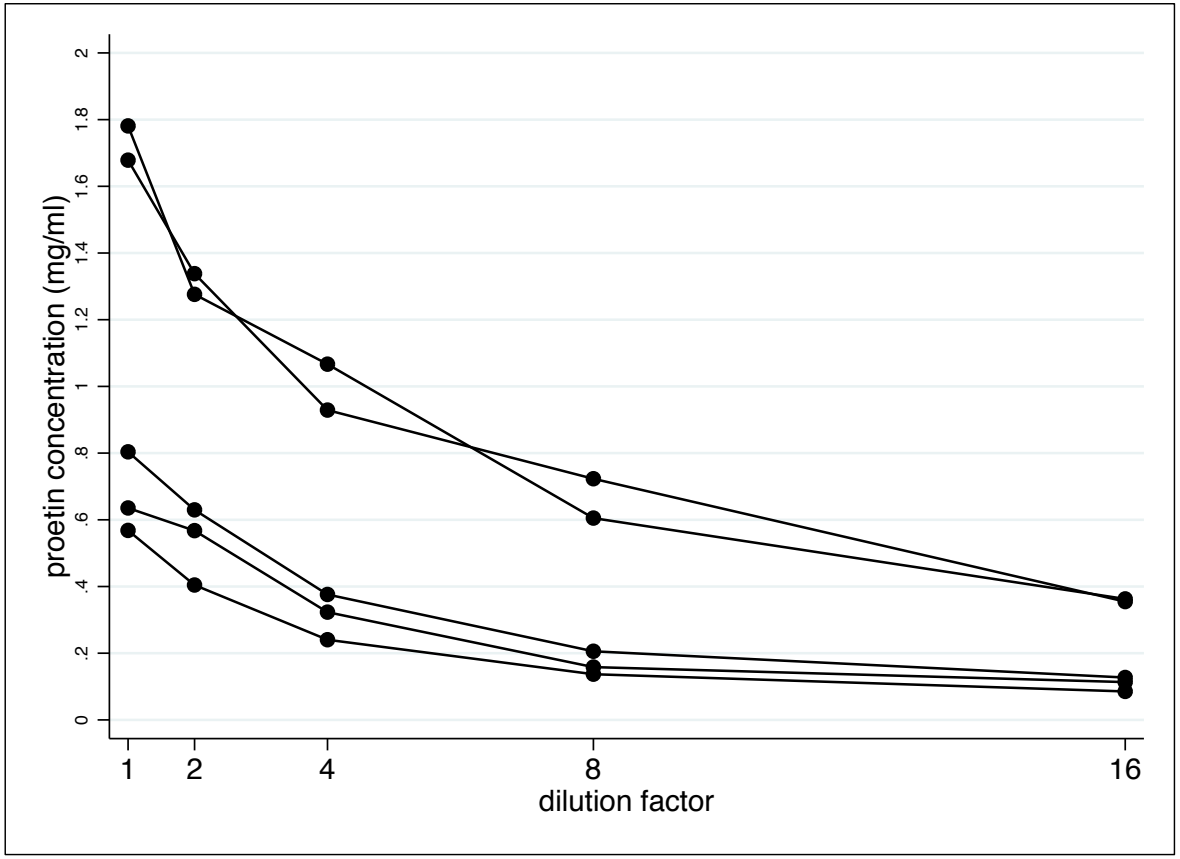

Fig 8. Leucocyte pellet dilution experiments showing protein concentration measured with a BCA assay against dilution factor used to dilute pellet.

pipette. Previously we had collected blood in a standard EDTA tube and pipetted the blood over the lysoprep, however this introduced inconsistency in terms of the sample volume "filtered" and produced a small and in some cases insufficient yield.

Conversely, the principle problem we encountered was that the pelleted leucocytes were too large. This meant that in the case of the larger pellets the BCA protein assay appeared to underestimate the protein concentration because the fluorescent substrate was saturated. Moreover there was substantial variation between size of the pellets. This compounded the problem as, for instance, it meant that a halving of the protein concentration would not lead to an estimated halving of the calculated protein concentration. In order to ascertain the optimal dilution factor which prevented saturation of the BCA assay whilst not overly diluting the sample we collected leucocyte pellet samples from five control subjects and serially diluted the pellet before carrying out a BCA assay on the dilutions. The results are listed below (table 3) and are graphed in Fig 8. On this basis of these results a x8 dilution appeared to represent the optimal dilution factor.

Table 3. Protein concentration following serial dilutions of leucocyte pellet

sample	x1 (mg/ml)	x2 (mg/ml)	x4 (mg/ml)	x8 (mg/ml)	x16 (mg/ml)
1	0.64	0.57	0.32	0.16	0.11
2	0.80	0.63	0.38	0.21	0.13
3	0.57	0.40	0.24	0.14	0.09
4	1.78	1.28	1.07	0.61	0.36
5	1.68	1.34	0.93	0.72	0.35

7.10 Liquid chromatography mass spectrometry assays

7.10a Ambroxol liquid chromatography mass spectrometry assay optomisation

Optimisation of the LCMS technique was carried out on our behalf by Laboratories of the Government Chemist (LGC). 50ul of ambroxol standard solution (or methanol in the case of blanks) and ambroxol-d5 internal standard was added to a 250uL matrix and vortexed. Protein was precipitated using 1ml acetonitrile. The sample was then vortexed and centrifuged (12min 13000rpm). The supernatant was diluted 50/50 and injected (10ul volume) onto an ACE Excel 2 C128-AR column. A Gradient comprised of of H20 + 0.1% formic acid, 15% methanol + 0.1% formic acid and methanol + 5% TetrahydroFuran was used. Flow was directed to the mass spectrometer between 2-12 minutes and to waster at all other times. Mass spectrometry was performed at 450°C, CUR 10, GS1:60 GS2 60 IS 5000v. For ambroxol, transitions were defined at 379 → 264, 277→262, 281→266 and for the internal standard at 384 → 264, 382 → 262.

For the validation a nine point calibration was performed at 0.1-500ng/ml with six replicate spikes at high and low concentrations. At least 3 batches were prepared on three separate days for each matrix. Triplicates spikes were performed at the limit of detection. Two pre-prepared QC samples were at stored at -80 degrees. Acceptance criteria were a retention time of +/- 0.1min, Calibration R^2 >0.995, signal to noise ratio > 3 for limits if detection and >10 for limits of quantification within ratios of primary transitions with 20% in both cases. Spike recovery between 70-120%. QC between 70-120%.

In serum a high spike at 250ng/ml and a low spike at 5ng/ml were supplemented by an additional spike at 1500ng/ml (diluted 1/10 post extraction). In cerebrospinal fluid a high spike at 100ng/ml and a low spike at 1ng/ml were used. In all cases acceptance criteria were met. In the case of the QC samples (50ng/ml in serum and cerebrospinal fluid) samples were run initially in duplicate. Initially in both cerebrospinal fluid and serum the acceptance criteria were not met in 2 batches (batch 1 and 2 cerebrospinal fluid, batch 2 and 3 serum). It was discovered that standard degraded upon storage at -80 degrees. The QC samples were repeated with fresh standards and all samples met acceptance criteria. This modification was incorporated into the final protocol. For both samples the limit of detection was 0.5ng/ml (1.3nmol) and limit of quantification was 1ng/ml (2.6 nmol). This is well below the anticipated concentrations of ambroxol found by found by Narita et al. at an equivalent dose (cerebrospinal fluid 60-830 nmol, serum 41–424nmol) [302].

7.10b Quantification of Glucosylceramide and Glucocerebrosidase cerebrospinal fluid protein levels by mass spectrometry

In order to measure glucosylceramide and GCase concentration within cerebrospinal fluid it was necessary to develop novel assays. We carried out a number of validation experiments to ensure these assays had sufficient sensitivity and specificity to detect and quantify the proteins/lipids. These were performed on our behalf by Jenny Hallqvist of the Centre for Translational Omics UCL Great Ormond Street Institute of Child Health.

7.11c Glucocerebrosidase

The samples were prepared in the following manner. 10g whole protein yeast enolase were added to 300 µL cerebrospinal fluid. 900 µL ice cold acetone was added whereupon the samples were vortexed and left at -20 °C overnight. The samples were centrifuged at 16 900 x *g*, +4 °C for 10 minutes. Supernatant was taken off and the pellet was washed twice with ice cold 80% acetone. The samples were freeze-dried overnight. The freeze-dried cerebrospinal fluid was re-suspended in 60 µL digest buffer (100 mM Tris, pH 7.8, 6M urea, 2M thiourea, 2% ASB14) and shaken for 30 minutes. 4.5 µL DTE solution were added and the samples were left shaking for 1 hour. 9 µL of IAA solution were added, the samples were shaken and left to incubate in darkness for 45 minutes. 496.5 µL of MilliQ water were added. 3 µg trypsin were added and the samples were incubated at +37 °C for 16 hours. The samples were cleaned of salts using C18 cartridges. Peptides were eluted with 70% acetone. Solvents were evaporated and the samples were reconstituted in 100 µL 3% ACN, 0.1% TFA prior to analysis by mass spectrometry. Mass spectrometry was performed at 450°C, CUR 10, GS1:60 GS2 60 IS 5000v.

The calibration curve consisted of a set of pooled cerebrospinal fluid samples spiked with known amounts of analyte. Samples were analysed on Waters Cortecs UPLC C18+, 1.6 µm, 2.1 x 50 mm (with a VanGuard pre-column). A solution of MilliQ water with 0.1% formic acid was added and acetone with 0.1 formic acid was slowly added to a target gradient of 40% over 7 minutes whereupon the flow was increased to 100% acetone. Quantifier and qualifier transitions were measured respectively at 731>1100 and 731>1199. The transition for the internal standard was measured at 790>805. The duplicate points for each calibrant in the

calibration curve consist of one measurement from a 20 µL injection, and one from a 10ul injection. The lowest point used for calculations in the calibration curve was 0.5 ng/µL spiked in pooled cerebrospinal fluid. Unfortunately GCase quantification in five cerebrospinal fluid samples were below the limits of quantification. In order to broaden the limits of quantification we increased the sample volume used to 500 µL cerebrospinal fluid. We also simplified the purification procedure in order to increase the sample yield, omitting the acetone cleaning step before reconstitution in 50 µL and injection. Following these changes it was possible to detect GCase with a revised limit of detection /quantification of 1nM respectively. In the pooled QC sample a concentration of 84ng/ml (58nM) was detected, whilst within the five sample tested concentrations ranged from 53-169 ng/ml (36-116nM).

7.11d Glucosylceramide

550uL ice cold $CHCl_3$:MeOH [2:1, v/v] containing the internal standards (IS) d_3-C16-Gb1 and dimethylpsychosine were added to 100 µL cerebrospinal fluid. The concentration of the internal standards in the extraction mixture were as follows; [D3]-C16:0-Gb1 : 4 ng/mL, Dimethylpsychosine: 0.05 ng/mL. The samples were shaken in room temperature at 7 x g for 20 minutes and thereafter left for 1 h at room temperature. The samples were centrifuged at +4 °C, 16 900 x g for 5 minutes. The organic phase lower phase was transferred to glass vials and dried under N_2. A calibration curve was created by spiking a set of pooled samples with known amounts of Gb1. The samples were reconstituted in 50 µL MeOH prior to analysis by mass spectrometry. Mass spectrometry was performed at 450°C, CUR 10, GS1:60 GS2 60 IS 5000v.

Detection of glucosylceramide is complicated by the existence of a number of isoforms of the lipid. Transitions are listed below:

Isoform	Monitored transitions
[D3]-C16:1 (internal standard)	725.67 > 563.67
Dimethyl psychosine (internal standard)	490.46 > 310.44
Lyso-Gb1	462.46 > 264.3/282.0
C16:0-CMH	722.7 > 542.6/560.6
C16:0-CMH-OH	738.6 > 264.3
C18:1-CMH	748.6 > 586.6
C18-CMH	750.6 > 588.6
C18:0-OH	766.6 > 264.3
C20-CMH	778.6 > 616.7
C20-CMH-OH	794.6 > 264.3
C22:1-CMH	804.7 > 642.7
C22-CMH	806.7 > 644.7
C22-CMH-OH	820.7 > 658.8
C24:1-CMH	832.7 > 670.7
C24-CMH	834.7> 672.7

Table 4. Mass spectrometry transitions used for detect glycosphingolipid isoforms

The Gb1 standard (Matreya ID 1521) consisted of a mixture of Gb1 isoforms. Gb1 is present in isoforms due to the varying fatty acids attached to it. For calculation of the total Gb1 content in the samples, a calibration curve with the sum of all isoforms' analyte/[D3]C16:0 ratios against total the Gb1 concentration was constructed. When estimating precision and limit of detection, the C16:0 isoform was used. We also attempted to detect lyso Gb1 a derivative of Gb1 in which the fatty acid group has been cleaved. This required a separate internal standard (Matreya 1306). The lipid is not normally detectable in bodily fluids, however it is found in Gaucher and Krabbe patients and is thought to be produced as a breakdown product of acid ceramidase mediated catalysis (when high levels of Gb1 are

present in these conditions). The QC samples consisted of non-spiked pooled cerebrospinal fluid samples measured on two different days. Acceptance criteria were spikes at expected transitions (+/- 0.1min), linear increase in signal with increase in standard concentration, a signal to noise ratio of X3 for limits of detection and x10 for limits of quantification. Additionally we carried out further QC samples on cerebrospinal fluid from five (non pooled) subjects to estimate endogenous levels of the lipids.

For total Gb1 the limit of detection/quantification was 0.04ng/ml (0.05nM) and 40ng/ml (51nM) respectively. Spikes of all isoforms were detected with standard alone, standard spiked in matrix and in QC samples. For our five additional QC samples total Gb1 levels were quantified at ≈ 120-190ng/ml (153 - 242 nM). A breakdown of individual concentrations of Gb1 isoforms is available in the appendices. Unfortunately, although we were able to detect the spiked standard in solvent and within the matrix, we were unable to detect lyso Gb1 within the pooled or separate QC samples.

7.12 Concluding remarks

In this chapter we have presented the design and optimisation work necessary to commence the AiM PD trial. Most of this work revolved around the frailties and pitfalls of the GCase assay. Clearly being able to reproducibly quantify this activity will be of critical importance to the success of the study and through the studies we have carried out we believe that in our hands the study is robust with excellent intra and inter assay/plate variability demonstrated. We have also carried out *in vitro* experiments which have allowed us to predict the effect of ambroxol on central nervous system GCase (although, as we have

described, we would not be surprised if the predicted fall in GCase activity did not occur, which would point to additional nuances to ambroxol's biological effect of GCase). In this case the metabolomics, proteomics and lipidomics screen in serum, cerebrospinal fluid and urine will be of key importance as it will hopefully highlight pathways (and potentially off target effects) of the drug. Moreover we have shown the successful optimisation of LCMS assays to detect ambroxol, glucosylceramide and GCase levels within the cerebrospinal fluid. The former will establish central nervous system penetration whilst the latter two will, as described, aid our definition of the precise mode of action of the drug.

Chapter 8 - Preliminary results from the AiM PD clinical trial

8.0 Characterisation of participants

We attempted to match participants in the *GBA* and idiopathic Parkinson disease group in terms of age, sex and Hohn and Yahr clinical staging. Details of the demographics are listed in table 1 together with significance tests between the two groups (Spearman rank unless otherwise stated) whilst the mutations of the *GBA* Parkinson disease group are listed in table 2. In terms of the individual mutations we opted to enrol a range of Parkinson disease causing mutations. These included four 'severe' mutations, two non severe (*N370S*) mutation carriers, three Parkinson disease associated variants (*E326K*) and one biallelic participant who carried the *T369M* polymorphism together with a null stop codon which gives rise to a non coding GCase protein. By including a diverse selection of mutations we hoped to establish the effect on a mix of categories of genotype in order to understand the potential scope of recipients for the treatment. Subjects were recruites by SM. Leucocyte GCase assays were carried out by Rob Baker. CSF GCase assats were carried out by SM or Laura Smith. Data analysis was carried out by SM.

	GBA **Parkinson disease**	**Idiopathic Parkinson disease**	**significance**	**combined**
Age, median (yr)	**61**	**60**	p=1.000	**60.5**
Male (%)	**90**	**80**	p=1.000	**85**
Age of onset (yr)	**47**	**54**	p=0.1661	**53**
Duration (yr)	**10**	**5.5**	p=0.2576	**7**
H&Y (% stage I / % stage II)	**10/90**	**10/90**	p=1.000	**10/90**
UPDRS(off), median	**64**	**51**	p=0.3151	**56**
MoCa, median	**26**	**25**	p=0.7506	**25**
NMS, median	**67**	**31**	p=0.1692	**34**
NMSQuest, median	**11.5**	**8**	p=0.1024	**10**

Table 1 Demographics

Table 2. *GBA* mutations of *GBA* Parkinson disease participants	
IVS 2+1	*N370S*
E326K	*N370S*
E326K	*RecNcil* (*L444P*/*A456P*/V460V)
E326K	*R463C*
T369M/W362STOP	*R463C*

* denotes Fishers exact test

8.1 cerebrospinal fluid and leucocyte GCase activity are strongly correlated.

As a potential biomarkers of Parkinson disease progression or Parkinson disease development, the correlation between central nervous system and peripheral blood leucocyte GCase activity is of interest. Clearly if the correlation is strong then there is no need to subject a patient to the expense and potential complications of a lumbar puncture as the biomarker can be measured in peripheral blood. To date no studies have looked at the correlation. Spearman's rank showed a strong correlation between cerebrospinal fluid

and leucocyte GCase (p=0.001). A scatter graph of the correlation is shown in Figure 1. As would be expected there were statistically significant differences in GCase activity in both leucocytes (Spearman coef -0.67, p<0.0001) and cerebrospinal fluid (Spearman oef =-0.689, p<0.0001). Box plots of both are displayed in Fig 2.

8.2 cerebrospinal fluid GCase does not correlate with markers of Parkinson disease severity

We explored whether cerebrospinal fluid GCase activity was associated with clinical markers of Parkinson disease severity namely age of Parkinson disease onset, duration of disease, UPDRSscore, NMS, NMSQuest, MoCa and *GBA* mutations severity (*GBA* group only). In order to minimise the risk of type 1 error caused by multiple comparisons we initially tested for correlations within the whole cohort, carrying out pairwise analyses only when a significant result was obtained. A summary of these tests is presented in table 3.

The NMSQuest was the only assessment where correlations were observed across the whole cohort and this was duplicated in the *GBA* Parkinson disease group o*nly.* A scatter graph of the correlation is shown in Fig 3. Trends were observed for the NMS (p=0.0991). It seems strange that correlations exist between the non motor features of Parkinson disease and cerebrospinal fluid activity, but not in terms of any other measures. This may be a question of power. Slight trends could be said to exist for UPDRS (coef. -0.2650, p=0.3039), disease duration (coef. -0.2741, p=0.3042) and age of onset (coef. 0.3004, p=0.2582), although they are far from convincing. Given a few of the participants had relatively mild Parkinson disease (e.g UPDRS23 and 29), non-motor features may provide a more prominent phenotype to correlate to. Nonetheless this data does add some weight to the

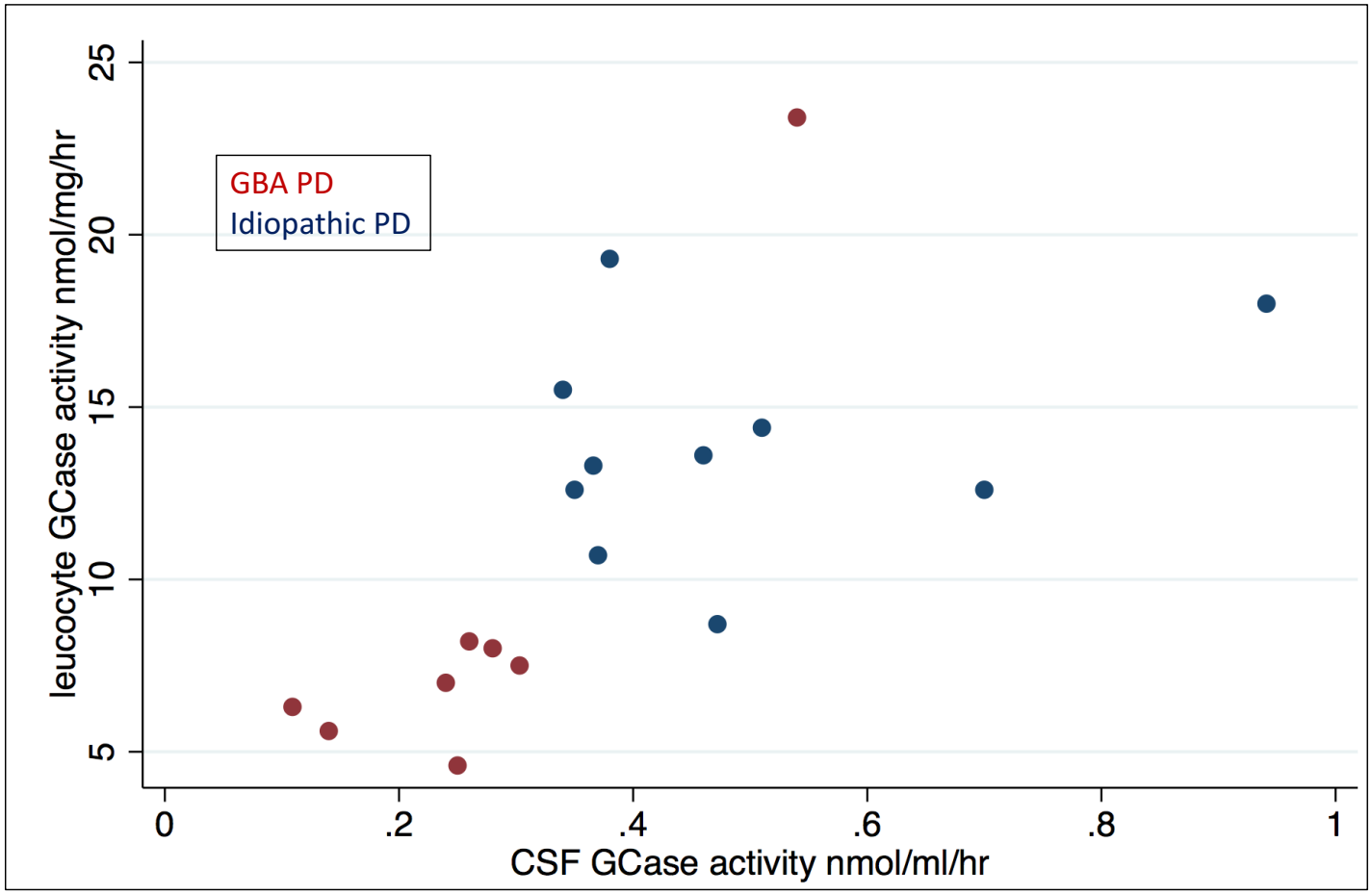

Fig 1. scatter graph of CSF (x) and leucocyte GCase (y) in GBA PD (red) and idiopathic PD (blue) subjects

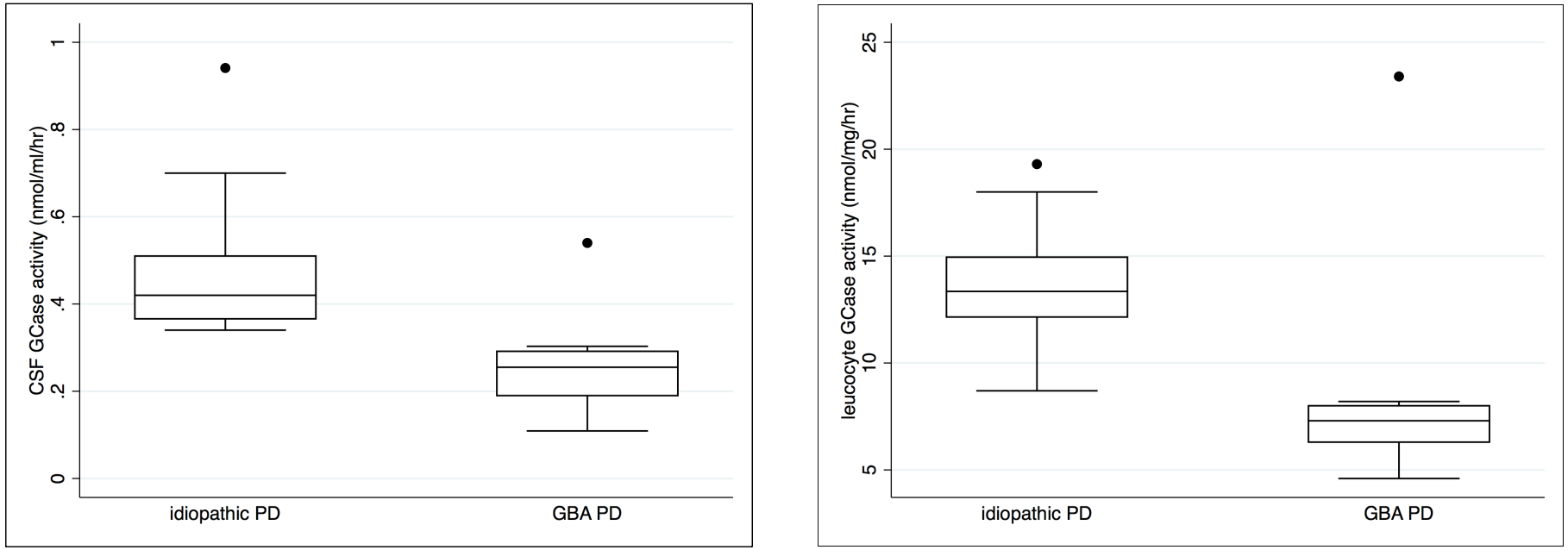

Fig 2. Box plots of CSF (left) and leucocyte GCase activity in GBA PD and idiopathic PD subjects

Table 3. Correlation of cerebrospinal fluid GCase activity with clinical markers of Parkinson disease severity			
	Combined Parkinson disease group	***GBA* Parkinson disease**	**Idiopathic Parkinson disease**
AAO	p=0.2582	-	-
duration	P=0.3042	-	-
UPDRS	p=0.3039	-	-
NMS	p=0.0991	-	-
NMSQuest	**p=0.0464**	**p=0.0017**	p=0.1802
MoCa	p=0.7889	-	-
Mutation severity	p=1.000*		

* denotes Fishers exact test

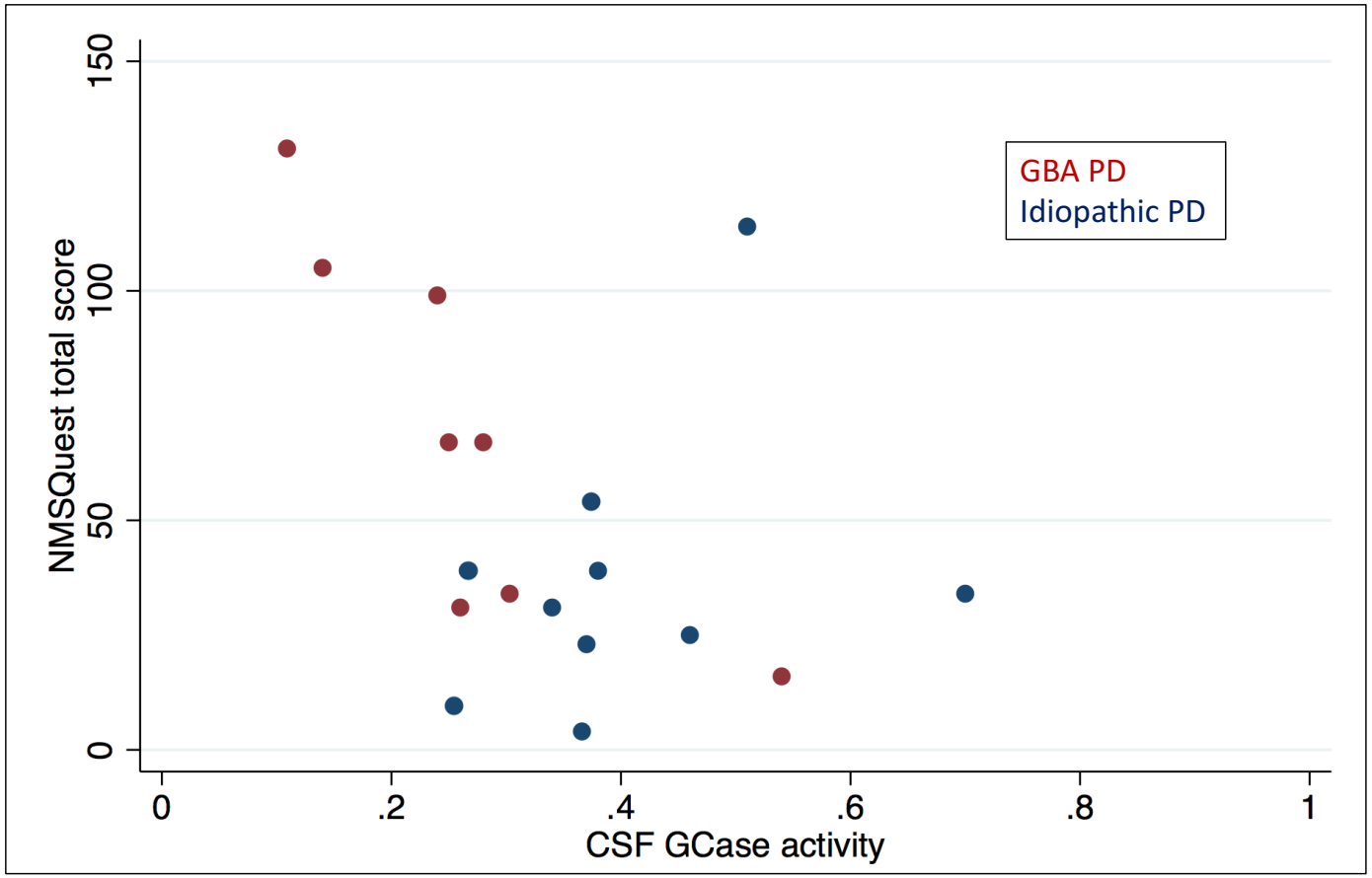

Fig 3. scatter graph of CSF GCase activity (x) and NMSQuest score (y) in GBA PD (red) and idiopathic PD (blue) subjects

hypothesis that GCase is a potential biomarker of Parkinson disease, although the result is far from conclusive.

8.3 Preliminary data shows ambroxol is tolerable at 1.26g/day

At the time of writing 16 participants had reached the target dose of 1260mg. Reported adverse events related to the IMP were nausea and burning at the back the throat when the tablets were not taken with food as advised (2 participants). One of these participants withdrew from the study, primarily on account of illness in the family, although dyspepsia was cited as a contributing factor. Another subject withdrew because the tablet burden (7 tablets 3 times a day) was too high. Otherwise participants have tolerated the ambroxol well with minimal side effects.

8.4 Ambroxol delivers a dose dependent increase in GCase activity in GBA Parkinson disease cases

Compared to baseline, ambroxol administration delivered a median 63% and 109% increase in GCase activity at 10 days (120mg TID) and 3 months 1260mg TID respectively, both of which reached statistical significance (Fig 4 and 5). For idiopathic Parkinson disease participants the median increase was 7% and 15%, although this failed to reach significance (Tables. 4 and 5). A graph of these results is shown in Fig 4.

It is unsurprising that the percentage GCase activity increases more prominently amongst *GBA* mutations carriers. Ambroxol's putative mode of action is to mobilise mutant ER

sequestered GCase to the lysosome. In idiopathic Parkinson disease subjects the degree of such sequestration is likely to be substantially less, hence the potential to increase GCase activity is reduced. None the less *in vitro* studies do suggest a lesser, although still detectable increase in GCase activity [35,37]. We would expect to see this effect mirrored in the idiopathic Parkinson disease group. There is a small, non significant increase detected amongst the idiopathic Parkinson disease group. Our recruitment strategy initially recruited *GBA* Parkinson disease cases and matched them with idiopathic Parkinson disease subjects. As such the number of participants who had reached 3 months on the IMP was a reflection of this (*GBA* Parkinson disease 5, idiopathic Parkinson disease 2). Accordingly it is likely that as numbers increase this trend will reach significance.

8.5 Concluding remarks

We have presented here preliminary data from the AiM PDtrial. The baseline result are of interest in themselves. In the first case they confirm that peripheral GCase activity is a good correlate of central nervous system GCase activity, alleviating (if in future GCase is advanced as a Parkinson disease biomarker) the need for collection of cerebrospinal fluid. We have also presented some limited data supporting at least some correlation with Parkinson disease disease severity, although as we have discussed the results are not conclusive. Finally we have shown dose dependent increases of GCase activity in peripheral blood leucocytes following ambroxol administration. Of course, the primary outcome of the study is to establish ambroxol's penetrance and target engagement within the central nervous system , but nonetheless these results are highly promising,

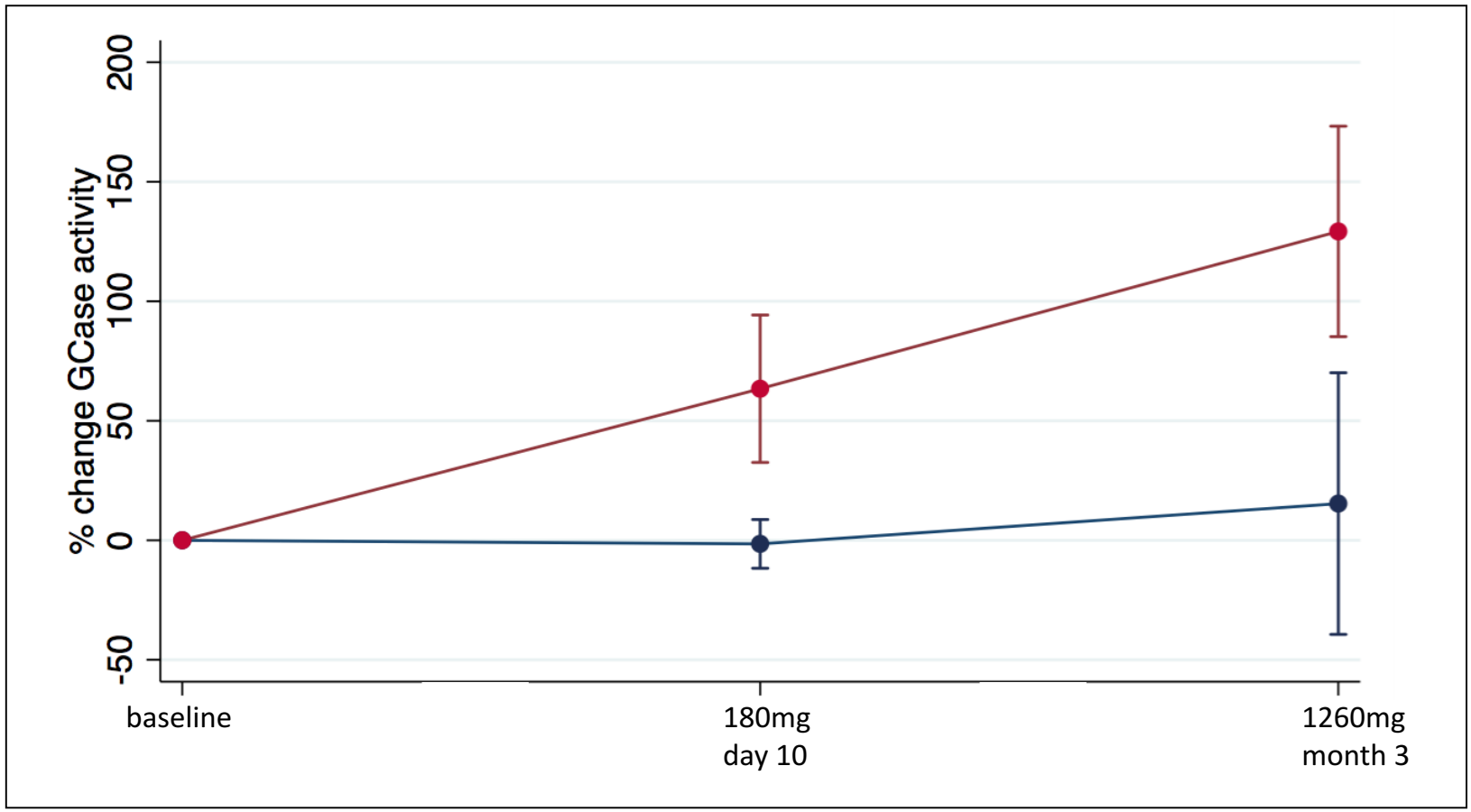

Fig 4. Graph of change in leucocyte GCase activity pre and post dose in GBA PD (red) and idiopathic PD (blue) patients

Table 4. statistical tests GCase activity pre and post dose	Day 10 (120mg TID)	3 month (1260mg TID)
***GBA* Parkinson disease**	**N=8 Z=-2.731 p=0.0063**	**N=5 Z=-3.646 p=0.0003**
Idiopathic Parkinson disease	N=8 Z=0.00 p=1.0000	N=2 Z=0.000 p=1.000

GBA	**baseline GCase nmol/mg/hr**	**GCase at day 10 (120mg) nmol/mg/hr**	**GCase at 3 months (1260mg) nmol/mg/hr**	**% change GCase at day 10 (120mg)**	**% change GCase at 3 months (1260mg)**	**baseline cerebrospinal fluid GCase nmol/ml/hr**
IPD mean	**13.65**	**13.45**	**14.95**	**-1.50**	**15.35**	**0.49**
IPD median	**13.35**	**13.1**	**14.3**	**7.28**	**15.36**	**0.42**
GBA PD mean	**8.65**	**13.85714**	**14.38**	**63.41**	**129.2234**	**0.26**
GBA median	**7.30**	**12.10**	**14.30**	**60.87**	**109.52**	**0.26**
Combined mean	**11.51**	**13.64**	**14.54**	**28.79**	**96.69**	**0.39**
combined median	**11.70**	**12.70**	**14.30**	**23.93**	**104.29**	**0.36**

Table 5. descriptive statistics of GCase activity pre and post dose

Chapter 9 - Conclusion

9.0 Two complementary disease models caused by the same genetic mutations

It is a unique and not fully exploited privilege for researchers examining the *GBA* gene, that two human disease models, one which is rare with a young onset and very debilitating course and one which is common, phenotypically heterogeneous and a disease of old age, coexist and are caused by mutations in the same gene. For Parkinson's researchers, twenty years of research and the proven therapeutic strategies Gaucher researchers have devised and demonstrated have doubtless advanced the field by years if not decades. The major question that remains unanswered is whether the disease mechanism underlying the two diseases the same. In **chapter 2** we presented data showing that many of the prodromal features present in Parkinson disease are also present in asymptomatic *GBA* carriers and Gaucher patients. Moreover in **chapter 4** we showed that amongst *GBA* carriers (which includes a substantial number of Gaucher patients) serum alpha synuclein levels are upregulated in those with the most prominent evidence of these Parkinson disease prodromal features and that there is a good correlation between serum alpha synuclein levels and the number of severe mutations carried. We have already discussed the commonalities of the clinical presentations of so called neuronopathic Gaucher disease and aspects of Parkinsonian disorders. These comparisons are brought further into focus by the finding that the mutations associated with neuronopathic Gaucher features are also those with the highest risk of Parkinson disease. The fact that penetrance of *GBA* Parkinson disease and neuronopathic Gaucher disease are both variable highlights further these striking commonalities. It is the responsibility of researchers from both fields to fully exploit

the outstanding opportunities that spawn from the appropriate investigation of these diseases, in tandem.

9.1 A common but heterogenous genetic cause of Parkinson's

The neurogenetics community has to date been extremely adept at identifying very rare and highly penetrant Parkinson disease causing gene mutations and conversely very common variants associated with marginal odds ratios of Parkinson disease. What is particularly remarkable about *GBA* is that it lies in between these two exemplars, namely it is a reasonably common genetic risk factor associated with an incomplete but none the less highly significant risk of developing Parkinson disease. Such intermediate frequency, intermediate penetrance alleles are perhaps the most pertinent because they mimic the inheritance of idiopathic Parkinson disease, in that a family history of Parkinson disease is the single greatest genetic risk factor for it, although most Parkinson disease is not inherited in a mendelian manner. *GBA* allele frequencies amongst the Parkinson disease population is around 0.05 (5%) and this makes *GBA* by some way the most significant genetic risk factor for Parkinson disease. Thus *GBA* (and *LRRK2*) are the only examples of a genetic risk factors which have significance to a large number of Parkinson disease patients. It may be that the *GBA* gene is even more important to our understanding of Parkinson disease, as only now has full exome sequencing (as opposed to targeted analysis of SNPs) becoming the norm. The very onerous practical difficulties of sequencing the *GBA* gene also mean that the identification of a number of very significant alleles (such as the splice variant IVS 2+1) are often not carried out. Another hugely promising but as yet largely unexplored area is the role of the autonomous pseudogene in the pathogenesis of Parkinson disease. It has been

said that the pseudogene is non coding, however there is evidence of protein transcription and it is known that there are high levels of variability associated with it [310-312]. If variants in the *GBA* pseudogene were implicated in Parkinson disease then this would be likely to broaden the scope of the involvement of *GBA* in Parkinson disease still further.

On a practical level the ubiquitous frequency and involvement of *GBA* in Parkinson disease pathogenesis provides a stable platform to understand the genetics of a complex polygenic disease such a Parkinson disease. **In chapter 2** using the work of Ziv Gan-Or and other as a prototype, we were able to demonstrate the epidemiological principle of ascribing a quantification "Parkinson disease risk" to individual *GBA* mutations. The stark variation demonstrated here between, for example, polymorphisms such as *E326K* and severe disease causing alleles such as *L444P* or *84GG,* speak to the complexity of the genetics that underlie *GBA* Parkinson disease, but moreover that stratification of the risk to an individual mutation carrier may be tangible. The fact that such a vast array of *GBA* mutations have been described in the context of Gaucher disease makes this process all the more tantalising because much of the leg work of deciphering which variants convey significant pathogenicity has been done (assuming that all Gaucher causing alleles also cause Parkinson disease which may well be an assumption which lacks nuance). The most pertinent take home message is the scale required to undertake this kind of analysis. Sample sizes in the tens of thousands are required and this makes conventional means of clinical assessment, such as those described **in chapter 3** largely redundant. Big data, collected in a sustainable and cost effective manner will be the key to these analyses and we provide a blue print for such assessment in **chapter 4.**

9.2 Towards a comprehensive stratified risk model accounting for the variable penetrance of GBA Parkinson disease

In **chapter 3** we described work which shows consistently that the prodromal Parkinson disease features of cognitive impairment and hyposmia seem to be worse amongst asymptomatic *GBA* carriers than age adjusted controls. We also show that these symptoms together with depression appear to cluster together in a number of "higher risk subjects" in a prototype model for disease stratification. Quite what the significance of such symptoms or clustering is unclear, nonetheless is seems plausible that they may be markers of the same ongoing neurodegeneration which ultimately leads to Parkinson disease in a subset of these patients. A screening approach by which sensitivity is progressively narrowed by successive more focussed methodologies seems a plausible and realistic possibility. With genetic classifications of Parkinson disease risk (such as the prototype described in **chapter 2**) a starting point of simple clinical assessments could be augmented with imaging and biochemical tests to achieve this end. A number of pilot approaches have been described in **chapter 5** of which PET imaging using the PK11195 ligand appears to be the most promising. In all cases further development is required, necessitating once again the establishment of large cohorts which have been reliably and accurately phenotyped. Once again this requires enlarging of cohorts using mechanisms such as the rapsodi platform described in **chapter 4.** In this chapter we describe the validation of a number of novel instruments for collecting clinical data as well as the adaptation of some established ones using questionnaires or smell identification kits. The numbers here are relatively small but do provide tantalising evidence that it may be feasible to detect these symptoms using an internet based platform. The assessments in question are by no means the finished product and will require not only

optimisation and improvement, but also maintenance of enough continuity to take full advantage of the prospective nature of the assessments. Such a platform will rise and fall on its ability to maintain the attention of participants without the motivating factor of an assessor present. It will require innovation in terms of approach and technology (like for instance the integration of touch screen technologies into future portals), but will provide insights into the genetic, epigenetic and epidemiological cofactors which may or may not contribute to penetrance of *GBA* Parkinson disease. The end product, of course, of such a complicated an involved process of disease stratification will (hopefully) be the targeting of bespoke therapies to *GBA* pathway, such ambroxol, *in vivo* human studies of which are described in **chapter 8**.

9.3 The structural, biochemical and biological basis for GBA mediated Parkinson disease pathogenesis

The pathological basis of *GBA* Parkinson disease remains unclear. In this thesis we have carried out experiments using a variety of methodologies which contribute to our understanding of the field. In **chapter 5** used PET imaging to estimate whether there was evidence of glial activation amongst asymptomatic *GBA* carriers. Small numbers accepted, these experiments found that nigral PK11195 signal is upregulated in the substantia but not in other brain regions. Moreover the signal correlated with evidence of hyposmia, a well described prodromal Parkinson disease feature occurring decades in advance of Parkinson disease onset. The fact that there is no correlation between this signal and the DAT signal recorded, implied that in advance of dopaminergic loss some form of targeted inflammation may occur in Parkinson disease affected brain regions, although whether this is a pathogenic

or protective mechanism is unclear. This data coincides with slightly inconsistent findings (also described in **chapter 5**) showing variously that biomarkers of peripheral immune activation are upregulated and together fit in with a prevailing literature related to neuroinflammation and Parkinson disease.

Equally in **chapter 6** we tested a hypothesis that sequestered GCase protein gives rise to a disruption of intracellular calcium signalling, but were not able to produce any evidence to corroborate it (this may be because of a poor choice of disease model). Finally across the thesis we have carried out various experiments that provide insights into the often presumed mode of action of Parkinson disease conversion, namely GCase activity levels. In **chapter 2** we correlated the generated odds ratios of the Parkinson disease risk of individual mutations with peripheral blood spot GCase measurements and found no evidence of a correlation. In **chapter 2** the failure of GCase activity to correlate with prodromal risk scores or in **chapter 5** the fact that no correlation of serum alpha synuclein levels with GCase activity. Finally in **Chapter 8,** we showed no correlation of cognitive impairment, Parkinson disease severity, mutation severity, age of onset or any other measures of Parkinson disease symptoms severity with leucocyte or cerebrospinal fluid GCase activity. There was however a strong correlation between cerebrospinal fluid and leucocyte GCase, activity, confirming that peripheral leucocyte measures are a stable representation of central nervous system GCase activity. On balance these findings disfavour the hypothesis that impaired GCase activity is the driving factor behind the pathogenesis of *GBA* Parkinson disease, although there are hints to the contrary, such as the fact that in the same chapter we showed that non motor Parkinson disease features did seem to correlate with this cerebrospinal fluid GCase .

A recurring theme is the utility of epidemiological and clinical studies to inform in terms of the basic mechanisms of *GBA* Parkinson disease pathogenesis. There is no more prescient example of this than the fact that astute clinical observation (and for that matter not on the part of neurologists) highlighted the initial link between the two conditions. As such the importance of appropriately scaled and designed clinical and cohort based research is once again emphasised.

9.4 The realisation and promise of targeted therapies for Parkinson disease and Gaucher disease

For Parkinson's investigators the field of *GBA* research is enhanced significantly by the large number of therapeutic strategies which have been devised and (in some cases proven) in the context of Gaucher disease. In **Chapters 7 and 8** I have described preparatory work and preliminary results of a phase II clinical trial of the mixed type inhibitory chaperone of GCase, ambroxol. The preliminary data is encouraging and shows that as expected the drug is able to upregulate GCase activity in leucocytes in a dose dependent manner. There are moreover Parkinson disease clinical trials underway of substrate reduction therapies for *GBA* Parkinson disease and together they hint at a beckoning era of medication targeted at the *GBA* pathway. This emphasises the importance of the proposed system of risk stratification of *GBA* carriers to successfully deliver neuroprotective drugs prior to the onset of Parkinson disease symptoms.

9.5 GBA: a prototype for idiopathic Parkinson disease

The single greatest promise of the *GBA* paradigm is that not only is there the realistic promise of neurotherapeutics targeted at *GBA* mutation carriers, but that these same strategies may be applied to idiopathic Parkinson disease patients as a whole. In **chapter 2** we discussed at length about the shared pattern of inheritance of *GBA* and idiopathic Parkinson disease and highlighted the potential (given the huge number of documented Gaucher causing mutations and Gaucher associated polymorphism) that *GBA* may plausibly account for as much as 10% of UK idiopathic Parkinson disease cases (in addition to the 25% of Israeli Parkinson disease cases are already known to be *GBA* positive). It is reasonable to speculate that other variants within the *GBA* gene may account for even more of the missing inheritance of *GBA* Parkinson disease.

Although this correlation between GCase activity and many of the biochemical, clinical and epidemiological markers of Parkinson disease is not absolute and has been interrogated throughout this thesis, it is established that compromise of the GCase enzyme is part of the pathological process underlying Parkinson disease development. At a cellular level autophagy is an established and well studied paradigm in Parkinson disease research. A number of studies have shown that at a population level peripheral and central GCase activity is lower in idiopathic Parkinson disease subjects. In **chapter 5** we also highlighted a role for neuroinflammation in *GBA* Parkinson disease, another well described association with the pathogenesis of idiopathic Parkinson disease. There are therefore multiple rationales to lead us to believe that *GBA* targeted neurotherapeutic strategies, such as those highlighted in **chapters 7 and 8,** may be applicable to idiopathic Parkinson disease as a

whole. Moreover, the data collected in terms of the prodromal course of Parkinson disease which may be present amongst *GBA* carriers (**chapter 3)** has already informed us as to how we might target such drugs in idiopathic and *GBA* Parkinson disease alike, whilst the promise of enlarged datasets such as those proposed in **chapter 4** may provide a practical mechanism to allow us to do so. The promise of the *GBA* gene in term of Parkinson disease is substantial. In the author's opinion, it is the most relevant of the various genetic forms of Parkinson's to idiopathic Parkinson disease as whole and may provide substantive neuroprotective therapies and screening strategies for targeting of these drugs within the near future.

Appendices

Chapter 1

10.0 Supplementary Methods

Forty one studies were identified and included in the final analysis. Mutations/variants were included if they were found in two or more separate studies. For all variants, please refer to Tables 1 and 2, Figures 2-4, Supplementary table 1 and Supplementary figures 1-6. We excluded two studies [31,313] from the *L444P*/*RecNcil* analyses because it was unclear whether the methodology was able to distinguish between *L444P* as a lone mutation or as part of the *RecNcil* haplotype.

Although pertinent meta-analyses of the role of *N370S*, *L444P* and all GD-causing *GBA* mutations in Parkinson disease[105,106] already exist [30,42,140,141], we attempted to carry out all three analyses on these mutations/pooled data to validate our methods in a context where established estimates were available.

10.1 Supplementary Results

10.1a All GD-causing mutations

Meta-analysis of all detected Gaucher disease causing *GBA* alleles (Fig 2. Supp. Fig 1 and 6) revealed an OR of 3.53 (95%CI 3.14-3.97, $p=3.61 \times 10^{-99}$), however Woolf's test revealed a

highly heterogeneous sample (I^2= 71.1, p=1.60x10^{-12}), an effect which has been demonstrated in other meta-analysis [30] Use of a random effects model did not resolve this heterogeneity (I^2= 71.1, p=1.60x10^{-12}), We explored through meta-regression the influence of ethnicity (p=0.498), the portion of familial/early onset cases (p=0.755) and the screening methodology (p=0.278) used; however we failed to show a significant contribution of these co-covariates. We considered whether the heterogeneity could be caused by publication bias, however Begg's test was not significant (p=0.180). Joint analysis revealed an OR of 2.45 (95%CI 2.18-2.73, p=3.88x10^{-55}). We attempted to carry out the meta analysis amongst studies individual ethnicities. Interestingly the Caucasian (OR 3.55 [95%CI 2.37-5.30] p=3.0x10^{-10}, heterogeneity I^2 = 73.7 p= 8.07x10^{-9}) cohort remained heterogeneous and Ashkenazi cohorts showed a strong trend towards heterogenicity (OR 4.46 [95%CI 3..07-6.49] p2.25x10^{-15}, heterogeneity I^2 = 58.8 p= 0.063); however the East Asian (OR 10.16 [95%CI 5.42-19.03] p2.08x10^{-13}, heterogeneity I^2=3.9 p=0.469), Hispanic (OR 21.12 [95%CI 3.74-119.28] p=0.0002, heterogeneity I^2=0.0 p=0.917) and North African cohorts did not (OR 5.15 [95%CI 1.30-20.32] heterogeneity I^2 = 0.0 p=0.947).

The joint analysis revealed an odds ratio of 2.44 (95%CI 2.18-2.73, p=3.64x10^{-56}).

10.1b *N370S* and *L444P*

In the case of joint analyses of *L444P* and *N370S* we excluded Ashkenazi cohorts to prevent skewing of results on the basis of the higher Ashkenazi allele frequency of these [21,314] in the (disproportionately large) control groups in two of these studies (respectively Parkinson disease/control groups were 1,000/3,805 and 99/1,543). Furthermore we confined the

N370S joint analysis to Caucasians, as *N370S* is largely specific to these and Ashkenazi populations [19,314-317]. This allowed us to augment *N370S* data with 66,666 subjects from the ExAc database. Because *L444P* is found amongst all ethnicites, we were not able to generate an adequately matched control group from the ExAc database.

N370S meta-analysis (Fig 2, Supp Fig. 2 and 6) gave rise to an OR of 3.11 (95%CI 2.60-3.72, $p=1.84x10^{-35}$, Woolf's p=0.078, Begg p=0.385). Joint analysis (Fig. 2) revealed an OR of 3.85 (95%CI 2.63-5.63, $p= 5.1x10^{-12}$) and 4.24 (95%CI 3.52-5.11, $p=7.2x10^{-52}$) including control subjects from the ExAc database.

L444P meta-analysis (Fig. 2, Supp Fig 2 and 6) revealed an OR of 8.76 (95%CI 6.01-12.76, $p=1.2x10^{-29}$, Woolf p=0.997, Begg p=0.691). Joint analysis (Fig. 2) produced an OR of 13.91 (95%CI 8.58-22.54, $p=1.0x10^{-26}$).

10.1c RecNcil (L444P; A456P; V460V)

RecNcil gives rise to a severe form of Gaucher diseaseand after *N370S*, *L444P*, *E326K* and *T369M* was the most frequent mutation identified in our analysis. It is present across the spectrum of ethnicities (apart from Ashkenazi studies which did not screen for the mutation), although proportionately it appears over represented in East Asian populations.

Meta-analysis (Fig. 2, Supp. Fig 3 and 6) revealed an OR of 3.08 (95%CI 1.65-5.76, $p=8.0x10^{-4}$, Woolf p=0.907, Begg p=0.921). Joint analysis (Fig 2.) showed an OR of 3.63 [95%CI 1.68-7.87] of developing Parkinson disease associated with mutation (p=0.002). Because *RecNcil*

is a haplotype consisting of 3 mutations the ExAc database did not include control data to augment the dataset.

10.1d 84GG

84GG is a null mutation caused by a glycine duplication leading to a frameshift and a premature stop codon 18 amino acids downstream.[318] Our study confirms previous findings that it is predominately an Ashkenazi mutation [149] in that 65.8% of Parkinson disease (25/38) and 90% of control (9/10) *84GG* alleles identified were in Ashkenazi cohorts even though they accounted for 10.5% (1,100/7,021) of Parkinson disease subjects and 56.7% (5,348/9,430) of control subjects surveyed.

Meta-analysis (Fig. 2, supp. Fig. 3 and 7) revealed a combined OR of 13.47 (95%CI 7.75-23.44 $p=2.26x10^{-20}$, Woolf p=0.907, Begg p=1.00)

Because *84GG* is overwhelmingly an Ashkenazi mutation (65.8% of case and 90% of control) we excluded non-Ashkenazi studies in our joint analysis in order not to unduly skew the case and control groups (lower allele frequency amongst other populations). Joint analysis (Fig. 2) concluded that *84GG* increased Parkinson disease risk with an OR of 14.42 (95%CI 6.96-29.88 $p=1.94x10^{-12}$). Although ExAc data was available it was not included due to an absence of Ashkenazi participants.

10.1e R120W

R120W is a severe GD-causing mutation. It was disproportionately prevalent amongst East Asian populations (89.3% of mutations were found within these populations) and in particular in Japan where two studies accounted for 24/28 mutations. Meta-analysis (Fig. 2, supp. Fig. 3 and 7) revealed an OR of 8.85 (95%CI 2.51-31.11, p=0.002, Woolf p=0.403, Begg p=0.221). The joint analysis (Fig. 2) derived OR of the risk of Parkinson disease was 51.92 (95%CI 3.15-853.3, p=0.016). ExAc control data was not available for this mutation.

10.1f H255Q

H255Q causes as a severe GD-causing mutation. It was solely found amongst Caucasians and interestingly all these were within Greek cohorts. Meta-analysis (Fig. 2 supp. Fig. 3 and 6) revealed an OR of 4.58 (95%CI 0.80-26.27, p=0.260, Woolf p=0.916 Begg p=0.296). The joint analysis (Fig. 2) showed a significance effect with (OR 4.71 [95%CI 2.06 – 10.63] p=0.0007) but not without (OR 9.38 [95%CI 0.53-164.39], p=0.375) the addition of Caucasian 66,702 control subjects from the ExAc database.

10.1g E326K

E326K is a mild mutation and causes Gaucher diseaseonly in combination with more severe GD-causing mutations.[150] This mutation has been shown to reduce enzyme activity.[23,35] Our meta-analysis (Fig 3., sup Fig. 3 and 6) revealed an OR of (1.51 [95%CI 1.15-1.99] p=0.006, Woolf p=0.589, Begg p=0.855). It was found almost exclusively in Caucasian populations

(146/148 Parkinson disease, 66/68 control), and accordingly for our pooled analysis (Fig. 3) we excluded studies in non-Caucasian groups (OR 1.78 [95%CI 1.33-2.38], $p=2.4x10^{-4}$) and then augmented the control group with 66,406 Caucasian controls from the ExAc database (OR 1.78 [95%CI 1.50-2.11], $p=1.6x10^{-11}$).

10.1h T369M

T369M is classified as a mild GD-causing mutation and is pathogenic only in conjunction with a severe GD-causing allele. It was found predominately amongst Caucasian populations (59/61 and 23/24 amongst case and control group respectively). Meta-analysis (Fig. 3, supp. Fig. 3 and 8) failed to show a significant effect (OR 1.69 95%CI 1.10-2.60, p=0.051, Woolf p=0.402,Begg p=0.087). Joint analysis (Fig. 3) of Caucasian subjects showed an OR of 1.39 (95%CI 0.86-2.25, p=0.516) and 1.06 (95%CI 0.81-1.28 p=0.99) with the addition of 64196 Caucasian controls from the ExAc database

10.1i D409H

D409H is classified as a severe GD-causing mutation. It is found amongst Caucasian and Asian populations within our study, with the latter being relatively over represented (6/14 in East Asian studies in the Parkinson disease group). Meta-analysis (Fig. 4, supp Fig. 5 and 8) revealed an OR of 2.58 (95%CI 1.04-6.39, p=0.123, Woolf test p=0.99, Begg's test p=0.876) and joint analysis (Fig. 3) (OR 6.89 95%CI 1.3-36.6 p=0.072) failed to reveal a significant effect although a further joint analysis which included 63,400 Caucasian and East Asian control subjects from the ExAc database did (OR 10.47 95%CI 4.71-23.3 $p=1.4x10^{-8}$).

10.0j D409H;H255Q

D409H;*H255Q* is classified as a severe GD-causing mutations. It was only found within Caucasian studies in our dataset. Meta-analysis (Fig. 3, supp. Fig. 5 and 8) revealed an OR of 3.99 (95%CI 1.12-14.2, p=0.066, Woolf p=0.990, Begg p=0.466) and of (OR 2.75 95%CI 0.84-8.93, p=0.27, Fig. 3 in our joint analysis. ExAc data was not available for this haplotype.

10.0k R463C

R463C is a severe GD-causing mutation. It was found only within Caucasian populations. Meta-analysis (Fig. 3, supp. Fig. 4 and 8) failed to reveal a significant effect (OR 3.87 95%CI 0.87-17.29, p=0.228, Woolf's test p=0.874 ,Begg's test p=0.734). This was replicated in joint analyses (Fig. 3) with (OR 1.63 95%CI 0.54-4.93, p=0.999] and without (OR 2.10 95%CI 0.85-51.65, p=0.999) the inclusion of 66,728 ExAc controls.

Supp table 1. Summary of individual study characteristics

Study	year	country	ethnicity	Mutations screened	familial	Total Parkinson disease	Total CTL
Asselta et al.[19]	2014	Italy	Caucasian	Exons 8-11	Y	2,766	1,111
Bras et al.[319]	2009	Portugal	Caucasian	sequencing	N	230	430
Choi et al.[320]	2012	Korea	E. Asian	sequencing	Y	277	291
Clark et al.[321]	2007	USA	Ashkenazi	sequencing	N	278	179
Duran et al.[16]	2013	UK	Caucasian	sequencing	Y	185	283
De Marco et al.[322]	2008	Italy	Caucasian	*N370S*, *L444P*	N	395	483

Emelyanov et al.[323]	2012	Russia	Caucasian	*N370S* *L444P*	Y	320	240
Gan-Or et al.[22]	2015	Israel	Ashkenazi	*84GG*, *N370S*, *L444P*	N	1,000	3,805
Guo et al.[324]	2015	China	E. Asian	*L444P*	N	1,061	1,066
Han et. Al.[325]	2015	Canada	Caucasian	sequencing	N	225	110
Hu et al.	2010	China	E. Asian	*N370S*	N	328	300
Huang et al.[326]	2011	China	E. Asian	*R120W*,*D409H*, *L444P*,	N	967	780
Kalinderi et al.[327]	2009	Greece	Caucasian	sequencing	N	172	132
Kumar et al.[328]	2013	Serbia	Caucasian	sequencing	N	360	348
Lesage et al.[18]	2011	France	Caucasian	sequencing	Y	1,391	391
Lesage et al.[329]	2011	Tunisia	N.African	sequencing	y	194	177
Li et al.[330]	2014	Japan	E. Asian	sequencing	Y	147	100
Mao et al.[331]	2010	China	E. Asian	*L444P*	N	616	411
Mata et al.[31]	2008	USA	Caucasian	*N370S*, *L444P*	N	721	554
Mitsui et al.[332]	2009	Japan	E. Asian	sequencing	Y	534	544
Moritau et al.[333]	2011	Greece	Caucasian	*N370S*, *D409H*, *H255Q*, *L444P*, *R120W*	N	205	206
Neumann et al.[334]	2009	UK	Caucasian	sequencing	Y	790	257
Nichols et al.[335]	2009	USA	Caucasian	sequencing	Y	1,325	359
Nishioka et al.[317]	2010	Tunisia	N.African	sequencing	Y	240	372
Noreau et al.[336]	2011	Canada	Caucasian	sequencing	N	212	189
Peretz et al.[21]	2004	Israel	Ashkenazi	*84GG*, *N370S*, *L444P*	N	99	1,543
Rincon et al.[316]	2013	Mexico	Latino	*N370S*, *L444P*	Y	128	252
Ran et al[337]	2016	Sweden	Caucasian	*N370S*, *L444P*, *E326K*	N	1,872	1,450
Sato et al.[338]	2005	Canada	Caucasian	*84GG*, *N370S*, *L444P*	Y	88	122

Seto Salvia et al. [339]	2012	Spain	Caucasian	sequencing	Y	225	182
Spitz et al.[340]	2007	Brazil	Latino	*N370S*, *L444P*	Y	65	267
Tan et al.[341]	2007	Singapore	East. Asian	*N370S*, *L444P*	N	331	347
Toft et al.[342]	2006	Norway	Caucasian	*N370S*, *L444P*	N	311	474
Vaz dos Santos et al.[343]	2010	Brazil	Latino	*RecNcil*, *N370S*, *L444P*	Y	110	155
Wu et al.[344]	2007	Taiwan	E. Asian	*RecNcil*, *R120W*	N	518	339
Yu et al.[345]	2015	China	E. Asian	sequencing	N	184	130
Zhang et al.[140]	2012	China	E. Asian	*R120W*, *N370S*, *L444P*	Y	195	443

CTL- control, Parkinson disease – Parkinson disease

Supp. table 2. Mutation/Variant characteristics and summary of count data										
Mutation/Variant	**exon**	**type**	**cDNA**	**severe/mild /null (GD)**	**Parkinson disease+**	**Parkinson disease-**	**CTL+**	**CTL-**	**CTL+ (Exac)**	**CTL- (Exac)**
***84GG* (Meta)**	2	Insertion/ frameshift	1910Ggdup	null	30	1,347	9	5,518	-	-
***84GG* (Joint)**					30	1,347	9	5,518	-	-
***R120W* (Meta)**	5	missense	475C>T	severe	28	2,840	0	1,553		
***R120W* (Joint)**					25	2,797	0	2,627	-	-
***H255Q* (Meta)**	7	missense	882T>G	severe	5	9,553	0	3,949		
***H255Q* (Jpint)**					5	4,068	0	2,501	24	73,332
***H255Q;D409H* (Meta)**	7,9	complex	882T>G 1342G>C	severe	12	553	3	551	-	-
***H255Q;D409H* (Joint)**					12	5,597	3	3,946	-	-
***E326K* (Meta)**	8	missense	1093G>A	mild	148	5,698	67	4,185	-	-
***E326K* (Joint)**					146	7,267	66	5,123	798	66,406
***T369M* (Meta)**	8	missense	1223 C>A	mild	58	4,016	23	1,758		
***T369M* (Joint)**					59	5,334	23	2,837	627	63,569
***N370S* (Meta)**	8	missense	1226 A>G	mild	360	13,112	350	13,262	-	-
***N370S* (Joint)**					208	11,623	32	7,981	242	58,286
***D409H* (Meta)**	9	missense	1342G>C	severe	14	4,405	0	2,657		
***D409H* (joint)**					14	9,328	0	5,840	8	63,392
***L444P* (Meta)**	9	missense	1448T>C	severe	299	17,139	20	16,472	-	-
***L444P* (Joint)**					292	15,441	18	12,155	-	-
***L444P;A456P*; V460V(*RecNcil*) (Meta)**	9,10	complex	1448T>C 1483G>C 1497G>C	severe	45	7,433	7	4,334	-	-

***L444P;A456P*; V460V(*RecNcil*) (Joint)**					45	11,045	7	6,480	-	-
***R463C* (Meta)**	10	missense	1504C>T	severe	11	2,715	0	1,279	-	-
***R463C* (Joint)**					11	5,999	0	4,204	4	66,724

CTL- control, cDNA – complementary DNA, Joint – Joint analysis, Meta – meta-analysis, Parkinson disease – Parkinson disease, Gaucher disease- Gaucher disease

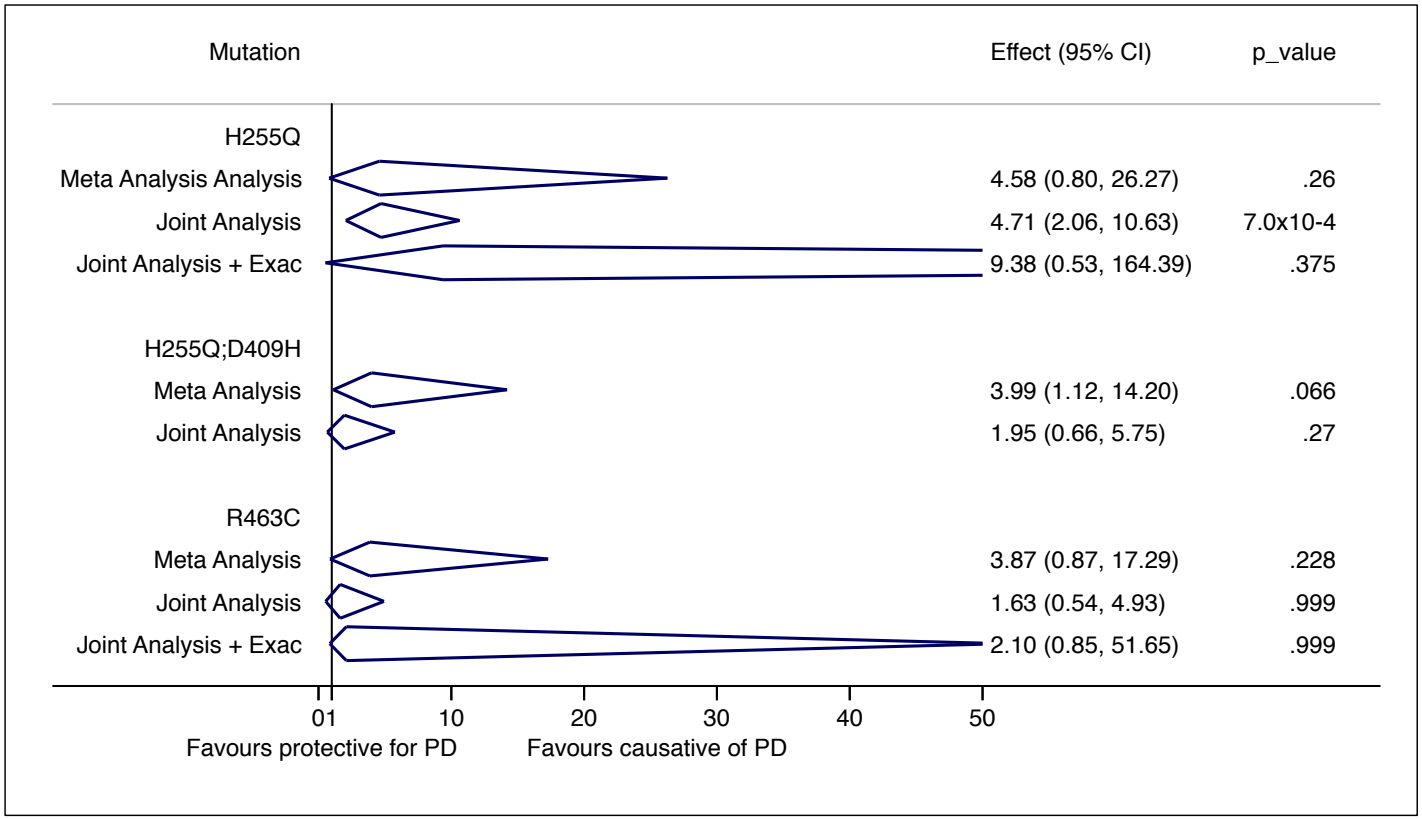

Sup Fig. 1. Effect size (OR) with 95% CI of PD risk associated with H255Q;D409H, and R463C mutations

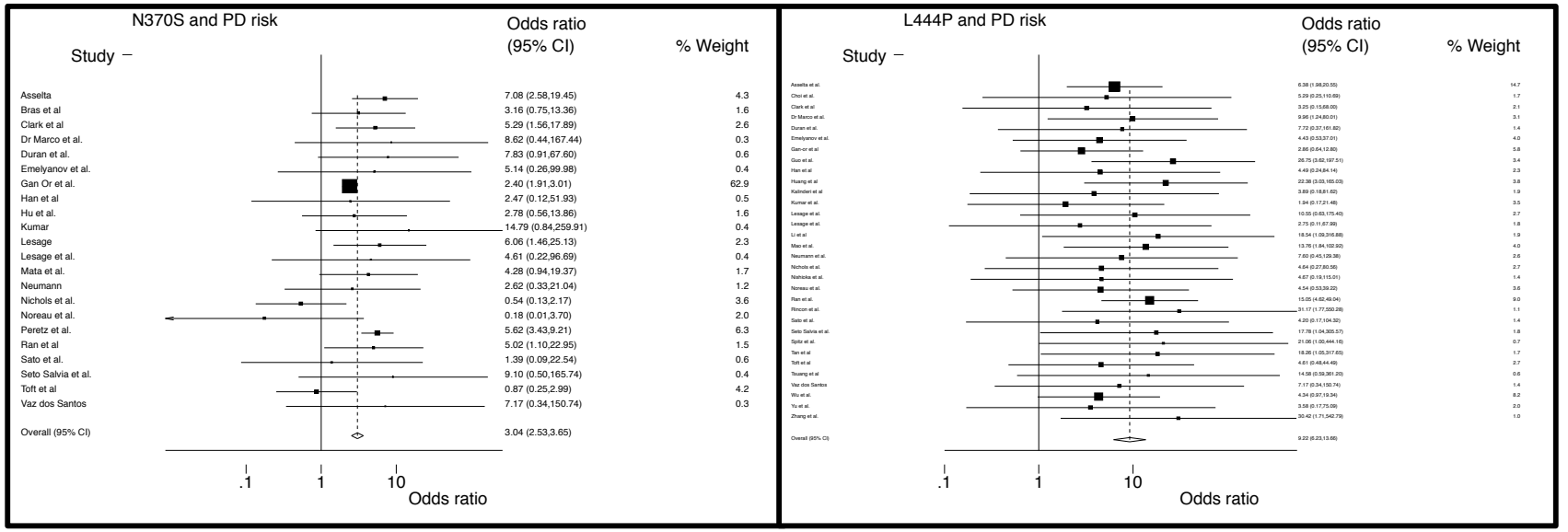

Supplementary Fig. 2. Forest plot of risk of PD (with 95%CI) associated with L444P and N370S mutations

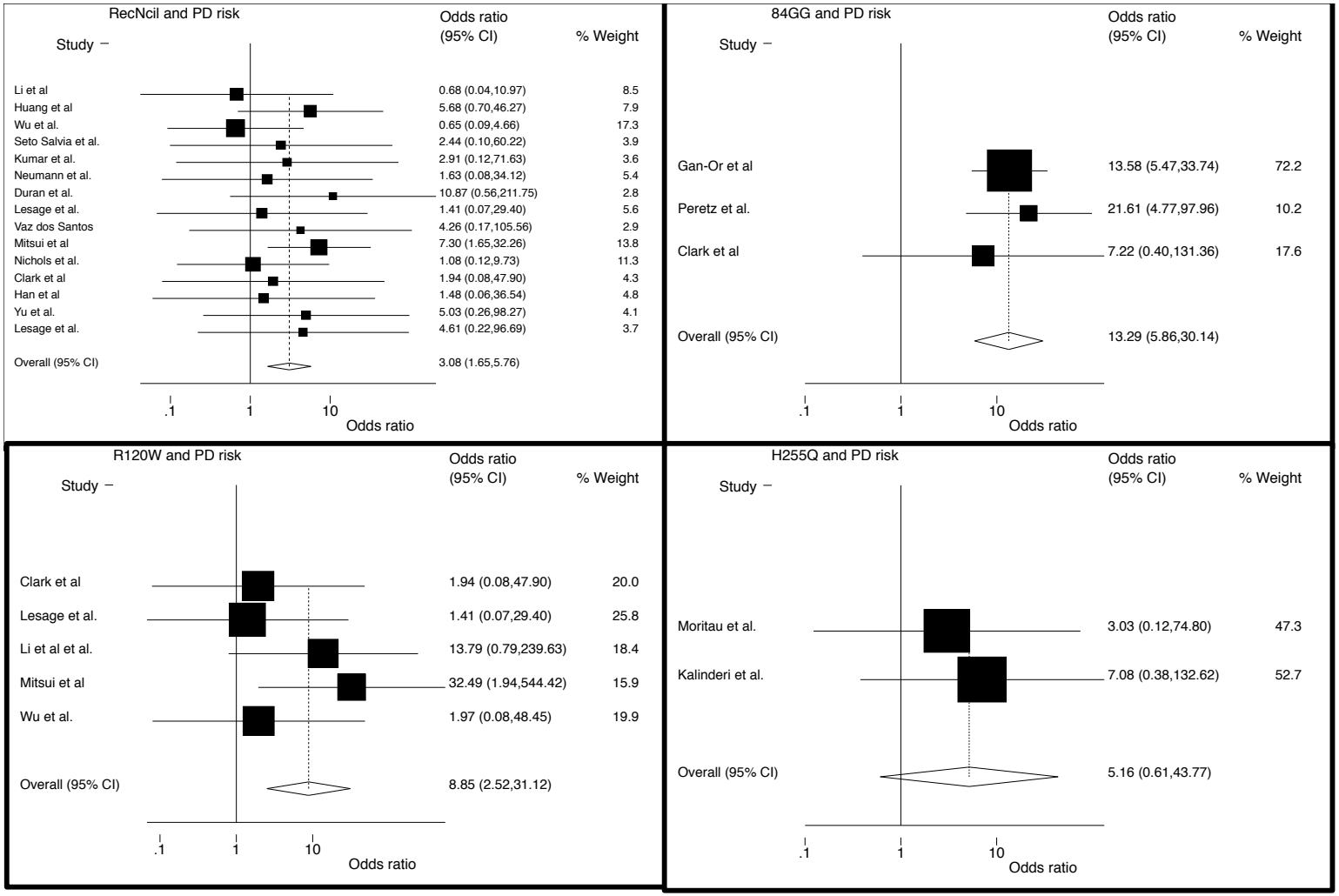

Supplementary Fig 3. Forest plots of risk of PD (with 95%CI) associated with 84GG, R120W, H255Q and L444P;A456P;V460V (RecNcil) mutations

Supplementary Fig 4. Forest plots of risk of PD (with 95%CI) associated with E326K, T369M and R463C mutations/variants

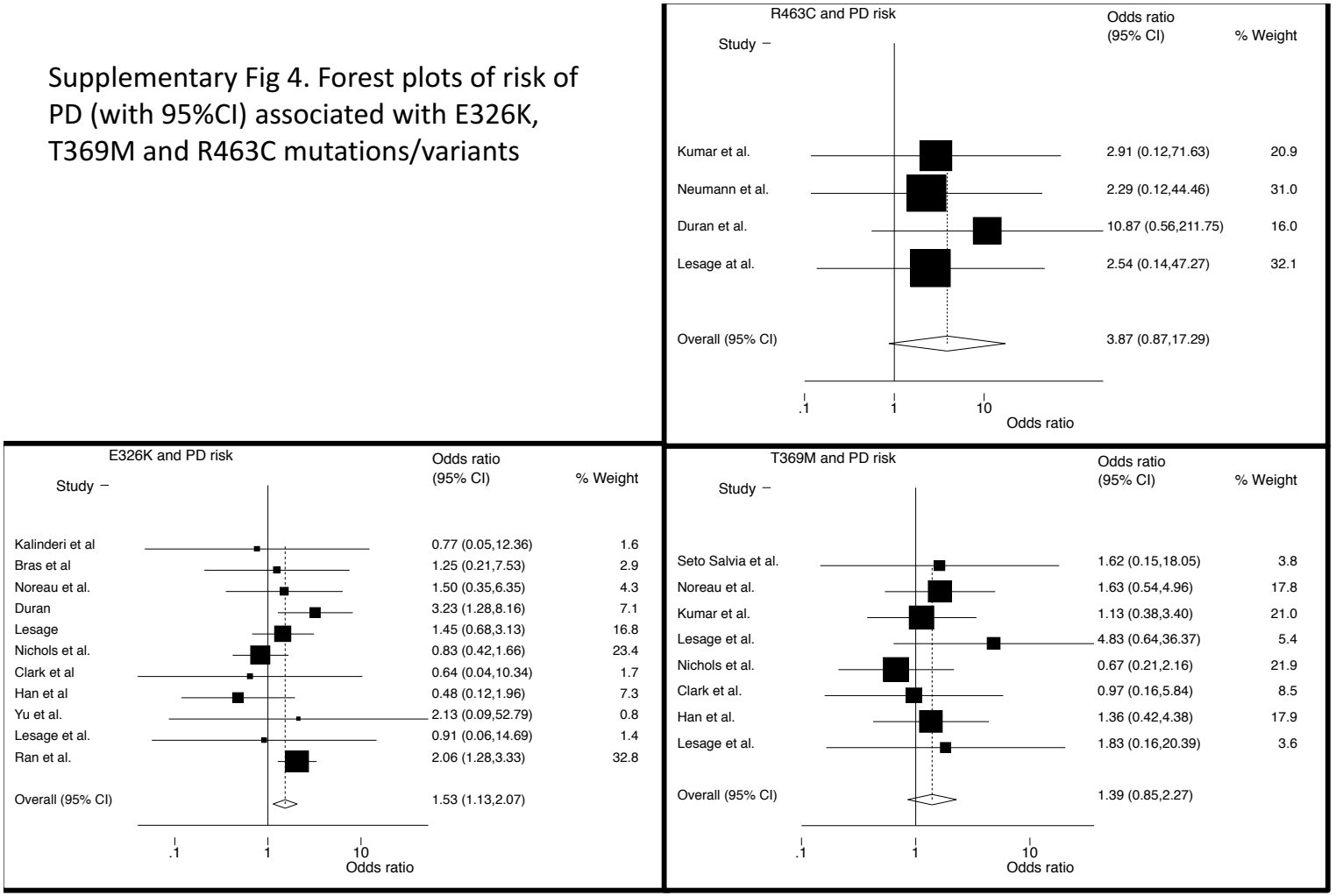

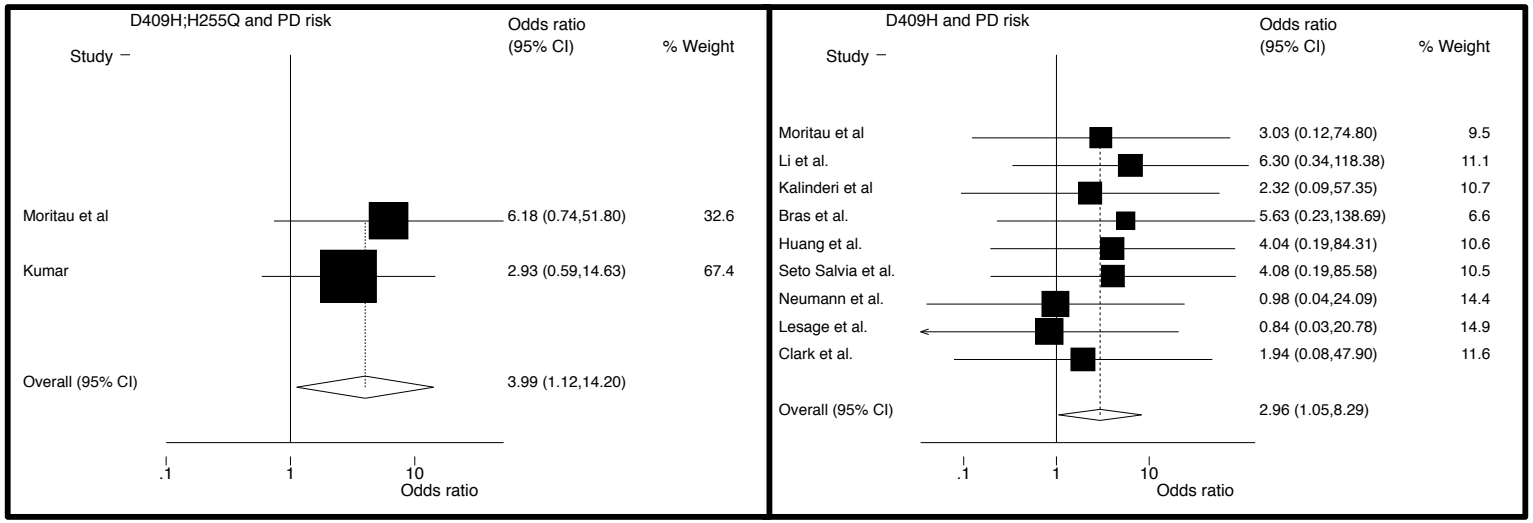

Supplementary Fig 5. Forest plot of risk of PD (with 95%CI) associated with D409H;H255Q and D409H mutations

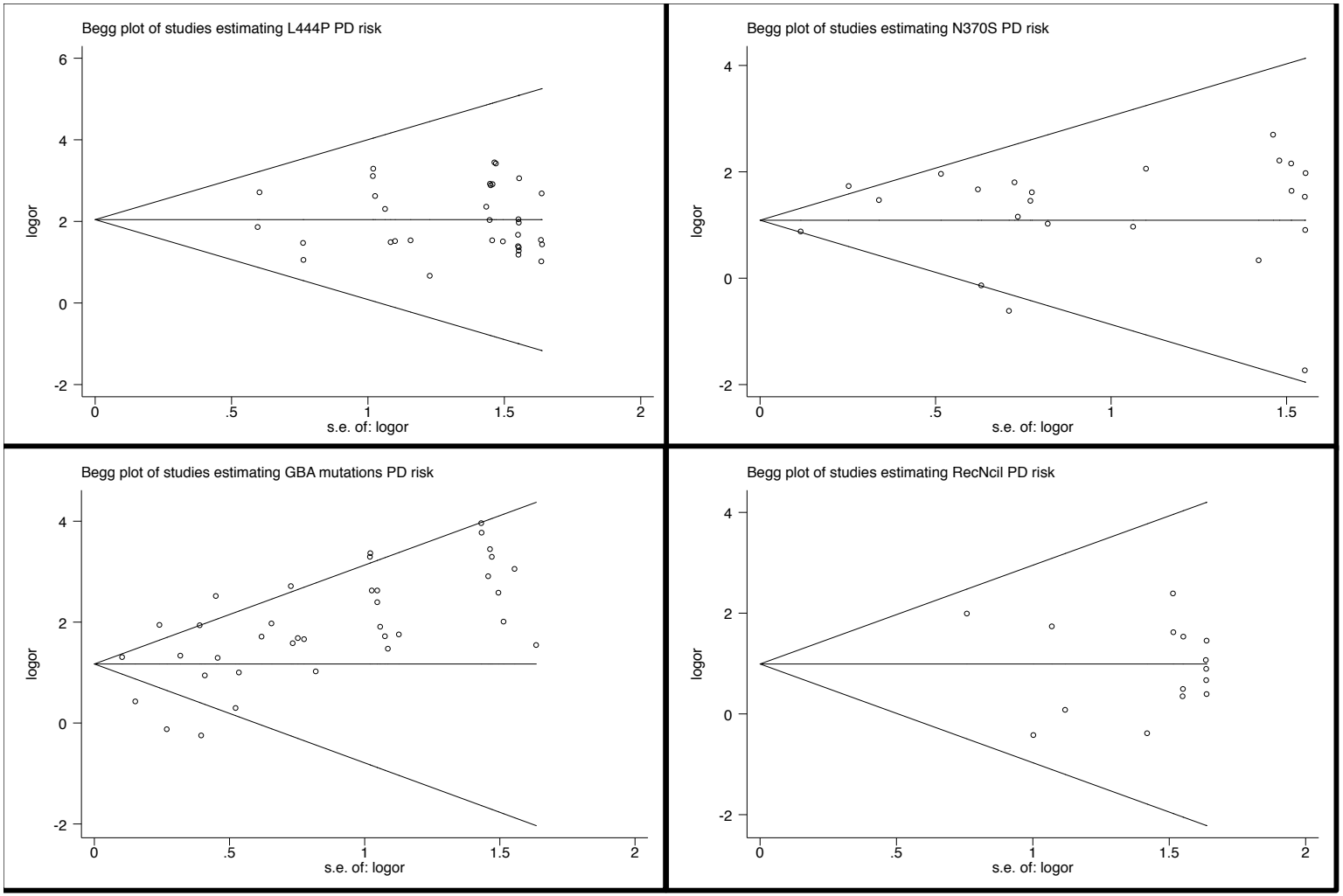

Supplementary Fig. 6. Begg plots of N370S, L444P, RecNcil and all GD causing mutations

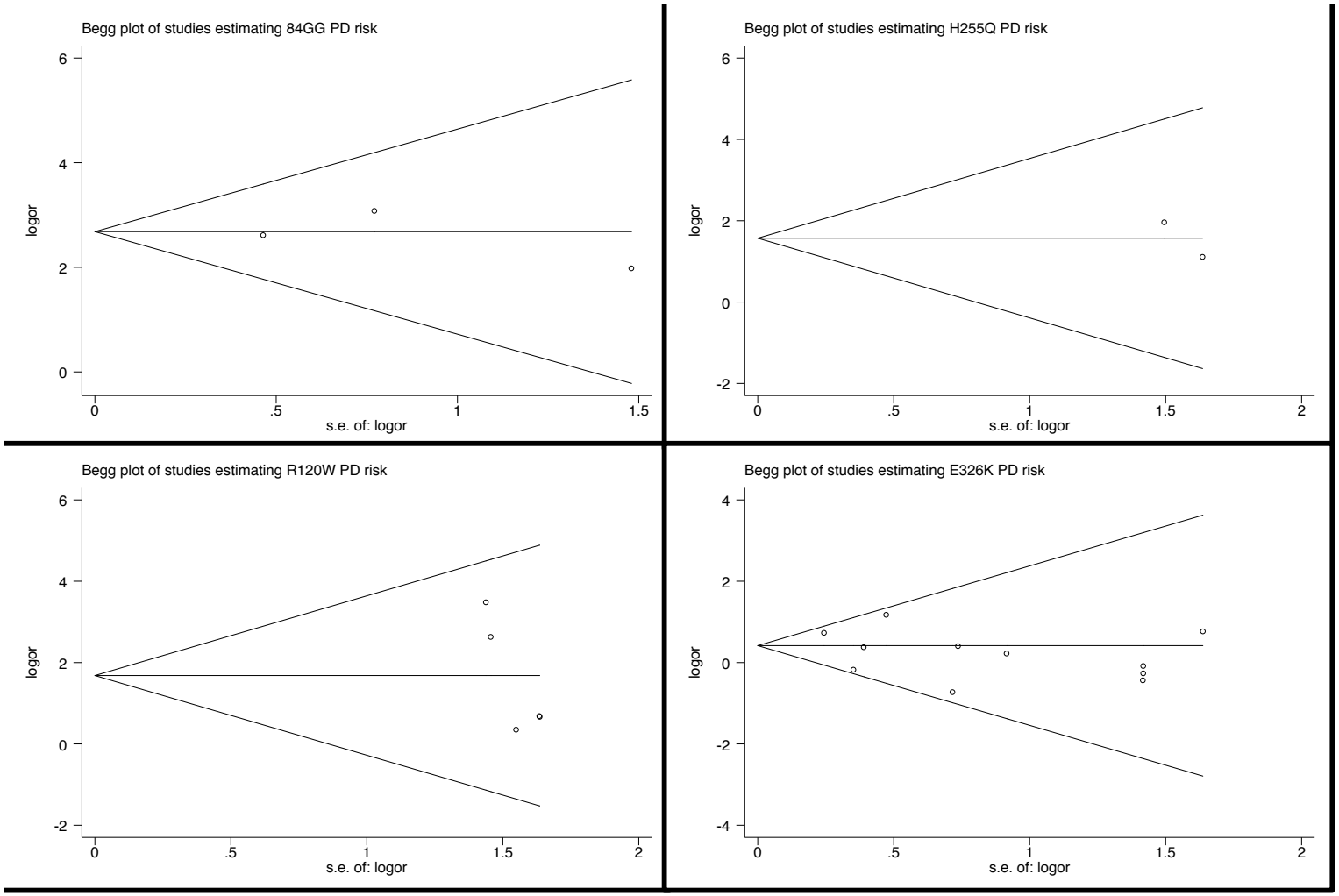

Supplementary Fig. 7. Begg plots of 84GG, H255Q, R120W and E326K mutations/variants

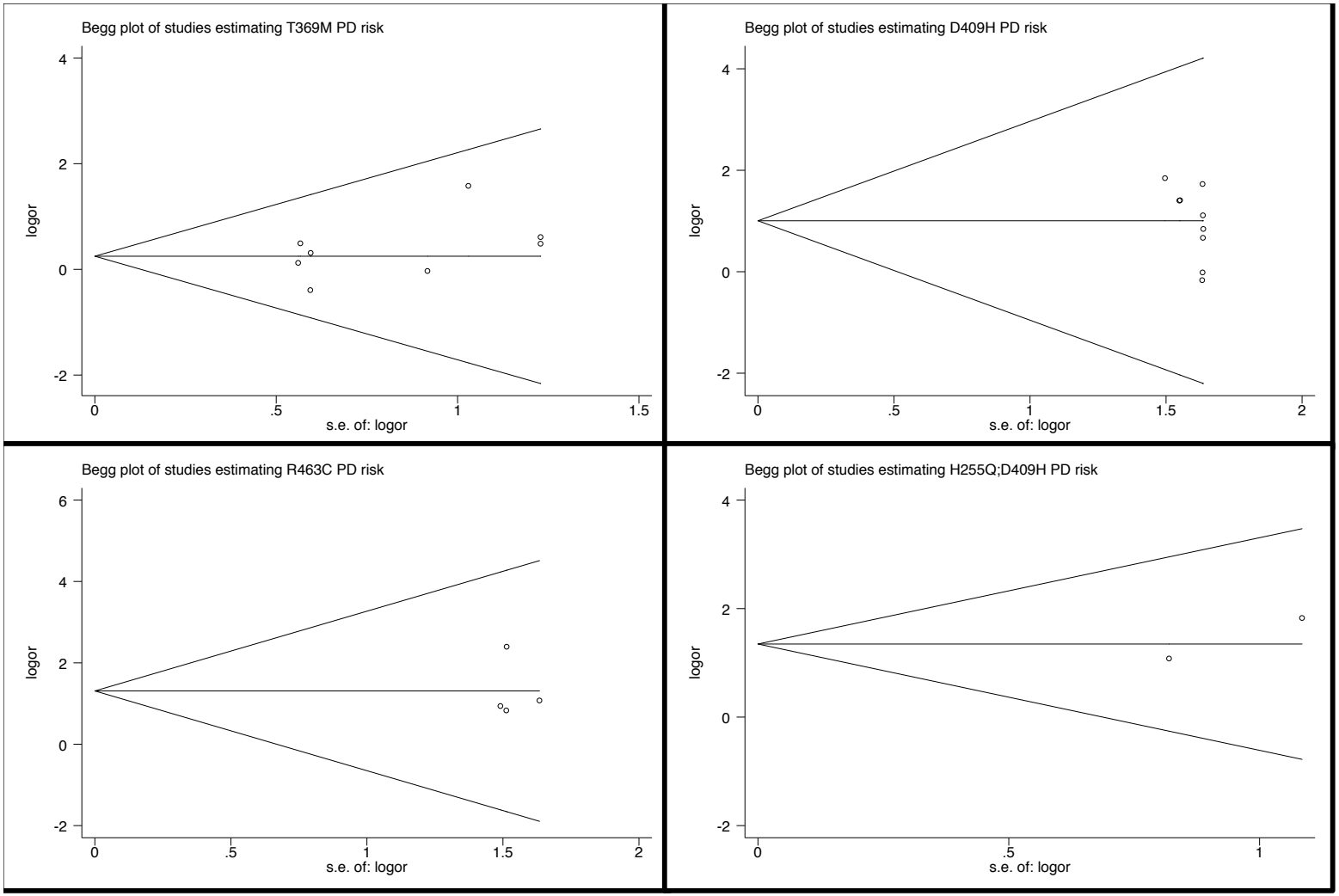

Supplementary Fig. 8. Begg plots of T369M, D409H R463C and H255Q;D409H mutations/variants

Chapter 3

10.2 Supplementary Methods

10.2a Participants

Type 1 Gaucher patients between over 40 years of age were recruited from the Royal Free London Hospital in 2010, heterozygous *GBA* mutation–positive relatives were recruited from their kindred (see supplementary materials for genotyping details). Controls were unrelated. All participants were free of any neurological symptoms or signs at inclusion[111,112] participants were assessed longitudinally from baseline (2010/2011), with target assessments in 2012/13 (timepoint 1) and 2014/15 (timepoint 2). It should be noted that previous studies referred to age matched populations whilst the present analysis encompasses these and additional cases drawn from our longitudinal database. The study was approved by the Hampstead Research Ethics Committee (10/H0720/21). All participants provided written informed consent.

10.2b Follow-up Evaluation

At each timepoint a standardised clinical history and neurological assessment was conducted, including the Unified Parkinson's Disease Rating Scale parts II and III, the University of Pennsylvania Smell Identification Test (UPSIT), the Montreal Cognitive

Supplementary table 3. Trimmed mean (+ exact confidence intervals) and median scores of prodromal features of Parkinson disease amongst control, homozygous, bi-allelic and combined group of *GBA* carriers

		baseline	Timepoint 1	Timepoint 2			baseline	Timepoint 1	timepoint 2
UPSIT ctl	**trimmed mean [95%CI]**	**34.6 [33.6-35.7]**	**34.2 [32.9-35.5]**	**33.1 [31.6-34.6]**	**UPDRS II ctl**	**trimmed mean [95%CI]**	**0.0**	**0.4 [0.1-0.7]**	**0.7 [0.0-1.3]**
	median	35.0	35.0	32.0		**median**	0.0	0.0	0.0
UPSIT hom	**trimmed mean [95%CI]**	**32.8 [31.4-34.2]**	**31.2 [29.3-33.0]**	**29.8 [2.7-31.9]**	**UPDRS II hom**	**trimmed mean [95%CI]**	**0.6 [0.1-1.2]**	**2.1 [1.1-3.0]**	**4.8 [2.0-7.5]**
	median	34.0	32.0	32.0		**median**	0.0	1.0	3.0
UPSIT het	**trimmed mean [95%CI]**	**31.6 [29.8-33.4]**	**30.6 [29.0-32.2]**	**29.1 [27.0-31.2]**	**UPDRS II het**	**trimmed mean [95%CI]**	**0.5 [0.13-0.8]**	**1.3 [0.8-1.7]**	**2.1 [1.0-3.2]**
	median	33.5	32.0	30.0		**median**	0.0	1.0	1.0
UPSIT gba	**trimmed mean [95%CI]**	**32.2 [31.1-33.5]**	**31.1 [30.1-32.1]**	**29.7 [28.2-31.2]**	**UPDRS II gba**	**trimmed mean [95%CI]**	**0.5 (0.1-0.9)**	**1.6 [1.0-2.1]**	**3.3 [1.8-4.8]**
	median	34.0	32.0	30.0		**median**	0.0	1.0	2.0
MOCA ctl	**trimmed mean [95%CI]**	**27.9 [27.3-28.4]**	**28.0 [27.5-28.7]**	**28.3 [27.7-29.0]**	**UPDRS III ctl**	**trimmed mean [95%CI]**	**0.0 [0.0-0.2]**	**1.9 [0.4-3.3]**	**2.5 [1.0-4.0]**
	median	28.0	28.0	28.5		**median**	0.0	0.0	1.0
MOCA hom	**trimmed mean [95%CI]**	**26.6 [25.8-27.4]**	**26.9 [25.8-28.0]**	**25.8 [24.5-27.0]**	**UPDRS III hom**	**trimmed mean [95%CI]**	**1.9 [0.2-3.6]**	**6.4 [3.0-9.7]**	**8.5 [4.8-12.2]**
	median	27.0	28.5	26.0		**median**	0.0	3.0	5.0
MOCA het	**trimmed mean [95%CI]**	**26.1 [25.1-27.1]**	**26.5 [25.4-27.6]**	**26.3 [24.9-27.7]**	**UPDRS III het**	**trimmed mean [95%CI]**	**2.4 [0.9-3.8]**	**8.0 [5.4-10.6]**	**6.5 [3.7-9.2]**

	median	27.0	27.0	26.5		**median**	0.0	8.0	7.0
MOCA gba	**trimmed mean [95%CI]**	**26.4 [25.8-27.1]**	**26.8 [26.0-27.5]**	**26.0 [25.1-26.9]**	**UPDRS III gba**	**trimmed mean [95%CI]**	**1.9 [0.9 - 3.0]**	**6.8 [4.7-8.9]**	**7.6 [5.2-9.9]**
	median	27.0	27.0	26.0		**median**	0.0	4.0	5.0
BDI ctl	**trimmed mean [95%CI]**	**0.72 [0.0-1.77]**	**2.1 [0.0-5.0]**	**3.44 [1.8-5.1]**	**UMSARS ctl**	**trimmed mean [95%CI]**	**0.1 [0.0-0.2]**	**0.1 [0.1-0.2]**	**0.3 [0.0-0.5]**
	median	0.0	0.0	3.5		**median**	0.0	0.0	0.0
BDI hom	**trimmed mean [95%CI]**	**1.24 [0.3-2.2]**	**5.3 [3.1-7.5]**	**9.3 [6.5-12.0]**	**UMSARS hom**	**trimmed mean [95%CI]**	**0.3 [0.1-0.5]**	**0.6 [0.3-0.9]**	**1.3 [0.7-1.8]**
	median	0.0	0.0	8.0		**median**	0.0	0.0	1.0
BDI het	**trimmed mean [95%CI]**	**1.41 [0.1-2.7]**	**3.8 [2.5-5.1]**	**6.0 [4.5-7.4]**	**UMSARS het**	**trimmed mean [95%CI]**	**0.4 [0.2-0.5]**	**0.5 [0.1-0.9]**	**0.6 [0.3-1.0]**
	median	0.0	3.0	5.0		**median**	0.0	0.0	1.0
BDI gba	**trimmed mean [95%CI]**	**1.3 [0.5-2.0]**	**4.4 [3.0-5.7]**	**7.5 [5.7-9.3]**	**UMSARS gba**	**trimmed mean [95%CI]**	**0.6 [0.3-0.9]**	**0.5 [0.3-0.8]**	**1.0 [0.6-1.3]**
	median	0.0	4.0	7.5		**median**	0.0	0.0	1.0
RBDQS ctl	**trimmed mean [95%CI]**	**0.1 [0.0-0.3]**	**1.0 [0.3-1.6]**	**1.8 [1.1-2.5]**	**RBDSQ het**	**trimmed mean [95%CI]**	**0.6 [0.1-1.0]**	**2.1 [1.2-3.0]**	**2.4 [1.6 3.1]**
	median	0.0	0.0	2.0		**median**	0.0	1.5	2.5
RBDSQ hom	**trimmed mean [95%CI]**	**0.6 [0.1-1.2]**	**2.8 [1.9-3.6]**	**2.5 [1.8-3.1]**	**RBDSQ gba**	**trimmed mean [95%CI]**	**0.5 [0.2-0.9]**	**2.4 [1.8-3.0]**	**2.4 [1.9-2.9]**
	median	0.0	2.0	2.0		**median**	0.0	2.0	2.0

Supplementary table 4 - full breakdown of analyses for cohort study

Ordinal logistic regression model looking for associations between *GBA* group and prodromal features (compared to controls) taking into account age, sex, education, smoking history and history of Parkinson disease or dementia (p<0.05)

***GBA* vs controls**	**OR [95%CI] bl**	**p bl**
UPSIT	**4.0 [1.6-10.4]**	**p=0.003**
MOCA	**6.0 [2.3-15.2]**	**p<0.001**
BDI	**1.0 [0.1-9.0]**	**p=0.977**
RBDSQ	1.5 [0.1-1.9]	p= 0.729
***GBA* vs controls**	**OR [95%CI] tp1**	**p tp1**
UPSIT	**7.6 [2.7-21.8]**	**p<0.001**
MOCA	**7.3 [2.1-24.9]**	**p=0.002**
BDI	**2.2 [0.0-440]**	**p=0.997**
RBDSQ	5.0 [0.9-41.2]	p=0.139
***GBA* vs controls**	**OR [95%CI] tp2**	**p tp2**
UPSIT	**6.8 [2.0-23.1]**	**p=0.002**
MOCA	**4.0 [1.2-13.6]**	**p=0.024**
BDI	**10.6 [1.3-90.0]**	**p=0.029**
RBDSQ	**2.2 [0.21-20.0]**	**p=0.486**

KEY
bia: bia-allelic
bl: baseline
Chi 2: Chi squared
ctl: control
***GBA*: glucocerebrosidase mutation**
hom: homozygous
OR: odds ratio
tp1: timepoint 1
tp2: timepoint 2

Ordinal logistic regression model looking for associations between bi-allelic/homozygous groups and prodromal features (compared to controls) taking into account taking into account age, sex, education, smoking history and history of Parkinson disease/dementia(p<0.05)

vs controls	**OR [95%CI] bl bia**	**p bl bia**
UPSIT [95%CI]	**4.2 [1.8 - 12.2]**	**p=0.006**
MOCA [95%CI]	**5.0 [0.9-14.4]**	**p=0.003**
BDI		
RBDSQ		

KEY
bia: bia-allelic

vs controls	OR [95%CI] bl het	p bl het
UPSIT [95%CI]	4.3 [1.5 - 12.2]	p=0.011
MOCA [95%CI]	6.8 [2.5-19.1]	p<0.001
BDI		
RBDSQ		
vs controls	OR [95%CI] tp1 bia	p tp1 bia
UPSIT [95%CI]	6.3 [2.0 - 19.7]	p=0.002
MOCA [95%CI]	2.9 [0.9-9.6]	p=0.069
BDI		
RBDSQ		
vs controls	OR [95%CI] tp1 het	p tp1 het
UPSIT [95%CI]	9.0 [2.8 - 28.8]	p<0.001
MOCA [95%CI]	2.9 [0.9-9.6]	p=0.072
BDI		
RBDSQ		
vs controls	OR [95%CI] tp2 bia	p tp2 bia
UPSIT [95%CI]	6.8 [1.8 - 26.0]	p=0.005
MOCA [95%CI]	5.9 [1.5 - 23.3]	p=0.011
BDI	18.5 [1.9 - 169.0]	p=0.010
RBDSQ		
vs controls	OR [95%CI] tp2 het	p tp2 het
UPSIT [95%CI]	7.2 [1.8- 27.4]	p=0.004
MOCA [95%CI]	2.6 [0.65-10.4]	p=0.175
BDI	4.8 [0.5 - 44.7]	p=0.173

KEY

bia: bia-allelic
bl: baseline
Chi 2: Chi squared
ctl: control
***GBA*: glucocerebrosidase mutation**
hom: homozygous
OR: odds ratio
tp1: timepoint 1
tp2: timepoint 2

RBDSQ		

Repeated measures regression model looking for associations between combined *GBA* group and prodromal features (compared to controls) taking into account age, sex, education, smoking history and history of Parkinson disease/dementia(p<0.05)

repeated measures	OR [95%CI] *GBA*	p *GBA*
UPSIT	**5.0 [1.6-16.1]**	**p=0.006**
MOCA	**5.7 [1.5-20.0]**	**p=0.007**
BDI	2.3 [0.7 - 7.4]	p=0.158
RBDSQ	3.2 [0.7-13.4]	p=0.120
repeated measures	**OR [95%CI] bia**	**p bia**
UPSIT	**4.7 [1.3-5.3]**	**p=0.020**
MOCA	**7.1 [1.69-29.3]**	**p=0.007**
BDI		
RBDSQ		
repeated measures	**OR [95%CI] het**	**p het**
UPSIT	**5.3 [1.6-17.5]**	**p=0.008**
MOCA	**4.4 [1.1-18.4]**	**p=0.042**
BDI		
RBDSQ		

KEY

bia: bia-allelic
bl: baseline
Chi 2: Chi squared
ctl: control
***GBA*: glucocerebrosidase mutation**
hom: homozygous
OR: odds ratio
tp1: timepoint 1
tp2: timepoint 2

Ordinal logistic regression model looking for associations between individual risk scores of prodromal features amongst *GBA* carriers taking into account age, sex, education, smoking history and history of Parkinson disease/dementia(p<0.05)(p<0.05)

high risk model	OR [95%CI] *GBA*	p *GBA*
MOCA	**1.5 [1.03-2.3]**	**p=0.033**

KEY

BDI	**1.3 [1.02-1.8]**	**p=0.030**
high risk model	**OR [95%CI] bia**	**p bia**
MOCA	**2.2 [1.3 - 4.0]**	**p=0.006**
BDI	1.2 [0.8 - 1.7]	p=0.333
high risk model	**OR [95%CI] het**	**p het**
MOCA	0.9 [0.4 - 1.7]	p=0.750
BDI	1.3 [1.2 - 0.3]	p=0.249

Ordinal logistic regression model looking for associations between individual risk scores of prodromal features amongst controls (p<0.05)

high risk model	**OR [95%CI]**	**p *GBA***
MOCA	**0.25 [0.0-2.8]**	**p=0.259**
BDI	**1.3 [0.6-2.8]**	**p=0.435**

Fishers exact test of ctl vs combined *GBA* group (p<0.05)

	p value bl
UMSARS	**p=0.040**
RBD	p=0.376
UPDRS II	p=0.490
UPDRS III	p=0.407
	p value tp1
UMSARS	p=0.096
RBD	p=0.493
UPDRS II	p=0.201

KEY

bia: bia-allelic
bl: baseline
Chi 2: Chi squared
ctl: control
***GBA*: glucocerebrosidase mutation**
hom: homozygous
OR: odds ratio
tp1: timepoint 1
tp2: timepoint 2

UPDRS III	**p=0.020**
	p value tp2
UMSARS	p=0.292
RBD	p=0.546
UPDRS II	**p=0.022**
UPDRS III	p=0.593
Fishers exact test of ctl vs bia (p<0.05)	
	p value bl
UMSARS	**p=0.028**
RBD	
UPDRS II	
UPDRS III	
	p value tp1
UMSARS	
RBD	
UPDRS II	
UPDRS III	**p=0.003**
	p value tp2
UMSARS	
RBD	
UPDRS II	**p=0.006**
UPDRS III	
Fishers exact test of ctl vs het (p<0.05)	
	p value bl

tp2: timepoint 2

KEY
bia: bia-allelic
bl: baseline
Chi 2: Chi squared
ctl: control
***GBA*: glucocerebrosidase mutation**
hom: homozygous
OR: odds ratio
tp1: timepoint 1
tp2: timepoint 2

KEY

UMSARS	**p=0.036**
RBD	
UPDRS II	
UPDRS III	
	p value tp1
UMSARS	
RBD	
UPDRS II	
UPDRS III	**p=0.004**
	p value tp2
UMSARS	
RBD	
UPDRS II	**p=0.030**
UPDRS III	
Fishers/Chi squared test bia vs het (p<0.05)	
	p value bl
UMSARS	**p=0.035**
RBD	
UPDRS II	
UPDRS III	
	p value tp1
UMSARS	
RBD	
UPDRS II	
UPDRS III (chi2)*	p=0.279
	p value tp2
UMSARS	

bia: bia-allelic
bl: baseline
Chi 2: Chi squared
ctl: control
***GBA*: glucocerebrosidase mutation**
hom: homozygous
OR: odds ratio
tp1: timepoint 1
tp2: timepoint 2

KEY
bia: bia-allelic
bl: baseline
Chi 2: Chi squared
ctl: control
***GBA*: glucocerebrosidase mutation**
hom: homozygous
OR: odds ratio
tp1: timepoint 1
tp2: timepoint 2

RBD		
UPDRS II	p=0.989	
UPDRS III		

Ordinal regression model taking into account age, sex, education, family history of dementia/Parkinson disease and smoking history, looking for associations between putative biomarkers and risk score

	OR [95% CI]	**p value**
alpha synuclein	**1.4 [1.0-1.9]**	**p=0.025**
Tau	1.6 [0.9-2.9]	p=0.111

ANOVA with FDR correction for multiple comparisons of levels of urine Ig Kappa light chain

	bia v ctl	
	p value	**Fold change**
Ig kappa chain V-I region AU	**p=0.005**	**3.5**
Ig kappa chain V-I region Ni	**p=0.025**	**2.8**
	het v ctl	
	p value	**Fold change**
Ig kappa chain V-I region AU	**p=0.028**	**3.2**
Ig kappa chain V-I region Ni	ns	ns

KEY

bia: bia-allelic
bl: baseline
Chi 2: Chi squared
ctl: control
***GBA*: glucocerebrosidase mutation**
hom: homozygous
OR: odds ratio

tp1: timepoint 1
tp2: timepoint 2

	bia v het	
	p value	**Fold change**
Ig kappa chain V-I region AU	ns	ns
Ig kappa chain V-I region Ni	ns	ns
	High risk v Low risk (*GBA*)	
	p value	**Fold change**
Ig kappa chain V-I region AU	**p=0.003**	**3.4**
Ig kappa chain V-I region Ni	**p=0.020**	**3.5**

Sensitivity analysis: ordinal regression model: taking into account age, sex, education, family history of dementia/Parkinson disease and smoking history, looking for associations with dependent variables and whether participant record contains any missing data. Across three timepoints

	baseline (OR [95%CI] p value)	**tp1 (OR [95%CI] p value)**	**tp2 (OR [95%CI] p value)**
UPSIT	1.9 [0.7 - 4.9] p=0.207	1.9 [0.6 - 6.2] p=0.321	2.0 [0.4 - 10.1] p=0.416
MOCA	0.6 [0.2 -1.8] p=0.366	1.1 [0.3-4.4] p=0.858	0.6 [0.1-4.3] p=0.574
BDI	3.9 [0.2-6.7] p=0.344	2.8 [0.3-30.4] p=0.395	1.4 [0.4-5.4] p=0.586
RBDSQ	0.9 [0.1-13.4] p=0.965	1.1 [0.15 - 7.8] p=0.941	2.4 [0.3-19.5] p=0.418

Assessment (MOCA), the Rapid Eye Movement Behaviour Disorder Sleep Questionnaire (RBDSQ), the Beck's Depression Inventory (BDI), and a Unified Multiple System Atrophy Rating Scale (UMSARS) subscale. Participants were examined independently by a physician trained in movement disorders (A.M, M.B or S.M). A blinded senior neurologist and expert in movement disorders (A.H.V.S.) evaluated participants upon deterioration in UPDRSscores.

10.2c Standardization of UPDRStesting

To ensure consistency in UPDRSpart III scoring a standardized approach to administration of testing was carried out. To test this approach investigators carried out a blinded assessment of patients with a clinical diagnosis of Parkinson disease and compared scores. Scores respectively for each participant showed a deviation of 0 points, 1 point, 2 points and 4 points out of 33.

10.2d Risk stratification procedure

To produce an indicator of overall worse/deterioration of performance, we devised a risk stratification system. From the first to last timepoint, for each half standard deviation fall in the assessment score of each prodromal feature, one point was scored (maximum of four). For each half standard deviation that the average score was below the trimmed mean of the combined *GBA* group a point was scored (maximum of four). The combined risk score out of eight was then produced.

10.3 Statistical analysis

10.3a Clinical data

Data was analysed using Stata version v.14.1 (StataCorp, Texas). Graphs were plotted using Stata and Microsoft excel v.15.17. Outliers with disproportionately poor scores in *GBA* carrier groups caused a non parametric distribution. To compensate trimmed means with exact confidence intervals were derived by excluding participants with scores more than two standard deviations from the mean (and recalculating). Primary analysis was carried out on the combined *GBA* vs controls groups. In the event of a significant association we carried out secondary analyses comparing bi-allelic/heterozygous groups with controls.

We assessed the confounding effect of study covariates and differences of groups demographics with descriptive statistics and a Kruskal–Wallis test.

Non-parametrically distributed raw data precluded analyses taking into account covariate risk factors, therefore where possible (MOCA, BDI, UPSIT, RBDSQ) data was categorised according to clinically validated thresholds:

UPSIT: <19 anosmia, 20-24 severe microsmia, 25-29 microsmia, 30-33 mild microsmia [169]

MOCA: <25 dementia, 25-26 mild cognitive impairment [170]

RBDSQ: >5 REM sleep disorder [172]

BDI: 9-19 mild depression, 20-29 moderate depression, > 29 severe depression [171]

Ordinal logistic regression was used to determine associations between the combined *GBA* cohort and controls adjusted for sex, education (university/non university educated), family

history of Parkinson disease and/or dementia, significant past smoking history (>1 pack year) and age (henceforth be referred to as study covariates).

Repeated measures logistic regression was used to determine associations between the change of prodromal features and study group, adjusted for study covariates using clinically validated thresholds:

UPSIT: <30 microsmia [169]
MOCA: <27 Mild cognitive impairment [170]
RBDSQ >5 REM sleep disorder [172]
BDI >8 mild depression [171]

Fisher's exact test was used to compare dependent variables which were not amenable to stratification (UMSARS subscale, UPDRS II/III)

Prodromal feature risk scores were entered into an ordinal regression model examining potential associations between the UPSIT and other risk scores, taking into account study co-variates. Successively the least statistically significant risk score was removed until only significant associations ($p<0.05$) remained. This model was then tested in heterozygous/bi-allelic carriers and the control group.

10.3b Missing data

We carried out a sensitivity analysis within the dataset to assess the impact of missing data. To do this we constructed a regression model which included the dependent variable in

questions at each timepoint, *GBA* carriers status (ctl/het/bia), all other study coovariates and whether data was missing for the participant and dependent variable in question. We concluded that missing data did not impact on any dependent variable and hence that data was missing at random (see supplementary table 1 for details).

Where appropriate (cross sectional and repeated measures analyses) we used multiple imputation using chained equations (m=50) to impute missing values. Because dependent variables were not parametrically distributed we were only able to impute variables which were amenable to transformation into ordinal datasets (MOCA, BDI, RBDSQ and UPSIT – see above). Dependent variables were included in the regression model if respectively there was a missing data rate in excess of 5%. This included at baseline UPSIT and BDI and at timepoints 1/2 UPSIT, BDI, MOCA and RBDSQ. All study covariates were included in the chained regression model in order to calculate these imputed values.

Chapter 4

10.4 Supplementary results

Supplementary table 5 – descriptive statistics of cogtrack validation assisted/unassisted experiments

	Choice reaction time	**Spatial working memory**	**Numeric working memory**	**Picture recognition**	**Digit Vigilance**
reaction time (msec) assisted					
median	544.4	1139.4	1005.3	1123.8	508.1
IQR	512.2-576.7	952.0-1326.9	811.8-1198.85	1038.0-1209.6	498.2-518.0
reaction time (msec) unassisted					
median	512.4	1175.25	898.9	1164.85	518.04
IQR	443.4-581.4	977.1-1373.4	727.7-1070.2	727.7-1349.4	498.9-537.14
accuracy (%) assisted					
median	96.3	93.8	96.7	100	100
IQR	92.95-99.65	87.55-100.05	92.25-101.15	97.5-102.5	98.9-101.1
accuracy (%) unassisted					
median	100	100	96.7	100	98.9
IQR	100-100	100-100	83.3-110.0	100-100	96.7-101.1
False alarms (#) assisted					
	-	-	-	-	3
	-	-	-	-	4.5-1.5
False alarms (#) assisted					
	-	-	-	-	1
	-	-	-	-	1.5-0.5

Supplementary table 6 – Descriptive statistics of cogtrack outputs.

group		SRT (msec)	SRTM (msec)	SRTSD (msec)	SRTCV (%)	VIGACC (%)	VIGRT (msec)	VIGFA (#)	VIGSD (msec)	VIGCV (msec)
control	**mean**	367.68	340.33	122.25	32.83	95.29	453.54	3.12	63.75	14.05
	median	348.77	333.90	102.16	26.15	97.78	456.89	3.00	65.94	14.71
carrier	**mean**	495.96	432.31	340.23	62.11	95.35	503.33	3.25	80.58	15.90
	median	404.78	353.40	151.77	35.91	97.78	509.43	3.00	77.06	14.65
biallellic	**mean**	455.74	392.46	255.92	45.99	96.15	473.42	2.44	71.24	14.93
	median	426.14	373.80	115.86	30.65	97.78	476.11	1.50	70.75	14.38
Parkinson disease	**mean**	431.46	380.35	210.97	42.92	95.26	497.62	5.24	79.05	15.78
	median	382.79	333.35	111.79	28.69	97.78	490.72	4.00	77.65	15.67

group		CRTACC (%)	CRT (msex)	CRTM (msec)	CRTSD (msec)	CRTCV (%)
control	**mean**	95.52	545.26	525.05	186.35	32.38
	median	96.00	562.86	561.10	108.77	22.38
carrier	**mean**	96.36	633.19	579.85	329.72	38.83
	median	98.00	597.14	587.70	112.33	18.79
biallellic	**mean**	96.08	580.03	548.33	198.31	28.39
	median	98.00	543.84	535.00	107.61	19.12
Parkinson disease	**mean**	95.16	628.46	575.06	313.48	43.51
	median	96.00	533.56	526.90	117.79	19.44

group		SPMOACC (%)	SPMNACC (%)	SPMORT (msec)	SPMNRT (msec)	SPMRT (msec)	SPMORTM (msec)	SPMNRTM (msec)	SPMRTM (msec)	SPMSD (msec)	SPMCV (%)
control	mean	93.50	86.40	1020.18	1081.51	1065.38	847.13	1010.61	895.74	667.00	54.02
	median	100.00	100.00	864.15	1015.49	954.49	859.50	888.00	868.00	279.65	26.49
carrier	mean	86.82	87.82	1369.96	1556.69	1483.40	1213.60	1264.74	1232.76	959.80	55.47
	median	93.75	100.00	1287.76	1436.08	1362.29	1147.80	1226.70	1154.50	553.83	38.21
biallellic	mean	87.14	84.23	1213.60	1415.29	1323.90	1056.40	1225.60	1141.14	670.14	47.81
	median	93.75	95.00	1141.22	1371.90	1294.75	910.10	1063.50	1065.40	518.40	44.98
Parkinson disease	mean	82.89	85.79	1332.26	1530.98	1440.51	1175.38	1241.36	1124.55	1139.98	69.74
	median	93.75	95.00	1122.30	1216.60	1217.17	1086.50	981.90	998.60	476.60	44.45

group		NWMOACC (%)	NWMNACC (%)	NWMORT (msec)	NWMNRT (msec)	NWMRT (msec)	NWMORTM (msec)	NWMNRTM (msec)	NWMRTM (msec)	NWMSD (msec)	NWMCV (%)
control	mean	94.40	94.93	839.13	972.26	904.42	798.92	936.14	854.66	248.73	26.63
	median	100.00	100.00	843.86	939.53	909.52	804.50	916.30	888.00	234.94	25.19
carrier	mean	91.27	94.91	981.09	1110.77	1044.30	894.69	973.27	933.07	453.02	38.33
	median	93.33	100.00	972.36	1054.60	1008.10	903.00	901.80	923.90	300.52	33.21
biallellic	mean	94.61	93.59	907.81	1031.96	969.11	825.22	923.82	866.87	352.64	35.08
	median	100.00	100.00	914.50	984.36	954.04	846.90	916.25	880.10	307.26	32.54
Parkinson disease	mean	92.81	95.26	1002.82	1161.58	1081.77	899.24	1072.87	1015.23	361.94	31.73
	median	100.00	100.00	937.71	1006.47	1004.08	842.05	953.10	948.35	318.54	31.56

group		DPICOA (%)	DPICNA (%)	DPICORT (msec)	DPICNRT (msec)	DPICRT (msec)	DPICORTM (msec)	DPICNRTM (msec)	DPICRTM (msec)	DPICSD (msec)	DPICCV (%)
control	mean	92.20	65.00	1385.45	1709.29	1499.26	1163.58	1529.28	1260.83	695.87	44.14
	median	90.00	70.00	1395.15	1572.60	1366.60	1134.50	1302.60	1240.90	676.38	40.56
carrier	mean	88.91	62.00	1475.09	1841.32	1599.90	1220.69	1477.54	1283.55	995.26	57.13
	median	90.00	65.00	1323.27	1679.11	1477.71	1172.20	1429.20	1242.70	732.27	47.31
biallellic	mean	88.85	58.75	1318.37	1754.44	1460.27	1091.08	1441.26	1173.81	797.32	50.69
	median	90.00	65.00	1140.44	1717.53	1297.92	996.65	1302.50	1042.70	598.66	46.41
Parkinson disease	mean	91.32	59.47	1333.96	1653.58	1446.88	1149.69	1457.03	1263.11	622.33	40.57
	median	95.00	62.50	1152.31	1606.39	1381.64	1106.70	1401.25	1167.90	499.44	40.99

Supplementary table 7. Schapiro Wilks tests for normality

control						heterozygote					
Variable		Obs W	V	z	Prob>z	Variable	Obs	W	V	z	Prob>z
SRT1	25	0.93095	1.919	1.332	0.0914	SRT1	55	0.53129	23.769	6.795	0
SRTM1	25	0.95061	1.372	0.647	0.25874	SRTM1	55	0.51863	24.411	6.852	0
SRTSD1	25	0.87971	3.343	2.467	0.00682	SRTSD1	55	0.76329	12.004	5.33	0
SRTCV1	25	0.85040	4.157	2.913	0.00179	SRTCV1	55	0.77828	11.244	5.19	0
VIGACC1	25	0.61153	10.794	4.863	0	VIGACC1	55	0.81881	9.188	4.757	0
VIGRT1	25	0.91318	2.412	1.8	0.03591	VIGRT1	55	0.97214	1.413	0.741	0.22929
VIGFA1	25	0.99471	0.147	-3.921	0.99996	VIGFA1	55	0.94261	2.91	2.291	0.01098
VIGSD1	25	0.92359	2.123	1.539	0.06189	VIGSD1	55	0.97837	1.097	0.198	0.42156
VIGCV1	25	0.92011	2.22	1.63	0.05153	VIGCV1	55	0.95502	2.281	1.768	0.03849

CRTACC1	25	0.87974	3.342	2.466	0.00683	**CRTACC1**	55	0.85399	7.404	4.294	0.00001
CRT1	25	0.92132	2.186	1.599	0.05491	**CRT1**	55	0.77858	11.228	5.187	0
CRTM1	25	0.91449	2.376	1.769	0.03843	**CRTM1**	55	0.96515	1.768	1.222	0.11095
CRTSD1	25	0.49242	14.104	5.41	0	**CRTSD1**	55	0.3782	31.533	7.401	0
CRTCV1	25	0.43843	15.604	5.617	0	**CRTCV1**	55	0.45582	27.596	7.115	0
SPMOACC1	25	0.52882	13.093	5.258	0	**SPMOACC1**	55	0.75547	12.401	5.4	0
SPMNACC1	25	0.34355	18.241	5.936	0	**SPMNACC1**	55	0.61337	19.607	6.382	0
SPMORT1	25	0.62048	10.546	4.816	0	**SPMORT1**	55	0.92764	3.669	2.788	0.00265
SPMNRT1	25	0.87576	3.25	2.397	0.00827	**SPMNRT1**	55	0.90562	4.786	3.358	0.00039
SPMRT1	25	0.77599	6.225	3.738	0.00009	**SPMRT1**	55	0.95082	2.494	1.96	0.025
SPMORTM1	25	0.96691	0.92	-0.171	0.56808	**SPMORTM1**	55	0.89145	5.505	3.658	0.00013
SPMNRTM1	25	0.88985	2.881	2.152	0.01571	**SPMNRTM1**	55	0.97642	1.196	0.383	0.3507
SPMRTM1	25	0.96371	1.008	0.017	0.49327	**SPMRTM1**	55	0.94956	2.558	2.014	0.02199
SPMSD1	25	0.54543	12.631	5.185	0	**SPMSD1**	55	0.66717	16.878	6.061	0
SPMCV1	25	0.53648	12.88	5.224	0	**SPMCV1**	55	0.65628	17.431	6.13	0
SPMSI1	25	0.53473	12.928	5.232	0	**SPMSI1**	55	0.66371	17.054	6.083	0
NWMOACC1	25	0.86808	3.666	2.655	0.00396	**NWMOACC1**	55	0.78892	10.705	5.084	0
NWMNACC1	25	0.72069	7.761	4.189	0.00001	**NWMNACC1**	55	0.5673	21.943	6.623	0
NWMORT1	25	0.96255	1.04	0.081	0.46767	**NWMORT1**	55	0.96646	1.701	1.139	0.12733
NWMNRT1	25	0.91742	2.295	1.698	0.04476	**NWMNRT1**	55	0.85668	7.268	4.254	0.00001
NWMRT1	25	0.95965	1.121	0.234	0.40752	**NWMRT1**	55	0.90578	4.778	3.354	0.0004
NWMORTM1	25	0.89147	3.016	2.256	0.01202	**NWMORTM1**	55	0.97124	1.459	0.809	0.20914
NWMNRTM1	25	0.83199	4.668	3.15	0.00082	**NWMNRTM1**	55	0.89437	5.357	3.599	0.00016
NWMRTM1	25	0.93661	1.761	1.157	0.12356	**NWMRTM1**	55	0.95818	2.121	1.612	0.05345
NWMSD1	25	0.91572	2.342	1.74	0.04097	**NWMSD1**	55	0.55092	22.774	6.703	0
NWMCV1	25	0.87747	3.405	2.505	0.00613	**NWMCV1**	55	0.65624	17.433	6.13	0
NWMSI1	25	0.85398	4.057	2.863	0.0021	**NWMSI1**	55	0.65239	17.628	6.154	0
DPICOACC1	25	0.98613	0.386	-1.948	0.97432	**DPICOACC1**	55	0.95849	2.105	1.596	0.05522
DPICNACC1	25	0.95569	1.231	0.425	0.3354	**DPICNACC1**	55	0.97344	1.347	0.639	0.2615

DPICORT1	25	0.94168	1.621	0.987	0.16184	**DPICORT1**	55	0.93693	3.198	2.493	0.00633
DPICNRT1	25	0.77218	6.33	3.772	0.00008	**DPICNRT1**	55	0.80842	9.715	4.876	0
DPICRT1	25	0.90601	2.612	1.962	0.02486	**DPICRT1**	55	0.90647	4.743	3.339	0.00042
DPICORTM1	25	0.94203	1.611	0.974	0.16491	**DPICORTM1**	55	0.91327	4.398	3.177	0.00075
DPICNRTM1	25	0.65905	9.474	4.597	0	**DPICNRTM1**	55	0.8651	6.841	4.124	0.00002
DPICRTM1	25	0.97212	0.775	-0.522	0.69923	**DPICRTM1**	55	0.9529	2.388	1.867	0.03095
DPICSD1	25	0.89084	3.033	2.268	0.01166	**DPICSD1**	55	0.70172	15.126	5.826	0
DPICCV1	25	0.96883	0.866	-0.294	0.61553	**DPICCV1**	55	0.70286	15.069	5.817	0
DPICSI1	25	0.96191	1.058	0.116	0.45388	**DPICSI1**	55	0.96406	1.822	1.287	0.09902
biallelic						**Parkinson disease**					
Variable Obs	**W**	**V**	**z**	**Prob>z**		**Variable Obs**	**W**	**V**	**z**	**Prob>z**	
SRT1	52	0.7832	10.516	5.03	0	**SRT1**	38	0.76007	9.118	4.637	0
SRTM1	52	0.83827	7.845	4.403	0.00001	**SRTM1**	38	0.67935	12.185	5.245	0
SRTSD1	52	0.62416	18.231	6.206	0	**SRTSD1**	38	0.54367	17.341	5.986	0
SRTCV1	52	0.78038	10.653	5.057	0	**SRTCV1**	38	0.56	16.721	5.909	0
VIGACC1	52	0.64181	17.375	6.103	0	**VIGACC1**	38	0.84296	5.968	3.748	0.00009
VIGRT1	52	0.98354	0.798	-0.481	0.6848	**VIGRT1**	38	0.98414	0.603	-1.062	0.85591
VIGFA1	52	0.86543	6.528	4.01	0.00003	**VIGFA1**	38	0.87593	4.715	3.253	0.00057
VIGSD1	52	0.97717	1.107	0.218	0.41371	**VIGSD1**	38	0.94391	2.132	1.588	0.05615
VIGCV1	52	0.97117	1.398	0.717	0.23673	**VIGCV1**	38	0.97953	0.778	-0.527	0.70083
CRTACC1	52	0.94125	2.85	2.239	0.01259	**CRTACC1**	38	0.97838	0.822	-0.412	0.65975
CRT1	52	0.63763	17.578	6.128	0	**CRT1**	38	0.72139	10.588	4.95	0
CRTM1	52	0.82163	8.652	4.612	0	**CRTM1**	38	0.69863	11.453	5.115	0
CRTSD1	52	0.41479	28.387	7.152	0	**CRTSD1**	38	0.63388	13.913	5.523	0
CRTCV1	52	0.52371	23.104	6.712	0	**CRTCV1**	38	0.64193	13.607	5.477	0
SPMOACC1	52	0.80242	9.584	4.831	0	**SPMOACC1**	38	0.59977	15.209	5.71	0
SPMNACC1	52	0.73149	13.025	5.487	0	**SPMNACC1**	38	0.82863	6.512	3.931	0.00004

SPMORT1	52	0.84035	7.744	4.375	0.00001	**SPMORT1**	36	0.6535	12.635	5.304	0
SPMNRT1	51	0.87567	5.939	3.804	0.00007	**SPMNRT1**	38	0.71019	11.013	5.033	0
SPMRT1	52	0.86133	6.726	4.074	0.00002	**SPMRT1**	38	0.82067	6.815	4.026	0.00003
SPMORTM1	52	0.90302	4.704	3.31	0.00047	**SPMORTM1**	36	0.62633	13.626	5.462	0
SPMNRTM1	51	0.85181	7.079	4.179	0.00001	**SPMNRTM1**	38	0.50741	18.719	6.146	0
SPMRTM1	52	0.80235	9.587	4.832	0	**SPMRTM1**	38	0.79405	7.826	4.316	0.00001
SPMSD1	52	0.69523	14.783	5.758	0	**SPMSD1**	38	0.72359	10.504	4.934	0
SPMCV1	52	0.81039	9.197	4.743	0	**SPMCV1**	38	0.72851	10.317	4.896	0
SPMSI1	52	0.81994	8.734	4.633	0	**SPMSI1**	38	0.73594	10.035	4.838	0
NWMOACC1	52	0.72422	13.377	5.544	0	**NWMOACC1**	38	0.77187	8.669	4.531	0
NWMNACC1	52	0.5597	21.358	6.544	0	**NWMNACC1**	38	0.4103	22.409	6.523	0
NWMORT1	52	0.92888	3.45	2.647	0.00406	**NWMORT1**	38	0.69527	11.58	5.138	0
NWMNRT1	52	0.96239	1.824	1.285	0.09938	**NWMNRT1**	38	0.62825	14.127	5.555	0
NWMRT1	52	0.97282	1.319	0.591	0.27723	**NWMRT1**	38	0.65347	13.169	5.408	0
NWMORTM1	52	0.95945	1.967	1.446	0.07406	**NWMORTM1**	38	0.85637	5.458	3.56	0.00019
NWMNRTM1	52	0.96181	1.853	1.318	0.09375	**NWMNRTM1**	38	0.69251	11.685	5.157	0
NWMRTM1	52	0.95954	1.963	1.441	0.07474	**NWMRTM1**	38	0.73177	10.193	4.871	0
NWMSD1	52	0.85184	7.187	4.216	0.00001	**NWMSD1**	38	0.59873	15.249	5.716	0
NWMCV1	52	0.85082	7.236	4.23	0.00001	**NWMCV1**	38	0.93138	2.608	2.011	0.02217
NWMSI1	52	0.69273	14.905	5.775	0	**NWMSI1**	38	0.87237	4.85	3.313	0.00046
DPICOACC1	52	0.95822	2.027	1.51	0.06551	**DPICOACC1**	38	0.93868	2.33	1.775	0.03796
DPICNACC1	52	0.95128	2.363	1.838	0.03302	**DPICNACC1**	38	0.91721	3.146	2.405	0.0081
DPICORT1	52	0.90505	4.606	3.265	0.00055	**DPICORT1**	38	0.8532	5.579	3.606	0.00016
DPICNRT1	52	0.92562	3.608	2.743	0.00305	**DPICNRT1**	38	0.94182	2.211	1.665	0.04799
DPICRT1	52	0.90534	4.592	3.258	0.00056	**DPICRT1**	38	0.89893	3.841	2.823	0.00238
DPICORTM1	52	0.87294	6.164	3.887	0.00005	**DPICORTM1**	38	0.93131	2.61	2.013	0.02206
DPICNRTM1	52	0.91334	4.203	3.069	0.00107	**DPICNRTM1**	38	0.87092	4.905	3.336	0.00042
DPICRTM1	52	0.86609	6.496	4	0.00003	**DPICRTM1**	38	0.93272	2.557	1.969	0.02446
DPICSD1	52	0.81967	8.747	4.636	0	**DPICSD1**	38	0.92238	2.95	2.269	0.01162
DPICCV1	52	0.86771	6.417	3.974	0.00004	**DPICCV1**	38	0.93609	2.429	1.862	0.03133

DPICSI1	52	0.95535	2.166	1.652	0.04927	**DPICSI1**	38	0.96827	1.206	0.393	0.34734

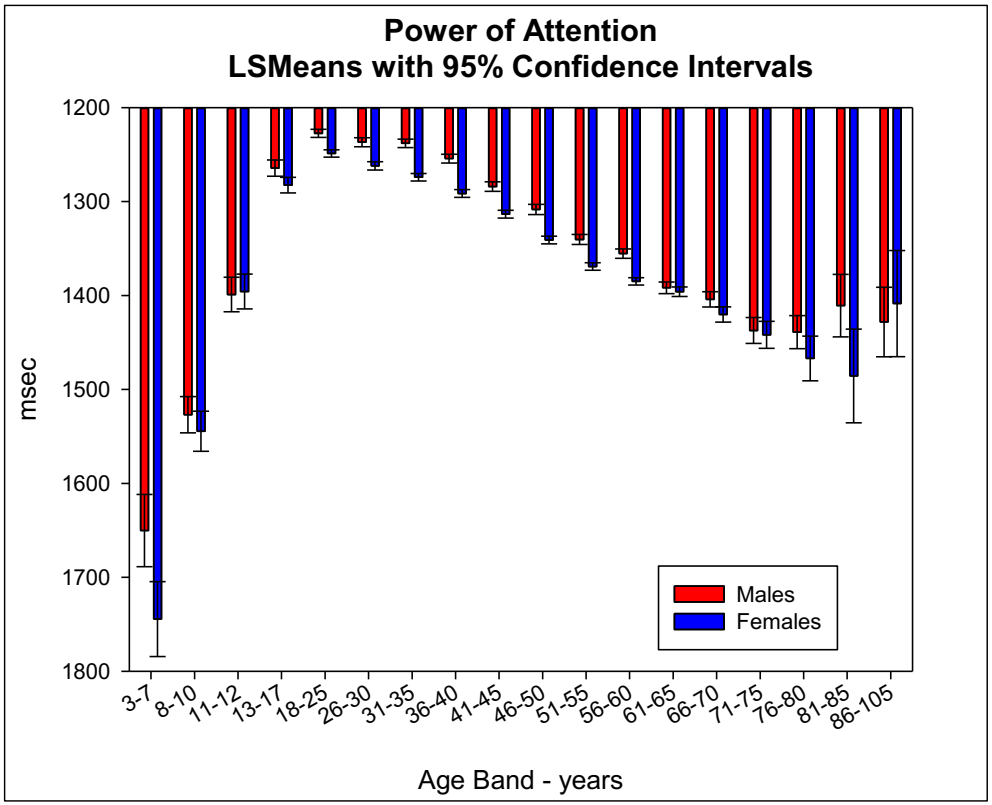

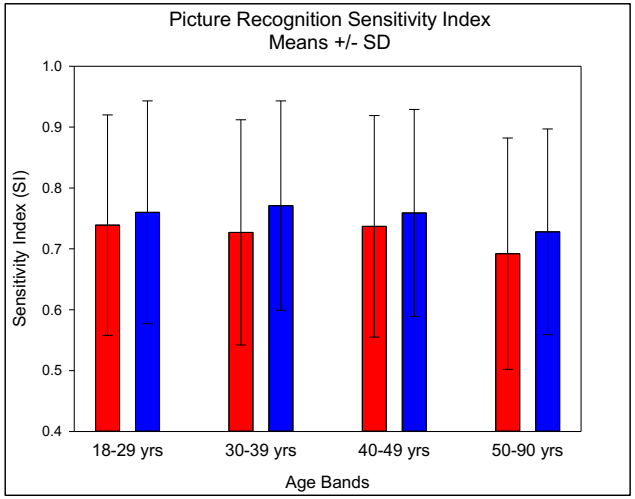

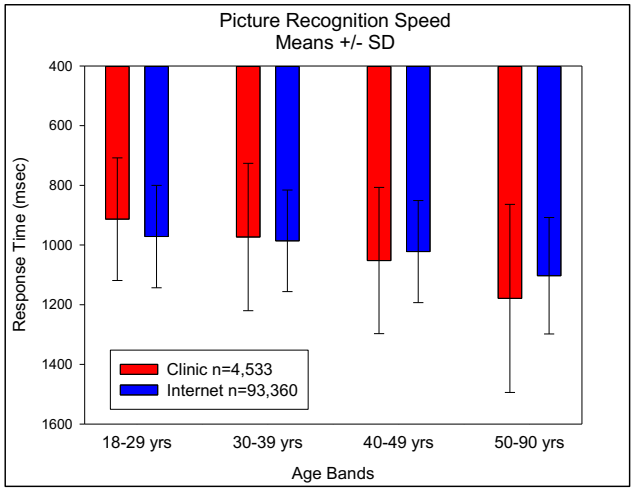

Supplementary Fig 9 . Validation data showing power of attention cogtrack task variation with sex. Picture sensitivity index and speed.

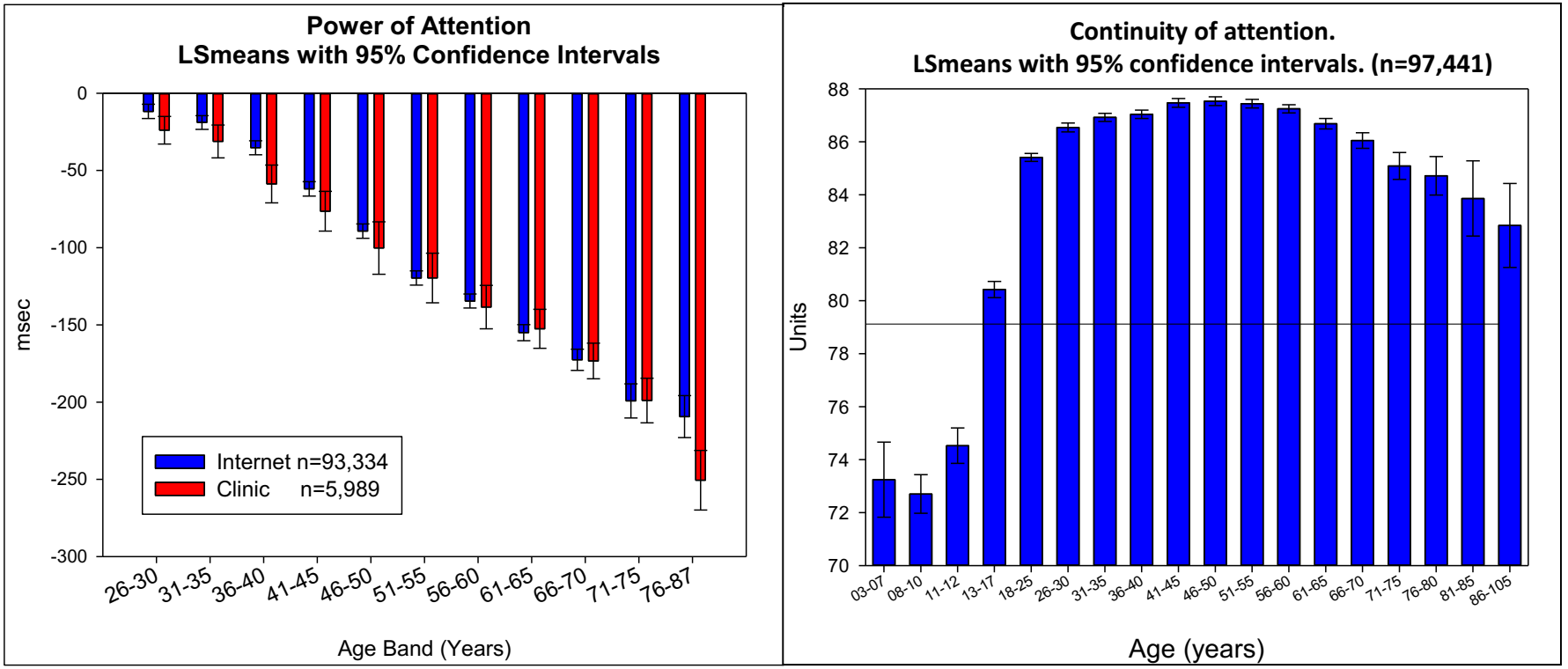

Supplementary Fig 10 .. Validation data for internet based version of cogtrack (CDR) battery. Power of Attention (left) and Continuity of attention (right). Study run over 12 months 2011-2012. Four tests from a computer based cognitive methodology, the CDR System, were internet enabled: simple reaction time, choice reaction time, digit vigilance and delayed picture recognition. 5 language versions were available: English, Greek, Hungarian, Portuguese & Spanish. 120,171 individuals logged on to a website, entered their age and gender, and performed the tests on-line. Male to female ratio 41% v 59%

Chapter 6

10.5 Mice

Mice were treated in accordance with local ethical committee guidelines and the UK Animals (Scientific Procedures) Act of 1986. All procedures were carried out in accordance with Home Office guidelines (United Kingdom). B6129SF1/J (101043) mice expressing wild-type *GBA1* (wild-type mice) and mice expressing the *N370S* mutation[346]

All mice were 10 to 12 weeks of age at sacrifice.

Genotyping of *N370S* alleles in primary mouse neurons was performed on brain samples samples from respective mouse embryos as previously described. [286] Briefly brains were extracted and digested in 15ml of extraction buffer + 15uL of proteinase K (55 degree for 5 hours, 99 degrees for 10minutes). Transgenic mice containing heterozygous/homozygous *N370S* mutation were identified by polymerase chain reaction (PCR) of ear genomic DNA using forward primer F: 5'CACAGATGTGTATGGCCATCGG-3 and reverse primer R: 5'-CTGAAGTGGCCAAGATGGTAG-3'.

10.6 Immunohistochemistry

Cells were fixed in 3.7% paraformaldehyde (pH 7.4), permeabilised with methanol for 10min at -20°C, blocked in 2% (v/v) goat serum in PBS with 0.1% (v/v) Triton X-100 (PBST) for 1h at RT, and then incubated with chicken polyclonal anti GFAP (abcam ab4674) or rabbit polyclonal anti beta 3 tubulin (abcam ab18207) antibodies overnight at 4°C. Following

washing of cover slips with PBS, cells were incubated with green goat anti chicken (abcam ab150173) or red goat anti rabbit (ab6719) antibody for 1h at 37 °C in PBST with 2% goat serum. Coverslips were then washed three times with PBS and mounted in citifluor containing DAPI.

10.7 Live-cell imaging

Ca^{2+} imaging Cells were loaded with the ratiometric fluorescent Ca^{2+} indicator Fura-2 after incubation with Fura-2 AM (2.5µM) and 0.005% (v/v) pluronic acid (Invitrogen) for 1 hour at room temperature in HEPES-buffered saline (HBS) consisting of 10 mM HEPES, 2 mM $MgSO_4$, 156 mM NaCl, 3 mM KCl, 2 mM $CaCl_2$, 1.25 mM KH_2PO_4 and 10 mM glucose (pH 7.4).

Following three washes in HBS, cells were stimulated with either GPN (200 µM; glycyl-L-phenylalanine-naphthylamide; SantaCruz Biotech), thapsigargin (1 µM; Merck), or KCL (52 mM; Sigma). Where indicated (thapsigargin), extracellular Ca^{2+} was removed using a modified HBS solution containing 1 mM EGTA (ethylene glycol tetraacetic acid) instead of $CaCl_2$.

10.8 Lysotracker imaging

Fibroblasts were incubated with 100 nM Lysotracker red (Invitrogen) for 30 minutes in HBS. After loading, cells were washed three times in HBS and imaged after stimulation with GPN.

10.9 GCase activity assay (brain lysate)

Brain samples were homogenized in 5mM ethylenediaminetetraacetic acid, 750mM sodium chloride, 50mM Tris (pH 7.4), 10% Triton X-100. Homogenate was centrifuged to remove insoluble materials, and protein concentration was determined using a Pierce BCA Protein Assay. Resulting lysate was diluted to 2mg/ml in distilled water and sonicated.

GCase activity was measured in lysate (20 µg protein) using 5mM 4-methylumbelliferyl β-D-glucopyranoside substrate in McIlvaine buffer (pH 5.4) supplemented with 22mM sodium taurocholate hydrate at 37 °C for 1 hour. The reaction was stopped by adding 0.25M glycine (pH 10.4), and substrate fluorescence was measured at excitation of 365nm, emission of 450nm with a PerkinElmer (Waltham, MA) fluorescence spectrometer. All GCase assays were performed in duplicate. GCase activity was expressed as nanomoles of substrate catalysed per milligram protein per hour.

10.10 GCase activity assay (fibroblasts)

Fibroblast pellets were lysed in 10% Triton X-100. protein concentration was determined using a Pierce BCA Protein Assay. Resulting lysate was diluted to 2mg/ml in distilled water and sonicated. GCase activity was measured in lysate (20 µg protein) using 5mM 4-methylumbelliferyl β-D-glucopyranoside substrate in McIlvaine buffer (pH 5.4) supplemented with 22mM sodium taurocholate hydrate at 37 °C for 1 hour. The reaction was stopped by adding 0.25M glycine (pH 10.4), and substrate fluorescence was measured

at excitation of 365nm, emission of 450nm with a PerkinElmer (Waltham, MA) fluorescence spectrometer. All GCase assays were performed in duplicate. GCase activity was expressed as nanomoles of substrate catalysed per milligram protein per hour.

10.11 GCase activity brain (homogenates)

Brain samples were homogenized in 5mM ethylenediaminetetraacetic acid, 750mM sodium chloride, 50mM Tris (pH 7.4), 10% Triton X-100, unless stated otherwise. Homogenate was centrifuged to remove insoluble materials, and protein concentration was determined using a Pierce BCA Protein Assay. Resulting lysate was diluted to 2mg/ml in distilled water and sonicated. GCase activity was measured in lysate (20 µg protein) using 5mM 4-methylumbelliferyl β-D-glucopyranoside substrate in McIlvaine buffer (pH 5.4) supplemented with 22mM sodium taurocholate hydrate at 37 °C for 1 hour. The reaction was stopped by adding 0.25M glycine (pH 10.4), and substrate fluorescence was measured at excitation of 365nm, emission of 450nm with a PerkinElmer (Waltham, MA) fluorescence spectrometer. All GCase assays were performed in duplicate. GCase activity was expressed as nanomoles of substrate catalysed per milligram protein per hour.

10.12 Demographics of fibroblast cell lines

Supplementary table 8. Characterstics of fibroblast lines TMRM experiments			
mutation	**disease**	**age/sex**	**passage**
wt	-	70F	9
wt/wt	-	52M	9
wt/wt	-	54M	7
wt/wt	-	65M	9
N370S/wt	-	75F	7
N370S/wt	-	45M	8
N370S/wt	-	52M	7
N370S/wt	-	71F	8
N370S/wt	Parkinson disease	78F	7
N370S/wt	Parkinson disease	57M	9
N370S/wt	Parkinson disease	63M	7
N370S/wt	Parkinson disease	57M	8
N370S/203insc	GD	61M	8
N370S/c1263del55	GD	50M	8
N370S/*N370S*	GD	70M	7
N370S/R359X	GD	54M	8

10.13TMRM image express methods

Cells were plated on 96 well glass bottomed plates in DMEM, 10% FBS, pen/strep, NEAA, pyruvate 48 hours prior to imaging at a density of 2000 cells/well.1 Hour before imaging cells were washed with 100uL HBS and then incubated with HBS with TMRM 25nM and Hoechst 2ug/ml was added Cells were imaged, HBS was removed and then 100uL 5uM oligomycin with 25nM TMRM was added and cells reimaged. Demographics and passage numbers of cell lines used are listed below.

Chapter 7

10.14 GCase activity cerebrospinal fluid

cerebrospinal fluid was centrifuged at 2200G for 10min and frozen at -80 degrees within an hour of collection in 250ul aliquots. Upon defrosting cerebrospinal fluid was vortexed and centrifuged at 8000rpm for 10 second. 10 repeats of 20ul of cerebrospinal fluid was added to a 96 well plate. The reaction was commenced by adding 40ul of 5uM 4-MU-β-D-glucopyranoside solution dissolved in McIlvaine citrate buffer (0.15M, pH 5.9). The plate was covered and incubated at 38 degrees for 3 hours whereupon the reaction was stopped using 240ul Glycine stopping buffer (1M, pH 10.4). A standard was prepared by preparing 5 repeats of 200ul 1mM 4-methylumbelliferone in distilled water and adding 100ul Glycine buffer. The plate was measured at excitation of 365nm, emission of 450nm with a

PerkinElmer (Waltham, MA) fluorescence spectrometer. GCase assays were expressed as nanomoles of substrate catalysed per millilitre of cerebrospinal fluid per hour.

Gain settings

The fluorescence readings for GCase are very low in cerebrospinal fluid. Therefore, in the initial trial of this assay, the same plate was read at several different gain settings (50, 55, 60, 65 and 75) in order to obtain a signal that could be better discriminated from the water blank wells. However, the choice of gain was constrained by the very high fluorescence for the standard solution. In the end we settled for a gain adjustment of 55 for all subsequent assays and also decided to use a 4-fold diluted standard solution in the plates, which was then accounted for in the final activity calculations.

Negative controls

Condruitol beta expoxide (CBE) is a known potent inhibitor of GCase. CBE stock solution (10mM) was made by dissolving the solute in dH_2O and was subsequently aliquoted and stored at -20°C. For the assay, the CBE was added in a 1:10 dilution directly to cerebrospinal fluid to obtain a working concentration of 1mM and incubated at 37°C for 15min before adding to the plate. As a second negative control, some of the cerebrospinal fluid sample was denatured prior to performing the assay. Denaturing was achieved by heating the cerebrospinal fluid to 80°C for a minimum of 15min in a dry bath incubator.

10.15 Small molecular chaperones in vitro studies

Both ambroxol and Isophagamine were dissolved in dimethyl sulfoxide (DMSO) to make a stock solution of 10mM. An intermediate stock of 100µM was made, aliquoted and stored at -20°C. For the assay ABX/IFG was added in a 1:200 dilution directly to cerebrospinal fluid to obtain a working concentration of 500nM and incubated at 37°C for 15min before adding to the plate. The concentration of 500nM was chosen and rounded to a workable concentration based on the cerebrospinal fluid penetration of ABX in Gaucher diseasepatients reported from the results of a recent clinical trial[302]

10.16 GCase activity leucocyte pellets

Leucocyte pellets were lysed in Fermantas ProteoJET Mammalian Cell Lysis Reagent and diluted 8X in McIlvaine citrate buffer (0.15M, pH 5.9). The reaction was commenced by adding 40ul of 5uM 4-MU-β-D-glucopyranoside solution dissolved in McIlvaine citrate buffer (0.15M, pH 5.9). The plate was covered and incubated at 38 degrees for 3 hours whereupon the reaction was stopped using 240ul Glycine stopping buffer (1M, pH 10.4). A standard was prepared by preparing 5 repeats of 200ul 1mM 4-methylumbelliferone in distilled water and adding 100ul Glycine buffer. The plate was measured at excitation of 365nm, emission of 450nm with a PerkinElmer (Waltham, MA) fluorescence spectrometer. Protein concentration was determined using a Pierce BCA Protein Assay. GCase assays were expressed as nanomoles of substrate catalysed per milligram of protein per hour.

References

1 Van Meer G, Wolthoorn J, Degroote S. The fate and function of glycosphingolipid glucosylceramide. *Philos Trans R Soc Lond, B, Biol Sci* 2003; **358**: 869–73.

2 Poorthuis B. Lysosomal Storage Disorders. Oxford University Press, 2016 DOI:10.1093/med/9780199972135.003.0046.

3 Platt FM. Sphingolipid lysosomal storage disorders. *Nature* 2014; **510**: 68–75.

4 Roze E, Sedel F. Gangliosidoses (GM1 and GM2). Oxford University Press, 2016 DOI:10.1093/med/9780199972135.003.0050.

5 West M, Linthorst G. Fabry Disease. Oxford University Press, 2016 DOI:10.1093/med/9780199972135.003.0049.

6 Chabás A, Cormand B, Balcells S, *et al.* Neuronopathic and non-neuronopathic presentation of Gaucher disease in patients with the third most common mutation (D409H) in Spain. *J Inherit Metab Dis* 1996; **19**: 798–800.

7 Tylki-Szymañska A, Keddache M, Grabowski GA. Characterization of neuronopathic Gaucher disease among ethnic Poles. *Genet Med* 2006; **8**: 8–15.

8 Grabowski GA, Zimran A, Ida H. Gaucher disease types 1 and 3: Phenotypic characterization of large populations from the ICGG Gaucher Registry. *Am J Hematol* 2015; **90**: S12–8.

9 Abdelwahab M, Blankenship D, Schiffmann R. Long-term follow-up and sudden unexpected death in Gaucher disease type 3 in Egypt. *Neurol Genet* 2016; **2**: e55.

10 Goker-Alpan O, Schiffmann R, Park JK, Stubblefield BK, Tayebi N, Sidransky E. Phenotypic continuum in neuronopathic gaucher disease: an intermediate phenotype between type 2 and type 3. *The Journal of Pediatrics* 2003; **143**: 273–6.

11 Rana HQ, Balwani M, Bier L, Alcalay RN. Age-specific Parkinson disease risk in GBA mutation carriers: information for genetic counseling. *Genet Med* 2013; **15**: 146–9.

12 Neudorfer O, Giladi N, Elstein D, *et al.* Occurrence of Parkinson's syndrome in type I Gaucher disease. *QJM* 1996; **89**: 691–4.

13 Rosenbloom B, Balwani M, Bronstein JM, *et al.* The incidence of Parkinsonism in patients with type 1 Gaucher disease: data from the ICGG Gaucher Registry. *Blood Cells Mol Dis* 2011; **46**: 95–102.

14 Anheim M, Elbaz A, Lesage S, *et al.* Penetrance of Parkinson disease in glucocerebrosidase gene mutation carriers. *Neurology* 2012; **78**: 417–20.

15 Sidransky E, Hart PS. Penetrance of PD in Glucocerebrosidase Gene Mutation Carriers. *Neurology* 2012; **79**: 106–7.

16 Duran R, Mencacci NE, Angeli AV, *et al.* The glucocerobrosidase E326K variant predisposes to Parkinson‘s disease, but does not cause Gaucher’s disease. *Movement Disorders* 2013; **28**: 232–6.

17 Neumann J, Bras J, Deas E, *et al.* Glucocerebrosidase mutations in clinical and pathologically proven Parkinson's disease. *Brain* 2009; **132**: 1783–94.

18 Lesage S, Anheim M, Condroyer C, *et al.* Large-scale screening of the Gaucher‘s disease-related glucocerebrosidase gene in Europeans with Parkinson’s disease. *Hum Mol Genet* 2011; **20**: 202–10.

19 Asselta R, Rimoldi V, Siri C, *et al.* Glucocerebrosidase mutations in primary parkinsonism. *Parkinsonism and realted Disorders* 2014; **20**: 1215–20.

20 Aharon-Peretz J, Rosenbaum H, Gershoni-Baruch R. Mutations in the glucocerebrosidase gene and Parkinson's disease in Ashkenazi Jews. *N Engl J Med* 2004; **351**: 1972–7.

21 Aharon-Peretz J, Badarny S, Rosenbaum H, Gershoni-Baruch R. Mutations in the glucocerebrosidase gene and Parkinson disease: phenotype-genotype correlation. *Neurology* 2005; **65**: 1460–1.

22 Gan-Or Z, Amshalom I, Kilarski LL, *et al.* Differential effects of severe vs mild GBA mutations on Parkinson disease. *Neurology* 2015; **84**: 880–7.

23 Horowitz M, Pasmanik-Chor M, Ron I, Kolodny EH. The enigma of the E326K mutation in acid beta-glucocerebrosidase. *Mol Genet Metab* 2011; **104**: 35–8.

24 Mallett V, Ross JP, Alcalay RN, *et al.* GBA p.T369M substitution in Parkinson disease: Polymorphism or association? A meta-analysis. *Neurol Genet* 2016; **2**: e104.

25 Mullin S, Schapira A. The genetics of Parkinson's disease. *Br Med Bull* 2015; **114**: 39–52.

26 Mata IF, Leverenz JB, Weintraub D, *et al.* GBA Variants are associated with a distinct pattern of cognitive deficits in Parkinson's disease. *Movement Disorders* 2015; published online Aug. DOI:10.1002/mds.26359.

27 Cilia R, Tunesi S, Marotta G, *et al.* Survival and dementia in GBA-

associated Parkinson's disease: The mutation matters. *Ann Neurol* 2016; published online Sept 15. DOI:10.1002/ana.24777.

28 Alcalay RN, Caccappolo E, Mejia-Santana H, *et al.* Cognitive performance of GBA mutation carriers with early-onset PD: the CORE-PD study. *Neurology* 2012; **78**: 1434–40.

29 Liu G, Boot B, Locascio JJ, *et al.* Neuropathic Gaucher's mutations accelerate cognitive decline in Parkinson's. *Ann Neurol* 2016; published online Sept. DOI:10.1002/ana.24781.

30 Sidransky E, Nalls MA, Aasly JO, *et al.* Multicenter analysis of glucocerebrosidase mutations in Parkinson's disease. *N Engl J Med* 2009; **361**: 1651–61.

31 Mata IF, Samii A, Schneer SH, *et al.* Glucocerebrosidase gene mutations: a risk factor for Lewy body disorders. *Arch Neurol* 2008; **65**: 379–82.

32 Tsuang D, Leverenz JB, Lopez OL, *et al.* GBA mutations increase risk for Lewy body disease with and without Alzheimer disease pathology. *Neurology* 2012; **79**: 1944–50.

33 Zokaei N, McNeill A, Proukakis C, *et al.* Visual short-term memory deficits associated with GBA mutation and Parkinson's disease. *Brain* 2014; **137**: 2303–11.

34 Manning-Boğ AB, Schüle B, Langston JW. Alpha-synuclein-glucocerebrosidase interactions in pharmacological Gaucher models: A biological link between Gaucher disease and parkinsonism. *NeuroToxicology* 2009; **30**: 1127–32.

35 McNeill A, Magalhaes J, Shen C, *et al.* Ambroxol improves lysosomal biochemistry in glucocerebrosidase mutation-linked Parkinson disease cells. *Brain* 2014; **137**: 1481–95.

36 Mazzulli JR, Xu Y-H, Sun Y, *et al.* Gaucher disease glucocerebrosidase and α-synuclein form a bidirectional pathogenic loop in synucleinopathies. *Cell* 2011; **146**: 37–52.

37 Yang S-Y, Beavan M, Chau K-Y, Taanman J-W, Schapira AHV. A Human Neural Crest Stem Cell-Derived Dopaminergic Neuronal Model Recapitulates Biochemical Abnormalities in GBA1 Mutation Carriers. *Stem Cell Reports* 2017; **8**: 728–42.

38 Alcalay RN, Levy OA, Waters CC, *et al.* Glucocerebrosidase activity in Parkinson's disease with and without GBA mutations. *Brain* 2015; **138**: 2648–58.

39 Gegg ME, Burke D, Heales SJR, *et al.* Glucocerebrosidase deficiency in

substantia nigra of parkinson disease brains. *Ann Neurol* 2012; **72**: 455–63.

40 Parnetti L, Chiasserini D, Persichetti E, *et al.* Cerebrospinal fluid lysosomal enzymes and alpha-synuclein in Parkinson's disease. *Movement Disorders* 2014; **29**: 1019–27.

41 Zhang X. Association of Common Variants in the Glucocerebrosidase Gene with High Susceptibility to Parkinson's Disease among Chinese. *Chin J Physiol* 2012; **55**: 398–404.

42 Zhao F, Bi L, Wang W, *et al.* Mutations of glucocerebrosidase gene and susceptibility to Parkinson's disease: An updated meta-analysis in a European population. *Neuroscience* 2016; : 1–9.

43 Reymond J-L, Flux VS, Maillard NL. Enzyme assays. *Chem Commun* 2008; **409**: 34–46.

44 Persichetti E, Chiasserini D, Parnetti L, *et al.* Factors Influencing the Measurement of Lysosomal Enzymes Activity in Human Cerebrospinal Fluid. *PLoS ONE* 2014; **9**: e101453.

45 Parnetti L, Balducci C, Pierguidi L, *et al.* Cerebrospinal fluid ?-glucocerebrosidase activity is reduced in Dementia with Lewy Bodies. *Neurobiol Dis* 2009; **34**: 484–6.

46 Burrow TA, Sun Y, Prada CE, *et al.* Molecular Genetics and Metabolism. *Mol Genet Metab* 2015; **114**: 233–41.

47 Enquist IB, Bianco Lo C, Ooka A, *et al.* Murine models of acute neuronopathic Gaucher disease. *Proc Natl Acad Sci USA* 2007; **104**: 17483–8.

48 Vitner EB, Farfel-Becker T, Eilam R, Biton I, Futerman AH. Contribution of brain inflammation to neuronal cell death in neuronopathic forms of Gaucher's disease. *Brain* 2012; **135**: 1724–35.

49 Ouchi Y, Yoshikawa E, Sekine Y, *et al.* Microglial activation and dopamine terminal loss in early Parkinson's disease. *Ann Neurol* 2005; **57**: 168–75.

50 Croisier E, Moran LB, Dexter DT, Pearce RKB, Graeber MB. Microglial inflammation in the parkinsonian substantia nigra: relationship to alpha-synuclein deposition. *J Neuroinflammation* 2005; **2**: 14.

51 Converse AK, Larsen EC, Engle JW, Barnhart TE, Nickles RJ, Duncan ID. 11C-(R)-PK11195 PET imaging of microglial activation and response to minocycline in zymosan-treated rats. *J Nucl Med* 2011; **52**: 257–62.

52 Kim S, Cho S-H, Kim KY, *et al.* α-Synuclein induces migration of BV-2

microglial cells by up-regulation of CD44 and MT1-MMP. *J Neurochem* 2009; **109**: 1483–96.

53 Zhang W, Wang T, Pei Z, *et al.* Aggregated alpha-synuclein activates microglia: a process leading to disease progression in Parkinson's disease. *The FASEB Journal* 2005; **19**: 533–42.

54 Lee E-J, Woo M-S, Moon P-G, *et al.* Alpha-synuclein activates microglia by inducing the expressions of matrix metalloproteinases and the subsequent activation of protease-activated receptor-1. *The Journal of Immunology* 2010; **185**: 615–23.

55 Reale M, Iarlori C, Thomas A, *et al.* Brain, Behavior, and Immunity. *Brain Behav Immun* 2009; **23**: 55–63.

56 Sardi SP, Clarke J, Viel C, *et al.* Augmenting CNS glucocerebrosidase activity as a therapeutic strategy for parkinsonism and other Gaucher-related synucleinopathies. *Proceedings of the National Academy of Sciences* 2013; **110**: 3537–42.

57 Murphy KE, Gysbers AM, Abbott SK, *et al.* Reduced glucocerebrosidase is associated with increased α-synuclein in sporadic Parkinson's disease. *Brain* 2014; **137**: 834–48.

58 Gegg ME, Sweet L, Wang BH, Shihabuddin LS, Sardi SP, Schapira AHV. No evidence for substrate accumulation in Parkinson brains with GBA mutations. *Movement Disorders* 2015; **30**: 1085–9.

59 Yap TL, Gruschus JM, Velayati A, *et al.* Alpha-synuclein interacts with Glucocerebrosidase providing a molecular link between Parkinson and Gaucher diseases. *J Biol Chem* 2011; **286**: 28080–8.

60 Yap TL, Velayati A, Sidransky E, Lee JC. Membrane-bound α-synuclein interacts with glucocerebrosidase and inhibits enzyme activity. *Mol Genet Metab* 2013; **108**: 56–64.

61 Yap TL, Gruschus JM, Velayati A, Sidransky E, Lee JC. Saposin C protects glucocerebrosidase against α-synuclein inhibition. 2013; **52**: 7161–3.

62 Tan C-C, Yu J-T, Tan M-S, Jiang T, Zhu X-C, Tan L. Autophagy in aging and neurodegenerative diseases: implications for pathogenesis and therapy. *Neurobiol Aging* 2014; **35**: 941–57.

63 Cuervo AM, Stefanis L, Fredenburg R, Lansbury PT, Sulzer D. Impaired degradation of mutant alpha-synuclein by chaperone-mediated autophagy. *Science* 2004; **305**: 1292–5.

64 Decressac M, Mattsson B, Weikop P, Lundblad M, Jakobsson J, Björklund A. TFEB-mediated autophagy rescues midbrain dopamine

neurons from α-synuclein toxicity. *Proceedings of the National Academy of Sciences* 2013; **110**: E1817–26.

65 Webb JL, Ravikumar B, Atkins J, Skepper JN, Rubinsztein DC. Alpha-Synuclein is degraded by both autophagy and the proteasome. *J Biol Chem* 2003; **278**: 25009–13.

66 Alvarez-Erviti L, Rodriguez-Oroz MC, Cooper JM, *et al.* Chaperone-Mediated Autophagy Markers in Parkinson Disease Brains. *Arch Neurol* 2010; **67**. DOI:10.1001/archneurol.2010.198.

67 Koga H, Cuervo AM. Neurobiology of Disease. *Neurobiol Dis* 2011; **43**: 29–37.

68 Majeski AE, Dice JF. Mechanisms of chaperone-mediated autophagy. *Int J Biochem Cell Biol* 2004; **36**: 2435–44.

69 Xilouri M, Brekk OR, Stefanis L. α-Synuclein and protein degradation systems: a reciprocal relationship. *Mol Neurobiol* 2013; **47**: 537–51.

70 Chau K-Y, Ching HL, Schapira AHV, Cooper JM. Relationship between alpha synuclein phosphorylation, proteasomal inhibition and cell death: relevance to Parkinson's disease pathogenesis. *J Neurochem* 2009; **110**: 1005–13.

71 Löhle M, Hughes D, Milligan A, *et al.* Clinical prodromes of neurodegeneration in Anderson-Fabry disease. *Neurology* 2015; **84**: 1454–64.

72 Shachar T, Bianco Lo C, Recchia A, Wiessner C, Raas-Rothschild A, Futerman AH. Lysosomal storage disorders and Parkinson's disease: Gaucher disease and beyond. *Movement Disorders* 2011; **26**: 1593–604.

73 Bendikov-Bar I, Ron I, Filocamo M, Horowitz M. Characterization of the ERAD process of the L444P mutant glucocerebrosidase variant. *Blood Cells Mol Dis* 2011; **46**: 4–10.

74 Schmitz M, Alfalah M, Aerts JMFG, Naim HY, Zimmer K-P. Impaired trafficking of mutants of lysosomal glucocerebrosidase in Gaucher's disease. *Int J Biochem Cell Biol* 2005; **37**: 2310–20.

75 Maor G, Rencus-Lazar S, Filocamo M, Steller H, Segal D, Horowitz M. Unfolded protein response in Gaucher disease: from human to Drosophila. *Orphanet J Rare Dis* 2013; **8**: 140.

76 Ron I, Horowitz M. ER retention and degradation as the molecular basis underlying Gaucher disease heterogeneity. *Hum Mol Genet* 2005; **14**: 2387–98.

77 Surmeier DJ, Schumacker PT. Calcium, bioenergetics, and neuronal

vulnerability in Parkinson's disease. *J Biol Chem* 2013; **288**: 10736–41.

78 Bravo R, Parra V, Gatica D, *et al.* Endoplasmic reticulum and the unfolded protein response: dynamics and metabolic integration. *Int Rev Cell Mol Biol* 2013; **301**: 215–90.

79 Nath S, Goodwin J, Engelborghs Y, Pountney DL. Molecular and Cellular Neuroscience. *Molecular and Cellular Neuroscience* 2011; **46**: 516–26.

80 Wright JA, Wang X, Brown DR. Unique copper-induced oligomers mediate alpha-synuclein toxicity. *The FASEB Journal* 2009; **23**: 2384–93.

81 Danzer KM, Haasen D, Karow AR, *et al.* Different species of alpha-synuclein oligomers induce calcium influx and seeding. 2007; **27**: 9220–32.

82 Li W-J, Jiang H, Song N, Xie J-X. Dose- and time-dependent alpha-synuclein aggregation induced by ferric iron in SK-N-SH cells. *Neurosci Bull* 2010; **26**: 205–10.

83 Cole NB, Murphy DD, Grider T, Rueter S, Brasaemle D, Nussbaum RL. Lipid Droplet Binding and Oligomerization Properties of the Parkinson's Disease Protein α-Synuclein. *Journal of Biological …* 2002.

84 Roostaee A, Beaudoin S, Staskevicius A, Roucou X. Aggregation and neurotoxicity of recombinant α-synuclein aggregates initiated by dimerization. *Mol Neurodegener* 2013; **8**: 5.

85 Lemkau LR, Comellas G, Kloepper KD, Woods WS, George JM, Rienstra CM. Mutant protein A30P α-synuclein adopts wild-type fibril structure, despite slower fibrillation kinetics. *J Biol Chem* 2012; **287**: 11526–32.

86 Nielsen SB, Macchi F, Raccosta S, *et al.* Wildtype and A30P mutant alpha-synuclein form different fibril structures. *PLoS ONE* 2013; **8**: e67713.

87 Moussa CE-H, Mahmoodian F, Tomita Y, Sidhu A. Dopamine differentially induces aggregation of A53T mutant and wild type alpha-synuclein: insights into the protein chemistry of Parkinson's disease. *Biochem Biophys Res Commun* 2008; **365**: 833–9.

88 Porcari R, Proukakis C, Waudby CA, *et al.* The H50Q mutation induces a 10-fold decrease in the solubility of α-synuclein. *Journal of Biological Chemistry* 2015; **290**: 2395–404.

89 Van Raaij ME, van Gestel J, Segers-Nolten IMJ, de Leeuw SW, Subramaniam V. Concentration dependence of alpha-synuclein fibril length assessed by quantitative atomic force microscopy and statistical-mechanical theory. *Biophys J* 2008; **95**: 4871–8.

90 Iljina M, Garcia GA, Horrocks MH, *et al.* Kinetic model of the aggregation of alpha-synuclein provides insights into prion-like spreading. *Proceedings of the National Academy of Sciences* 2016; **113**: E1206–15.

91 Winner B, Jappelli R, Maji SK, *et al.* In vivo demonstration that alpha-synuclein oligomers are toxic. *Proc Natl Acad Sci USA* 2011; **108**: 4194–9.

92 Luth ES, Stavrovskaya IG, Bartels T, Kristal BS, Selkoe DJ. Soluble, prefibrillar α-synuclein oligomers promote complex I-dependent, Ca2+-induced mitochondrial dysfunction. *Journal of Biological Chemistry* 2014; **289**: 21490–507.

93 Celej MS, Sarroukh R, Goormaghtigh E, Fidelio GD, Ruysschaert J-M, Raussens V. Toxic prefibrillar α-synuclein amyloid oligomers adopt a distinctive antiparallel β-sheet structure. *Biochem J* 2012; **443**: 719–26.

94 Hinault MP, Cuendet AFH, Mattoo RUH, *et al.* Stable -Synuclein Oligomers Strongly Inhibit Chaperone Activity of the Hsp70 System by Weak Interactions with J-domain Co-chaperones. *Journal of Biological Chemistry* 2010; **285**: 38173–82.

95 Conway KA, Lee S-J, Rochet J-C, Ding TT, Williamson RE, Lansbury PT. Acceleration of oligomerization, not fibrillization, is a shared property of both α-synuclein mutations linked to early-onset Parkinson's disease: Implications for pathogenesis and therapy. *Proceedings of the …* 2000.

96 Rivers RC, Kumita JR, Tartaglia GG, *et al.* Molecular determinants of the aggregation behavior of alpha- and beta-synuclein. *Protein Sci* 2008; **17**: 887–98.

97 Li J-Y, Englund E, Holton JL, *et al.* Lewy bodies in grafted neurons in subjects with Parkinson's disease suggest host-to-graft disease propagation. *Nat Med* 2008; **14**: 501–3.

98 Luk KC, Kehm VM, Zhang B, O'Brien P, Trojanowski JQ, Lee VMY. Intracerebral inoculation of pathological α-synuclein initiates a rapidly progressive neurodegenerative α-synucleinopathy in mice. *J Exp Med* 2012; **209**: 975–86.

99 Luk KC, Kehm V, Carroll J, *et al.* Pathological α-synuclein transmission initiates Parkinson-like neurodegeneration in nontransgenic mice. *Science* 2012; **338**: 949–53.

100 Rey NL, Petit GH, Bousset L, Melki R, Brundin P. Transfer of human α-synuclein from the olfactory bulb to interconnected brain regions in mice. *Acta Neuropathol* 2013; **126**: 555–73.

101 Kordower JH, Chu Y, Hauser RA, Freeman TB, Olanow CW. Lewy body–like pathology in long-term embryonic nigral transplants in Parkinson's

disease. *Nat Med* 2008; **14**: 504–6.

102 Kordower JH, Dodiya HB, Kordower AM, *et al.* Transfer of host-derived alpha synuclein to grafted dopaminergic neurons in rat. *Neurobiol Dis* 2011; **43**: 552–7.

103 Bultron G, Kacena K, Pearson D, *et al.* The risk of Parkinson's disease in type 1 Gaucher disease. *J Inherit Metab Dis* 2010; **33**: 167–73.

104 Noyce AJ, Bestwick JP, Silveira-Moriyama L, *et al.* Meta-analysis of early nonmotor features and risk factors for Parkinson disease. *Ann Neurol* 2012; **72**: 893–901.

105 Beutler E, Gelbart T, Scott CR. Hematologically important mutations: Gaucher disease. *Blood Cells Mol Dis* 2005; **35**: 355–64.

106 Hruska KS, LaMarca ME, Scott CR, Sidransky E. Gaucher disease: mutation and polymorphism spectrum in the glucocerebrosidase gene (GBA). *Hum Mutat* 2008; **29**: 567–83.

107 Schrag A, Horsfall L, Walters K, Noyce A, Petersen I. Prediagnostic presentations of Parkinson's disease in primary care: a case-control study. *Lancet Neurol* 2015; **14**: 57–64.

108 Wolters EC, Braak H. Parkinson's disease: premotor clinico-pathological correlations. *J Neural Transm Suppl* 2006; : 309–19.

109 Siderowf A, Lang AE. Premotor Parkinson's disease: concepts and definitions. *Movement Disorders* 2012; **27**: 608–16.

110 Siderowf A, Jennings D, Eberly S, *et al.* Impaired olfaction and other prodromal features in the Parkinson At-Risk Syndrome Study. *Movement Disorders* 2012; **27**: 406–12.

111 McNeill A, Duran R, Proukakis C, *et al.* Hyposmia and cognitive impairment in Gaucher disease patients and carriers. *Movement Disorders* 2012; **27**: 526–32.

112 Beavan M, McNeill A, Proukakis C, Hughes DA, Mehta A, Schapira AHV. Evolution of Prodromal Clinical Markers of Parkinson Disease in a GBA Mutation-Positive Cohort. *JAMA Neurol* 2014; published online Dec 15. DOI:10.1001/jamaneurol.2014.2950.

113 Gan-Or Z, Mirelman A, Postuma RB, *et al.* GBA mutations are associated with Rapid Eye Movement Sleep Behavior Disorder. *Ann Clin Transl Neurol* 2015; **2**: 941–5.

114 Kohn DB, Nolta JA, Weinthal J, *et al.* Toward gene therapy for Gaucher disease. *Hum Gene Ther* 1991; **2**: 101–5.

115 Brennan PJ, Tatituri RVV, Brigl M, *et al.* Invariant natural killer T cells recognize lipid self antigen induced by microbial danger signals. *Nat Immunol* 2011; **12**: 1202–11.

116 Fink JK, Correll PH, Perry LK, Brady RO, Karlsson S. Correction of glucocerebrosidase deficiency after retroviral-mediated gene transfer into hematopoietic progenitor cells from patients with Gaucher disease. *Proc Natl Acad Sci USA* 1990; **87**: 2334–8.

117 Dunbar CE, Kohn DB, Schiffmann R, *et al.* Retroviral Transfer of the Glucocerebrosidase Gene into CD34+ Cells from Patients with Gaucher Disease: In Vivo Detection of Transduced Cells without Myeloablation. *Hum Gene Ther* 2004; **9**: 2629–40.

118 Cucchiarini M. Human gene therapy: novel approaches to improve the current gene delivery systems. *Discov Med* 2016; **21**: 495–506.

119 Dahl M, Doyle A, Olsson K, *et al.* Lentiviral Gene Therapy Using Cellular Promoters Cures Type 1 Gaucher Disease in Mice. *Molecular Therapy* 2015; **23**: 835–44.

120 Weinreb NJ, Charrow J, Andersson HC, *et al.* Effectiveness of enzyme replacement therapy in 1028 patients with type 1 Gaucher disease after 2 to 5 years of treatment: a report from the Gaucher Registry. *The American Journal of Medicine* 2002; **113**: 112–9.

121 The clinical effectiveness and cost-effectiveness of enzyme replacement therapy for Gaucher's disease: a systematic review. *Clinical Governance: An International Journal* 2007; **12**: cgij.2007.24812cae.008.

122 Begley D. The Significance of the Blood-Brain Barrier for Gaucher Disease and Other Lysosomal Storage Diseases. In: Gaucher Disease. CRC Press, 2009: 397–421.

123 Brady RO, Yang C, Zhuang Z. An innovative approach to the treatment of Gaucher disease and possibly other metabolic disorders of the brain. *J Inherit Metab Dis* 2013; **36**: 451–4.

124 Nag S. Pathophysiology of Blood–Brain Barrier Breakdown. In: Blood-Brain Barrier. New Jersey: Humana Press, 2003: 97–120.

125 LeBowitz J. A breach in the blood–brain barrier. *Proceedings of the National Academy of Sciences* 2005; **102**: 14485–6.

126 Shire, editor. Study of Intrathecal Idursulfase-IT Administered in Conjunction With Elaprase® in Pediatric Patients With Hunter Syndrome and Early Cognitive Impairment (AIM-IT) . https://clinicaltrials.gov/ct2/show/NCT02055118 (accessed March 22, 2017).

127 Cox TM, Amato D, Hollak CE, *et al.* Evaluation of miglustat as maintenance therapy after enzyme therapy in adults with stable type 1 Gaucher disease: a prospective, open-label non-inferiority study. *Orphanet J Rare Dis* 2012; **7**: 102.

128 Serratrice C, Swiader L, Serratrice J. Switching from imiglucerase to miglustat for the treatment of French patients with Gaucher disease type 1: a case series. *J Med Case Rep* 2015; **9**: 146.

129 Schiffmann R, Fitzgibbon EJ, Harris C, *et al.* Randomized, controlled trial of miglustat in Gaucher's disease type 3. *Ann Neurol* 2008; **64**: 514–22.

130 ENGAGE Randomized Clinical Trial Evaluating Cerdelga® (eliglustat) for Treatment-Naïve Patients with Gaucher Disease Type 1 Published in The Journal of the American Medical Association. Sanofi http://news.genzyme.com/press-release/engage-randomized-clinical-trial-evaluating-cerdelga-eliglustat-treatment-naive-patien (accessed March 22, 2017).

131 Sanofi. A Global Study to Assess the Drug Dynamics, Efficacy, and Safety of GZ/SAR402671 in Parkinson's Disease Patients Carrying a Glucocerebrosidase (GBA) Gene Mutation (MOVES-PD). https://clinicaltrials.gov/ct2/show/NCT02906020.

132 Bendikov-Bar I, Maor G, Filocamo M, Horowitz M. Ambroxol as a pharmacological chaperone for mutant glucocerebrosidase. *Blood Cells Mol Dis* 2013; **50**: 141–5.

133 Maegawa GHB, Tropak MB, Buttner JD, *et al.* Identification and characterization of ambroxol as an enzyme enhancement agent for Gaucher disease. *J Biol Chem* 2009; **284**: 23502–16.

134 Luan Z, Li L, Higaki K, Nanba E, Suzuki Y, Ohno K. The chaperone activity and toxicity of ambroxol on Gaucher cells and normal mice. *Brain Dev* 2013; **35**: 317–22.

135 Jung O, Patnaik S, Marugan J, Sidransky E, Westbroek W. Progress and potential of non-inhibitory small molecule chaperones for the treatment of Gaucher disease and its implications for Parkinson disease. *Expert Rev Proteomics* 2016; **13**: 471–9.

136 Yang C, Rahimpour S, Lu J, *et al.* Histone deacetylase inhibitors increase glucocerebrosidase activity in Gaucher disease by modulation of molecular chaperones. *Proc Natl Acad Sci USA* 2013; **110**: 966–71.

137 Cuervo AM, Wong E. Chaperone-mediated autophagy: roles in disease and aging. *Cell Res* 2014; **24**: 92–104.

138 Clarke GM, Anderson CA, Pettersson FH, Cardon LR, Morris AP, Zondervan KT. Basic statistical analysis in genetic case-control studies. *Nature Protocols* 2011; **6**: 121–33.

139 Arkadir D, Dinur T, Mullin S, *et al.* Trio approach reveals higher risk of PD in carriers of severe vs. mild GBA mutations. *Blood Cells Mol Dis* 2016; published online Nov 12. DOI:10.1016/j.bcmd.2016.11.007.

140 Zhang X, Bao Q-Q, Zhuang X-S, *et al.* Association of Common Variants in the Glucocerebrosidase Gene with High Susceptibility to Parkinson's Disease among Chinese. *Chin J Physiol* 2012; **55**: 398–404.

141 Chen J, Li W, Zhang T, Wang Y-J, Jiang X-J, Xu Z-Q. Glucocerebrosidase gene mutations associated with Parkinson's disease: a meta-analysis in a Chinese population. *PLoS ONE* 2014; **9**: e115747.

142 Day NE, Byar DP. Testing Hypotheses in Case-Control Studies-Equivalence of Mantel-Haenszel Statistics and Logit Score Tests. *Biometrics* 1979; **35**: 623.

143 Paul SR, Donner A. A comparison of tests of homogeneity of odds ratios in K 2 x 2 tables. *Stat Med* 1989; **8**: 1455–68.

144 Begg CB, Mazumdar M. Operating characteristics of a rank correlation test for publication bias. *Biometrics* 1994; **50**: 1088–101.

145 Lek M, Karczewski KJ, Minikel EV, *et al.* Analysis of protein-coding genetic variation in 60,706 humans. *Nature* 2016; **536**: 285–91.

146 GBA entry - ExAC database. http://exac.broadinstitute.org/gene/ENSG00000177628 (accessed Nov 27, 2016).

147 Ma C, Blackwell T, Boehnke M, Scott LJ, GoT2D investigators. Recommended joint and meta-analysis strategies for case-control association testing of single low-count variants. *Genet Epidemiol* 2013; **37**: 539–50.

148 Holm S. A Simple Sequentially Rejective Multiple Test Procedure. *scandanavian journal of statistics* 1979; : 65–70.

149 Diaz GA, Gelb BD, Risch N, *et al.* Gaucher disease: the origins of the Ashkenazi Jewish N370S and 84GG acid beta-glucosidase mutations. *Am J Hum Genet* 2000; **66**: 1821–32.

150 Beutler E, Gelbart T, Balicki D, *et al.* Gaucher disease: four families with previously undescribed mutations. *Proc Assoc Am Physicians* 1996; **108**: 179–84.

151 Zimran A, Horowitz M. RecTL: a complex allele of the glucocerebrosidase

gene associated with a mild clinical course of Gaucher disease. *Am J Med Genet* 1994; **50**: 74–8.

152 Premkumar L, Futerman A, Silman I, Sussman J. The X-Ray Structure of Human Acid-beta-Glucosidase. In: Gaucher Disease. CRC Press, 2009: 85–96.

153 Dvir H, Harel M, McCarthy AA, *et al.* X-ray structure of human acid-β-glucosidase, the defective enzyme in Gaucher disease. *EMBO reports* 2003; **4**: 704–9.

154 Wei RR, Hughes H, Boucher S, *et al.* X-ray and Biochemical Analysis of N370S Mutant Human Acid ?-Glucosidase. *J Biol Chem* 2010; **286**: 299–308.

155 Steet RA, Chung S, Wustman B, Powe A, Do H, Kornfeld SA. The iminosugar isofagomine increases the activity of N370S mutant acid beta-glucosidase in Gaucher fibroblasts by several mechanisms. *Proc Natl Acad Sci USA* 2006; **103**: 13813–8.

156 Offman MN, Krol M, Silman I, Sussman JL, Futerman AH. Molecular basis of reduced glucosylceramidase activity in the most common Gaucher disease mutant, N370S. *Journal of Biological Chemistry* 2010; **285**: 42105–14.

157 Liou B, Kazimierczuk A, Zhang M, Scott CR, Hegde RS, Grabowski GA. Analyses of variant acid beta-glucosidases: effects of Gaucher disease mutations. *J Biol Chem* 2006; **281**: 4242–53.

158 Lieberman RL, Wustman BA, Huertas P, *et al.* Structure of acid beta-glucosidase with pharmacological chaperone provides insight into Gaucher disease. *Nat Chem Biol* 2007; **3**: 101–7.

159 Schrag A, Ben-Shlomo Y, Quinn NP. Cross sectional prevalence survey of idiopathic Parkinson's disease and Parkinsonism in London. *BMJ* 2000; **321**: 21–2.

160 Chen H, Zhao EJ, Zhang W, *et al.* Meta-analyses on prevalence of selected Parkinson's nonmotor symptoms before and after diagnosis. *Transl Neurodegener* 2015; **4**: 1.

161 Zhang J, Xu C-Y, Liu J. Meta-analysis on the prevalence of REM sleep behavior disorder symptoms in Parkinson's disease. *BMC Neurol* 2017; **17**: 23.

162 Braak H, Tredici KD, Rüb U, de Vos RAI, Jansen Steur ENH, Braak E. Staging of brain pathology related to sporadic Parkinson’s disease. *Neurobiol Aging* 2003; **24**: 197–211.

163 Boeve BF, Silber MH, Saper CB, *et al.* Pathophysiology of REM sleep

behaviour disorder and relevance to neurodegenerative disease. *Brain* 2007; **130**: 2770–88.

164 Pare P, Ferrazzi S, Thompson WG, Irvine EJ, Rance L. An epidemiological survey of constipation in canada: definitions, rates, demographics, and predictors of health care seeking. *Am J Gastroenterol* 2001; **96**: 3130–7.

165 Mullol J, Alobid I, Mariño-Sánchez F, *et al.* Furthering the understanding of olfaction, prevalence of loss of smell and risk factors: a population-based survey (OLFACAT study). *BMJ Open* 2012; **2**. DOI:10.1136/bmjopen-2012-001256.

166 Roberts R, Knopman DS. Classification and epidemiology of MCI. *Clin Geriatr Med* 2013; **29**: 753–72.

167 Bandelow B, Michaelis S. Epidemiology of anxiety disorders in the 21st century. *Dialogues Clin Neurosci* 2015; **17**: 327–35.

168 Lam SP, Zhang J, Wing Y-K. REM sleep behavior disorder: from epidemiology to heterogeneity. *Sleep* 2013; **36**: 1117–9.

169 Muirhead N, Auerbach E, Saleh H. Is The University Of Pennsylvania Smell Identification Test (UPSIT) Valid for the UK Population? *The Otorhinolaryngologist* 2013; **2**: 99–103.

170 Hoops S, Nazem S, Siderowf AD, *et al.* Validity of the MoCA and MMSE in the detection of MCI and dementia in Parkinson disease. *Neurology* 2009; **73**: 1738–45.

171 Leentjens AF, Verhey FR, Luijckx GJ, Troost J. The validity of the Beck Depression Inventory as a screening and diagnostic instrument for depression in patients with Parkinson's disease. *Movement Disorders* 2000; **15**: 1221–4.

172 Nomura T, Inoue Y, Kagimura T, Uemura Y, Nakashima K. Utility of the REM sleep behavior disorder screening questionnaire (RBDSQ) in Parkinson's disease patients. *Sleep Med* 2011; **12**: 711–3.

173 Wenning GK, Tison F, Seppi K, *et al.* Development and validation of the Unified Multiple System Atrophy Rating Scale (UMSARS). *Movement Disorders* 2004; **19**: 1391–402.

174 Azur MJ, Stuart EA, Frangakis C, Leaf PJ. Multiple imputation by chained equations: what is it and how does it work? *Int J Methods Psychiatr Res* 2011; **20**: 40–9.

175 Lesage S, Anheim M, Condroyer C, *et al.* Large-scale screening of the Gaucher‘s disease-related glucocerebrosidase gene in Europeans with Parkinson’s disease. *Hum Mol Genet* 2011; **20**: 202–10.

176 Biegstraaten M, Mengel E, Marodi L, *et al.* Peripheral neuropathy in adult type 1 Gaucher disease: a 2-year prospective observational study. *Brain* 2010; **133**: 2909–19.

177 Rucker J. Neural Control and Clinical Disorders of Supranuclear Eye Movements. *Advances in clinical neuroscience and rehabilitation* 2012; **12**: 1–3.

178 Dickson DW, Rademakers R, Hutton ML. Progressive supranuclear palsy: pathology and genetics. *Brain Pathol* 2007; **17**: 74–82.

179 Erikson A. Gaucher disease--Norrbottnian type (III). Neuropaediatric and neurobiological aspects of clinical patterns and treatment. *Acta Paediatr Scand Suppl* 1986; **326**: 1–42.

180 Conradi NG, Sourander P, Nilsson O, Svennerholm L, Erikson A. Neuropathology of the Norrbottnian type of Gaucher disease. Morphological and biochemical studies. *Acta Neuropathol* 1984; **65**: 99–109.

181 Noyce AJ, Bestwick JP, Silveira-Moriyama L, *et al.* PREDICT-PD: identifying risk of Parkinson's disease in the community: methods and baseline results. *Journal of Neurology, Neurosurgery & Psychiatry* 2014; **85**: 31–7.

182 Noyce AJ, Schrag A, Masters JM, Bestwick JP, Giovannoni G, Lees AJ. Subtle motor disturbances in PREDICT-PD participants. *Journal of Neurology, Neurosurgery & Psychiatry* 2017; **88**: 212–7.

183 Noyce AJ, Nagy A, Acharya S, *et al.* Bradykinesia-akinesia incoordination test: validating an online keyboard test of upper limb function. *PLoS ONE* 2014; **9**: e96260.

184 Wesnes KA, McKeith IG, Ferrara R, *et al.* Effects of rivastigmine on cognitive function in dementia with lewy bodies: a randomised placebo-controlled international study using the cognitive drug research computerised assessment system. *Dement Geriatr Cogn Disord* 2002; **13**: 183–92.

185 Schrag A, Barone P, Brown RG, *et al.* Depression rating scales in Parkinson's disease: critique and recommendations. Movement Disorders. 2007; **22**: 1077–92.

186 Biegstraaten M, Wesnes KA, Luzy C, *et al.* The cognitive profile of type 1 Gaucher disease patients. *J Inherit Metab Dis* 2012; **35**: 1093–9.

187 Weil RS, Schrag AE, Warren JD, Crutch SJ, Lees AJ, Morris HR. Visual dysfunction in Parkinson’s disease. *Brain* 2016; **139**: 2827–43.

188 Suwijn SR, van Boheemen CJ, de Haan RJ, Tissingh G, Booij J, de Bie

RM. The diagnostic accuracy of dopamine transporter SPECT imaging to detect nigrostriatal cell loss in patients with Parkinson?s disease or clinically uncertain parkinsonism: a systematic review. *EJNMMI Res* 2015; **5**: 10.

189 Kollack-Walker S, Liu CY, Fleisher AS. The Role of Neuroimaging in the Assessment of the Cognitively Impaired Elderly. *Neurologic Clinics* 2017; **35**: 231–62.

190 Kraoua I, Stirnemann J, Ribeiro MJ, *et al.* Parkinsonism in Gaucher's disease type 1: ten new cases and a review of the literature. *Movement Disorders* 2009; **24**: 1524–30.

191 Goker-Alpan O, Masdeu JC, Kohn PD, *et al.* The neurobiology of glucocerebrosidase-associated parkinsonism: a positron emission tomography study of dopamine synthesis and regional cerebral blood flow. *Brain* 2012; **135**: 2440–8.

192 Kono S, Ouchi Y, Terada T, Ida H, Suzuki M, Miyajima H. Functional brain imaging in glucocerebrosidase mutation carriers with and without parkinsonism. *Movement Disorders* 2010; **25**: 1823–9.

193 Sunwoo M-K, Kim S-M, Lee S, Lee PH. Parkinsonism associated with glucocerebrosidase mutation. *J Clin Neurol* 2011; **7**: 99–101.

194 McNeill A, Wu R-M, Tzen K-Y, *et al.* Dopaminergic neuronal imaging in genetic Parkinson's disease: insights into pathogenesis. *PLoS ONE* 2013; **8**: e69190.

195 McGeer PL, Itagaki S, Boyes BE, McGeer EG. Reactive microglia are positive for HLA-DR in the substantia nigra of Parkinson‘s and Alzheimer’s disease brains. *Neurology* 1988; **38**: 1285–5.

196 Imamura K, Hishikawa N, Sawada M, Nagatsu T, Yoshida M, Hashizume Y. Distribution of major histocompatibility complex class II-positive microglia and cytokine profile of Parkinson's disease brains. *Acta Neuropathol* 2003; **106**: 518–26.

197 Hirsch EC, Hunot S. Neuroinflammation in Parkinson's disease: a target for neuroprotection? *The Lancet Neurology* 2009; **8**: 382–97.

198 Banati RB. Visualising microglial activation in vivo. *Glia* 2002; **40**: 206–17.

199 Chen H, Zhang SM, Hernán MA, *et al.* Nonsteroidal anti-inflammatory drugs and the risk of Parkinson disease. *Arch Neurol* 2003; **60**: 1059–64.

200 Chen H, Jacobs E, Schwarzschild MA, *et al.* Nonsteroidal antiinflammatory drug use and the risk for Parkinson's disease. *Ann Neurol* 2005; **58**: 963–7.

201 Hernán MA, Logroscino G, García Rodríguez LA. Nonsteroidal anti-inflammatory drugs and the incidence of Parkinson disease. *Neurology* 2006; **66**: 1097–9.

202 Krüger R, Hardt C, Tschentscher F, *et al.* Genetic analysis of immunomodulating factors in sporadic Parkinson's disease. *J Neural Transm (Vienna)* 2000; **107**: 553–62.

203 Wu Y-R, Feng I-H, Lyu R-K, *et al.* Tumor necrosis factor-alpha promoter polymorphism is associated with the risk of Parkinson's disease. *Am J Med Genet B Neuropsychiatr Genet* 2007; **144B**: 300–4.

204 Rentzos M, Nikolaou C, Andreadou E, *et al.* Circulating interleukin-10 and interleukin-12 in Parkinson's disease. *Acta Neurol Scand* 2009; **119**: 332–7.

205 Scalzo P, Kümmer A, Cardoso F, Teixeira AL. Serum levels of interleukin-6 are elevated in patients with Parkinson's disease and correlate with physical performance. *Neurosci Lett* 2010; **468**: 56–8.

206 Dobbs RJ, Charlett A, Purkiss AG, Dobbs SM, Weller C, Peterson DW. Association of circulating TNF-alpha and IL-6 with ageing and parkinsonism. *Acta Neurol Scand* 1999; **100**: 34–41.

207 Tantawy AAG. Cytokines in Gaucher disease: Role in the pathogenesis of bone and pulmonary disease. *Egyptian Journal of Medical Human Genetics* 2015; **16**: 207–13.

208 Mucci JM, Rozenfeld P. Pathogenesis of Bone Alterations in Gaucher Disease: The Role of Immune System. *J Immunol Res* 2015; **2015**: 192761.

209 Pandey MK, Grabowski GA. Immunological cells and functions in Gaucher disease. *Crit Rev Oncog* 2013; **18**: 197–220.

210 Arends M, van Dussen L, Biegstraaten M, Hollak CEM. Malignancies and monoclonal gammopathy in Gaucher disease; a systematic review of the literature. *Br J Haematol* 2013; **161**: 832–42.

211 Wong K, Sidransky E, Verma A, *et al.* Neuropathology provides clues to the pathophysiology of Gaucher disease. *Mol Genet Metab* 2004; **82**: 192–207.

212 Mistry PK, Liu J, Yang M, *et al.* Glucocerebrosidase gene-deficient mouse recapitulates Gaucher disease displaying cellular and molecular dysregulation beyond the macrophage. *Proceedings of the National Academy of Sciences* 2010; **107**: 19473–8.

213 Allen MJ, Myer BJ, Khokher AM, Rushton N, Cox TM. Pro-inflammatory cytokines and the pathogenesis of Gaucher's disease: increased release

of interleukin-6 and interleukin-10. *QJM* 1997; **90**: 19–25.

214 Cagnin A. In vivo visualization of activated glia by[11C] (R)-PK11195-PET following herpes encephalitis reveals projected neuronal damage beyond the primary focal lesion. *Brain* 2001; **124**: 2014–27.

215 Pappata S, Levasseur M, Gunn RN, *et al.* Thalamic microglial activation in ischemic stroke detected in vivo by PET and [11C]PK1195. *Neurology* 2000; **55**: 1052–4.

216 Gerhard A, Pavese N, Hotton G, *et al.* In vivo imaging of microglial activation with [11C](R)-PK11195 PET in idiopathic Parkinson's disease. *Neurobiol Dis* 2006; **21**: 404–12.

217 Martinez-Martin P, Chaudhuri KR, Rojo-Abuin JM, *et al.* Assessing the non-motor symptoms of Parkinson's disease: MDS-UPDRS and NMS Scale. *Eur J Neurol* 2015; **22**: 37–43.

218 Chaudhuri KR, Martinez-Martin P, Schapira AHV, *et al.* International multicenter pilot study of the first comprehensive self-completed nonmotor symptoms questionnaire for Parkinson's disease: the NMSQuest study. *Movement Disorders* 2006; **21**: 916–23.

219 Parbo P, Ismail R, Hansen KV, *et al.* Brain inflammation accompanies amyloid in the majority of mild cognitive impairment cases due to Alzheimer's disease. *Brain* 2017; **140**: 2002–11.

220 Surmeier DJ, Obeso JA, Halliday GM. Selective neuronal vulnerability in Parkinson disease. *Nat Rev Neurosci* 2017; **18**: 101–13.

221 Brichta L, Greengard P. Molecular determinants of selective dopaminergic vulnerability in Parkinson's disease: an update. *Front Neuroanat* 2014; **8**: 494.

222 Ponsen MM, Stoffers D, Twisk JWR, Wolters EC, Berendse HW. Hyposmia and executive dysfunction as predictors of future Parkinson's disease: a prospective study. *Movement Disorders* 2009; **24**: 1060–5.

223 Xiao Q, Chen S, Le W. Hyposmia: a possible biomarker of Parkinson's disease. *Neurosci Bull* 2014; **30**: 134–40.

224 Ikemoto S. Dopamine reward circuitry: two projection systems from the ventral midbrain to the nucleus accumbens-olfactory tubercle complex. *Brain Res Rev* 2007; **56**: 27–78.

225 Wile DJ, Agarwal PA, Schulzer M, *et al.* Serotonin and dopamine transporter PET changes in the premotor phase of LRRK2 parkinsonism: cross-sectional studies. *The Lancet Neurology* 2017; **16**: 351–9.

226 A randomized controlled trial comparing pramipexole with levodopa in

early Parkinson's disease: design and methods of the CALM-PD Study. Parkinson Study Group. *Clin Neuropharmacol* 2000; **23**: 34–44.

227 Whone AL, Watts RL, Stoessl AJ, *et al.* Slower progression of Parkinson's disease with ropinirole versus levodopa: The REAL-PET study. *Ann Neurol* 2003; **54**: 93–101.

228 Fahn S, Parkinson Study Group. Does levodopa slow or hasten the rate of progression of Parkinson's disease? *J Neurol* 2005; **252 Suppl 4**: IV37–IV42.

229 Miller DW, Hague SM, Clarimon J, *et al.* Alpha-synuclein in blood and brain from familial Parkinson disease with SNCA locus triplication. *Neurology* 2004; **62**: 1835–8.

230 El-Agnaf OMA, Salem SA, Paleologou KE, *et al.* Alpha-synuclein implicated in Parkinson's disease is present in extracellular biological fluids, including human plasma. *The FASEB Journal* 2003; **17**: 1945–7.

231 Yanamandra K, Gruden MA, Casaite V, Meskys R, Forsgren L, Morozova-Roche LA. α-Synuclein Reactive Antibodies as Diagnostic Biomarkers in Blood Sera of Parkinson's Disease Patients. *PLoS ONE* 2011; **6**: e18513.

232 Foulds PG, Diggle P, Mitchell JD, *et al.* A longitudinal study on α-synuclein in blood plasma as a biomarker for Parkinson's disease. *Sci Rep* 2013; **3**: 2540.

233 Marques O, Outeiro TF. Alpha-synuclein: from secretion to dysfunction and death. *Cell Death Dis* 2012; **3**: e350–7.

234 Emmanouilidou E, Melachroinou K, Roumeliotis T, *et al.* Cell-Produced - Synuclein Is Secreted in a Calcium-Dependent Manner by Exosomes and Impacts Neuronal Survival. *Journal of Neuroscience* 2010; **30**: 6838–51.

235 Lee H-J, Suk J-E, Bae E-J, Lee J-H, Paik SR, Lee S-J. Assembly-dependent endocytosis and clearance of extracellular alpha-synuclein. *Int J Biochem Cell Biol* 2008; **40**: 1835–49.

236 Jang A, Lee H-J, Suk J-E, Jung J-W, Kim KP, Lee S-J. Non-classical exocytosis of alpha-synuclein is sensitive to folding states and promoted under stress conditions. *J Neurochem* 2010; **113**: 1263–74.

237 Bae E-J, Yang N-Y, Song M, *et al.* Glucocerebrosidase depletion enhances cell-to-cell transmission of α-synuclein. *Nat Commun* 2014; **5**: 4755.

238 Avila Jl, Convit J, Velazquez-Avila G. Fabry's disease: normal ?-galactosidase activity and urinary-sediment glycosphingolipid levels in two obligate heterozygotes. *British Journal of Dermatology* 2006; **89**:

149–57.

239 Chatterjee S, Gupta P, Pyeritz RE, Kwiterovich PO Jr. Immunohistochemical Localization of Giycosphingolipid in Urinary Renal Tubular Cells in Fabry?s Disease. *American Journal of Clinical Pathology* 1984; **82**: 24–8.

240 Ritter MM, Geiss HC, Richter WO, Schwandt P. Lipoprotein(a) is increased in patients with familial hypercholesterolemia. *Atherosclerosis* 1995; **115**: S91.

241 Manwaring V, Heywood WE, Clayton R, *et al.* The identification of new biomarkers for identifying and monitoring kidney disease and their translation into a rapid mass spectrometry-based test: evidence of presymptomatic kidney disease in pediatric Fabry and type-I diabetic patients. *J Proteome Res* 2013; **12**: 2013–21.

242 Bennett K, Callard R, Heywood W, *et al.* New role for LEKTI in skin barrier formation: label-free quantitative proteomic identification of caspase 14 as a novel target for the protease inhibitor LEKTI. *J Proteome Res* 2010; **9**: 4289–94.

243 Zhao H, Peddada SD, Cui X. Mixed directional false discovery rate control in multiple pairwise comparisons using weighted p-values. *Biom J* 2015; **57**: 144–58.

244 Cox TM, Rosenbloom BE, Barker RA. Gaucher disease and comorbidities: B-cell malignancy and parkinsonism. *Am J Hematol* 2015; 90 Suppl 1: S25–8.

245 St-Amour I, Paré I, Alata W, *et al.* Brain Bioavailability of Human Intravenous Immunoglobulin and its Transport through the Murine Blood–Brain Barrier. *Journal of Cerebral Blood Flow & Metabolism* 2013; **33**: 1983–92.

246 Bard F, Cannon C. Peripherally administered antibodies against amyloid β-peptide enter the central nervous system and reduce pathology in a mouse model of Alzheimer disease . *Nat Med* 2000; **6**: 1–4.

247 Gilman S, Koller M, Black RS, *et al.* Clinical effects of Abeta immunization (AN1792) in patients with AD in an interrupted trial. *Neurology* 2005; **64**: 1553–62.

248 Lehrer R, Lichtenstein A, Ganz T. DEFENSINS: Antimicrobial and Cytotoxic Peptides of Mammalian Cells. *Annual Review Immunology* 1993; : 105–28.

249 Braak H, Sastre M, Del Tredici K. Development of alpha-synuclein immunoreactive astrocytes in the forebrain parallels stages of intraneuronal pathology in sporadic Parkinson's disease. *Acta*

Neuropathol 2007; **114**: 231–41.

250 Stokholm MG, Danielsen EH, Hamilton-Dutoit SJ, Borghammer P. Pathological alpha-synuclein in gastrointestinal tissues from prodromal parkinson's disease patients. *Ann Neurol* 2016; published online March 26. DOI:10.1002/ana.24648.

251 Hilton D, Stephens M, Kirk L, *et al.* Accumulation of α-synuclein in the bowel of patients in the pre-clinical phase of Parkinson's disease. *Acta Neuropathol* 2013; **127**: 235–41.

252 Devos D, Lebouvier T, Lardeux B, *et al.* Colonic inflammation in Parkinson's disease. *Neurobiol Dis* 2013; **50**: 42–8.

253 Xu M-Q, Cao H-L, Wang W-Q, *et al.* Fecal microbiota transplantation broadening its application beyond intestinal disorders. *World J Gastroenterol* 2015; **21**: 102–11.

254 Sindic A. Current Understanding of Guanylin Peptides Actions. *International Scholarly Research Notices* 2013; **2013**: 1–17.

255 Xu J, Kao S-Y, Lee FJS, Song W, Jin L-W, Yankner BA. Dopamine-dependent neurotoxicity of alpha-synuclein: a mechanism for selective neurodegeneration in Parkinson disease. *Nat Med* 2002; **8**: 600–6.

256 McCarthy A, McKinley J, Lynch T. The inherent susceptibility of dorsal motor nucleus cholinergic neurons to the neurodegenerative process in Parkinson's Disease. *Front Neurol* 2012; **3**: 189.

257 Matzuk MM, Saper CB. Preservation of hypothalamic dopaminergic neurons in Parkinson's disease. *Ann Neurol* 1985; **18**: 552–5.

258 Damier P, Hirsch EC, Agid Y, Graybiel AM. The substantia nigra of the human brain. II. Patterns of loss of dopamine-containing neurons in Parkinson's disease. *Brain* 1999; **122 (Pt 8)**: 1437–48.

259 Puopolo M, Raviola E, Bean BP. Roles of subthreshold calcium current and sodium current in spontaneous firing of mouse midbrain dopamine neurons. 2007; **27**: 645–56.

260 Guzman JN, Sánchez-Padilla J, Chan CS, Surmeier DJ. Robust pacemaking in substantia nigra dopaminergic neurons. 2009; **29**: 11011–9.

261 Brini M, Calì T, Ottolini D, Carafoli E. Neuronal calcium signaling: function and dysfunction. *Cell Mol Life Sci* 2014; published online Jan 19. DOI:10.1007/s00018-013-1550-7.

262 Islam MS. Calcium signaling in the islets. *Adv Exp Med Biol* 2010; **654**: 235–59.

263 Hay JC. Calcium: a fundamental regulator of intracellular membrane fusion? *EMBO reports* 2007; **8**: 236–40.

264 Whitaker M. Calcium at fertilization and in early development. *Physiol Rev* 2006; **86**: 25–88.

265 Berridge MJ, Lipp P, Bootman MD. The versatility and universality of calcium signalling. *Nat Rev Mol Cell Biol* 2000; **1**: 11–21.

266 Bootman MD, Collins TJ, Peppiatt CM, *et al.* Calcium signalling--an overview. *Semin Cell Dev Biol* 2001; **12**: 3–10.

267 Rizzuto R, De Stefani D, Raffaello A, Mammucari C. Mitochondria as sensors and regulators of calcium signalling. *Nat Rev Mol Cell Biol* 2012; **13**: 566–78.

268 Mullin S, Schapira A. α-Synuclein and mitochondrial dysfunction in Parkinson's disease. *Mol Neurobiol* 2013; **47**: 587–97.

269 Ascherio A, Tanner CM. Use of antihypertensives and the risk of Parkinson disease. *Neurology* 2009; **72**: 578–9.

270 Ritz B, Rhodes SL, Qian L, Schernhammer E, Olsen JH, Friis S. L-type calcium channel blockers and Parkinson disease in Denmark. *Ann Neurol* 2010; **67**: 600–6.

271 Hockey LN, Kilpatrick BS, Eden ER, *et al.* Dysregulation of lysosomal morphology by pathogenic LRRK2 is corrected by two-pore channel 2 inhibition. *J Cell Sci* 2014; published online Nov 21. DOI:10.1242/jcs.164152.

272 Kilpatrick BS, Magalhaes J, Beavan MS, *et al.* Endoplasmic reticulum and lysosomal Ca(2+) stores are remodelled in GBA1-linked Parkinson disease patient fibroblasts. *Cell Calcium* 2016; **59**: 12–20.

273 Schöndorf DC, Aureli M, McAllister FE, *et al.* iPSC-derived neurons from GBA1-associated Parkinson's disease patients show autophagic defects and impaired calcium homeostasis. *Nat Commun* 2014; **5**: 4028.

274 Horowitz M, Pasmanik-Chor M, Borochowitz Z, *et al.* Prevalence of glucocerebrosidase mutations in the Israeli Ashkenazi Jewish population. *Hum Mutat* 1998; **12**: 240–4.

275 McPherson PS, Kim YK, Valdivia H, *et al.* The brain ryanodine receptor: a caffeine-sensitive calcium release channel. *Neuron* 1991; **7**: 17–25.

276 Osellame LD, Rahim AA, Hargreaves IP, *et al.* Mitochondria and quality control defects in a mouse model of Gaucher disease--links to Parkinson's disease. *Cell Metab* 2013; **17**: 941–53.

277 Scaduto RC, Grotyohann LW. Measurement of mitochondrial membrane potential using fluorescent rhodamine derivatives. *Biophys J* 1999; **76**: 469–77.

278 Kilpatrick BS, Eden ER, Schapira AH, Futter CE, Patel S. Direct mobilisation of lysosomal Ca2+ triggers complex Ca2+ signals. *J Cell Sci* 2013; **126**: 60–6.

279 Hettiarachchi NT, Parker A, Dallas ML, *et al.* alpha-Synuclein modulation of Ca2+ signaling in human neuroblastoma (SH-SY5Y) cells. *J Neurochem* 2009; **111**: 1192–201.

280 Adamczyk A, Strosznajder JB. Alpha-synuclein potentiates Ca2+ influx through voltage-dependent Ca2+ channels. *NeuroReport* 2006; **17**: 1883–6.

281 Cullen V, Sardi SP, Ng J, *et al.* Acid β-glucosidase mutants linked to Gaucher disease, Parkinson disease, and Lewy body dementia alter α-synuclein processing. *Ann Neurol* 2011; **69**: 940–53.

282 Vaccaro A, Salvioli R, Tatti M, Ciaffoni F. Saposins and Their Interaction with Lipids*. *Neurochem Res* 1998; : 1–8.

283 Tamargo RJ, Velayati A, Goldin E, Sidransky E. The role of saposin C in Gaucher disease. *Mol Genet Metab* 2012; **106**: 257–63.

284 Christomanou H, Chabás A, Pámpols T, Guardiola A. Activator protein deficient Gaucher's disease. *Klin Wochenschr* 1989; **67**: 999–1003.

285 McNeill A, Duran R, Hughes DA, Mehta A, Schapira AHV. A clinical and family history study of Parkinson's disease in heterozygous glucocerebrosidase mutation carriers. *Journal of Neurology, Neurosurgery & Psychiatry* 2012; **83**: 853–4.

286 Migdalska-Richards A, Daly L, Bezard E, Schapira AHV. Ambroxol effects in glucocerebrosidase and α-synuclein transgenic mice. *Ann Neurol* 2016; **80**: 766–75.

287 Choubey V, Safiulina D, Vaarmann A, *et al.* Mutant A53T alpha-synuclein induces neuronal death by increasing mitochondrial autophagy. *J Biol Chem* 2011; **286**: 10814–24.

288 Rajawat YS, Hilioti Z, Bossis I. Aging: Central role for autophagy and the lysosomal degradative system. *Ageing Res Rev* 2009; **8**: 199–213.

289 Lashuel HA, Overk CR, Oueslati A, Masliah E. The many faces of α-synuclein: from structure and toxicity to therapeutic target. *Nat Rev Neurosci* 2012; **14**: 38–48.

290 Gonzalez A, Valeiras M, Sidransky E, Tayebi N. Lysosomal integral

membrane protein-2: A new player in lysosome-related pathology. *Mol Genet Metab* 2014; **111**: 84–91.

291 Sun Y, Liou B, Xu YH, *et al.* Ex Vivo and in Vivo Effects of Isofagomine on Acid ?-Glucosidase Variants and Substrate Levels in Gaucher Disease. *J Biol Chem* 2012; **287**: 4275–87.

292 Khanna R, Benjamin ER, Pellegrino L, *et al.* The pharmacological chaperone isofagomine increases the activity of the Gaucher disease L444P mutant form of ?-glucosidase. *FEBS Journal* 2010; **277**: 1618–38.

293 Mazzulli JR, Zunke F, Tsunemi T, *et al.* Activation of -Glucocerebrosidase Reduces Pathological -Synuclein and Restores Lysosomal Function in Parkinson's Patient Midbrain Neurons. *Journal of Neuroscience* 2016; **36**: 7693–706.

294 Wauer R, Schmalisch G, Kurze D, Rachmann B, Grauel EL. The use of ambroxol (bromhexine metabolite VIII) in the prevention and treatment of hyaline membrane disease (HMD). *European Journal of Obstetrics & Gynecology and Reproductive Biology* 1983; **15**: 421–4.

295 Wu X, Li S, Zhang J, *et al.* Meta-analysis of high doses of ambroxol treatment for acute lung injury/acute respiratory distress syndrome based on randomized controlled trials. *The Journal of Clinical Pharmacology* 2014; **54**: 1199–206.

296 Leffler A, Reckzeh J, Nau C. Block of sensory neuronal Na+ channels by the secreolytic ambroxol is associated with an interaction with local anesthetic binding sites. *Eur J Pharmacol* 2010; **630**: 19–28.

297 Fois G, Hobi N, Felder E, *et al.* A new role for an old drug: Ambroxol triggers lysosomal exocytosis via pH-dependent Ca2+ release from acidic Ca2+ stores. *Cell Calcium* 2015; **58**: 628–37.

298 Boehringer Pharmaceuticals. Summary of product characteristics Ambrosan 60mg. 2015; : 1–4.

299 Suzuki Y, Ichinomiya S, Kurosawa M, *et al.* Chemical chaperone therapy: clinical effect in murine GM1-gangliosidosis. *Ann Neurol* 2007; **62**: 671–5.

300 Takamura A, Higaki K, Kajimaki K, *et al.* Enhanced autophagy and mitochondrial aberrations in murine G(M1)-gangliosidosis. *Biochem Biophys Res Commun* 2008; **367**: 616–22.

301 Migdalska-Richards A, Ko WKD, Li Q, Bezard E, Schapira AHV. Oral ambroxol increases brain glucocerebrosidase activity in a nonhuman primate. *Synapse* 2017; **256**: e21967.

302 Narita A, Shire, Itamura S, *et al.* Ambroxol chaperone therapy for neuronopathic Gaucher disease: A pilot study. *Ann Clin Transl Neurol*

2016; **3**: 200–15.

303 Zimran A, Altarescu G, Elstein D. Pilot study using ambroxol as a pharmacological chaperone in type 1 Gaucher disease. *Blood Cells Mol Dis* 2013; **50**: 134–7.

304 Narita A, Kubota N, Takayama R, *et al.* Chaperone therapy for neuronopathic Gaucher disease. *Mol Genet Metab* 2013; **108**: S69.

305 Oosterhuis B, Storm G, Cornelissen PJ, Su CA, Sollie FA, Jonkman JH. Dose-dependent uricosuric effect of ambroxol. *Eur J Clin Pharmacol* 1993; **44**: 237–41.

306 Baranwal AK, Murthy AS, Singhi SC. High-dose Oral Ambroxol for Early Treatment of Pulmonary Acute Respiratory Distress Syndrome: an Exploratory, Randomized, Controlled Pilot Trial. *J Trop Pediatr* 2015; published online June 30. DOI:10.1093/tropej/fmv033.

307 Visani L, Daniotti S. SHORT SAFETY REPORT - Post marketing surveillance on tolerability of high dose ambroxol in pregnant women and newborns and on efficacy in preventing IRDS . 1992; : 1–3.

308 Balducci C, Pierguidi L, Persichetti E, *et al.* Lysosomal hydrolases in cerebrospinal fluid from subjects with Parkinson's disease. *Movement Disorders* 2007; **22**: 1481–4.

309 Rocha EM, Smith GA, Park E, *et al.* Sustained Systemic Glucocerebrosidase Inhibition Induces Brain α-Synuclein Aggregation, Microglia and Complement C1q Activation in Mice. *Antioxid Redox Signal* 2015; **23**: 550–64.

310 Martínez-Arias R, Comas D, Mateu E, Bertranpetit J. Glucocerebrosidase pseudogene variation and Gaucher disease: Recognizing pseudogene tracts in GBA alleles. *Hum Mutat* 2001; **17**: 191–8.

311 Sorge J, Gross E, West C, Beutler E. High level transcription of the glucocerebrosidase pseudogene in normal subjects and patients with Gaucher disease. *J Clin Invest* 1990; **86**: 1137–41.

312 Martínez-Arias R, Calafell F, Mateu E, Comas D, Andrés A, Bertranpetit J. Sequence variability of a human pseudogene. *Genome Res* 2001; **11**: 1071–85.

313 Benitez BA, Davis AA, Jin SC, *et al.* Resequencing analysis of five Mendelian genes and the top genes from genome-wide association studies in Parkinson's Disease. *Mol Neurodegener* 2016; **11**: 29.

314 Gan-Or Z, Giladi N, Rozovski U, *et al.* Genotype-phenotype correlations between GBA mutations and Parkinson disease risk and onset. *Neurology* 2008; **70**: 2277–83.

315 Hu F-Y, Xi J, Guo J, *et al.* Association of the glucocerebrosidase N370S allele with Parkinson's disease in two separate Chinese Han populations of mainland China. *Eur J Neurol* 2010; **17**: 1476–8.

316 González-Del Rincón M de L, Monroy Jaramillo N, Suárez Martínez AI, *et al.* The L444P GBA mutation is associated with early-onset Parkinson's disease in Mexican Mestizos. *Clin Genet* 2013; **84**: 386–7.

317 Nishioka K, Vilarino-Guell C, Cobb SA, *et al.* Glucocerebrosidase mutations are not a common risk factor for Parkinson disease in North Africa. *Neurosci Lett* 2010; **477**: 57–60.

318 Beutler E, Gelbart T, Kuhl W, Sorge J, West C. Identification of the second common Jewish Gaucher disease mutation makes possible population-based screening for the heterozygous state. *Proc Natl Acad Sci USA* 1991; **88**: 10544–7.

319 Bras J, Paisán-Ruíz C, Guerreiro R, *et al.* Complete screening for glucocerebrosidase mutations in Parkinson disease patients from Portugal. *Neurobiol Aging* 2009; **30**: 1515–7.

320 Choi JM, Kim WC, Lyoo CH, *et al.* Association of mutations in the glucocerebrosidase gene with Parkinson disease in a Korean population. *Neurosci Lett* 2012; **514**: 12–5.

321 Clark LN, Ross BM, Wang Y, *et al.* Mutations in the glucocerebrosidase gene are associated with early-onset Parkinson disease. *Neurology* 2007; **69**: 1270–7.

322 De Marco EV, Annesi G, Tarantino P, *et al.* Glucocerebrosidase gene mutations are associated with Parkinson's disease in southern Italy. *Movement Disorders* 2008; **23**: 460–3.

323 Emelyanov A, Boukina T, Yakimovskii A, *et al.* Glucocerebrosidase gene mutations are associated with Parkinson's disease in Russia. *Movement Disorders* 2012; **27**: 158–9.

324 Guo J-F, Li K, Yu R-L, *et al.* Polygenic determinants of Parkinson's disease in a Chinese population. *Neurobiol Aging* 2015; **36**: 1765.e1–6.

325 Han F, Grimes DA, Li F, *et al.* Mutations in the glucocerebrosidase gene are common in patients with Parkinson's disease from Eastern Canada. *Int J Neurosci* 2015; : 1–7.

326 Huang C-L, Wu-Chou Y-H, Lai S-C, *et al.* Contribution of glucocerebrosidase mutation in a large cohort of sporadic Parkinson's disease in Taiwan. *Eur J Neurol* 2011; **18**: 1227–32.

327 Kalinderi K, Bostantjopoulou S, Paisán-Ruíz C, Katsarou Z, Hardy J, Fidani L. Complete screening for glucocerebrosidase mutations in

Parkinson disease patients from Greece. *Neurosci Lett* 2009; **452**: 87–9.

328 Kumar KR, Ramirez A, Gobel A, *et al.* Glucocerebrosidase mutations in a Serbian Parkinson's disease population. *Eur J Neurol* 2013; **20**: 402–5.

329 Lesage S, Condroyer C, Hecham N, *et al.* Mutations in the glucocerebrosidase gene confer a risk for Parkinson disease in North Africa. *Neurology* 2011; **76**: 301–3.

330 Li Y, Sekine T, Funayama M, *et al.* Clinicogenetic study of GBA mutations in patients with familial Parkinson's disease. *Neurobiol Aging* 2014; **35**: 935.e3–8.

331 Mao X-Y, Burgunder J-M, Zhang Z-J, *et al.* Association between GBA L444P mutation and sporadic Parkinson's disease from Mainland China. *Neurosci Lett* 2010; **469**: 256–9.

332 Mitsui J, Mizuta I, Toyoda A, *et al.* Mutations for Gaucher disease confer high susceptibility to Parkinson disease. *Arch Neurol* 2009; **66**: 571–6.

333 Moraitou M, Hadjigeorgiou G, Monopolis I, *et al.* beta-Glucocerebrosidase gene mutations in two cohorts of Greek patients with sporadic Parkinson's disease. *Mol Genet Metab* 2011; **104**: 149–52.

334 Neumann J, Bras J, Deas E, *et al.* Glucocerebrosidase mutations in clinical and pathologically proven Parkinson's disease. *Brain* 2009; **132**: 1783–94.

335 Nichols WC, Pankratz N, Marek DK, *et al.* Mutations in GBA are associated with familial Parkinson disease susceptibility and age at onset. *Neurology* 2009; **72**: 310–6.

336 Noreau A, Rivière J-B, Diab S, *et al.* Glucocerebrosidase mutations in a French-Canadian Parkinson's disease cohort. *Can J Neurol Sci* 2011; **38**: 772–3.

337 Ran C, Brodin L, Forsgren L, *et al.* Neurobiology of Aging. *NBA* 2016; : 1–7.

338 Sato C, Morgan A, Lang AE, *et al.* Analysis of the glucocerebrosidase gene in Parkinson's disease. *Movement Disorders* 2005; **20**: 367–70.

339 Setó-Salvia N, Pagonabarraga J, Houlden H, *et al.* Glucocerebrosidase mutations confer a greater risk of dementia during Parkinson's disease course. *Movement Disorders* 2012; **27**: 393–9.

340 Spitz M, Rozenberg R, Pereira LDV, Reis Barbosa E. Association between Parkinson's disease and glucocerebrosidase mutations in Brazil. *Parkinsonism and realted Disorders* 2008; **14**: 58–62.

341 Tan E-K, Tong J, Fook-Chong S, *et al.* Glucocerebrosidase mutations and risk of Parkinson disease in Chinese patients. *Arch Neurol* 2007; **64**: 1056–8.

342 Toft M, Pielsticker L, Ross OA, Aasly JO, Farrer MJ. Glucocerebrosidase gene mutations and Parkinson disease in the Norwegian population. *Neurology* 2006; **66**: 415–7.

343 Santos dos AV, Pestana CP, Diniz KRDS, *et al.* Mutational analysis of GIGYF2, ATP13A2 and GBA genes in Brazilian patients with early-onset Parkinson's disease. *Neurosci Lett* 2010; **485**: 121–4.

344 Wu Y-R, Chen C-M, Chao C-Y, *et al.* Glucocerebrosidase gene mutation is a risk factor for early onset of Parkinson disease among Taiwanese. *Journal of Neurology, Neurosurgery & Psychiatry* 2007; **78**: 977–9.

345 Yu Z, Wang T, Xu J, *et al.* Mutations in the glucocerebrosidase gene are responsible for Chinese patients with Parkinson's disease. *J Hum Genet* 2015; **60**: 85–90.

346 Sanders A, Hemmelgarn H, Melrose HL, Hein L, Fuller M, Clarke LA. Transgenic mice expressing human glucocerebrosidase variants: utility for the study of Gaucher disease. *Blood Cells Mol Dis* 2013; **51**: 109–15.